The effect of compounds on copper homeostasis in *Plasmodium falciparum* and neuroblastoma cells

Natasha C. Jansen van Vuuren

A dissertation submitted to the Faculty of Health Sciences, University of Witwatersrand, Johannesburg, in the fulfilment of the requirements for the degree of Master of Science in Medicine.

2020

Candidate's declaration

I Natasha C. Jansen van Vuuren declare that this Dissertation is my own, unaided work. It is being submitted for the Degree of Master of Science in Medicine at the University of the Witwatersrand, Johannesburg. It has not been submitted before for any degree or examination at any other University.

(Signature of candidate)

15th day of October 20 20 in Bloemfontein

Dedication

This work is dedicated to my parents and family for their continuous love, support, and encouragement.

Presentations arising from this research project

- Jansen van Vuuren, N.C., van Zyl, R. 2012.
  Poster Presentation: The haemolytic protective properties of 8-hydroxyquinoline copper chelating agents. 5th All Africa Congress of Basic and Clinical Pharmacology. Accra, Ghana. 11-13 July 2012.
- Jansen van Vuuren, N.C., van Zyl, R. 2012.
  Oral Presentation: The anti-neoplastic properties of 8-hydroxyquinolone copper chelating agents. Annual Congress of the South African Society for Basic and Clinical Pharmacology and Toxicology Society of South Africa. Pretoria, South Africa. 29 September – 2 October 2012
- Jansen van Vuuren, N.C., van Zyl, R. 2014.
  Poster Presentation: The effect of 8-hydroxyquinoline derivatives on copper homeostasis in Plasmodium falciparum. University of the Witwatersrand. Faculty of Health Sciences Research Day and Postgraduate Expo. Johannesburg, South Africa. 17 September 2014.
- Jansen van Vuuren, N.C., van Zyl, R. 2014.
  Poster Presentation: The copper chelation and antimalarial activity of 8-hydroxyquinoline and its derivatives. 17th World Congress of Basic and Clinical Pharmacology. Cape Town, South Africa. 13-18 July 2014.
- Jansen van Vuuren, N.C., van Zyl, R. 2014.
  Oral Presentation: The copper chelation and antimalarial activity of 8-hydroxyquinoline and its derivatives. University of the Witwatersrand, 6th Cross Faculty Postgraduate Symposium. Johannesburg, South Africa. September 2014.
- Jansen van Vuuren, N.C., van Zyl, R. 2015.
  Poster Presentation: (±)-Menthone, a copper chelator with antimalarial activity. Annual Congress of the South African Society for Basic and Clinical Pharmacology and Toxicology Society of South Africa. Johannesburg, South Africa. 31 August – 2 September 2015.
- Jansen van Vuuren, N.C., van Zyl, R. 2016.
  Poster presentation: The ovicidal, larvicidal and toxicological effect of 8-hydroxyquinoline derivatives. All Africa Congress on Pharmacology and Pharmacy. Muldersdrift, South Africa. 5-7 October 2016.
  Won best poster presentation for young toxicologist competition.

Abstract

Adverse changes in copper ion homeostasis can be harmful to living organisms, where an excess of copper can cause oxidative damage leading to carcinogenesis, neurogenerative diseases and the conditions such as Wilson's and Parkinson's disease. However, copper is a crucial metal required for metabolism and growth, as in the malaria parasite. Malaria is a global health problem that is further amplified by resistance to antimalarials and insecticides. Consequently, novel copper chelators that diminish metal ion redox effects and inhibit malaria metabolism are required to prevent disease progression. Two potential groups selected for investigation included 8-hydroxyquinoline (8-OH) derivatives and essential oils constituents (EOCs), which are known antioxidants, metal chelators, with antimicrobial properties. Thus, the aim of the study was to determine the interaction of twenty-one 8-OHs and fifty-five EOCs with copper and to determine their chemotherapeutic effect on *Plasmodium falciparum* (3D7), *Anopheles gambiae* (KGB) and neuroblastoma cells (SHSY5Y), as well as the toxicological effects on human red blood cells and *Artemia*. The most potent 8-OH derivative, N-butyl-2,2-imino-di-(8-OH) preferentially chelated Cu(I) (IC_{50}: 12.90 ± 0.80 µM) over Cu(II) (IC_{50}: 44.37 ± 2.52 µM), compared to tetrathiomolybdate (IC_{50} Cu(I): 44.37 ± 2.52 µM; IC_{50} Cu(II): 45.79 ± 10.54 µM). It interacted synergistically with tetrathiomolybdate to chelate Cu(I) (ΣFIC = 0.40) and in an additive manner to chelate Cu(II) (ΣFIC = 0.75); whilst retaining its ability to chelate copper *in vitro*. This 8-OH derivative had notable *in vitro* antimalarial activity (IC_{50}: 0.58 ± 0.03 µM) affecting the progression of trophozoites to schizonts by inhibiting haemozoin formation comparable to chloroquine and interacted synergistically with chloroquine *in vitro*. N-butyl-2,2-imino-di-(8-OH) possessed larvicidal activity, but not as potently as *2*-benzyl-8-OH and DDT. It was twice as cytotoxic to neuroblastoma cells compared to camptothecin, but not as toxic to *Artemia* as potassium dichromate. Furthermore, 8-OH derivatives with functional groups at positions 5 and 7 displayed improved copper chelating, antioxidant, anticancer, antimalarial and larvicidal activity. The EOCs displayed a diverse pharmacological profile, with the widest range of activity belonging to (±)-menthone. It effectively chelated Cu(II) in preference to Cu(I) (IC_{50}: 12.69 ± 3.69 µM; 10.78 ± 2.00 µM, respectively) compared to trientine (30.97 ± 0.64 µM; 27.34 ± 5.96 µM, respectively); along with promising copper reducing ability. However, this promising chelating ability did not correspond to its ability to inhibit malaria (51.22 ± 8.21 µM). (±)-Menthone possessed significant larvicidal activity (73.00 ± 5.70%) compared to DDT (100.00 ± 0.00%), but was not as active as carvacrol (93.0 ± 5.70%). Although (+)-α-pinene had poor copper chelating activity, it potently inhibited parasite growth (IC_{50}: 0.009 ± 0.002 µM) by inhibiting haemozoin formation, whilst interacting synergistically *in vitro* with chloroquine (ΣFIC =0.45). The diverse properties of 8-OH derivatives and EOCs give rise to the potential that these compounds may be useful in the management of diseases caused by copper excess, oxidative stress, the malaria parasite and cancer.

Acknowledgements

I would like to thank my supervisor, Prof. Robyn L van Zyl, for her consistent advice, knowledge and all the time and effort that she dedicated to this project.

I would earnestly like to thank Mr C.T Chen and Mrs N. Shunmoogum-Gounden for their support in the laboratory and most importantly their friendship. Thank you Mrs F. Kathrada and Mrs O. Mustapha for their assistance in the laboratory and interesting chats.

Sincerest thanks to the staff of the Department of Pharmacy and Pharmacology for all their help and support.

I would like to acknowledge Prof Christiaan Brink for his generous donation of the SH-SY5Y cell line.

Thank you to Dr Shune Oliver for her guidance with the larvicidal studies and for providing the larvae for my study.

Sincerest thanks to the University of Witwatersrand, the National Research Foundation, The Belgium Technical Corporation and Faculty Research Committee for providing financial support.

Table of Contents

List of Figures

List of Tables

List of Equations

List of Abbreviations

AA	Ascorbic acid
ADP	Adenosine diphosphate
APP	Amyloid precursor protein
ATOX1	Antioxidant-1 copper transport protein
ATP	Adenosine triphosphate
ATPase	Adenosine triphosphatase
ATP7A	Adenosine triphosphatase-7A
ATP7B	Adenosine triphosphatase 7B
BC	Background control
BCS	Bathocupreine disulphonate
BHA	Butylated hydroxyanisole
BHT	2,6-Di-tert-butyl-4-methylphenol
CC	Colour control
CCS	Capsanthin-capsorubin synthase
CO_2	Carbon dioxide
COX	Cyclo-oxygenase
CTR1	Copper transport protein-1
CuCl	Cuprous chloride
$CuCl_2$	Cupric chloride
CuCN	Copper cyanide
$CuSO_4.H_2O$	Hydrated copper sulphate
ddH_2O	Double distilled water
DDT	Dichlorodiphenyltrichloroethane
DHA	Dihydroartemisinin
DMEM	Dulbecco's modified eagle's medium
DMSO	Dimethyl sulfoxide
DNA	Deoxyribonucleic acid
$DPPH^{\bullet}$	2,2-Diphenyl-1-picrylhydrazyl
EDTA	Ethylenediamine tetra acetic acid
EOC	Essential oil constituents
FAD	Flavin adenine dinucleotide
$FADH_2$	Flavin adenine dinucleotide hydroquinone
FBIT	Ferriprotoporphyrin biomineralization formation inhibited
FBS	Fetal bovine serum

FIC	Fractional inhibitory concentration
FPIX	Ferriprotoporphyrin IX
GABA	γ-Aminobutyric acid
GIT	Gastrointestinal tract
hCTR1	Human copper transporter-1
HEPES	4-(2-Hydroxyethyl)-1-piperazineethanesulfonic acid
H_2O_2	Hydrogen peroxide
IC_{50}	Half maximal inhibitory concentration
IUPAC	International Union of Pure and Applied Chemistry
JAK	Janus kinase
LD_{50}	Median lethal dose
mRNA	Mitochondrial ribonucleic acid
MTT	3-(4, 5-dimethyl-2-thiazol-2-yl)-2, 5- diphenyl-2H-tetrazolium bromide
MW	Molecular weight
NADH	Nicotinamide adenine dinucleotide
NBT	Nitro blue tetrazolium
ND	Not determined
NDoH	National Department of Health
NED	*N*-(1-Naphthyl)ethylenediamine dihydrochloride
NS	Not significant
2-OH	2-Hydroxyquinoline
4-OH	4-Hydroxyquinoline
8-OH	8-Hydroxyquinoline
PBS	Phosphate buffered saline
PBT2	5,7-Dichloro-2-[(dimethylamino)methyl]quinolin-8-ol
PES	Phenazine ethosulfate
PGE2	Prostaglandin-E2
pLDH	Parasite lactate dehydrogenase
RBC	Red blood cells
ROS	Reactive oxygen species
RT	Room Temperature
SOD	Superoxide dismutase
SRB	Sulphorhodamine B
TC	Test compound
TCA	Trichloroacetic acid

TEAC	Trolox™ equivalent antioxidant capacity
TET	Trientine
TETA	Triethylenetetramine
TMB	Tetrathiomolybdate
TNF-α	Tumour necrosis factor-α
UV- VIS	Ultraviolet–visible
WHO	World Health Organization

Chapter 1. Introduction

Metal ions such as iron and copper are utilized in many metabolic processes in the human body as well as in parasitic protozoa, such as *Plasmodium falciparum* (Rasoloson *et al.*, 2004; Zatta and Frank, 2007; Crisponi *et al.*, 2010). Iron and copper undergo oxidation reactions and when in contact with free radicals such as hydrogen peroxide (H_2O_2), lipid peroxidation is initialized in cellular membranes which lead to their dysfunction and death (McCord, 2004). When in excess, copper ions react with nitric oxide and the reactive species of these molecules cause cellular membrane damage (Valko *et al.*, 2006; Tisato *et al.*, 2010). Changes in metal homeostasis can adversely affect living organisms, where an excess of copper can cause oxidative damage which may contribute to carcinogenesis, neurogenerative diseases and the pathogenesis of conditions such as Wilson's and Menkes disease (Blincoe, 1993; Shi, Hudson and Liu, 2004; Singh, Sharad and Kapur, 2004). Whereas a deficiency in these metal ions can result in cell death of microorganisms due to the interruption of anabolic processes, which could be advantageous when trying to eliminate an infection that relies on copper or iron for its rapid replication (Rasoloson *et al.*, 2004). Copper and iron are essential in the metabolism of the malaria parasite and compounds that can cause a deficiency in the malaria parasite are needed to aide in the treatment against the parasite (Rasoloson *et al.*, 2004). In contrast, compounds that stabilise or chelate metal ions and reduce their pathology are needed to prevent diseases that are aggravated by metal ion accumulation such as Alzheimer's, Parkinson's and Huntington's disease (Chen, Miah and Aschner, 2016).

An overabundance of free copper ions in intracellular and extracellular sites may lead to the production of pro-oxidant reactions causing damage to cellular organelles and membranes (Bertinato and L'Abbé, 2004; Crisponi *et al.*, 2010; Scheiber, Mercer and Dringen, 2010). Changes in copper homeostasis contributes to the pathogenesis of diseases such as Wilson's, Huntington's, aceruloplasminemia and neurodegenerative disorders (Bertinato and L'Abbé, 2004). Wilson's disease is a rare, inherited, autosomal, recessive disease caused by a mutation in the gene encoding the adenosine triphosphatase 7B (ATP7B) copper translocation protein found in hepatocytes (Lang *et al.*, 2007; Niederau, 2018). In the presence of high concentration of the ion, this protein translocates copper into the bile (Lang *et al.*, 2007). The mutation decreases copper excretion through the bile resulting in copper to accumulate in various organs such as the liver, brain, kidney and cornea (Niederau, 2018). Accumulation of copper activates reactive oxygen species (ROS) that disrupt the functioning of lysosomes and mitochondria, which triggers the formation of lipid peroxides and inhibition of antioxidants (Lang *et al.*, 2007).

Currently, research is required to find new copper chelators that can be used in the management of copper excess disorders and since the compounds in this study have shown the potential to both chelate and/or reduce metal ions, they will be examined to determine whether they are effective in decreasing the accumulation copper and their preliminary toxicity profile.

Malaria is an infectious protozoal disease and is transmitted by an infected *Anopheles* mosquito to the bloodstream of a human host (WHO, 2019). Of the five species of malaria parasite: *Plasmodium falciparum* is the deadliest (WHO, 2019).The parasite is transmitted into the bloodstream of a human host where it invades the hepatocytes and proliferates such that merozoites infect new red blood cells (RBC) which proliferate and mature before lysing the RBCs to continue the next cycle of the parasite (Bartoloni and Zammarchi, 2012; WHO, 2019).

Artemisinin combined with lumefantrine is used as first line therapy because of its favourable tolerance in patients and its high potency against malaria. Increased resistance is the largest problem in the management of malaria, which results in the increased risk of death (WHO, 2019). Growing resistance to artemisinin demands the development of new classes of antimalarial agents (WHO, 2016). New targets, such as the parasitic enzymes responsible for copper homeostasis could be a viable option. Individuals infected with *P. falciparum* have a 33-39% decrease in serum copper levels as compared to healthy, uninfected individuals (109-149 µg/dL) (Garba, Ubom and Ejiogu, 2006). The loss of copper in the serum was due to haemolysis and the parasite incorporating the free copper ions for its own growth and synthesis (Garba, Ubom and Ejiogu, 2006). The copper chelator, neocuproine has been shown to inhibit the *in vitro* growth and metabolism of *Plasmodium* during the transition from ring to trophozoite stage. Thus, indicating the sensitivity of the parasite to changes in its own copper homeostasis and could be a potential drug target. The hepatic parasitaemia is decreased when iron concentration is lowered. Several studies have shown that iron chelators such as desferrioxamine, deferiprone and daphnetin derivatives inhibit parasitic metabolism. The development of novel chelators that may act as antimalarials are needed to combat the growing resistance to antimalarial drugs.

The 8-hydroxyquinoline (8-OH) derivatives are used as antibacterial, antiseptic, and antifungal agents (Moret *et al.*, 2009) and have been shown to possess the potential as being antioxidant, metal reducers; as well as to form weak chelates with ferrous (II) ions and fairly stable, strong chelates with copper (II) ions (Phillips and Stanley, 2011). These favourable copper chelating properties show potential to be used in various pathological conditions to limit the concentration of free copper. Thus, various derivatives of these compounds were selected

and their interaction with copper determined, before being evaluated on malaria parasites, *Anopheles* larvae and human neuronal cells.

Essential oil constituents (EOCs) have been reported to possess antiseptic, antidepressant and antimicrobial properties (Pramod and Ansari, 2010). EOCs, including eugenol and its derivatives have been shown to be potent free radical scavengers and to reduce iron and copper. EOCs have also demonstrated antipyretic properties that could also provide a dual mechanism of action to alleviate some clinical symptoms of malaria. EOCs possess inhibitory activity against *P. vivax* and *P. falciparum*. These properties favour further study of EOCs and structurally related compounds to further determine their potential as copper chelators and influence on biological activity.

Thus, the aim of the study was to determine the interaction of 8-OHs and EOCs with copper and to determine their chemotherapeutic effect on *Plasmodium*, *Anopheles* and human neuroblastoma cells.

Chapter 2. Literature Review

2.1. The essential and toxic nature of copper

Copper is a vital micronutrient and an essential co-factor to several metabolic enzymes found in all living organisms. Copper homeostasis is a tightly controlled process such that it is stored in very low concentrations and is usually rapidly utilized (Bertinato and L'Abbé, 2004; Abou Zeid and Kaler, 2019). Copper has numerous physical and chemical properties (Table 2.1), is an important constituent in several food sources, metabolic and essential enzymes.

Table 2.1: The International Union of Pure and Applied Chemistry (IUPAC) name and physiochemical properties of copper ions (Hammond, 2005).

IUPAC Name	Synonyms	Copper compounds	Appearance	Melting point (°C)	Boiling point (°C)
Copper (I) Cu^{1+}	Cuprous	Cuprous chloride (CuCl)	Green, powder	426	1490
		Copper cyanide (CuCN)	Pale, yellow powder	474	25.7 at 760mmHg
Copper (II) Cu^{2+}	Cupric	Hydrated copper sulphate ($CuSO_4.H_2O$)	Blue, crystalline, powder	110-150	650
		Cupric Chloride ($CuCl_2$)	Yellow, brown powder	100	993

Copper is potentially toxic to sensitive intracellular organelles and extracellular components. Copper toxicity has been associated with neurological diseases such as Wilson's and Alzheimer's disease (Bertinato and L'Abbé, 2004). Excess copper has induced the formation of ROS in erythrocytes, which may be mitigated by the use of antioxidants (Husain and Mahmood, 2019).

The aim of this review is to summarise the importance of copper in the normal functioning of humans and malaria parasite, its role in excess or deficient diseases and the standard treatments of these diseases. Additionally, this review intends to determine if any recent research has been conducted in support of novel copper toxicity related treatments.

2.2. The importance of maintaining copper homeostasis

To ensure the careful maintenance of copper in eukaryotic cells and in the human body copper absorption, distribution and excretion is regulated by copper chaperones and enzymes (Culbertson *et al.*, 2020). Approximately 2 to 4 mg of copper is ingested through a normal diet.

Copper is mostly found in the brain, liver, kidney, plasma and blood (Latorre, Troncoso and Uauy, 2019).

2.2.1. Copper absorption, distribution, and excretion in the human body

2.2.1.1. Absorption

The process of copper absorption involves the uptake of the copper (II) ion in the gastrointestinal tract by binding the ion to the enterocyte-based enzyme human copper transporter-1 (hCTR1). This enzyme reduces the cupric ion to the cuprous ion and transports it across the permeable membrane (Figure 2.1) (Bertinato and L'Abbé, 2004; Crisponi *et al.*, 2010; De Romaña *et al.*, 2011; Latorre, Troncoso and Uauy, 2019).

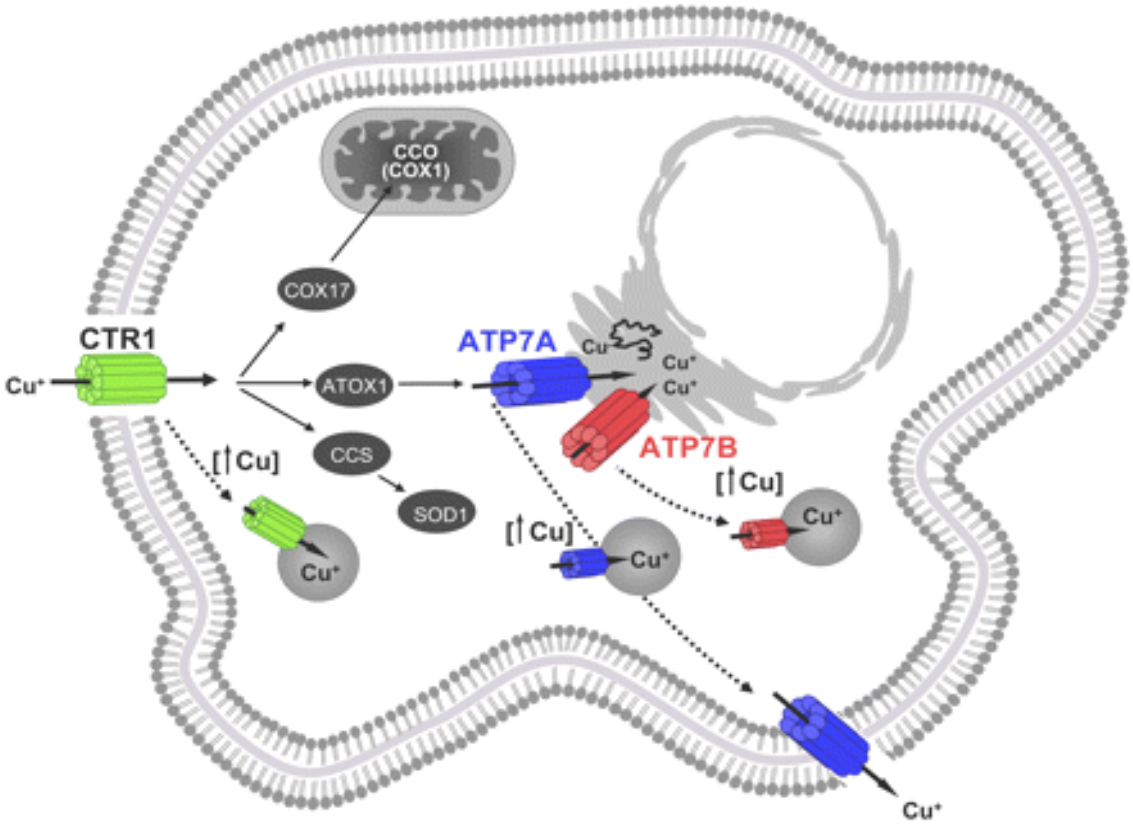

Figure 2.1: The intestinal absorption and excretion of copper (Wang *et al.*, 2017).
Copper (Cu), Copper (I) ion (Cu^{+}), copper transport protein-1 (CTR1), cyclo-oxygenase-17 (COX17), antioxidant-1 copper transport protein (ATOX1), capsanthin-capsorubin synthase (CCS), superoxide dismutase-1 (SOD1), cyclo-oxygenase-1 (COX1), Adenosine triphosphatase (ATP7A; ATP7B).

The copper (I) ion is then bound to metallothioneins that regulate the transport of copper across the intestinal epithelium (Crisponi *et al.*, 2010; Latorre, Troncoso and Uauy, 2019). As seen in Figure 2.1, the intracellular ATPase enzyme, ATP7A oxidises copper (I) to copper (II)

ion and translocates it across the enterocyte membrane into the portal bloodstream, where it is transported to various tissues and utilized (Crisponi *et al.*, 2010).

2.2.1.2. Distribution

Normal serum copper concentration is in the range of 10-20 µM and 0-1.6 µM in urine. The approximate distribution of copper in the body consists of 5.45% in the blood, 8% in the brain, 9.1% in the liver, 23.6% in the skeletal muscles and 41.8% in the skeleton and bone marrow (Crisponi *et al.*, 2010). In blood copper is bound to proteins such as ceruloplasmin, albumin and transcupreine (Zatta and Frank, 2007). Copper is distributed to the tissues bound to complexes or chaperone proteins such as glutathione. Glutathione along with other metalloenzymes are the main detoxification and storage sites for intracellular copper (La Fontaine and Mercer, 2007). Glutathione reduces copper (II), binds to it, delivers it to metallothionein's and acts as a protective agent against copper toxicity (Tapiero, Townsend and Tew, 2003). When high concentrations of copper are present in the plasma, the production of metalloenzymes are induced to protect the cellular components from free copper ions.

2.2.1.3. Distribution in the brain

Metallothionein protects and delivers metal ions ,such as copper, zinc and iron, to sites in the brain, plus also act as chaperones by assisting proper protein folding (Zatta and Frank, 2007). Astrocytes are important neuronal cells in the maintenance of copper homeostasis in the brain and have an elevated capacity to avoid metal toxicity (Scheiber, Mercer and Dringen, 2010). These cells express a large concentration of metallothionein's and glutathione and are localized between neuronal tissue and the capillary endothelial tissue (Scheiber, Mercer and Dringen, 2010).

2.2.1.4. Distribution in hepatic and gastrointestinal system

In hepatocytes and enterocytes, copper is shuttled via the trans-golgi network and delivered to P-type ATPases, ATP7A (enterocytes) and ATP7B (hepatocytes) (Tapiero, Townsend and Tew, 2003).

2.2.1.5. Excretion

Copper excretion begins with the copper (II) ion binding to albumin and transcupreine in the portal bloodstream where it is transported to the hepatocyte membrane. It is transferred into the hepatocyte via anion exchange between sodium and carbonate (Crisponi *et al.*, 2010; De Romaña *et al.*, 2011). Copper is reduced and excreted as unabsorbed copper (I) by the hepatic translocator protein ATP7B into the bile (Figure 2.1) (Tapiero, Townsend and Tew,

2003; De Romaña *et al.*, 2011). If the excretion process is interrupted or fails, copper accumulates in the liver and can cause toxicity.

2.2.1.6. The metabolic functions of copper

Copper is involved in many essential biological processes such as the growth of new blood vessels and the functioning of essential enzymes (Crisponi *et al.*, 2010). Copper is an important component of many metabolic enzymes and proteins such as: cytochrome c oxidase, lysyl oxidase, ceruloplasmin and metallothionein's (Tapiero, Townsend and Tew, 2003; Bertinato and L'Abbé, 2004). These enzymes and proteins carry out significant metabolic functions including electron transport, respiration, and connective tissue formation (Table 2.2). Therefore copper is an ion that is associated with numerous processes critical to normal functioning as outlined below (MacPherson and Murphy, 2007).

Table 2.2: Summary of the enzymes and proteins which are dependent on, or contain copper (Tapiero, Townsend and Tew, 2003; Balamurugan and Schaffner, 2006).

Enzymes			**Proteins**		
Name	**Function**	**Species**	**Name**	**Function**	**Species**
Cytochrome c oxidase	Respiration	Mammals, bacteria, yeast, malaria parasite & fungi	Ceruloplasmin	Ferroxidase (Iron reducer)	Mammals, bacteria, fungi, parasites & plants
Lysyl oxidase	Connective tissue formation		Metallothionein	Metal ion chelators	Mammals, yeast, plants
Cu ATPases	Cu absorption & excretion		Transcupreine	Cu plasma transport	Mammals
Ascorbate Oxidase			Hemocyanin	Blood pigment	Molluscs & crustacea
Cu/Zn superoxide dismutase	Catalyses superoxide → H_2O_2	Mammals, all eukaryotes & prokaryotes	Copper transporter 1	Copper uptake mediator	Mammals, yeast, plants, *P. falciparum*
Tyrosinase	Melanin production	Mammals, plants, malaria vector & fungi	Plastocyanin	Photosynthesis electron transport	Plants
Dopamine β-mono oxidase	Dopamine → norepinephrine	Mammals	Cerebrocuprein	Cu storage in brain	Mammals

2.2.2. Copper-dependent enzymes and their functions

The main physiological role of copper is to form part of metabolic enzymes. An enzyme that relies on copper to carry out its normal functions is known as a copper-dependent enzyme. These enzymes may have copper binding sites that require a copper ion to bind and facilitate certain tasks or the copper ion is a central constituent of the enzyme (MacPherson and Murphy, 2007; Latorre, Troncoso and Uauy, 2019). The enzymes in Table 2.2 were selected because they require copper to function, their highly conserved nature, and the important functions that they carry out.

2.2.2.1. Cytochrome c oxidase

Cytochrome c oxidase is the terminal oxidase enzyme in mitochondrial respiration in several organisms (Figure 2.2) where oxygen is reduced to water. It is a proton pump with two copper binding sites located within the inner membrane of the mitochondria and is vital in the production of cellular energy (Figure 2.2) (Tapiero, Townsend and Tew, 2003; De Luca *et al.*, 2019). In the presence of copper deficiency, the oxidase is unable to carry out its function. Consequences of this dysfunction include, a general skeletal myopathy, cardiomyopathy, motor neuron disease, hepatic failure, renal failure and lactic acidosis (Hamza and Gitlin, 2002; Tapiero, Townsend and Tew, 2003). Cytochrome c oxidase in *P. falciparum* is involved in the oxidative phosphorylation pathway and facilitates copper transport across the mitochondrial membrane (MPMP, 2020; UniProtKB, 2020a). Inhibition of this protein may inhibit aerobic respiration and electron transport within the parasitic (Section 2.4.2.1) (UniProtKB, 2020a).

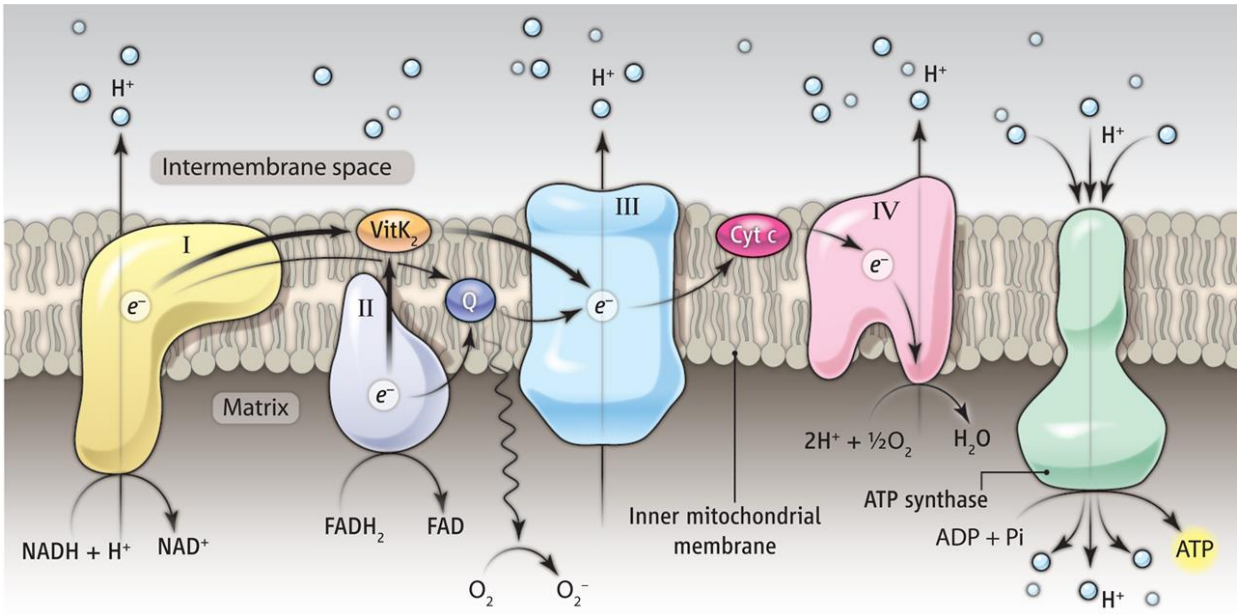

Figure 2.2: The electron transport chain showing cytochrome c (Cyt c) transporting electrons to complex IV in order to reduce molecular oxygen (Bhalerao and Clandinin, 2012).

Flavin adenine dinucleotide (FAD), Flavin adenine dinucleotide hydroquinone ($FADH_2$), nicotinamide adenine dinucleotide (NADH), proton (H^+), ubiquinone (Q), vitamin K ($VitK_2$), adenosine triphosphate (ATP), adenosine diphosphate (ADP), electron (e^-), inorganic phosphate (Pi), complex I (I), complex II (II), complex III (III) and complex IV (IV).

2.2.2.2. Lysyl oxidase

Copper is an important supportive component of lysyl oxidase that is central in the development of connective tissue by catalysing the formation of aldehydes from lysine residues (Shanbhag *et al.*, 2019). Errors in the arrangement of connective tissue lead to malformations in the extracellular matrix of tissues and organs (Di Ferrante *et al.*, 1975). Such that in severe copper deficiencies as caused by Menke's disease, the decreased copper concentration in the body leads to deformed connective tissue resulting in Ehlers-Danlos syndrome type IV, certain types of lung cancers and arterial dissection (Di Ferrante *et al.*, 1975; Tapiero, Townsend and Tew, 2003; Sibon *et al.*, 2005). Similarly, inhibition of lysyl oxidase within the *Anopheles gambiae* malaria parasite vector would result in disruptions of copper binding, endocytosis facilitation, and redox reaction mediation (UniProtKB, 2020b).

2.2.2.3. Copper/Zinc superoxide dismutase

Copper/Zinc superoxide dismutase (SOD) located in the nucleus, cytoplasm, peroxisomes and inner mitochondrial membrane is responsible for the conversion of superoxide anions to peroxide and has an antioxidant, protective effect on somatic cells (Tapiero, Townsend and

Tew, 2003; Valentine, Doucette and Potter, 2005; Tiwari *et al.*, 2019). Mutations of this enzyme are associated with the development of diseases such as amylotrophic lateral sclerosis, which is a neurodegenerative disease affecting the motor neurons of the frontal horn of the spinal cord leading to a decrease in muscular tone and eventual death from respiratory failure (Tapiero, Townsend and Tew, 2003; Valentine, Doucette and Potter, 2005; Desai and Kaler, 2008; Tiwari *et al.*, 2019). Copper/Zinc SOD is important in the protection of cellular components from reactive oxygen species by catalysing and controlling the production of free radicals (Figure 2.3 and Figure 2.4) and when this enzyme dysfunctions, free radicals can cause damage to cellular and organelle membranes (Tiwari *et al.*, 2019).

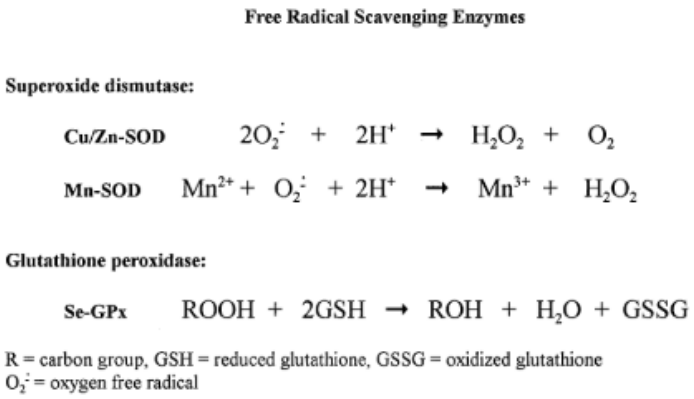

Figure 2.3: Free radical scavenging enzymes and the tightly controlled reactions that are catalysed (Leung, 1998).

Copper is a vital constituent of this enzyme and is central to its normal function (Desai and Kaler, 2008; Rivera-Mancía *et al.*, 2010). It has been proposed that copper plays a role in the pathogenesis of amylotrophic lateral sclerosis by augmenting the production of reactive oxygen species (Figure 2.4) (Desai and Kaler, 2008; Tiwari *et al.*, 2019). SOD binds metal ions and impedes free radical formation within the *P. falciparum* parasite (Section 2.4.2.4) which prevents damage to membranes by removing toxic ROS (UniProtKB, 2020c).

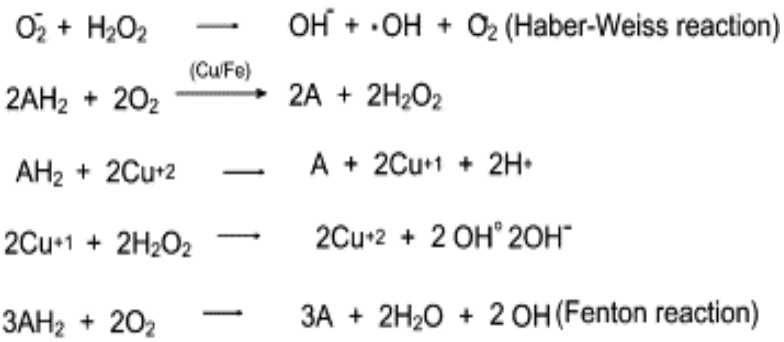

Figure 2.4: The Haber-Weiss and Fenton reactions with metal ion catalysed resulting in the production of free radicals (Tapiero and Tew, 2003).

2.2.2.4. Copper adenosine triphosphatases

The copper adenosine triphosphatases (ATPases), such as ATP7A (Menke's protein) and ATP7B (Wilson's protein) are crucial in the secretion and excretion of copper. These are P-type, transmembrane ATPases with copper binding receptors at the N-terminus (Bertinato and L'Abbé, 2004; De Luca *et al.*, 2019). The function of ATP7B is dependent on the concentration of copper present within the hepatocytes, where an increased concentration of intracellular copper leads to conformational changes of ATP7B and the subsequent binding to and excretion of copper into the bile (Terada and Sugiyama, 2002). The ATP7B protein is comprised of three sections, namely, a transductal, a nucleotide-binding and a cytosolic six-copper binding domain. Copper binds the cytosolic domain, whilst ATP is bound to the nucleotide binding domain (Figure 2.1) (Terada and Sugiyama, 2002). The ATP is hydrolysed, which momentarily phosphorylates the ATP7B protein. Energy is released from the subsequent dephosphorylating and this energy is utilized by copper-containing vesicles that are pumped across the cellular membrane (Terada and Sugiyama, 2002; Bertinato and L'Abbé, 2004).

ATP7A is responsible for the cationic uptake of copper into cells of the brain, muscle, kidney, small intestine, and lungs; in contrast, ATP7B is responsible for the biliary excretion of copper and is localized in the liver and kidneys. If the concentration of copper is higher than normal, this enzyme collects copper into vesicles that combine with the apical membrane of the hepatocytes for excretion (Crisponi *et al.*, 2010; De Romaña *et al.*, 2011). ATP7A oxidises the copper (I) ion to the copper (II) and transports it across the enterocyte membrane into the portal bloodstream where it is transported to various tissues and utilized by copper chaperones (Crisponi *et al.*, 2010).

Both of these enzymes are located in the trans-Golgi network which allows for copper transport across membranes (Bertinato and L'Abbé, 2004). A defective gene in the ATP7A protein causes a progressive, rare, X-linked recessive syndrome of copper metabolism, namely Menke's disease (Wang, Garrick and Collins, 2019). Symptoms include an overall copper deficiency in vital organs, bone abnormalities, mental impediments and seizures (Latorre, Troncoso and Uauy, 2019). The neuronal symptoms are a result of deficiency of crucial cupro-enzymes, such as cytochrome c oxidase, dopamine β-hydroxylase and superoxide dismutase (Strausak *et al.*, 2001; Tapiero, Townsend and Tew, 2003; Latorre, Troncoso and Uauy, 2019). When these enzymes dysfunction, the consequences result in deficiency of neurotransmitters such as dopamine, as well as potentiation of superoxide damage. Treatment includes copper replacement therapy with copper-histidine complexes that cross the blood brain barrier and normalize the cuproenzymes levels (Strausak *et al.*, 2001; Tapiero, Townsend and Tew, 2003; Vairo *et al.*, 2019).

2.2.3. Copper binding proteins

Proteins that bind to copper ensure the maintenance of the metal cations homeostasis. Copper is an essential component of certain transporter proteins, where in its absence the formation of the protein would not occur correctly, leading to its dysfunction in metal ion transport (Tapiero, Townsend and Tew, 2003). Those copper-dependent proteins and enzymes include: cytochrome c oxidase, hemocyanin, amicyanin and plastocyanin (Tapiero, Townsend and Tew, 2003; Balamurugan and Schaffner, 2006; Arciello *et al.*, 2011; Atzori *et al.*, 2011).

2.2.3.1. Ceruloplasmin

Ceruloplasmin is the main copper transporter protein that acts as a ferroxidase (iron ion reducer) (Tapiero, Townsend and Tew, 2003; Prohaska, 2008). Copper is an essential constituent of this protein and if a copper deficiency occurs, a severe accumulation of free iron ion takes place in the hepatocytes and peripheral tissues (Tapiero, Townsend and Tew, 2003). High blood serum levels of ceruloplasmin have been used as an indicator of disease progression in regards to inflammatory and malignant conditions; whereas low blood serum ceruloplasmin can indicate the presence of Wilson's disease (Nittis and Gitlin, 2002; Arnal *et al.*, 2010). In patients with stable *P. falciparum* infections, it was discovered that their ceruloplasmin levels were raised in comparison to lower levels of other antioxidant enzymes, such as glutathione and metallothioneins (Percário *et al.*, 2012; Gitau *et al.*, 2013). Contrastingly, the ceruloplasmin levels of children with acute infections of malaria were considerably reduced because the enzyme was expended to stabilize the severe oxidative stress (Narsaria *et al.*, 2012).

2.2.3.2. Metallothioneins

Metallothioneins act as free radical scavengers, remove and isolate excess metal ions present in the cytosol and thereby maintain copper homeostasis (Maarman, 2020). Metallothioneins are expressed in neuronal, cardiac, renal, epithelial, erythrocytic and monocytic tissue (Sullivan, Burnett and Cousins, 1998; Ryvolova *et al.*, 2011). In patients with Wilson's disease, the excess copper accumulates in the tissues and the expression of these enzymes is increased to decrease copper associated toxicity. Copper has a high affinity and binds tightly to this enzyme ($K_{Cu1} = 2 \times 10^{16}\ M^{-1}$). Consequently, dietary copper is bound to enterocytes and is not present in the blood (Banci *et al.*, 2007; Krężel and Maret, 2017; Hedera, 2019).

2.2.3.3. Human copper transporter receptor-1

hCtr1 is a transmembrane protein that allows for copper to enter the cells and is the primary mediator of copper uptake (Prohaska *et al.*, 1990; La Fontaine and Mercer, 2007; Scheiber, Mercer and Dringen, 2010). hCtr1 is expressed in all tissues and organs with a very high affinity for copper ($K_{Cu1} = 4.0 \times 10^{-19}\ M$) (Peña, Lee and Thiele, 1999).

2.3. Copper toxicity and treatments

Copper excess leads to the presence of free copper ions in intracellular and extracellular sites of neurological, hepatic, retinal and renal tissue. These free copper ions have a highly susceptible redox activity leading to the production of ROS, such as hydroxyl ions (Bertinato and L'Abbé, 2004; Crisponi *et al.*, 2010; Scheiber, Mercer and Dringen, 2010; Joshi *et al.*, 2019). This causes oxidative damage to extracellular membranes. In the hepatocytes, high copper excretion increases intracellular calcium concentration, leading to the initiation of catalytic enzymes responsible for tissue breakdown such as phospholipases, proteases and endonucleases (Crisponi *et al.*, 2010). The organ that endures the most damage from copper excess is the liver since it is the primary organ of copper homeostasis (Bertinato and L'Abbé, 2004; De Romaña *et al.*, 2011; Kardos *et al.*, 2018). The presence of excess copper causes the displacement of transition metal cofactors from innate binding sites. For example, to carry out hormonal signal transduction, zinc binds the deoxyribonucleic acid (DNA) domain of the oestrogen receptor. When the free copper ion concentration increases, the zinc is replaced and hormonal signal transduction is changed (Peña, Lee and Thiele, 1999; Tapiero, Townsend and Tew, 2003). Copper toxicity also leads to the inhibition of various proteins function, including: lactate dehydrogenase, glutathione S-transferase and poly-ADP-ribose polymerase (Scheiber, Mercer and Dringen, 2010).

It is apparent that copper is essential for numerous metabolic functions but needs to be carefully monitored and controlled to maintain a safe copper homeostasis.

2.3.1. Disorders of copper homeostasis

A discrepancy of copper in the brain can enhance the pathogenesis of several diseases such as, Wilson's disease, aceruloplasminemia, Alzheimer's disease and Parkinson's disease (Desai and Kaler, 2008).

2.3.1.1. Wilson's disease

Wilson's disease is caused by a mutation in the gene encoding the ATP7B copper translocation protein found in hepatocytes (Lang *et al.*, 2007; Kardos *et al.*, 2018; Niederau, 2018). Symptoms of Wilson's disease include depression, anxiety, tremor, jaundice and liver cirrhosis, which are difficult to distinguish from other hepatic and neurological diseases (Ala *et al.*, 2007; Dienes and Schirmacher, 2019; Litwin, Dusek and Członkowska, 2019). Zinc salts are given to prevent the uptake of copper by the small intestine (Niederau, 2018). D-Penicillamine and trientine (TET) are chelators that bind to copper in the bloodstream and the chelates are excreted into urine (Ferenci, 2019; Roberts, 2019). The management of Wilson's disease is currently approved for only these two chelators and they have been used as the standard treatment for decades (Ferenci, 2019; Roberts, 2019). Copper chelators and zinc salts are used in combination, which has an additive effect in preventing symptoms (Houwen, 2019). Untreated Wilson's disease leads to liver cirrhosis and eventually liver failure, thereafter a liver transplant is needed to manage the disease (Ala *et al.*, 2007; Niederau, 2018).

2.3.1.2. Aceruloplasminemia

Aceruloplasminemia is an inherited autosomal recessive disease characterised by the deficiency of the protein ceruloplasmin in serum, and is often misdiagnosed as Wilson's disease as patients with this disorder also presents with low serum ceruloplasmin (Harris, Klomp and Gitlin, 1998; Nittis and Gitlin, 2002; Ondrejkovičová *et al.*, 2020). Ceruloplasmin contains most of the copper present in human serum. This cuproprotein is important in the homeostasis of iron and an absence of this protein leads to a toxic accumulation of iron in neurons, specifically in the retina and basal ganglia (Harris, Klomp and Gitlin, 1998; Nittis and Gitlin, 2002). A lack of this enzyme causes an accumulation of iron in the liver, a decrease in the transport of copper and iron and the production of reactive oxygen species (Brewer, 2003). The disease presents with progressive neurodegeneration causing dystonia, dysarthria and dementia and patients suffering from aceruloplasminemia often exhibit Parkinson-type symptoms (Manto, 2014). The resultant iron accumulation is treated with desferrioxamine, a ferric ion chelator; however the disease is often fatal (Harris, Klomp and Gitlin, 1998; Nittis and Gitlin, 2002; Miyake *et al.*, 2020).

2.3.1.3. Alzheimer's disease

The transmembrane protein, amyloid precursor protein (APP) contains metal ion binding domains, mainly copper and zinc. It reduces copper (II) to copper (I) and forms toxic complexes with copper (I) that in turn produces reactive oxygen species (Strausak *et al.*, 2001; Kepp and Squitti, 2019). As the brain ages, proteolytic cleavage of APP becomes less efficient leading to formation of Aβ peptide (Donnelly, Xiao and Wedd, 2007). Copper is reported to react with the Aβ peptides to form reactive oxygen species. Alzheimer's disease is proposed to be caused by the aggregation of neurotoxic Aβ peptide (Strausak *et al.*, 2001; Donnelly, Xiao and Wedd, 2007; Desai and Kaler, 2008). This disease is the predominate form of dementia presenting with progressive cognitive and memory abnormalities (Donnelly, Xiao and Wedd, 2007; Desai and Kaler, 2008; Rivera-Mancía *et al.*, 2010)**.** Alzheimer's disease characteristically presents with normal serum copper and increased copper concentration in the cerebrospinal fluid. This increase in copper ions may cause oxidative damage and increase the neurodegeneration seen in the disease (Desai and Kaler, 2008; Wang *et al.*, 2020). The APP forms toxic complexes with free copper ions that produces reactive oxygen species by reducing hydrogen peroxide to form hydroxyl radicals, that in turn destroy neuronal tissue via the process of lipid peroxidation (Strausak *et al.*, 2001; Wang *et al.*, 2020). The Aβ peptide is formed through the cleavage of the APP by β- and γ-secretase enzymes and with age this cleavage becomes increasingly ineffective. This causes the malformation and aggregation of the Aβ peptide (Donnelly, Xiao and Wedd, 2007; Wang *et al.*, 2020). The aggregation process of Aβ peptides leads to the formation of senile plaques which have been found to contain a large concentration of transition metal ions which are proposed to be inducers of the pathogenesis of Alzheimer's disease (Strausak *et al.*, 2001; Donnelly, Xiao and Wedd, 2007; Rivera-Mancía *et al.*, 2010; Asili *et al.*, 2019). The excess concentration of copper is believed to react with the Aβ peptides to form reactive oxygen species. Metalloenzymes, such as glutathione, are utilized as a protective mechanism against toxicity by binding excess copper. However, these enzymes are soon depleted and oxidative damage occurs (Strausak *et al.*, 2001; Braidy *et al.*, 2019). This induces the production of more Aβ amyloid and the consequential production of neurological pathogenesis, including neurofibrillary fibres and senile plaques (Strausak *et al.*, 2001; Donnelly, Xiao and Wedd, 2007; Desai and Kaler, 2008).

2.3.1.4. Parkinson's disease

Parkinson's disease is a widespread, neurodegenerative motor affliction, with symptoms including musculoskeletal stiffness, tremors, bradykinesia and postural unsteadiness (Desai and Kaler, 2008). Lewy bodies are protein aggregates of the α-synuclein protein and accumulator plaque analogous to that of the senile plaques found in Alzheimer's disease

(Desai and Kaler, 2008; Mezzaroba *et al.*, 2019; Falcone *et al.*, 2020). It is believed that excess cerebral copper contributes to the formation of aggregates by inducing oxidative damage to the α-synuclein protein, which consequently causes dopaminergic neuronal cell death and leads to the development of Parkinson's disease (Donnelly, Xiao and Wedd, 2007; Desai and Kaler, 2008; Rivera-Mancía *et al.*, 2010; Mezzaroba *et al.*, 2019)**.** The concentration of serum copper ions is decreased in Parkinson's disease patients, however it is increased in the cerebrospinal fluid, which may lead to oxidative reactions and the potentiation of inflammation (Boll *et al.*, 2008; Manto, 2014).

It is therefore important to find novel compounds that can be used in the management of diseases associated with copper homeostasis. The test compounds in this study have shown both chelating and reducing actions against metal ions and have been examined to determine whether they are effective in decreasing the accumulation copper and redox activity of copper.

2.3.2. Chelators used to treat copper excess

Copper toxicity disorders such as Wilson's disease are normally treated with standard copper chelating agents, such as D-penicillamine and TET and inhibitors of copper absorption, including Zinc (Table 2.3) (Brewer, 2017).

2.3.2.1. Zinc

Zinc prevents the absorption of copper from dietary sources by binding to the metallothionein in the intestinal cell. The attachment of the zinc occupies the metallothionein receptors, thereby preventing any interactions with other transition metal ions (Houwen, 2019). Zinc stimulates the synthesis of metallothionein in the intestinal, hepatic and neuronal cells (Bremner and Beattie, 1990; Houwen, 2019). The tight link between metallothionein and copper prevents its absorption into systemic circulation. This promotes the loss of copper in the faeces as the enterocytes are shed during the normal cell turnover (Brewer, 2002; Lawson *et al.*, 2016). This treatment is well tolerated but may cause gastric irritation which can be resolved by replacing it with zinc acetate. In cases where zinc alone does not manage the copper levels, it can be used in combination with TET (Brewer, 2002; Houwen, 2019).

2.3.2.2. D-Penicillamine

D-Penicillamine contains two methyl groups in its structure and a sulfhydryl group that chelates copper (II) (Figure 2.5A). Two molecules of D-penicillamine bind to one molecule of copper (Figure 2.5B) and mobilize copper by forming copper-penicillamine complexes that are excreted into the urine (Ala *et al.*, 2007; Ferenci, 2019). D-Penicillamine is a metal ion chelator used in the treatment of rheumatoid arthritis, Wilson's disease and cystinuria (Figure 2.5). D-

Penicillamine is a cysteine elimination inhibitor and was discovered as a metabolite of penicillin antibiotics (Kosnett, 2012).

Table 2.3: The chemical and biological properties of copper chelators (Ding, Xie and Kang, 2011).

Copper Chelator		**Solubility/ Permeability**		**Mechanism of Chelation**	**Copper Affinity**
IUPAC Name	**Generic Term**	**Solubility**	**Membrane Permeable**	**Donor Groups**	**Stability constant K[a]**
3-Mervapto-D-valline	D-penicillamine	Water	Yes	NH_2, SH, COOH	7.1 for Cu^{2+}
Triethylenetetramine	TET	Lipid	Yes	Four NH_2	20.4 for Cu^{2+}
Bis-(sulfanylidene) molybdenum sulfanide	Tetrathiomolybdate	Water	No	Mo & S	8.0 for Cu^{2+}
2,9-Dimethyl-1,10-phenanthroline	Neocuproine	Lipid	Yes	2.2'-bipyridine & 1,10-phenanthroline	19.1 for Cu^{1+}
Ethylenediamine tetra acetic acid	EDTA	Water	Yes	NH_2, COOH	18.8 for Cu^{2+}
5-Chloro-7-iodo-8-OH	Clioquinol	Lipid	Yes	OH, I, Cl, N	8.9 for Cu^{2+}
Bathocupreine disulphonate	BCS	Water	No	2.2'-bipyridine & 1,10-phenanthroline	6.1 for Cu^{1+} & 19.8 for Cu^{1+}
2,9-Dimethyl-4,7-diphenyl-1,10-Phenanthroline	Bathocupreine	Lipid	Yes	2.2'-bipyridine & 1,10-phenanthroline	N/A
Diethylcarbamodithioic acid	DDC	Lipid	Yes	S, SH	14.9 for Cu^{2+}
N, N,N′,N′-tetrakis (2-pyridylmethyl)	TPEN	Lipid	Yes	4 heterocyclic nitrogen, 2 NH_2	20.5 for Cu^{2+}
Triethylenetetramine	TETA	Lipid	Yes	Cyclam & cyclone	>27 for Cu

In Wilson's disease, it enhances the urinary excretion of copper (II) by binding to and reducing it to copper (I). This drug is also useful in other heavy metal related toxicities as it can bind to lead, mercury, iron and cysteine, before being excreted into the urine (Brewer, 2003; Kosnett, 2012). Once the copper concentration decreases, the hepatic and neurological function increases and as an inhibitor of cysteine excretion it prevents cystinuria.

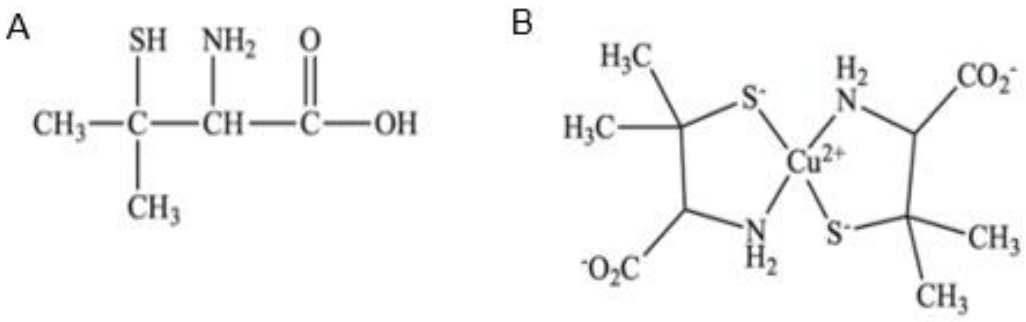

Figure 2.5: The chemical structure of D-penicillamine (A) and the copper-penicillamine complex (B) (Katerji *et al.*, 2017).

D-Penicillamine acts as an immunosuppressant by decreasing the number of T-lymphocytes, macrophages and interleukin-1 in severe rheumatoid arthritis (Ala *et al.*, 2007; Ferenci, 2019). D-Penicillamine also stimulates the synthesis of metallothionein which in turn chelates copper endogenously (Ala *et al.*, 2007; Ferenci, 2019). Thus, D-penicillamine facilitates the increased excretion of excess copper and removes excess extracellular copper by increasing the concentration of metallothionein (Ala *et al.*, 2007; Lawson *et al.*, 2016; Ferenci, 2019).

The oral bioavailability of D-penicillamine is approximately 70% and is excreted in the urine, along with copper, as a disulphide product (Figure 2.5). D-Penicillamine should be taken on an empty stomach to enhance its absorption (Ala *et al.*, 2007; Niederau, 2018) . The time taken to accomplish improvement of hepatic Wilson's disease symptoms is between approximately two to twelve months (Medici, Rossaro and Sturniolo, 2007).

D-Penicillamine has however been shown to worsen the neuropathy associated with Wilson's disease by inducing a pyridoxine (vitamin B_6) and iron deficiency (Brewer, 2003; Kosnett, 2012). To prevent these adverse effects, a daily dose of 25 mg pyridoxine is recommended (Medici, Rossaro and Sturniolo, 2007). Many patients reported to experience a transient hypersensitive reaction in the first month of treatment with fever, rash and/or lymphadenopathy being reported. This reaction can be corrected by temporarily withdrawing the drug and administering a corticosteroid may be recommended (Ala *et al.*, 2007). Long term side effects of this drug include: skin degeneration, joint arthropathy, immunological effects (lupus reactions, nephritic syndrome, myasthenia gravis, and good pasture syndrome), aplastic anaemia, neutropenia and thrombocytopaenia (Medici, Rossaro and Sturniolo, 2007; Lawson *et al.*, 2016; Ferenci, 2019).

D-Penicillamine may inhibit the cupric enzymes, thereby inducing side-effects such as skin lesions (Atzori *et al.*, 2011). D-Penicillamine increases the permeability of the blood brain barrier in Wilson's patients and thereby copper ions effectively cross through the barrier (Chen *et al.*, 2012). To prevent the possibility of adverse effects, routine monitoring of urinary protein content and blood count is advised (Brewer, 2003; Ferenci, 2019). This form of treatment is highly recommended for patients suffering mainly from hepatic symptoms and has been shown to improve the hepatic function of these patients. In 20 to 50% of those patients presenting with mainly neurological symptoms, the symptoms have worsened as a result of D-penicillamine treatment (Brewer, 2003; Ferenci, 2019).

2.3.2.3. Trientine dihydrochloride

Trientine dihydrochloride (triethylenetetramine; Figure 2.6A) is indicated for patients with Wilson's disease who show intolerance to D-penicillamine (Lawson *et al.*, 2016). Its mechanism of action is comparable to D-penicillamine, as it binds to excess copper (II) and increases its urinary excretion (Lawson *et al.*, 2016). It does not however have the same toxicity profile as D-penicillamine, with fewer side effects being experienced due to its lack of sulfhydryl groups. Adverse effects do however include anaemia (Byrns and Penning, 2011; Lawson *et al.*, 2016). TET forms a toxic complex with iron and is therefore not recommended that an iron supplement be taken with TET (Roberts and Schilsky, 2008; Crisponi *et al.*, 2010).

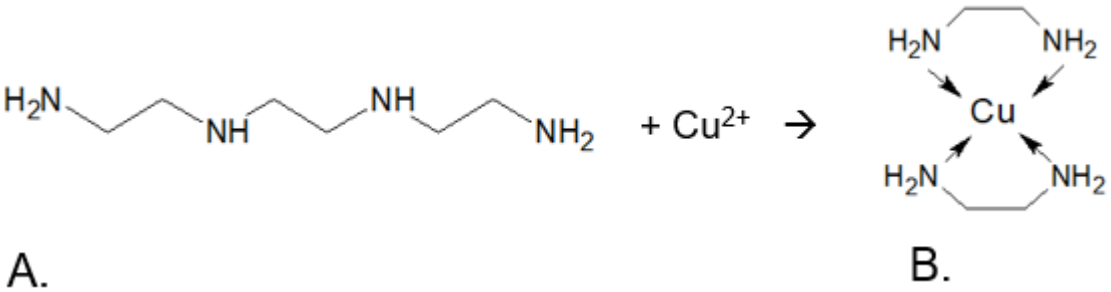

Figure 2.6: The chemical structure of TET (A) and the copper chelation complex of TET (B) (Yu *et al.*, 2010).

TET chelates copper (II) by forming a stable complex with the nitrogen atoms that are present within its structure (Figure 2.6B) (Roberts and Schilsky, 2008). TET is poorly absorbed from the gastrointestinal tract (GIT) and this is compensated for by increasing the prescribed dose. However, some studies have suggested that the large presence of unabsorbed TET in the GIT prevents the further absorption of copper (Crisponi *et al.*, 2010). The starting dose is generally 750 to 1000 mg, 2 to 3 times daily. This treatment should be taken before meals or 2 hours after a meal. No hypersensitivity reactions have been reported at the beginning of

treatment (Roberts and Schilsky, 2008). However, hypersensitivity reactions can occur in the later stages of treatment and these include, lupus-like syndrome, proteinuria and/or moderate sideroblastic anaemia. There is a 26% risk to worsening the neurological syndrome seen in Wilson's disease (Roberts and Schilsky, 2008).

2.3.2.4. Combination Therapy

D-Penicillamine and zinc are not recommended for combination therapy as D-penicillamine will chelate the zinc and be renally excreted (Roberts and Schilsky, 2008). However, initial treatment with a low dose D-penicillamine, high dose zinc sulphate followed with maintenance therapy of zinc sulphate alone, was found to improve the symptoms of Wilson's disease (Chang *et al.*, 2013). TET and zinc have been found to work well together in less serious cases of the Wilson's disease, where they are taken together for a 6-week period and then zinc is used as a daily maintenance therapy (Roberts and Schilsky, 2008). This form of treatment has a low patient compliance because the medications cannot be taken concurrently and each medication must be taken 3 times a day (Roberts and Schilsky, 2008).

2.3.2.5. Tetrathiomolybdate

Tetrathiomolybdate (TMB) is not yet considered as a standard treatment, however it has shown promise in the chelation of copper for the treatment of Wilson's disease (Figure 2.7). It has a twofold effect against copper toxicity, whereby it prevents nutritional absorption of copper (I) (when given with food) and forms chelates with the existing copper (II) sources (when given without food) (Brewer, 2003; Rupp and Weiss, 2019). It does so by binding to both copper (II) and albumin to form a complex of three molecules. Therefore, copper becomes inaccessible for absorption and is excreted from the body (Brewer, 2003; Rupp and Weiss, 2019). TMB was effective in preventing further progression of the neurotoxicity associated with Wilson's disease and did not display the same penchant as TET to worsen neurological symptoms believed to be caused by excess copper accumulation in the basal ganglia (Brewer *et al.*, 2009; Rupp and Weiss, 2019).

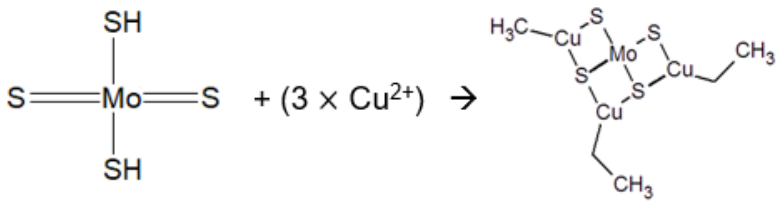

A. B.

Figure 2.7: The chemical structure of TMB (A) and TMB -copper complex (B) (Kodama, Fujisawa and Bhadhprasit, 2012)**.**

Its side effects are less severe than that of D-penicillamine and TET and are generally associated with bone marrow toxicity (anaemia, thrombocytopaenia, and neutropenia) and an increase in transaminase enzymes. All of these side effects were transient and normalised following suspension of the drug (Ferenci, 2004). An open label study was conducted to determine whether TMB prevented the augmentation of the neurological symptoms found in Wilson's disease patients. A follow up, double blind study compared the effect of TET and TMB on Wilson's disease patients with neurological symptoms (Brewer *et al.*, 2009; Brewer, 2015). TMB prevented the neurological deterioration in 53 patients, while it caused it in two patients. The neurological symptoms of 4% of TMB patients deteriorated in comparison to 26% of TET patients (Brewer *et al.*, 2009). Patients showed a marked improvement in clinical symptoms associated with Wilsons disease when treated with TMB in a phase 2 clinical trial (Weiss *et al.*, 2017). D-Penicillamine and TET have a higher incidence of neurological symptoms decline because they release free copper from hepatic storage sites, into the bloodstream leading to an increase in serum copper concentration symptoms (Brewer *et al.*, 2009; Weiss *et al.*, 2017). TMB controls free copper levels in the early stages of treatment by lowering the levels quickly and significantly, thereby preventing the development of acute neurological symptoms (Brewer *et al.*, 2009; Rupp and Weiss, 2019).

The effectiveness of TMB indicates that the discovery of new chelating compounds with fewer side effects would be beneficial in the treatment of copper toxicity related diseases. Compounds that have been shown to effectively bind to copper are the 8-OHs and several EOCs and warrant further investigation.

2.3.2.6. Chelators used in pathologies with metal ion excess

Copper excess has shown itself to be problematic within the human body as is the excess of any metal ion. Therefore chelation therapy such desferrioxamine for excesses of common metal ions such as iron, lead, mercury or arsenic is necessary (South African Department of Health, 2020).

2.3.2.7. Malaria treatment in South Africa

The first-line treatment for malaria in South Africa is artemether/lumefantrine 20/120 mg (South African Department of Health, 2020). The possible mechanism of actions for artemether, a derivative of artemisinin, include free radical production through endoperoxide interaction with parasitic iron-haem which results in a build-up of toxic molecules within the parasite, inhibition of parasitic transport proteins and inhibition of plasmodial mitochondrial processes (Stover, Travis King and Robinson, 2012; Gandhi and Elshaboury, 2020).

Lumefantrine is a schizonticide which is believed to inhibit haemozoin formation causing a toxic build-up within the parasite, similar to that of chloroquine (Stover, Travis King and Robinson, 2012). The dual mechanism of action of this combination give rise to an early decrease in parasitaemia clearance by artemether and the subsequent elimination of the residual parasites by lumefantrine (Gandhi and Elshaboury, 2020). Compounds that inhibit the formation of β-haematin and thereby prevent detoxification processes within the parasite have been shown to be effective in the management of malaria and it would be advantageous to find novel compounds with this ability.

2.4. Antimicrobial infections and copper homeostasis

2.4.1. Malaria and Copper

Both copper and iron are essential in the metabolism of protozoa such as *Plasmodium falciparum* and *P. vivax* (Baloch *et al.*, 2011; Khan, Kaushik and Singh, 2019; Parkinson *et al.*, 2019). Atomic absorption spectrometry determined that there was a significant increase in serum copper concentration of individuals infected with *P. vivax* malaria (2.26 ± 0.203 ppm) in comparison to uninfected individuals (2.07 ± 0.126 ppm). In contrast, iron, magnesium and zinc decreased in concentration in infected patients compared to uninfected individuals (Baloch *et al.*, 2011). The increased copper levels were also seen in cases of *P. falciparum* cerebral malaria (Baloch, 2012). A comparative study of children with acute (serum copper: 212.1-301.8 µg/mL) and uncomplicated (serum copper: 196.1-277.3 µg/mL) infections of *P. falciparum* with uninfected (serum copper: 162.4-224.2 µg/mL) children showed that the infected patients had significantly higher levels of serum copper and decreased levels of zinc (Saad *et al.*, 2013). An excess of extracellular copper increases the production of free radicals and the degree of resultant damage to the phospholipid membranes within the host.

A deficiency in these metal ions within the parasite will most likely result in cell death due to the interruption of anabolic and catabolic processes, which could be advantageous when trying to eliminate an infection that relies on copper for its rapid replication (Rasoloson *et al.*, 2004). Compounds that can cause a deficiency in this protozoal parasite are needed to aide in the campaign against this pathogen. The selective copper (I) chelator, neocuproine has been shown to inhibit the *in vitro* growth and metabolism of *Plasmodium falciparum* during the transition from ring to trophozoite stage (Rasoloson *et al.*, 2004). Thus, indicating the sensitivity of the parasite to changes in its own copper homeostasis and could be a potential drug target.

2.4.2. Copper-dependent enzymes, copper absorption, distribution, excretion, and homeostasis in the *Plasmodium falciparum*

P-type ATPase copper proteins similar to human and yeast ATP7A and ATP7B, as well as a copper transport protein similar to Ctr1, have been identified in *P. falciparum* (Choveaux, Przyborski and Goldring, 2012; Kenthirapalan *et al.*, 2014). These enzymes and proteins functioned in stabilizing the reduced form of copper, transporting copper, and utilizing copper in metabolic functions. Therefore these proteins and enzymes that act in a similar manner to those present in mammalian cells are responsible for the copper metabolism of the parasite (Choveaux, Przyborski and Goldring, 2012). The malaria parasite ingests host erythrocytic Cu/Zn superoxide dismutase and incorporates this enzyme into its own metabolic pathways, where it serves the same function as it did in the human host (Choveaux, Przyborski and Goldring, 2012). The existence of these proteins and enzymes within the parasite and the utilization of the infected erythrocyte copper imply that *P. falciparum* uses copper in its metabolism (Kenthirapalan *et al.*, 2014). The removal of plasmodial ATPase resulted in the inhibition of the parasite sexual stage and the inability of the malaria vector to infect a mouse model host. However, the absence of plasmodial ATPase had no effect on the asexual life cycle of the malaria parasite (Kenthirapalan *et al.*, 2014). The restriction and removal of copper from the parasite could therefore be a potential target to induce parasitic cell death.

2.4.2.1. Mitochondrial electron transport chain proteins

The parasitic mitochondrial translation DNA codes for 3 protein subunits (cytochrome b oxidase and cytochrome c oxidase subunits I and III) and are dependent on copper ions for function (Ling *et al.*, 2020). These proteins are integral in the parasitic mitochondrial protein translation process and were identified as targets for antimalarials such as atovaquone (Ling *et al.*, 2020). Metal ion binding could disrupt the important processes that these proteins are responsible for and inhibit the malaria parasite.

2.4.2.2. Aldolase

Aldolase functions as a copper binding enzyme and is believed to aid in the infiltration of erythrocytes (Kim *et al.*, 1998; Yeh and Altman, 2006; Diaz *et al.*, 2014). When inhibited with antisense oligonucleotides within the *P. falciparum* parasite, the stage development of the parasite is decreased (Kim *et al.*, 1998; Yeh and Altman, 2006). Thus, the inhibition of this enzyme through copper restriction may lead to parasitic death.

2.4.2.3. Superoxide dismutase

In *P. falciparum,* superoxide dismutase is proposed to inhibit the formation of toxic reactive oxygen species during haemoglobin degradation and copper binding is important in this

process (Rasoloson *et al.*, 2004; Boucher *et al.*, 2006). Targeting this enzyme with chalcones and piperazine derivatives resulted in the decreased stage development of the malaria parasite (Yeh and Altman, 2006). Chelation of copper ions and thereby the inhibition of copper binding could lead to the dysfunction of this enzyme.

2.4.2.4. Adenosine triphosphatase

The *P. falciparum* ATPase efflux enzyme is located in the parasite plasma membrane and the membrane surface of the host red blood cell during the trophozoite and schizont stages of the parasites asexual cycle (Choveaux, Przyborski and Goldring, 2012; Kenthirapalan *et al.*, 2014). The presence of this ATPase on the host cell suggests that the copper used in parasitic metabolism is obtained from the host erythrocyte (Choveaux, Przyborski and Goldring, 2012). Chemotherapeutic targeting of these enzymes could result in copper overload within the parasite and parasitic cell death.

2.4.3. Copper-containing proteins in *Plasmodium falciparum*

P. falciparum CTR1 protein has been reported to be relocated from the host erythrocytic membrane following invasion by the parasite, to be included in the parasitic membrane where it transports the host's erythrocytic copper. This membrane bound protein reduces copper (II) to copper (I) for transport. The *P. falciparum* copper transporter was reported to have a similar genetic sequence to the mammalian CTR1 (Choveaux, Przyborski and Goldring, 2012; Kenthirapalan *et al.*, 2014). Metallothionein motifs were also identified. In the presence of excess copper, the expression of these proteins increased and proceeded to bind to the copper in order to remove it from extracellular sites (Choveaux, Przyborski and Goldring, 2012).

Due to growing resistance to malaria treatments, new therapeutic targets are needed. The copper ion is essential for *P. falciparum* growth and homeostasis that could be beneficial when seeking new chemotherapeutic drug targets.

2.4.4. The malaria burden

Malaria is an infectious protozoal disease transmitted by an infected female *Anopheles* mosquito into the bloodstream of a human host (WHO, 2019). There are approximately 155 million cases of malaria each year resulting in approximately 260 000 deaths worldwide, each year. These deaths (93%) mostly occur in Africa and are frequently pregnant women and children under the age of five (WHO, 2019). A global fund of approximately 2.7 billion dollars a year is set aside to combat and control malaria (WHO, 2019). There are five species of malaria parasite: *P. vivax*, *P. ovale*, *P. malariae*, *P. knowlesi* and *P. falciparum,* with the latter

being the most common in South Africa and the most pathogenic and deadliest (Warrell *et al.*, 2010; Govender, 2019; WHO, 2019). *P. falciparum* mostly occurs in Africa and can be fatal within hours. Factors which now potentiate the burden of this disease and increase the risk of death, is the development of resistance not only in the vector, but also in the parasite (WHO, 2019). Artemisinin resistance has emerged in South-East Asia and molecular markers of resistance, such as *P. falciparum kelch 13* and *P. falciparum plasmepsin 2* gene augmentation have been detected (Ringwald, 2014; Kakolwa *et al.*, 2018). The *Anopheles* mosquito has developed resistance to synthetic insecticides used to control their breeding and the parasite has developed resistance to standard treatments (Table 2.4) (Tikar *et al.*, 2011; Venter *et al.*, 2017; Wiebe *et al.*, 2017; Yunta *et al.*, 2019).

2.4.5. Malaria parasite life cycle

The malaria parasite life cycle consists of several stages including the liver stage, the blood stage, and the mosquito stage (Figure 2.8).

2.4.5.1. Liver stage (Exo-erythrocytic cycle)

The female *Anopholes* mosquito introduces sporozoite parasites into the human bloodstream when having a blood meal (Brooks *et al.*, 2013). These sporozoites invade hepatocytes where they mature from the ring to trophozoite to schizont stage over a 24 to 72-hour period (Figure 2.8). Following 24 to 72 hours after entering the cell, they rupture to free the daughter merozoites from the hepatocyte (Brooks *et al.*, 2013). In the *P. ovale* and *P. vivax* species, latent hypnozoites can linger in the liver for months and years before causing a relapse and re-infecting erythrocytes. Once merozoites are released from hepatocytes, they enter the blood (Brooks *et al.*, 2013).

2.4.5.2. The blood or asexual stage or intra-erythrocytic cycle

This stage is the cause of the clinical symptoms experienced by a malaria-infected patient. In the asexual stage, the merozoites infect the RBCs and mature from rings to trophozoites to schizonts which rupture the RBCs to release 16 to 32 daughter merozoites (Brooks *et al.*, 2013). The lysed RBC also release toxins which cause the clinical symptoms of malaria, namely high fever, cold chills, sweating, joint and muscle pains and headaches) (WHO, 2019). In the sexual stage, select merozoites differentiate into sexual gametocytes, namely microgametocyte (male) and macrogametocytes (female), which are ingested during the *Anopheles* mosquito next blood meal, ensuring the continuation of the life cycle of the malaria parasite (Figure 2.8) (Brooks *et al.*, 2013).

Table 2.4: The developing resistance to antimalarials in reference to region (Wongsrichanalai *et al.*, 2002; Ringwald, 2014, 2016; NDoH South Africa, 2018; WHO, 2019).

Antimalarial	Region/s where resistance has developed	Year of first reported resistance
Atovaquone/ Proguanil	Parts of South East Asia & parts of Central Africa	1996/ 1949
Chloroquine	Asia, South America, Pacific Ocean islands, Australia & Africa (including South Africa)	1957
Mefloquine	South-East Asia & Parts of Africa & South America	1982
Quinine	Asia, North & South America, Pacific Ocean islands, Australia & Africa	1910
Sulfadoxine-pyrimethamine	South-East Asia, Parts of South America, East & Central Africa	1967
Artemisinin • **Dihydroartemisinin (DHA)-** • **Primaquine*** • **Artemether-Lumefantrine** • **Artesunate-Mefloquine**	Cambodia, Myanmar, and Thailand	2001 (Year theorised resistance emerged, detected in 2006).
	Laos	2013
	Vietnam	2009

* Tests conducted confirmed that this combination is an effective treatment in resistant areas (>95%) despite resistance (high parasite load) shown in first days of treatment (Ringwald, 2016; WHO, 2019).

2.4.5.3. Mosquito stage (sporogony cycle)

Following ingestion into the gut of the mosquito, the microgametocytes fuse with the macrogametocytes to form zygotes that become motile and elongate into ookinetes (Figure 2.8). These invade the midgut wall and mature into oocytes which differentiate into sporozoites (Brooks *et al.*, 2013; WHO, 2019). The latter then travel to the salivary glands of the mosquito and during the next blood meal, the sporozoites are injected into a human host (Brooks *et al.*, 2013).

2.4.6. The diagnosis and treatments of malaria

It is essential that malaria infection be identified accurately to ensure early treatment which could reduce the severity of the disease and potential mortality (Blumberg, 2015; WHO, 2019; DoHRSA, 2020).

2.4.6.1. Diagnosis

The diverse species of malaria can be differentiated by the appearance of their gametocytes, trophozoites, schizonts and the structure of the erythrocytes that they have infected (WHO, 2019). A blood smear observed under a microscope can conclude whether a patient is infected and the species of malaria parasite.

The cheapest and most rapid diagnostic tools consist of antigen-based rapid diagnostic tests (Murray, 2009; WHO, 2019). These immuno-chromatographic tests function by placing a blood sample within the test “cassette” where the dye-labelled antibody attaches to the parasitic antigen target and a positive test results in a the formation of a coloured band (Murray, 2009; WHO, 2019).

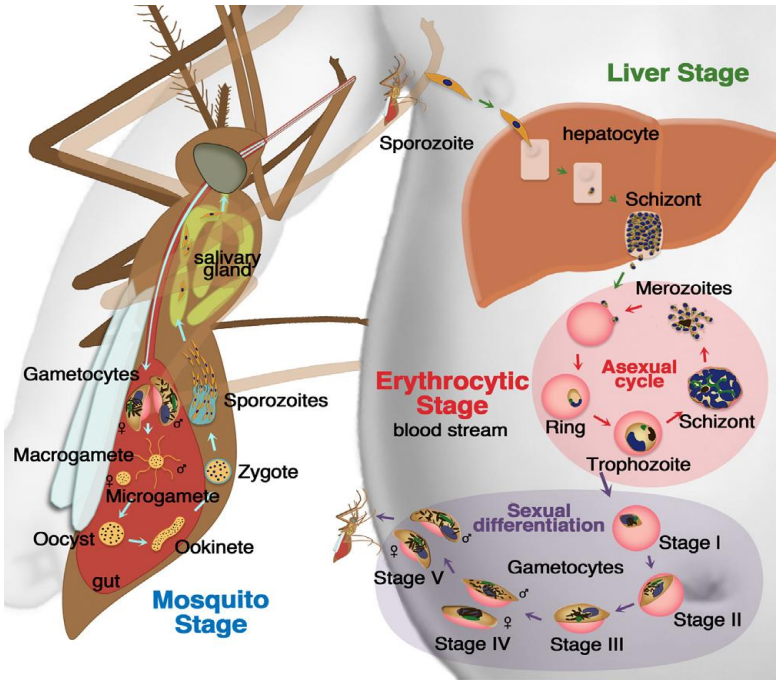

Figure 2.8: The malaria parasite life-cycle within the human host (Biamonte, Wanner and Le Roch, 2013).

2.4.6.2. The management of malaria infection

Monotherapy in the treatment of malaria (not including prophylactic treatment) is no longer possible due to the continued increase in development of resistance by malaria, namely *P. falciparum* (Phan Trong Giao *et al.*, 2001; WHO, 2019). Therefore, most treatments are used in combination of two or more antimalarial compounds.

2.4.6.2.1. Prophylaxis

To avoid the infection and transmission of malaria, certain steps such as chemotherapeutic prophylaxis and preventative strategies need to be taken (Table 2.5).

Table 2.5: The chemotherapeutic and preventative prophylaxis of malaria (Bloland, 2001; Schwartz, 2012; Blumberg, 2015; Rosenthal, 2015; Van Zyl, 2016; WHO, 2019; DoHRSA, 2020).

Prophylaxis	Parasite species	Mechanism of action	Side effects	Notable information
Mefloquine	*P. falciparum* and *P. vivax*	Schizonticidal in RBC phase	Dizziness, headache, rash, nausea & vomiting	Used in endemic regions
Doxycycline	Multi-drug resistant strain *P. falciparum*	Protein synthesis at apicoplast	Photosensitivity, GIT symptoms & candidiasis infection	Antibiotic
Atovaquone	*P. falciparum*	Inhibitor of parasitic pyrimidine synthesis in the schizont stage. Selective inhibition of malaria cytochrome bc_1 complex → disassembling mitochondrial membrane potential.	Rash & GIT symptoms	Used in combination with proguanil
&				
Proguanil				
		Inhibits parasitic dihydrofolate reductase resulting in folate synthesis inhibition	Mouth ulcers, vomiting & diarrhoea	Side effects of the combination: vomiting & elevated hepatic enzymes
Mosquito repellent (Citronella oil, di-ethyl toluamide) and insecticide treated nets used when sleeping				
Gauze screened windows and use of air conditioner/ fan				

2.4.6.2.2. Treatment

There are several antimalarial combinations used around the world with combinations including artemisinin derivatives being the most popular (Table 2.6). The artemisinin derivatives include: artesunate-amodiaquine (used in parts of Africa), artesunate-mefloquine (South-East Asia and South America), dihydroartemisinin-piperaquine (South-East Asia) and

artesunate-sulfadoxine-pyrimethamine (Rosenthal, 2015). The most common artemisinin derivative combination that is used in South Africa and most countries is artemether-lumefantrine (NDoH South Africa, 2018; WHO, 2019).

An increase of 10% in resistance to common malaria vector controls such as pyrethroids, carbamates and organophosphates were reported from 2010 to 2018. Several molecular mechanisms of resistance were reported in the malaria vector including changes to insecticidal enzymatic target sites (WHO, 2019).The continued development of resistance by the malaria parasite to antimalarials in Africa and Asia has demanded the investigation into and development of new classes or combinations of antimalarial agents (WHO, 2019).

Table 2.6: The standard antimalarials used for treatment (Fitch, Kanjananggulpan and Mruk, 1986; Bloland, 2001; Olliaro *et al.*, 2001; Fitch, 2004; Schwartz, 2012; Braga *et al.*, 2015; NDoH South Africa, 2018; Camarda *et al.*, 2019).

Generic name	Parasite strain targeted/ Treatment indication	Mechanism of action/ drug targets	Side effects and/or adverse reactions
Monotherapy			
Chloroquine	*P. vivax*.	Stops ferriprotoporphyrin (FPIX) incorporation to haemozoin → toxic accumulation of FPIX-chloroquine → parasite death	Headache, nausea, vomiting, diarrhoea, retinopathy, seizures, pruritus, abdominal cramps, metallic taste, alopecia, rash, tinnitus.
Primaquine	Prevent relapse of dormant *P. vivax & P. ovale*	Targets the liver stage of malaria by producing high concentrations of H_2O_2	Nausea, abdominal pain & headache. In patients with a glucose-6-phosphate deficiency induces methemoglobinemia& haemolysis
Combination therapy			
Lumefantrine and Artemether	1st line treatment for all species (except in 1st trimester of pregnancy)	Artemether: haem facilitated breakdown of endoperoxide bridge to produce ROS. Lumefantrine: with same mechanism of action as chloroquine; ↓ parasitic metabolism	Artemether: allergic reactions, dizziness, nausea, vomiting & diarrhoea Lumefantrine inhibits cytochrome CYP3A4. Combination: rash & headache
Quinine and Doxycycline/ Clindamycin	*P. falciparum, P. vivax & P. ovale*	Targets intraerythrocytic stages	Well tolerated in combination with quinine & ↓ risk of quinine toxicity. Vomiting, diarrhoea, fever, chills & confusion, nausea, and skin rashes
Artesunate	Severe, complicated *P. falciparum*	Targets blood schizont stage. Artesunate: see artemether.	Hypersensitivity, bradycardia, dizziness, and leukopenia.

Novel agents need to be developed in order to treat disorders caused by imbalances in copper homeostasis. Resistance of the malaria parasite and its vector to standard treatments have become more prevalent; this resistance demands the need for new antimalarial treatments.

2.5. The 8-hydroxyquinoline derivatives

8-OH and its derivatives are a group of heterocyclic compounds mainly used as complex forming agents and has been used for the quantitative determination of metal ions in the chemical, pharmaceutical and cosmetic industry (Jeon, Lee and Lee, 2009). 8-OH is widely used as a topical antiseptic (Merriam-Webster, 2020). Substitution of functional groups to the 8-OH rings results in a diversity of properties (Gershon, Gershon and Clarke, 2003).The chelation ability of these compounds has been investigated as possible treatments against infectious organisms, neurodegenerative diseases, inflammatory diseases and certain cancers (Scheibel and Stanton, 1986; Ding *et al.*, 2006; Wang *et al.*, 2010; Singh *et al.*, 2019).

2.5.1. The chemistry of 8-OH

8-OH with the molecular formula C_9H_7NO, consists of a basic quinoline ring as its central structure (Karpińska, Mazurek and Dobrowolski, 2011). 8-OH was derived from quinoline and its derivatives are formed by the addition of several different functional groups to the quinoline ring (Neldner, 1977). Halogenated 8-OHs are formed by the chemical substitution of the methylene double bond at the 5 and/or 7 positions on the heterocyclic ring with iodine, chlorine, or bromine. The additions/substitutions of functional groups and the tautomeric nature affect the behaviour and properties of the 8-OH derivatives (Neldner, 1977). The unique chemical properties of these compounds also allow for different mechanisms of action incurring its inhibitory activity against numerous diseases with diverse causes.

2.5.2. The metal ion chelation properties of 8-OHs

The 8-OH derivatives contain one or more hydroxyl groups and the divalent cations bind to the dissociated hydroxyl group oxygen anion in an alkaline pH causing chelation (Fraser and Creanor, 1975). 8-OH form chelates with several metal ions including Mn^{2+}, Mg^{2+}, Fe^{3+} and Zn^{2+}. The halogenated derivatives such as clioquinol (5-chloro-7-iodo-8-OH) has shown to possess activity in the management of neurodegenerative diseases, such as Alzheimer's disease by chelating free copper in neurons and preventing the development of β-amyloid plaques in the brain (Ferrada *et al.*, 2007; Adlard *et al.*, 2008; Bareggi and Cornelli, 2012). It has also shown potential in the management of Parkinson's disease, Huntington's disease and Prion disease (Di Vaira *et al.*, 2004; Bareggi and Cornelli, 2012). In addition, antineoplastic activity has been reported against several cell lines including: cervical carcinoma, lymphoma, leukaemia and pancreatic carcinoma (Ding *et al.*, 2006; Choroba *et al.*, 2020). Derivatives of

8-OH have been reported to stimulate the growth of neuronal cells through oxidative signalling which suggests that they possibly promote the healing of neurodegeneration (Haigh *et al.*, 2016). Proteasomes are intracellular protein degraders and regulate protein concentration. This important cellular function is amplified in cancerous cells and thereby the inhibition of proteasomes in the presence of cancer would be an advantageous therapeutic target (Oliveri *et al.*, 2017).

2.5.3. The antimicrobial, antiviral, antifungal and antimalarial properties of 8-OHs

Several 8-OH derivatives have been used clinically as antifungals, antibiotics and amebicides (Jeon, Lee and Lee, 2009). 8-OH possesses activity against several microorganisms, namely *Clostridium difficile*, *C. perfringens* and *Escherichia coli* (Jeon, Lee and Lee, 2009). 8-OH was able to enter cells with bacterial infections without damaging the cell itself and that a metal ion chelate with 8-OH had a higher level of antibacterial activity (Scheibel and Adler, 1981). It can be proposed that 8-OH chelated essential metal ions needed for the function of the microorganisms and that their important metabolic functions were disrupted leading to the inhibition (Jeon, Lee and Lee, 2009). The copper complexing effect of 8-OH resulted in the inhibition of *Mycobacterium tuberculosis* through the augmentation of copper toxicity within the bacteria (Shah *et al.*, 2016). It was also found that 8-OH selectively targeted *M. tuberculosis* within macrophages by operating as a copper ionophore (Shah *et al.*, 2016). The SOD enzymes of *Candia albicans* are dependent on copper for their function (Robinett *et al.*, 2019). Inhibition of SOD5 results in an increase in toxic oxidative stress of *C. albicans* and 5-chloro-7-iodo-8-OH was found to selectively inhibit SOD-5 resulting in a decrease of *C. albicans* pathogenesis (Robinett *et al.*, 2019).

The diverse mechanisms possessed by 8-OH derivatives are useful in the management of several diseases, including those that are infectious, inflammatory-mediated, neurodegenerative, and cancerous.

2.6. Essential oil constituents

EOCs from plants have traditionally been used to aide in the treatment of digestive problems, flu symptoms and difficulty sleeping (Baptista-Silva *et al.*, 2020). They are important components of essential oils whose unique composition will determine their fragrance, biological and medicinal activity (Bakkali *et al.*, 2008). Essential oils serve as a protective entity in plants against herbivores and microorganism infections (Pauli, 2001; Bakkali *et al.*, 2008). The essential oil from the leaves or flowers is obtained from aromatic plants through boiling and/or steaming distillation. They are used as components in products produced by the pharmaceutical, agricultural and cosmetic industries, such as creams, soaps, perfumes, food preservatives and analgesics (Bakkali *et al.*, 2008; Baptista-Silva *et al.*, 2020).

2.6.1. The antioxidant properties of essential oils

It has been shown that EOCs have been shown to possess potent antioxidant activity when in combination to form an essential oil compared to the individual EOCs (Lado *et al.*, 2004). Antioxidants are essential molecules in preventing cellular damage caused by the oxidative reactions of superoxide molecules; where these reactions impair DNA and important cellular components, therefore EOCs could be useful in preventing such reactions (Gülçin, 2011). *Salvia officinalis* contains large concentrations of EOCs, such as α-thujone, β-thujone, camphor, 1,8-cineole, borneol, α-humulene and β-caryophyllene and is reported to be a potent antioxidant with potential activity in cancer patients and to improve memory in the treatment of Alzheimer's disease (Hasanein, Sharifi and Emamjomeh, 2017). Furthermore, the essential oils from lavender and rosemary improved the short term memory in subjects (Filiptsova *et al.*, 2018). EOCs have been shown to influence the immune system through the macrophages and cytokines (Kedzia *et al.*, 1998; Standen, Connellan and Leach, 2006). Immune system modulators have the potential to selectively activate the immune system to fight diseases such as chronic inflammation and certain cancers (Kedzia *et al.*, 1998; Standen, Connellan and Leach, 2006). The antioxidant effects of several essential oils were dependent on dose and on the unique chemical profile of the EOCs of the essential oil mixture (Sacchetti *et al.*, 2005).

2.6.2. The antimicrobial, antimalarial and insecticidal properties of EOCs

Kalemba and Kunicka (2003) reported the variable antimicrobial activity of numerous essential oils against several microorganisms. It was also noted that the antimicrobial activity was dependent on the constituents of the essential oil, the concentration of the EOC and the strain of microorganism (Kalemba and Kunicka, 2003). The EOC rich plant, *Salvia officinalis L* has been used in traditional medicines to treat bacterial and fungal infections (Hasanein, Sharifi and Emamjomeh, 2017). EOCs rich in monoterpenes such as eugenol, carvacrol and thymol demonstrated potent antimicrobial activity against *Listeria monocytogenes, Escherichia coli* and *C. albicans* (Chami *et al.*, 2005; Zivanovic, Chi and Draughon, 2005; Stefanakis *et al.*, 2013). The essential oils of several plants that had a high concentration of thymol, limonene and α-pinene all demonstrated inhibition of both chloroquine-sensitive and resistance strains of *P. falciparum in vitro* with thymol being the most potent (Dell'Agli *et al.*, 2012). The authors theorised that the EOC antimalarial activity was due to trophozoite-schizont inhibition. This study also demonstrated that these EOCs have larvicidal and insecticidal activity against *An. gambiae* (Dell'Agli *et al.*, 2012). Thereby further demonstrating that the EOCs may potentially be used in both the treatment of malaria and management of the malaria vector. A number of the constituents have repellent activity against the malaria mosquito *An. stephensi* namely: carvone, ρ-cymene, α-pinene and eucalyptol (Rajkumar and Jebanesan, 2007). Limonene

and α-pinene as components of *Cupressus arizonica* essential oil were larvicidal against mosquitoes, which indicates that they have potential to be used in the control of the malaria vector (Sedaghat *et al.*, 2011). The antioxidant, anti-inflammatory, antimalarial, immune system activation and antimicrobial properties of EOCs' favour further study of the EOCs and structurally related compounds.

2.7. Aim and Objectives

The aim of the study was to determine the interaction of 8-OHs and EOCs with copper and to determine their chemotherapeutic effect in the treatment of malaria and effect on neuroblastoma cells.

Twenty-one 8-OH derivatives and fifty-five EOCs were selected and investigated to determine their pharmacological properties.

The following objectives were investigated to achieve the aim of the project:

2.7.1 Determined whether the test compounds could alter copper homeostasis by chelating or reducing copper.

2.7.2 Determined the *in vitro* chelating ability of the copper active compounds in neuroblastoma (SH-SY5Y) cell lines in the presence of excess levels of copper and thereby possible uses in copper excess diseases.

2.7.3 The antioxidant and pro-oxidant properties were assessed by determining the 2,2-diphenyl-1-picrylhydrazyl (DPPH•) and lipid peroxidation activity of these compounds.

2.7.4 The antimalarial properties of the test compounds were determined *in vitro* against chloroquine-resistant strain of 3D7 *Plasmodium falciparum* using the *Plasmodium* lactate dehydrogenase assay.

2.7.5 The drug interactions between the most active compounds against *P. falciparum* with standard antimalarials were determined using the *Plasmodium* lactate dehydrogenase assay.

2.7.6 The effects of the compounds on malarial β-haemozoin formation and thereby metabolism was determined.

2.7.7 The cytotoxic effects of the compounds on red blood cells and neuroblastoma cell line were determined using tetrazolium and sulphorhodamine B based assays.

2.7.8 The toxicity of the compounds against whole organisms was determined using the *Artemia* assay.

2.7.9 The effect of compounds against the *Anopheles* malaria vector was determined using the larvicidal lethality assay.

2.7.10 The structure-activity relationship of the test compounds was evaluated to determine the pharmacological interactions that existed between the most active compounds and control compounds.

Chapter 3. Methodology

3.1. Compounds, essential oils, and solvents

3.1.1. 8-OH and derivatives

All 4-hydroxyquinoline (4-OH), 2-hydroxyquinoline (2-OH) (Table 3.1) and 8-OH (Table 3.2; Figure 3.1) derivatives were dissolved in dimethyl sulfoxide (DMSO; ≥ 99.0%; Sigma-Aldrich) to prepare a stock solution of 10 mM. Depending on the assay, the stock solution was diluted in DMSO or RPMI-1640 or Dulbecco's modified eagle's media (DMEM) to prepare a starting concentration of 200 µM. Stock solutions were stored at -70°C in microcentrifuge tubes until required and dilutions were freshly prepared for each experiment.

Table 3.1: The molecular structure and chemical properties of 2- and 4-OH derivatives purchased from Sigma-Aldrich (Pubchem, 2020a).

Compounds	Molecular Formula	Molecular Weight (g/mol)
4-OH	C_9H_7NO	145.16
8-Fluoro-4-OH	C_9H_6FNO	168.15
8-Chloro-2-OH	C_9H_6ClNO	179.61

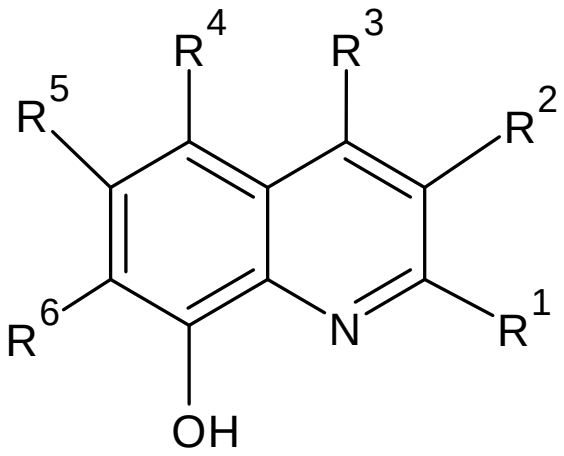

Figure 3.1: The general structure of the 8-OH derivatives, with a hydroxyl group at the 8th position carbon (Pubchem, 2020a).

Table 3.2: The chemical structure and properties (molecular weight (MW) and purity) of the 8-OH derivatives in reference to Figure 3.1 *Calbiochem; $Fluka; #Sigma-Aldrich.

Compound	$-R_1$	$-R_2$	$-R_3$	$-R_4$	$-R_5$	$-R_6$	MW (g/mol)	Purity (%)
5,7-dimethyl-8-OH$	H	H	H	CH_3	H	CH_3	173.21	≥98.0
5-nitro-8-OH#	H	H	H	NO_2	H	H	190.16	96.0
8-OH$	H	H	H	H	H	H	145.16	99.0
5-amino-8-OH#	H	H	H	NH_2	H	H	233.10	95.0
5-chloro-7-bromo-8-OH#	H	H	H	Cl	H	Br	285.50	97.0
5,7-dichloro-8-OH#	H	H	H	Cl	H	Cl	214.05	99.0
2-amino-8-OH$	NH_2	H	H	H	H	H	160.18	98.0
5-chloro-8-OH$	H	H	H	Cl	H	H	179.61	95.0
5-HSO_3-7-iodo-8-OH$	H	H	H	H_2SO_3	H	I	351.12	≥98.5
2-methyl-8-OH$	CH_3	H	H	H	H	H	159.11	98.0
5,7-dichloro-2-methyl-8-OH#	CH_3	H	H	Cl	H	Cl	228.08	95.0
5,7-dibromo-8-OH#	H	H	H	Br	H	Br	302.96	98.0
5-chloro-7-iodo-8-OH$	H	H	H	Cl	H	I	305.50	≥95.0
5,7-diiodo-8-OH#	H	H	H	I	H	I	396.95	97.0
N-butyl-2,2-imino-di-8-OH#	$C_{13}H_{15}N_2O$	H	H	H	H	H	359.45	≥98.0
5-HSO_3-8-OH#	H	H	H	H_2SO_3	H	H	225.22	98.0
2-benzyl-8-OH#	$C_6H_5CH_2$	H	H	H	H	H	258.28	95.0
5-carboxy-8-OH*	H	H	H	COOH	H	H	169.17	≥97.0

3.1.2. The essential oil constituents

The EOCs were stored in their stock form at 4°C and lids were sealed with Parafilm“M”® (Pechiney Plastic Packaging) in sealed plastic containers. All EOCs were diluted in DMSO to a 10 mM working stock (Table 3.3and Table 3.4). Depending on the assay, the stock solution was further diluted in DMSO to prepare a starting concentration of 200 µM. The diluents were freshly prepared before each experiment to avoid evaporation of the volatile constituents.

Table 3.3: The chemical properties of EOCs (Pubchem, 2020a) (*SAFC®; $Fluka;#Sigma-Aldrich; ^Merck).

Compound	MW (g/mol)	Density (g/ml)	Stock Molarity (M)	Compound	MW (g/mol)	Density (g/ml)	Stock Molarity (M)
***Cis*-nerolidol**[$]	222.37	0.88	3.90	**(+)-α-Pinene**[#]	136.23	0.86	6.30
***Trans*-nerolidol**[$]	222.37	0.88	3.93	**(-)-α-Pinene**[$]	136.23	0.86	6.30
***Trans*-geraniol**[$]	154.25	0.88	5.70	**(-)-β-Pinene^**	136.23	0.87	6.40
Cis*-geraniol	154.25	0.88	5.68	**(+)-β-Pinene**[$]	136.23	0.87	6.40
Citral[$]	152.23	0.89	5.83	**(-)-Fenchone**[$]	152.23	0.94	6.21
Geranyl acetate	196.29	0.92	4.67	**(+)-Fenchone**[$]	152.23	0.94	6.21
Farnesol[$]	222.37	0.89	3.98	**(+)-Borneol**[#]	154.25	*	*
(±)-Linalool[$]	154.25	0.87	5.64	**(-)-Borneol**[$]	154.25	*	*
(-)-Linalool**	154.25	0.86	5.59	**(-)-Bornyl acetate**[#]	196.29	0.99	5.02
Linalyl acetate[#]	154.25	0.87	5.64	**(±)-Camphor**[$]	152.23	(solid)	(solid)
(-)-Citronellal[$]	154.25	0.85	5.52	**(1R)-(+)-Camphor**[#]	152.23	(solid)	(solid)
(S)-(-)-β-Citronellol	156.27	0.90	5.47	**(-)-Camphor**[$]	152.23	(solid)	(solid)
(±)-Menthone[$]	154.25	0.90	5.81	**(1R)-(-)-Camphorquinone**[#]	166.22	(solid)	(solid)
(-)-Menthone^	154.25	0.89	5.80	**(±)-Camphorquinone**[#]	166.22	(solid)	(solid)
(±)-Menthol[#]	156.27	0.89	5.70	**(1S)-(+)-Camphorquinone**[$]	166.22	(solid)	(solid)
Carvacrol[#]	150.22	0.98	6.50	**(-)-Caryophyllene oxide**[$]	220.35	(solid)	(solid)
(+)-Carvone[$]	150.22	0.96	6.39	***(+)-Trans*-caryophyllene**[$]	204.35	0.90	4.41
(-)-Carvone^	150.22	0.96	6.39	**(-)-α-Thujone**[$]	152.23	0.91	6.00
(-)-Pulegone**	152.23	0.94	6.15	**(±)-α-β-Thujone**[$]	152.23	0.93	6.08
(+)-Pulegone[$]	152.23	0.94	6.14	**Thymol**[$]	150.22	0.97	6.42
(R)-(+)-Limonene[$]	136.23	0.84	6.18	**2-Thiazoline-2 thiol**[$]	119.21	(solid)	(solid)
(S)-(-)-Limonene[#]	136.23	0.84	6.20	**Artemisia ketone**[$]	152.23	0.87	5.71
(+)-Terpinen-4-ol[$]	154.25	0.93	6.05	**α-Humulene**[$]	204.35	0.89	4.35
(-)-Terpinen-4-ol[$]	154.25	0.93	6.06	**Ocimene**[$]	136.23	0.82	6.00
Eugenol[$]	164.2	1.07	6.50	**(±)-Lavandulol acetate**[$]	196.29	0.91	4.62
1,8-Cineole	154.25	0.92	5.97	**Myrcene**[$]	154.25	0.86	5.59
1,4-Cineole**	154.25	0.89	5.75	**ρ-Cymene**[#]	134.22	0.86	6.41
α-Bisabolol**	222.37	0.92	4.14				

Table 3.4: The molecular structures of EOCs (Pubchem, 2020a).

Compound	Molecular structure	Compound	Molecular structure	Compound	Molecular structure	Compound	Molecular structure
***Cis*-nerolidol**	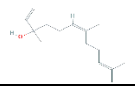	**(±)-Menthol**	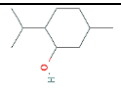	**(+)-α-Pinene**	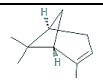	**(1S)-(+)-Camphorquinone**	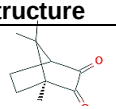
***Trans*-nerolidol**	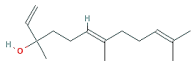	**Carvacrol**	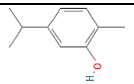	**(-)-α-Pinene**		**(-)-Caryophyllene oxide**	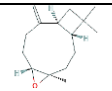
***Trans*-geraniol**	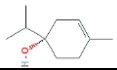	**(+)-Carvone**	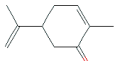	**(-)-β-Pinene**	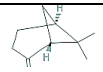	***(+)-Trans*-caryophyllene**	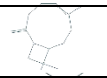
***Cis*-geraniol**	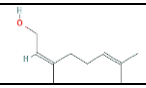	**(-)-Carvone**	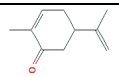	**(+)-β-Pinene**	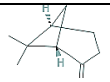	**(-)-α-Thujone**	
Citral	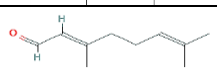	**(-)-Pulegone**	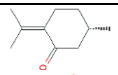	**(-)-Fenchone**	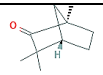	**(±)-α-β-Thujone**	
Geranyl acetate	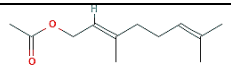	**(+)-Pulegone**	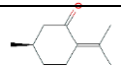	**(+)-Fenchone**		**Thymol**	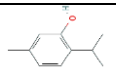
Farnesol	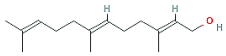	**(R)-(+)-Limonene**	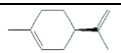	**(+)-Borneol**		**2-Thiazoline-2 thiol**	
(±)-Linalool	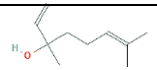	**(S)-(-)-Limonene**	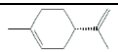	**(-)-Borneol**		**Artemisia ketone**	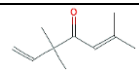
(-)-Linalool	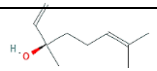	**(+)-Terpinen-4-ol**	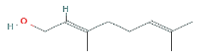	**(-)-Bornyl acetate**	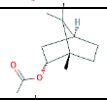	**α-Humulene**	
Linalyl acetate	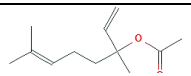	**(-)-Terpinen-4-ol**	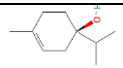	**(±)-Camphor**		**Ocimene**	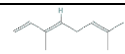
(-)-Citronellal		**Eugenol**		**(1R)-(+)-Camphor**		**(±)-Lavandulol acetate**	
(S)-(-)-β-Citronellol		**1,8-Cineole**		**(-)-Camphor**		**Myrcene**	
(±)-Menthone		**1,4-Cineole**		**(1R)-(-)-Camphorquinone**		**ρ-Cymene**	
(-)-Menthone		**α-Bisabolol**		**(±)-Camphorquinone**			

3.1.3. Reference control compounds

Seventeen compounds were used as standard references in the various assays (Table 3.5). Compounds that were water soluble were dissolved in double distilled water (ddH_2O) and filter sterilized using 0.2 µm filters (GVS™).

Table 3.5: The molecular formula and chemical properties of reference/control compounds used in several assays throughout the study.

Compound	Formula	MW (g/mol)	Solvent	Source
Neocuproine	$C_4H_{12}N_2$	262.74	ddH_2O	Fluka
TET	$C_6H_{18}N_4$	219.16	DMSO	Fluka
Cupral	$C_5H_{10}NNaS_2$	225.31	DMSO	Fluka
Butylated hydroxyanisole (BHA)	$C_{11}H_{16}O_2$	180.25	DMSO	Sigma-Aldrich
2,6-Di-tert-butyl-4-methylphenol (BHT)	$C_{15}H_{24}O$	220.36	DMSO	Fluka
6-Hydroxy-2,5,7,8-tetra-methylchroman-2-carboxylic acid (Trolox™)	$C_{14}H_{18}O_4$	250.26	DMSO	Sigma-Aldrich
Cupferron	$C_6H_9N_3O_2$	155.16	DMSO	Merck
Ascorbic acid (AA)	$C_6H_8O_6$	176.12	DMSO	Riedel deHaën
Ethylenediaminetetraacetic acid (EDTA)	$C_{10}H_{16}N_2O_8$	292.24	ddH_2O	Rochelle chemicals
Chloroquine	$C_{18}H_{26}ClN$	515.90	ddH_2O	Sigma-Aldrich
Quinine hydrochloride	$HCl(C_{20}H_{24}N_2O_2)$	360.90	ddH_2O	Sigma-Aldrich
Camptothecin	$C_{20}H_{16}N_2O_4$	348.35	DMSO	Sigma-Aldrich
D-Penicillamine	$C_5H_{11}NO_2S$	149.21	ddH_2O	Fluka
Ammonium tetrathiomolybdate	$H_8N_2MoS_4$	260.28	DMSO	Sigma-Aldrich
Dihydroartemisinin	$C_{15}H_{24}O_5$	284.35	DMSO	Fluka
Copper (I) chloride	CuCl	98.99	3% HCl	Sigma-Aldrich
Copper (II) sulphate	$CuSO_4.5H_2O$	249.68	ddH_2O	Fluka

3.2. Copper homeostasis investigations

3.2.1. Effect of copper on compounds and essential oil constituents

The test compounds at 200 µM (50 µL) were incubated in a 96 well plate at a ratio of 1:1 with either copper (I) chloride dissolved in 3% hydrochloric acid (200 µM; 50 µL; Sigma-Aldrich) or copper (II) sulphate dissolved in sterile ddH_2O (Říha *et al.*, 2013). For each compound the absorption spectrum of 200-750 nm was recorded and the absorption maxima were

determined (Mazor *et al.*, 2006). The percentage copper complexation to the test or control compound was calculated as per Equation 1.

$$\% \text{ Metal complexation} = \frac{Abs_{TC+Cu} - Abs_{TC\ alone} - Abs_{Cu}}{Abs_{TC+Cu}}$$

Equation 1: The percentage metal complexation on a test compound (Říha *et al.*, 2013)**.**
Where, Abs = Absorbance; TC = Test Compound; and Cu = Copper (I) or Copper (II).

3.2.2. Copper chelation assay

The copper chelation assay was used to determine the copper chelating properties of the test compounds and whether they could be utilized in the same manner as standard, therapeutic metal ion chelators. An adjusted protocol to that described by Říha *et al.* (2013) was used. Neocuproine is a copper (I) chelator that changes from a clear solution to a bright yellow solution when chelated to copper (I) ions (Figure 3.2) (Syed and Syeda, 2007).
Hydroxylamine (oxidizer) was added after the incubation of the compounds with copper (II) to ensure that the unchelated copper (II) ions were oxidized to copper (I) ions. Thereafter, neocuproine was added as a colourimetric detector of the remaining copper (I) ions (Říha *et al.*, 2013).

Copper (I) chloride (5 mM) was prepared in a 1:1 ratio solution of NaCl (5 mM) and HCl (6.9 M) and further diluted in ddH_2O to 1 mM to prepare a working solution. Copper (II) sulphate (5 mM) was prepared in ddH_2O and further diluted to 1 mM to prepare a working solution. An acetate buffer (pH 4) consisting of 847 mL of 0.1 M acetic acid and 15.3 mL of 0.1 M sodium acetate, was prepared for the copper (I) chelation assay. A 4-(2-hydroxyethyl)-1-piperazineethanesulfonic acid (HEPES) buffer (pH = 7.4; 3.574 g/L ddH_2O) was prepared for the copper (II) chelation assay. The working copper solution was incubated with the test compound or EOC and the relevant buffer for 15 minutes at room temperature (RT) in the dark (Figure 3.2). The solutions were further incubated with hydroxylamine and subsequently with neocuproine (Říha *et al.*, 2013). The plate was read using the Labsystems iEMS Reader MF, ultraviolet–visible (UV-VIS) plate reader at an absorbance of 450 nm. The percentage copper chelation was calculated using Equation 2.

$$\% \text{ Copper chelation} = 100 - \left[\frac{Abs_{TC} - Abs_{Blank}}{Abs_{100\%} - Abs_{Blank}} \times 100\right]$$

Equation 2: The percentage copper chelation of a test compound (Říha *et al.*, 2013).
Where Abs = Absorbance; TC = Test Compound; 100% = 100% copper chelation control and BC = Background control.

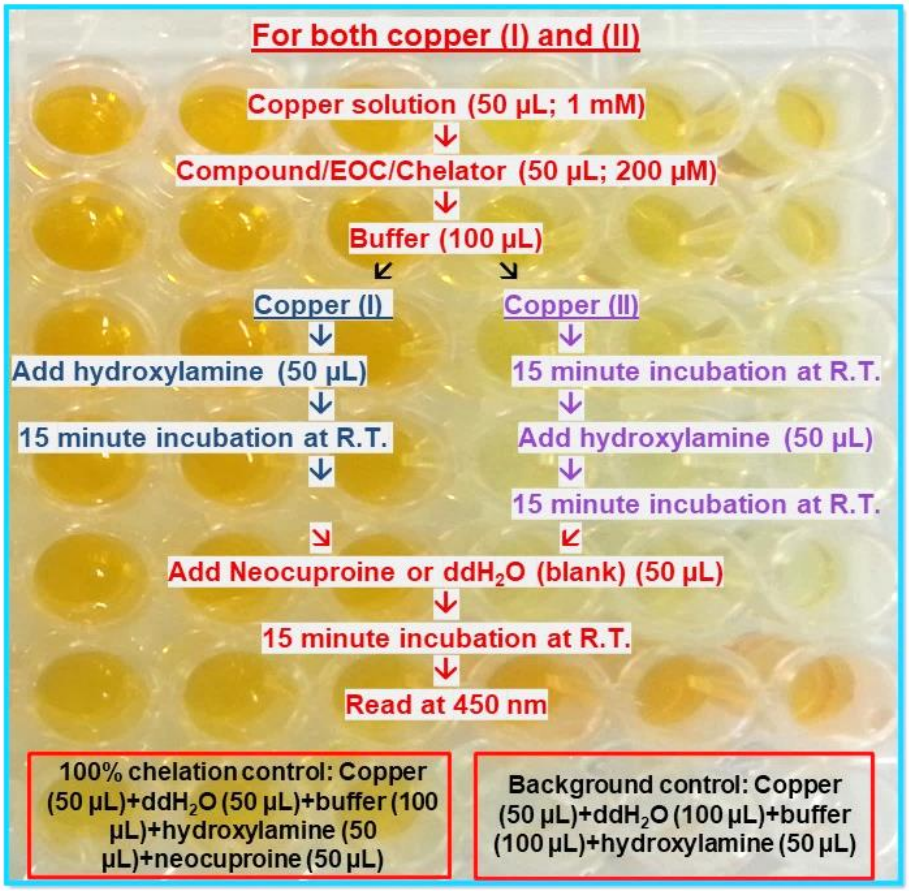

Figure 3.2: Copper chelation assay methodology as seen in a 96 well microtiter plate. The principle of the colourimetric copper chelation assay, where the higher the concentration of free copper ions in solution the brighter the yellow colour of the solution and therefore the lower the percentage copper chelated.

3.2.3. Copper reduction assay

The copper reduction assay was used to measure the concentration of reducing compounds in relation to their ability to reduce copper (II) to copper (I). There was a colour change from clear to green when the copper (II) was reduced to copper (I) by a compound (Mazor *et al.*, 2006) (Figure 3.4). $CuSO_4$ was prepared at a concentration of 10 mM in ddH_2O and diluted (17 mL) in 0.65 M (34 mL) ammonium acetate buffer (pH = 7; MW: 77.0825 g/mol; Sigma-Aldrich). Neocuproine was prepared to a concentration of 7.5 mM. ethylenediaminetetraacetic acid (EDTA) was used as the negative control, 6-hydroxy-2,5,7,8-tetramethylchroman-2-carboxylic acid (Trolox™) and butylated hydroxyanisole (BHA) were the positive controls with a DMSO background control was utilized (Mazor *et al.*, 2006). Each compound had a colour control (to compensate for spectral overlap absorbances) which consisted of the test compound/EOC and DMSO and were repeated in triplicate. The compounds were freshly diluted from a stock solution of 10 mM to a screening concentration of 200 µM.

To a 96 well microtiter plate (Figure 3.4), compounds/EOCs (50 µL) were added to row A (four columns for each compound). In row H, column 1 to 12, no compound was added since this was the background control. To all wells 50 µL of $CuSO_4.5H_2O$ was added, the plates were incubated in the dark for 10 minutes, then 50 µL of neocuproine was added to all wells and the plates were incubated in the dark for 30 minutes.

Copper reduction was determined using Equation 3 (Mazor *et al.*, 2006) where the absorbance was read at 450 nm on the Labsystems iEMS Reader MF. A standard curve was constructed using the Trolox™ positive control by means of Graphpad Prism® (Version 5.02) software and the absorbance values of the compounds were then interpolated from the standard curve (Figure 3.4). Those that showed activity relative to the antioxidant control, Trolox™, i.e. the Trolox™ equivalent antioxidant capacity (TEAC; Figure 3.3) were then further investigated to determine the copper reducing activity at different concentrations using serial dilutions (Mazor *et al.*, 2006).

$$\textbf{Copper reduction} = Abs_{TC} - Abs_{CC}$$

Equation 3: The copper reduction equation (Mazor *et al.*, 2006).
Where Abs = Absorbance; TC = Test compound and CC = Colour control

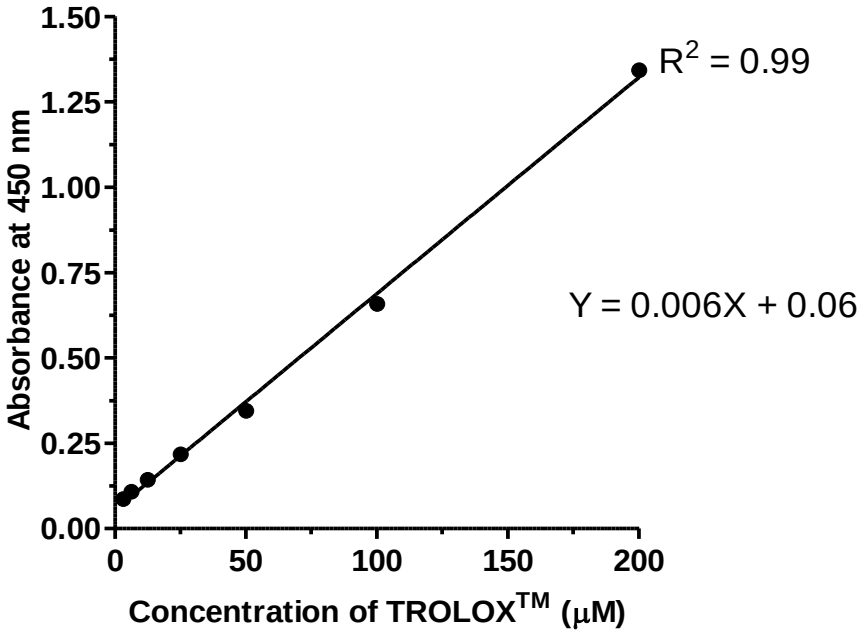

Figure 3.3: The linear regression curve of Trolox™ copper (II) ion reducing antioxidant capacity used to determine the TEAC of the test and control compounds.

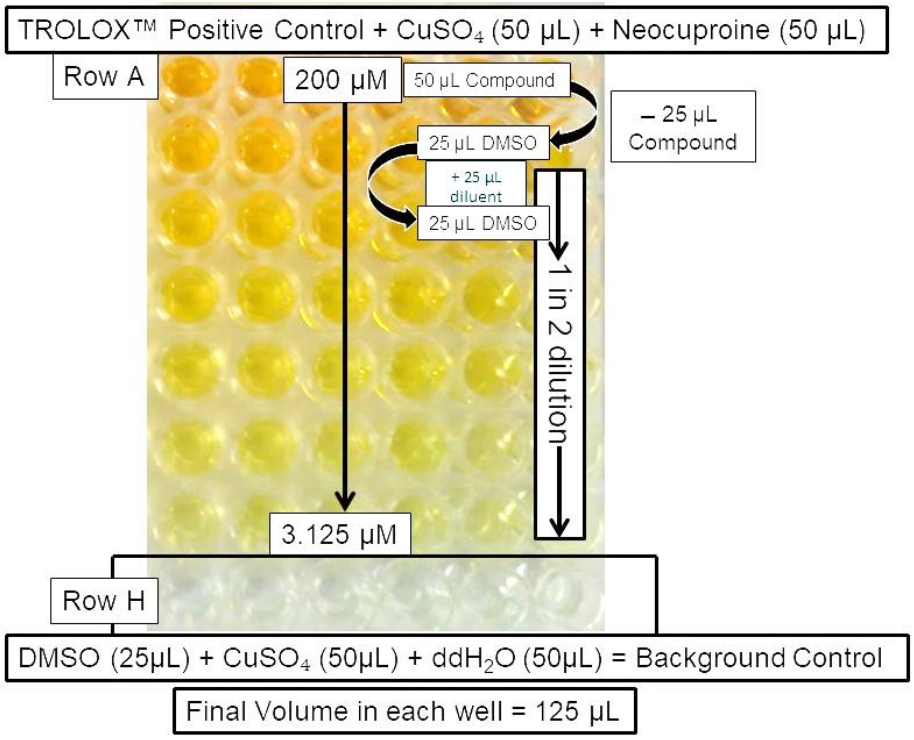

Figure 3.4: The copper reduction assay of Trolox™ in a 96 well microtiter plate. The antioxidant activity of test compounds/EOCs were determined against the reference compound Trolox™.

3.3. Antimalarial investigations

The tritiated hypoxanthine incorporation assay (Appendix B.1) was initially used to determine the antimalarial properties of the compounds and EOCs (Desjardins *et al.*, 1979; Van Zyl *et al.*, 2008). However, the Wallac™ beta scintillation counter was deemed irreparable before triplicate results could be obtained. Triplicate results were obtained using the parasite lactate dehydrogenase (pLDH) assay (Section 3.3.2) and this assay was validated using literature.

3.3.1. Malaria culturing

3.3.1.1. Preparation of media

The incomplete culture medium was prepared by dissolving RPMI-1640 (10.4 g; Gibco™), HEPES buffer (5.9 g; Sigma-Aldrich), D-glucose (40 g; Merck), hypoxanthine (44 mg; Sigma-Aldrich) and 50 mg/mL gentamicin sulphate (100 µL; Sigma-Aldrich) in 1 L of sterile, ddH_2O (Trager and Jensen, 1976; Van Zyl *et al.*, 2008). Experimental culture media was prepared as for the latter however gentamicin was excluded. These solutions were sterilised using the Sterivex™ 0.22 µm filter unit and stored at 4°C until needed (Trager and Jensen, 1976; Van Zyl *et al.*, 2008). To prepare complete culture media for culture maintenance and pLDH antimalarial assay, complete culture media was prepared with 15% (v/v) Albumax II™ (Gibco™;

Section 3.3.1.2) and 5% (w/v) $NaHCO_3$ (Saarchem; Section 3.3.1.3) in incomplete media (100 mL) (Trager and Jensen, 1976; Radfar *et al.*, 2009).

3.3.1.2. Preparation of Albumax II™

Albumax II™ (5 mg/100 mL) was used as a replacement for the plasma (Ringwald *et al.*, 1999) used by Trager and Jensen (1976) for culture maintenance only. It was prepared in incomplete culture media and sterile filtered (0.2 µm filters; GVS™). This was stored at -20°C and thawed when needed (Preechapornkul *et al.*, 2010).

3.3.1.3. Preparation of phosphate buffered saline, sodium bicarbonate and D-sorbitol

Phosphate buffered saline (PBS) was prepared by dissolving 8.0g NaCl (Saarchem), 0.3g KCl (Sigma-Aldrich), 0.73g $Na_2HPO_4.2H_2O$ (Sigma-Aldrich) and 0.2g KH_2PO_4 (Fluka) in 1 L of sterile MilliQ™ water (Radfar *et al.*, 2009). This was autoclaved at 120°C and stored at 4°C. Sodium bicarbonate ($NaHCO_3$; 0.6 M) was dissolved in 1 L of sterile MilliQ™ water to prepare a 5% (w/v) solution. D-sorbitol (0.27 M; Saarchem) was dissolved in 1 L of MilliQ™ water to prepare a 5% (w/v) working solution. Both solutions were sterilized by a 0.22 µm filter and stored at 4°C (Radfar *et al.*, 2009).

3.3.1.4. Preparation of erythrocyte suspension

With the assistance of a phlebotomy technician, blood was drawn from healthy volunteers into anti-coagulant blood tubes that contain citrate phosphate dextrose-1 (Clearance certificate No. M140669; Appendix A.1). The whole blood was stored at 4°C until required. At which time, the tubes were centrifuged at 252 X G for 5 minutes on the Thermo Scientific Heraeus™ Megafuge™ 40 Centrifuge, the supernatant and buffy coat discarded. The blood was washed in PBS and centrifuged as described at least three times to ensure all white blood cells and plasma were discarded and only red blood cells remained for culturing and experimental purposes. The erythrocytes (50% haematocrit) was resuspended in incomplete culture media and stored at 4°C in the citrate phosphate dextrose adenine tubes and used within 7 days of preparation (Radfar *et al.*, 2009).

3.3.1.5. *In vitro* culture maintenance of 3D7 *Plasmodium falciparum*

A chloroquine-sensitive strain of *Plasmodium falciparum* (3D7) was continuously maintained *in vitro*, with an approximate parasitaemia of 5% (Trager and Jensen, 1976; Van Zyl *et al.*, 2008). The complete culture medium (Section 3.3.1.1; 37°C) was replaced daily and culture diluted with fresh, uninfected human erythrocytes (Section 3.3.1.4) when the parasites were predominantly in the trophozoite/schizont stage. The parasites were maintained in a 5%

carbon dioxide (CO_2), 3% O_2 and 92% N_2 atmosphere and incubated at 37°C. The rapid stain technique (BIO LAB Diagnostics) was used to stain the thin blood smears prepared daily to examine the culture, determine the percentage parasitaemia and stage (Trager and Jensen, 1976; Van Zyl *et al.*, 2008; Radfar *et al.*, 2009). After the air-dried slides were fixed with methanol, the slide was first dipped into the red eosin stain for 10-20 seconds, rinsed with tap water, dipped into the methylene blue stain for 25-35 seconds, rinsed with tap water, air dried and viewed under oil immersion at 1000x magnification (Van Zyl *et al.*, 2008).

3.3.1.6. Synchronization of 3D7 *Plasmodium falciparum* culture

To ensure a culture consisting predominantly of ring infected erythrocytes, the 5% D-sorbitol technique described by Lambros and Vanderberg (1979) was used. The parasite culture (predominately ring stage) was centrifuged at 252 X G for 5 minutes on the Thermo Scientific Heraeus™ Megafuge™ 40 centrifuge and the supernatant was discarded (Radfar *et al.*, 2009). The pellet was resuspended in 10 mL warmed D-sorbitol and vortexed for 30 seconds to rupture old red blood cells and mature parasite forms and incubated at 37°C for 15 minutes. Following which the suspension was vortexed for 15 seconds, centrifuged at 252 X G for 5 minutes and the supernatant was discarded (Lambros and Vanderberg, 1979; Radfar *et al.*, 2009). Thereafter, normal culture maintenance procedures were carried out (Section 3.3.1.5) and the parasites were incubated at 37°C.

3.3.2. The *Plasmodium* lactate dehydrogenase assay

The pLDH assay was established in the Pharmacology Division and found to generate reliable, repeatable results and as such was used to determine the *in vitro* antimalarial activity of compounds and EOCs against the malaria parasite. pLDH is an enzyme that is crucial in the production of ATP and is found in high concentrations peaking in the trophozoite stage and was found to generate accurate means of parasite viability (Makler *et al.*, 1993).

3.3.2.1. Preparation of Malstat™ solution

To prepare Malstat™ solution: 40 µL Triton X-100, 0.2 g calcium-L-lactate and 2.5 mg 3-acetylpyridine adenine dinucleotide were dissolved in 10 mL of Tris base (6.6 g/L ddH_2O; pH=9.1) (Basco *et al.*, 1995). This was sterilized (0.22 µm) covered in foil and stored at 4°C for 1 week. Phenazine ethosulfate (PES; 0.0003 M) was dissolved in autoclaved, ddH_2O and nitro blue tetrazolium (NBT; 0.002 M) was dissolved in sterilized (0.22 µm), ddH_2O before being combined in a 1:1 ratio, immediately before use (Basco *et al.*, 1995).

3.3.2.2. Preparation of experimental plates

The parasite suspension (100 µL) in a predominately ring stage was adjusted to 2% parasitaemia and 2% haematocrit in freshly washed red blood cells that were at least three days old (to ensure a low level of platelets and low LDH levels in the erythrocytes) (Figure 3.5). The plates were incubated using the candle jar method for 24 hours at 37°C to guarantee an ideal environment for parasitic homeostasis (Trager and Jensen, 1976).

After incubation, the test compounds/EOCs (12.5 µL) were added in duplicate (at mid-trophozoite stage) and incubated for 48 hours at 37°C in the candle jar. After incubation, the plates were placed in a sterile, sealed container and frozen at -70°C for 1 hour and subsequently thawed for 30 minutes at 37°C. The process of freeze-thawing produced a parasite red blood cell lysate that was added to the Malstat™ solution (Basco *et al.*, 1995).

3.3.2.3. Addition of Malstat™ solution to parasites

To a new, sterile 96 well plate, the parasite red blood cell lysate (25 µL), Malstat™ solution (100 µL) and NBT/PES (20 µL) solution were added. The plates were incubated for 40 minutes at 37°C (Basco *et al.*, 1995). Thereafter, 5% acetic acid (50 µL) was added to stop the colour reaction and bubbles were removed. The plate was then read at 620 nm and the percentage inhibited parasite growth was calculated using Equation 4 (D'Alessandro *et al.*, 2013). A half maximal inhibitory concentration (IC_{50}) value was determined from log sigmoid dose response curves for compounds/EOCs that inhibited more than 60% at 50 µM.

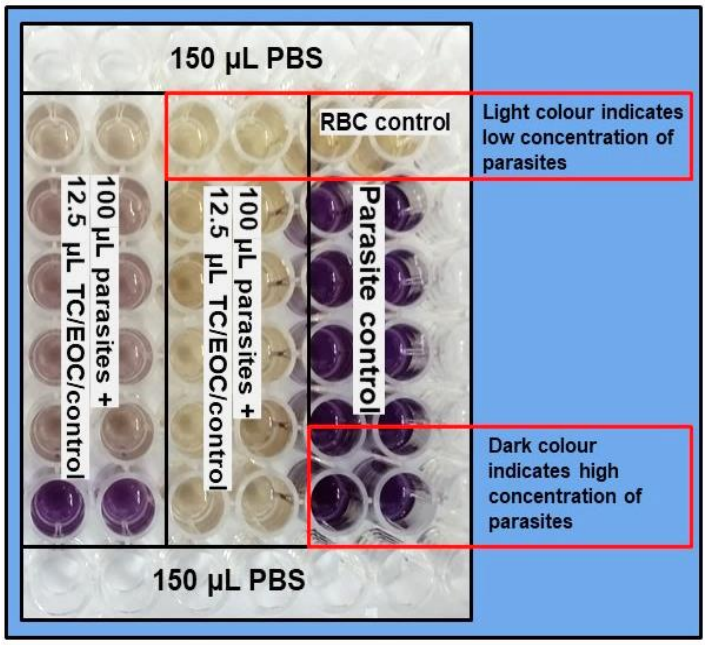

Figure 3.5: The layout of a 96-well microtiter plate in the pLDH assay.
The pLDH assay accurately determines the activity of test compounds/EOCs against malaria parasites.

$$\% \text{ Parasite growth inhibited} = 100 - \left[\frac{Abs_{TC} - Abs_{Mean\ RBC\ control}}{Abs_{mean\ parasite\ control} - Abs_{Mean\ RBC\ control}} \times 100 \right]$$

Equation 4: The percentage parasite growth inhibited in response to incubation to test compounds (Basco *et al.*, 1995).

Where TC = Test compound, RBC = red blood cell

3.3.3. The effect of compounds and EOCs on *Plasmodium* stage development

The effect of compounds and EOCs on the stage development of *P. falciparum* was assessed over a 72-hour period. Parasites were incubated with the most active compounds at their respective IC_{50} values as determined by the pLDH drug sensitivity studies. Thin blood smears were prepared every 4-6 hours for 72 hours, then Giemsa stained and viewed microscopically under oil immersion at 1000X magnification to determine the percentage parasitaemia in at least 10 fields. In addition, the stages sensitive to the compounds and the morphologically induced changes were determined. The total parasitaemia, % rings, % trophozoites, % schizonts and % gametocytes were documented at each time point.

3.3.4. Ferriprotoporphyrin biomineralization inhibition assay

To obtain essential amino acids for parasitic protein synthesis and metabolism, the malaria parasite digests haemoglobin in the food vacuole of the parasite. A by-product of this digestion is insoluble haem that is toxic to the parasite; but following biocrystallization it is converted into inert, insoluble haemozoin. The haemozoin can be observed under light microscopy as orange/brown crystals (Fitch, 2004). This assay was used to determine whether the compounds inhibited the formation of haemozoin or β-haematin, where the latter is the synthetic product produced under acidic conditions and is chemically identical to parasite-produced haemozoin. Inhibition of β-haematin would be similar to the mechanism of action of standard antimalarial agents, chloroquine, and quinine.

As shown in Figure 3.6, a haemin solution (1 mg/mL) in DMSO was added to test compounds or positive controls (chloroquine and quinine) at 200 µM. A sodium acetate buffer (0.5 M) was prepared by adding 0.5 M acetic acid (30.5 mL; BDH) and 0.5 M sodium acetate (19.5 mL; Sigma-Aldrich) to 50 mL ddH_2O. Beta-haematin formation was initiated by the addition of the sodium acetate buffer (pH 4.8) and the plates were incubated at 37°C for 24 hours. The plate was centrifuged at 1008 X G for 10 minutes using the Thermo Scientific Heraeus™ Megafuge™ 40 centrifuge, 150 µL supernatant was replaced with 150 µL DMSO. This DMSO wash was repeated twice and the pellet was further washed twice with ddH_2O, to decrease the DMSO concentration to ensure complete dissolution of the crystals. The beta-haematin

crystals were dissolved in 0.2 M sodium hydroxide (150 µL; Fisher Chemicals), placed in an MRC lab Thermo Shaker for 2 minutes at 161 X G before the absorbance was measured at 405 nm. The percentage beta-haematin formed was calculated using Equation 5.

$$\% \text{ Beta haematin inhibited} = 100 - \left(\frac{Abs_{TC} - Abs_{BC}}{Abs_{100\%} - Abs_{BC}} \times 100\right)$$

Equation 5: The percentage beta haematin inhibition calculation (Fitch, 2004).

Where Abs = absorbance; TC = test compound; BC = background control; 100% = 100% control.

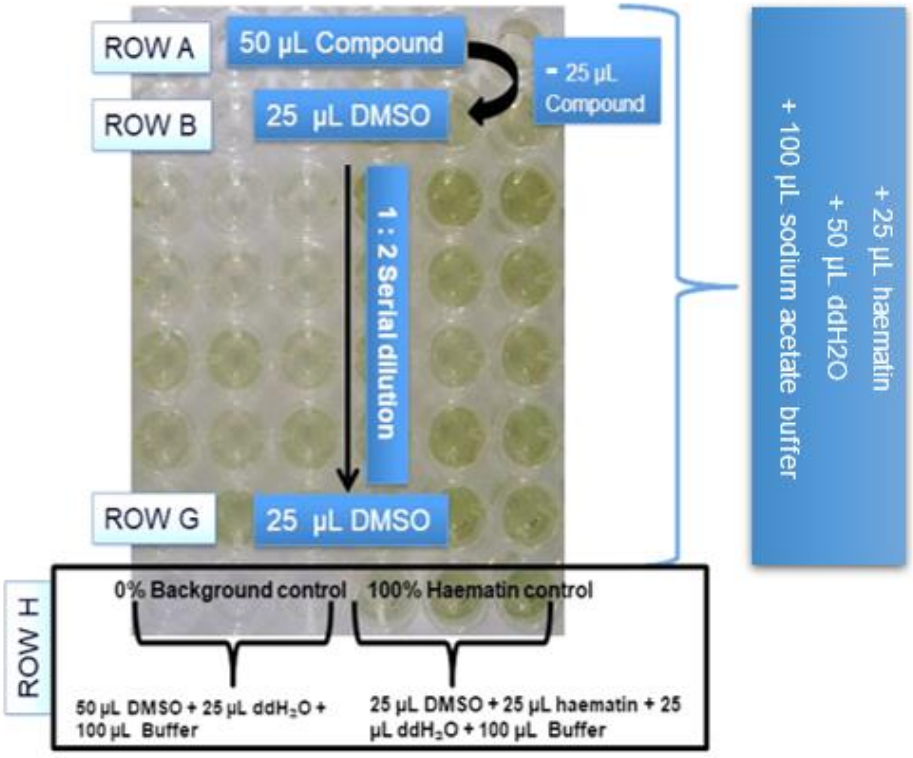

Figure 3.6: The microtiter plate organisation of the ferriprotoporphyrin biomineralization inhibition assay**.**

The method of haemoglobin breakdown in the food vacuole of the malaria parasite is a possible mechanism of action in which new antimalarial medicines may be developed.

3.4. The haemolytic effect of compounds and EOCs

3.4.1. The haemolysis assay

To establish whether the test compounds have a toxic effect on red blood cells, the method as described by Hayat *et al.* (2011) was used. Blood was obtained as described in Section 3.3.1.4 and blood no older than 3 days was used to ensure optimal membrane integrity. A 1% haematocrit of freshly washed red blood cell suspension was prepared in complete culture

medium (v/v) using 10% plasma or Albumax™ II (Section 3.3.1.2), 4.2% sodium bicarbonate (Section 3.3.1.3) and 85.8% RPMI-1640 (Section 3.3.1.1). The experimental microcentrifuge tubes contained red blood cells (200 µL), RPMI-1640 (25 µL) and 200, 100, 50 or 10 µM test/control compounds (25 µL), with matching colour controls prepared with an appropriate concentration of compound and complete culture medium (200 µL). The positive control (100% haemolysis) consisted of 0.2% (v/v) Triton X100 (25 µL; BDH Chemicals Ltd), the negative control (0% haemolysis) consisted of 50 µL RPMI-1640 and 200 µL 1% haematocrit red blood cell suspension; whilst the background control consisted of 50 µL RPMI-1640 and 200 µL complete culture medium. The microcentrifuge tubes were incubated for 48 hours at 37ºC. Thereafter the red blood cell pellet was gently disrupted, and the microcentrifuge tubes centrifuged at 252 X G for 5 minutes in the Thermo Scientific Heraeus™ Megafuge™ 40 centrifuge. The supernatant (50 µL) was removed from each tube and placed into a non-sterile 96 well microtiter plate along with 150 µL sterile ddH_2O. Plate was incubated at RT (approximately 25°C) for 10 minutes and the absorbance was then read at 412 nm on the Labsystems iEMS Reader MF. The percentage haemolysis was calculated according to Equation 6 (Hayat *et al.*, 2011).

$$\% \text{ Haemolysis} = \frac{Abs_{TC} - Abs_{BC}}{Abs_{Triton} - Abs_{BC}} \times 100$$

Equation 6: The percentage haemolysis induced by test compounds (Hayat *et al.*, 2011)**.**
Where Abs = Absorbance; TC = test compound; BC = background control.

3.4.2. The haemolytic protective assay

By following the same protocol as described in Section 3.4.1, the haemolytic protective assay determined if there was a dose-dependent protective effect of the EOCs and 8OH compounds against copper (I)- or (II)-induced haemolysis. Test/control compounds (25 µL of 200, 100, 50 or 10 µM;) with copper (I) or (II) (25 µL of 200, 100, 50 or 10 µM) were incubated with 1% haematocrit red blood cell suspension (200 µL) for 48 hours at 37°C. As in Section 3.4.1, the microcentrifuge tubes were centrifuged, the supernatant plated out and the absorption read on the Labsystems iEMS Reader MF. Equation 7 was used to determine the percentage haemolysis and the protective effect was determined using Equation 7. A negative value indicated an increase in haemolysis and a positive value indicated a decrease in haemolysis.

$$\text{Protective effect} = \%\ \text{Haemolysis}_{\text{TC alone}} - \%\ \text{Haemolysis}_{\text{TC+Copper}}$$

Equation 7: The protective effect of test compounds against copper induced haemolysis (Hayat *et al.*, 2011)**.**
Where TC = test compound.

3.5. The effect of compounds and EOCs on neuroblastoma cells

To determine the compounds toxicological effect against a neuroblastoma cell line (SH-SY5Y), two cellular viability assays were implemented using 3-(4, 5-dimethyl-2-thiazol-2-yl)-2, 5- diphenyl-2H-tetrazolium bromide (MTT; Duchefa Biochemies) and sulphorhodamine B (SRB; Sigma-Aldrich). The MTT assay is a standard colorimetric assay used to measure the cytotoxic concentration of a compound. MTT (yellow) is a tetrazolium salt which undergoes a cleavage reaction (catalysed by endoplasmic reticulum and mitochondrial enzymes) to form a purple formazan by metabolically active cells and as such the number of viable cells can be quantitatively determined (Mosmann, 1983). In comparison, the SRB assay was used to measure viable cells by staining protein content (Lin *et al.*, 1999). Amino acids in cells allow for uptake of the negatively charged SRB dye and the larger protein content resulted a greater absorbance (Houghton *et al.*, 2007).

3.5.1. Cell culturing

The human neuroblastoma (SH-SY5Y) cell line donated by Professor C. Brink (North-West University) and maintained at 37°C and 5% CO_2 in complete culture media consisting of a 1:1 ratio of DMEM (Biochrome) and Hams F12 media supplemented with 10% heat-inactivated foetal bovine serum (FBS; HyClone), 1% penicillin-streptomycin (Sigma-Aldrich), 1% glutamine (Sigma-Aldrich) and 1% sodium pyruvate (Sigma-Aldrich) (Kovalevich and Langford, 2013). Experimental DMEM used exclusively in cell line studies consisted of 10% FBS, 1% glutamine and 1% sodium pyruvate in DMEM and stored at -20°C until required. FBS was inactivated at 56°C for 30 minutes, aliquoted into 50 mL tubes and stored at -20°C. The morphology and growth of the cell line was observed under an inverted confocal microscope (20X magnification) and the complete media was changed every 48 to 72 hours or when the cells were 80-90% confluent. When confluent, the cells were trypsinized with 0.2% trypsin-EDTA (HyClone) at 37°C and for two minutes, before the trypsin-EDTA reaction was halted by adding complete DMEM. A single cell suspension was prepared and either used to reseed the culture (at approximately 20%) or used for experimental purposes (Kovalevich and Langford, 2013). This cell line was used for all *in vitro* investigations involving cell line studies as described in Sections 3.5.2, 3.5.3, 3.5.4, 3.5.5 and 3.5.6.

3.5.2. The trypan blue exclusion assay

To ensure optimal growth of the cells under experimental conditions, the cell number per mL and viability of the cells were determined using the trypan blue exclusion assay. The selective permeability of living cell membranes prevents the uptake of the trypan blue stain through the membrane; therefore, the live cells were translucent. In contrast, all non-viable cells were stained blue (Strober, 1997). In Figure 3.7, the cells were stained with trypan blue; Figure 3.7A

shows an example of cells in a field without using phase contrast on the microscope so that the clear, unstained, viable cells and the non-viable, trypan blue stained cells were visible. Phase contrast was used to demonstrate the morphology of the untreated cells (Figure 3.7B, 3.7C).

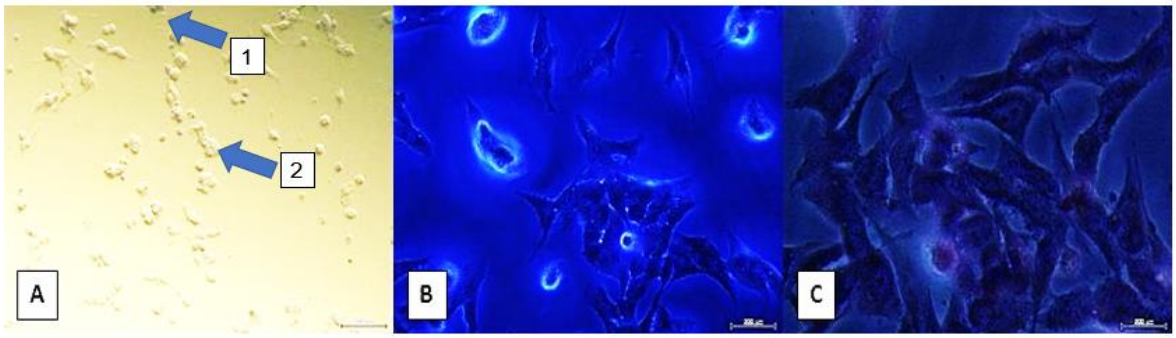

Figure 3.7: The viable cells at 0 hours, at magnifications of 10X (A), 20X (B) and 40X (C). Where 1 represents a non-viable cell and 2 represents viable cells

Cell suspension (20 µL) and 0.2% trypan blue solution (w/v; 20 µL; Sigma-Aldrich) were combined in a microcentrifuge tube and gently mixed before 20 µL of this suspension was placed onto the haemocytometer. The cells were counted and viability assessed using an inverted microscope (1000X magnification) and the number of translucent and blue stained cells were counted to determine the percentage of viable or dead cells, respectively (Strober, 1997). If the percentage dead cells was ≥ 2-5%, the cell culture was not used for experimental purposes, but returned to the culture flask to reinitiate the culture to optimise the viability of the cells. The number of cells per ml was calculated using Equation 8.

$$\frac{\textbf{Cells}}{\textbf{ml}} = \textbf{Average cells counted} \times \textbf{dilution factor} \times 10\,000$$

Equation 8: The cells per mL in each count on a haemocytometer (Strober, 1997).

The number of viable and non-viable cells were counted at 1, 24 and 48 hours and images taken using the Olympus microscope at 20X magnification to determine the effect of the compounds on the number of cells. The percentage change in cellular viability was calculated using Equation 9.

$$\%\,\Delta \text{ in viability} = \frac{\%\text{ alive after 24 hours of TC}}{\%\text{ alive after 24 hours of 100\% cell control}} - \frac{\%\text{ alive after 48 hours of TC}}{\%\text{ alive after 48 hours of 100\% cell control}}$$

Equation 9: The percentage change in cellular viability for the adherent cell counting (Strober, 1997).
Where TC = test compound

3.5.3. The MTT Cytotoxicity Assay

3.5.3.1. Cell number optimization

To determine the optimal cell number for uninhibited cell growth in the cytotoxicity assay under the departmental laboratory conditions based on Mosmann methodology (Mosmann, 1983), the cell density standard curve was determined (Figure 3.8). The cell suspension was prepared as described in Section 3.5.2 and the cell density was determined before being adjusted to 1.0x10⁶ cells/mL and diluted in approximately 1.0x10⁴ cells/mL increments. MTT (5 mg/ml) was dissolved in sterile PBS and filter-sterilized through a 0.2 µM filter into a sterile, light protected container. The MTT solution was stored at 4°C. To a 96 well microtiter plate, 90 µL cell suspension was added in triplicate wells and incubated for 44 hours under humidified conditions at 37°C and in 5% CO_2 before the MTT was added to determine the associated absorbance (Section 3.5.1). From the standard curve using Graphpad Prism® software (version 5.02), the optimal cell number per mL was determined to be approximately 55,000 cells/mL and this was adjusted to 50,000 cells per millilitre to account for variability between experiments.

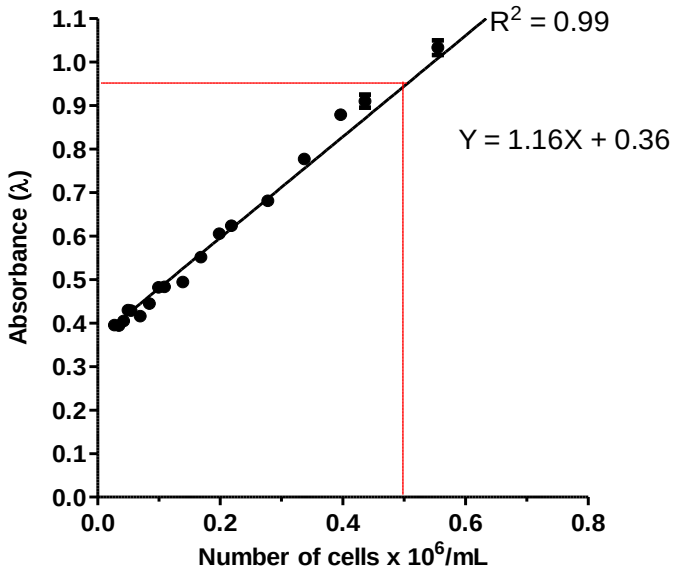

Figure 3.8: The standard curve of the SH-SY5Y cell line for the MTT assay (n=4).
The MTT-cell number standard curve was constructed to evaluate the optimal cell number to plate per well to ensure cell growth was not affected during the MTT assay.

The positive control was camptothecin (Sigma-Aldrich), an apoptotic inducing agent (Efferth *et al.*, 2007). The negative control was incomplete experimental culture media. The absorbance of each wells was read at the test wavelength of 540 nm and reference

wavelength of 690 nm on the Labsystems iEMS Reader MF (Mosmann, 1983). The percentage cellular viability was calculated using Equation 10:

$$\% \text{ Cellular viability} = \frac{\text{Abs TC}_{(540\text{-}690)} - \text{Abs cell free media}_{(540\text{-}690)}}{\text{Abs drug free control}_{(540\text{-}690)} - \text{Abs cell free control}_{(540\text{-}690)}}$$

Equation 10: The percentage cellular viability determined from MTT toxicological assays (Mosmann, 1983).

Where Abs = absorbance; TC = test compound; (540-690) = Absorbance of test wavelength – absorbance of reference wavelength.

3.5.3.2. MTT drug sensitivity assay

To determine the effect of compounds/EOCs on the neuronal cells, 180 µL cell suspension (50,000 cells/ml) were plated with 20 µL compound/EOC for 44 hours in an humidified environment at 37°C in 5% CO_2, before 40 µL MTT was added for 4 hours (Figure 3.9). The media (100 µL) was replaced with 100 µL of DMSO. To dissolve formazan crystals, the plate was shaken on the MRC lab Thermo Shaker for 10 minutes at 161 X G. The absorbance of each well was read at 540 nm and 690 nm. MTT was not added to colour control wells for the control/test compounds, PBS (50 µL) was added instead.

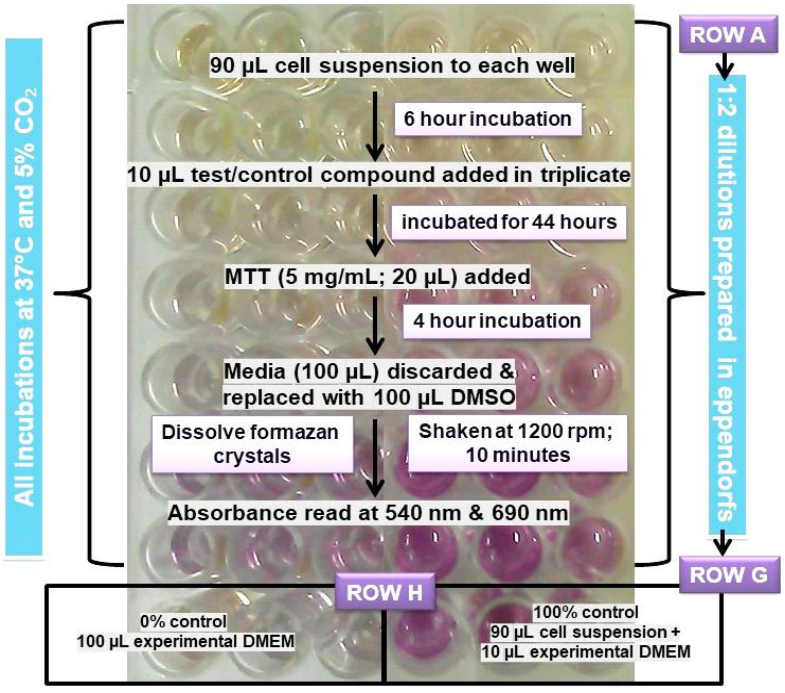

Figure 3.9: Resultant colour change of an MTT cellular viability assay following described protocol.

3.5.4. Sulphorhodamine B assay

To determine the optimal cell number per mL, a standard curve was prepared as described in Section 3.5.3.1; (Figure 3.10) however the method used to determine the cell viability after the 44 hour incubation differed (Keepers *et al.*, 1991).

The SRB protocol as described by Keepers *et al*, 1991 was undertaken following the 44 hour incubation period, where cold trichloroacetic acid (TCA; 4°C; 100 µL; UnivAR) was added to all the wells and the plate incubated at 4°C for 1 hour . The experimental culture media and TCA were discarded, and the cells washed with sterile ddH_2O and centrifuged for 5 minutes at 161 X G using the Thermo Scientific Heraeus™ Megafuge™ 40 centrifuge. The cells were washed four times. The plates were air dried at RT overnight. 0.4% SRB (w/v; 50 µL) was prepared in 1% acetic acid (v/v) and stored at 4°C. SRB was added for 1 hour at RT before the plate was washed with 1% acetic acid and centrifuged at 252 X G for 5 minutes. This procedure was repeated 4 times. Plates were then air dried for 1 hour at RT and unbuffered Tris base (pH 10.5; 100µL; BDH) was placed into the wells to solubilise the cellular protein content. The plates were shaken at 161 X G for 5 minutes on the MRC lab Thermo Shaker to ensure complete dissolution of the protein content (Keepers *et al.*, 1991).

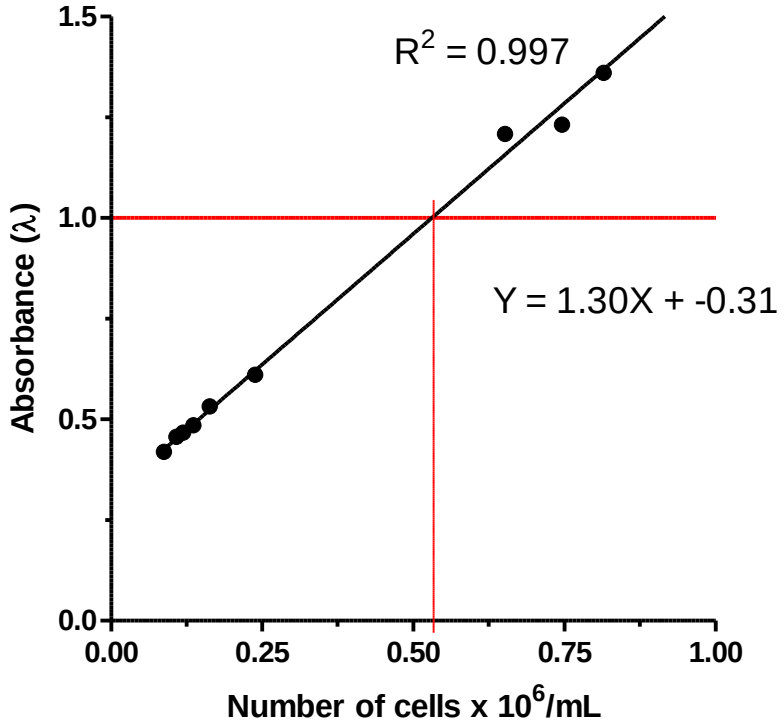

Figure 3.10: The standard curve to determine cell density of the SH-SY5Y cell line for the SRB assay (n=4).

The SRB standard curve was constructed to evaluate the cell number for optimal density attained from the SRB assay.

At an absorbance of 1.0, the optimal cell number per mL was approximately 50,300 cells/mL and this was adjusted to 50,000 cells per mL to equate cell number between cell lines being tested. Control/test compounds were screened at a concentration of 200 µM and the IC_{50} values of those with a cellular viability of less than 60% were determined. SRB was not added to colour control wells for the control/test compounds, PBS (50 µL) was added instead. The positive controls were camptothecin (topoisomerase inhibitor) and methotrexate (folic acid antagonist) (Bischoff *et al.*, 1971; Efferth *et al.*, 2007) and the negative control was incomplete experimental culture media. The absorbance was read at 540 nm on the Labsystems iEMS Reader MF and the IC_{50} values were determined from a log sigmoidal dose response curve using Graphpad Prism® (Version 5.02) software and the percentage cellular viability was determined (Equation 11).

$$\textbf{\% Cellular viability} = \frac{\textbf{Abs}_{\textbf{TC}}\textbf{-Abs}_{\textbf{cell free media}} \textbf{ - Abs}_{\textbf{colour control}}}{\textbf{Abs}_{\textbf{drug free control}} \textbf{ - Abs}_{\textbf{cell free control}}}$$

Equation 11: The calculation for cellular viability for the SRB assay**.**
Where Abs = absorbance; TC = test compounds.

3.5.5. The cellular viability protective effect of compounds and essential oils following copper exposure

Compounds that demonstrated the highest activity in the copper reduction and copper chelation assays (Sections 3.2.2 and 3.2.3) were tested to see whether they reduced copper toxicity within cells.

Following the same protocol as described in Sections 3.5.1, 3.5.2 and 3.5.3; cells were incubated with copper (I) and (II) for 24 hours at 37°C and 5% CO_2. A log sigmoidal dose response curve of copper (I) and (II) were generated to determine concentration of copper that inhibited cellular growth (Figure 4.21). The media was removed and compounds (10 µL; 200 µM) were added and the cells were further incubated at 37°C and in 5% CO_2 humidified environment for 20 hours. The MTT assay protocol (Section 3.5.3) was followed and the cellular viability determined using Equation 10. The cellular viability of the compounds/controls that were incubated in the absence and presence of copper were compared to determine the effect of the compounds on copper toxicity of neuroblastoma cells.

3.5.6. The effect of excess copper on cellular structure

To visualise the effect by which copper (I) and (II) toxicity was affected by test/control compounds, cells were stained with orcein. Orcein is a natural dye used to view copper

proteins and elastic fibres (Kumar and Kiernan, 2010). To a 24-microtiter plate, a cell suspension (360 µL) of 5,000 cells/mL was added and incubated for 6 hours under humidified conditions at 37°C and 5% CO_2. Copper (I) and copper (II) (40 µL), starting at a concentration of 0.25 mM and serially diluted (1:2) to 0.008 mM were added and incubated for 44 hours at 37°C and 5% CO_2. Similarly, a copper free plate was prepared. After incubation, 400 µL of the media was replaced with fresh experimental culture media (360 µL) along with control/ test compounds (40 µL) and further incubated for 4 hours 37°C and 5% CO_2. The cells were fixed in 100% methanol (200 µL) at 4ºC for 6 minutes and washed three times with PBS (200 µL) (Brock, Hamelers and Jovin, 1999). The cells were then stained with 5% eosin (v/v; 200 µL) for 30 minutes at RT being washed three times with sterile ddH_2O (200µL) (Kiernan, 2015). The nuclei of the cells were stained with 0.05% methylene blue (v/v; 200 µL) for 30 minutes at RT and washed three times with sterile ddH_2O (200 µL) (Kiernan, 2015). A 1% (w/v) orcein solution (200 µL; Sigma-Aldrich) was added to each well and incubated for 5 minutes at RT (Shousha and Mitchell, 1983). The cells were treated with an acid-alcohol solution (1 mL 25% hydrochloric acid in 99 mL 70% ethanol) for 10-20 seconds. The cells were washed with sterile ddH_2O and viewed under an inverted microscope at 100X magnification (Shousha and Mitchell, 1983). The copper was stained an orange-red colour against a blue-purple background (Figure 4.24 and Figure 5.16) (Kumar and Kiernan, 2010).

3.6. Antioxidant and pro-oxidant effects of compounds and EOCs

Oxidants may be either destructive or valuable in physiological responses. Beneficial responses include effects against infections and harmful responses are due to oxidant damage of cellular structures such as membranes, lipids and proteins (Halliwell, 2013). Several assays were used to test the antioxidant and pro-oxidant effect of compounds including the DPPH$^{\bullet}$ free radical scavenging assay, the lipid peroxidation inhibition assay, and the nitric oxide concentration (Griess reagent) assay.

3.6.1. The DPPH$^{\bullet}$ free radical scavenging assay

The DPPH$^{\bullet}$ assay determined the antioxidant activity of test compounds in relation to known antioxidant agents such as AA and Trolox™ (Sharma and Bhat, 2009). DPPH$^{\bullet}$ is a stable free radical that has an unpaired valence electron and when it reacts with a compound with antioxidant properties, the latter substance donates a hydrogen atom to the DPPH$^{\bullet}$ (Sharma and Bhat, 2009). When the deep violet colour of DPPH$^{\bullet}$ is reduced it changes to a pale yellow colour, allowing for UV-VIS spectrophotometric detection (Sharma and Bhat, 2009). A factor which affected the stability of DPPH$^{\bullet}$ was light, therefore the stock solution was stored in the dark at 4°C and the reaction plate was incubated in the dark at RT (Sharma and Bhat, 2009; Gülçin, 2011).

The stock solution was prepared to a concentration of 0.1 mM DPPH• (Sigma-Aldrich) in methanol (High performance liquid chromatography grade; Sigma-Aldrich) and this was stored in the dark at 4ºC for 24 hours before being used (Di Mambro *et al.*, 2003). Test compounds (50 µL) were screened at 200 µM and placed in a 96-well microtiter plate in rows B to G in triplicate with a fourth column for colour controls (Figure 3.11).

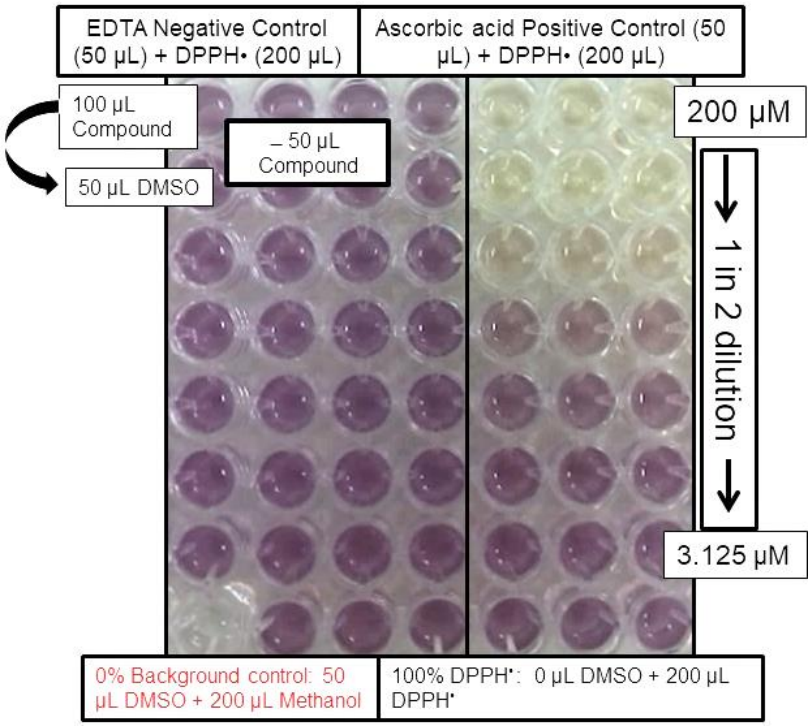

Figure 3.11: The free radical scavenging assay for EDTA and AA.
Free radical scavenging effects of EDTA and AA at various concentrations.

The compounds with activity greater than 60% were further investigated by determining the respective IC_{50} values from log sigmoidal dose response curves. In doing so, eight 1:2 serial dilutions of these compounds (in DMSO) were prepared and 50 µL plated in triplicate from rows B to G, along with 200 µL DPPH•. The 0% background control consisted of 50 µL DMSO and 200 µL methanol, whilst the 100% DPPH• control consisted of 50µL DMSO and 200 µL DPPH•. The colour controls consisted of 50 µL compound and 200 µL methanol. The positive control had 50 µL of the standard antioxidants namely AA, 2,6-Di-tert-butyl-4-methylphenol (BHT), BHA and Trolox™ (Di Mambro *et al.*, 2003). Once the DPPH• (200 µL) was added to the appropriate wells, the plate was placed in the dark for 30 minutes (Gülçin, 2011). The absorbance was then read at 540 nm in the Labsystems iEMS Reader MF, UV-VIS plate reader. The percentage of free radical scavenged by the compound was calculated using

Equation 12. A log sigmoidal dose response curve was plotted using Graphpad Prism® software from which the IC_{50} value was determined.

$$\% \text{ Free radical scavenged} = \frac{Abs_{TC} - Abs_{CC}}{Abs_{100\%} - Abs_{BC}} \times 100$$

Equation 12: The percentage free radical scavenged of test compounds (Gülçin, 2011).
Where Abs = absorbance; TC = Test compound; CC = colour control; BC = background control and 100% = the 100% DPPH control.

3.6.2. The lipid peroxidation inhibition assay

This assay was used to determine whether the test compounds can inhibit the formation of lipid peroxides (Gülçin *et al*., 2007). The sodium phosphate buffer (pH 7.0) was prepared by mixing solution A and solution B in a 122:78 ratio where solution A consisted of 7.12 g $Na_2HPO_4.2H_2O$ (BDH) in 200 mL sterile ddH_2O and solution B consisted of 2.76g $NaH_2PO_4.H_2O$ (Sigma-Aldrich) in 100 mL sterile ddH_2O. The test compounds (50 µL; 200 µM) were incubated in the dark at 37ºC with 125 µL linoleic acid solution, which consisted of 0.5% linoleic acid (51.2 µL; Fluka), 0.5% Tween 20 (51.2 µL; Sigma-Aldrich) and 0.2 M sodium phosphate buffer (10 mL). After 48 hours, 20 µL of this latter solution was reacted with ferrous chloride (40 µL; 20 mM, Fluka), 70% ethanol (900 µL; Rochelle Chemicals) and ammonium thiocyanate (40 µL; 300 g/L Sigma-Aldrich) for 30 minutes in the dark at 37°C. By doing so, the linoleic acid formed peroxides oxidising the ferrous ions to ferric ions, which formed complexes with thiocyanate that resulted in a colour complex that could be spectrophotometrically quantitated (Gülçin *et al*., 2007). The background control consisted of linoleic acid and sodium phosphate buffer and the positive controls were AA and Trolox™. The absorbance was read at 492 nm on the Labsystems iEMS Reader MF and the percentage lipid peroxidation inhibition was calculated using Equation 13 (Gülçin *et al*., 2007).

$$\% \text{ Lipid peroxidation inhibition} = \frac{Abs_{BC} - Abs_{TC}}{Abs_{BC}} \times 100$$

Equation 13: The percentage lipid peroxidation inhibition calculation for test compounds (Gülçin, Elmastat and Aboul-Enein, 2007)**.**
Where Abs = Absorbance; TC = Test Compound and BC = Background Control.

3.6.3. The nitric oxide concentration (Griess reagent) assay

3.6.3.1. Standard curve generation

The nitric oxide concentration or Griess reagent assay was used to verify the colourimetric nitrate/nitrite concentration in cell lines (Chaulya *et al.*, 2010; Ajjuri and O'Donnell, 2013). A

modified method as described by Griess, (1879) was used to determine the concentration of nitric oxide that accumulates in the cells, whilst incubated with the test compounds.

A nitrite standard reference curve (Figure 3.11) was prepared for each experiment and for each medium/buffer to accurately quantify nitrite levels in experimental samples. The 0.1 M nitrite standard was prepared by dissolving sodium nitrite (Sigma-Aldrich) in ddH_2O (Chaulya *et al*., 2010). This solution was diluted to 100 µM in DMEM culture media and DMSO. Three columns were designated in the 96-well microtiter plate for the nitrite standard reference curve. The DMEM culture media or DMSO was dispensed (50 µL) into the wells in rows B–H. The 100 µM nitrite solution (100 µL) was dispensed to the remaining 3 wells in row A and a serial twofold dilution was performed to generate the nitrite standard reference curve. A 0% nitrite control consisted of 50 µL of DMEM culture media or DMSO alone. To each well, 50 µL sulfanilamide solution (10 mg/mL in 5% phosphoric acid) was added, and the incubated for 10 minutes at RT in the dark (Waitumbi and Warburg, 1998). To all wells, 50 µL *N*-(1-naphthyl)ethylenediamine dihydrochloride (NED; 1 mg/mL in sterile ddH_2O) was added. This was incubated in the dark for 10 minutes at RT and the absorbance measured at 520nm using the on the Labsystems iEMS Reader MF. The standard nitrite curve was generated using GraphPad Prism® (Figure 3.12) (Waitumbi and Warburg, 1998; Chaulya *et al.*, 2010).

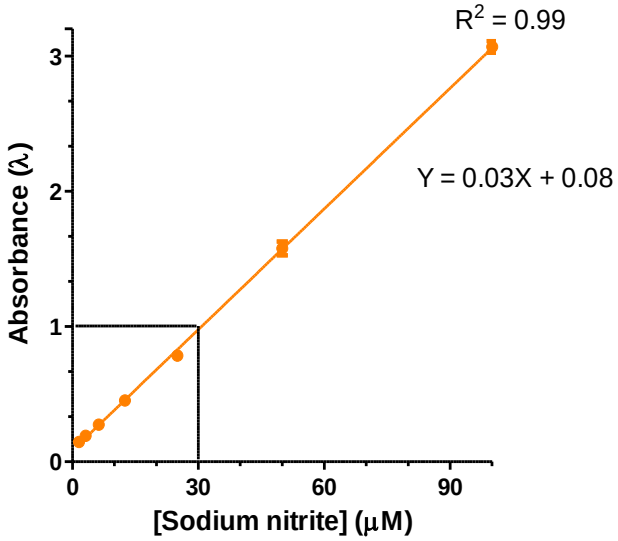

Figure 3.12: Griess standard nitrite curve of sodium nitrite.
A nitrite standard curve was determined by plotting the absorbance value versus the nitrite concentration.

The concentration of nitrite for DMEM at an absorbance value of 1 was determined to be 30 µM and as such this concentration was used when quantifying the nitrite concentration of the sample.

3.6.3.2. Antioxidant activity of compounds and EOCs

Nitric oxide is a well-known mediator in inflammatory reactions leading to cell damage. Nitric oxide has a short half-life, therefore nitric oxide is quantified using its breakdown metabolites, nitrite and nitrate (Li *et al.*, 2017). The metabolites of nitric oxide were measured using the following described methods. Cells were prepared as described in Section 3.5.1. To a 96-well microtiter plate, 50 µL of cells were added and incubated for 2-4 hours at 37°C in 5% CO_2. The compounds/EOCs (200 µM; 50 µL) were then added and incubated for 24 hours at 37°C in 5% CO_2. The 96-well microtiter plate was centrifuged at 252 X G for 5 minutes and 50 µL of supernatant was transferred to a new plate (Waitumbi and Warburg, 1998; Chaulya *et al.*, 2010). The sodium nitrite solution (0.1M) was diluted with ddH_2O to 30 µM and with sulfanilamide (1% w/v; 50 µL) was added to each well and incubated for a further 10 minutes at RT in the dark before NED (0.1 % w/v; 50 µL) was added to each well and incubated for 10 minutes at RT in the dark. The absorbance was measured at 520 nm (Waitumbi and Warburg, 1998; Chaulya *et al*., 2010). The positive controls were AA and gallic acid. The blank control consisted of ddH_2O PBS, sulfanilamide and NED, whilst the untreated control consisted of culture media, sodium nitrite, sulfanilamide and NED. The percentage nitrite formation inhibition was calculated using Equation 14.

$$\% \text{ NO formation inhibited} = 100 - \left(\frac{Abs_{TC} - Abs_{Negative\ control}}{Abs_{100\%\ NO\ control} - Abs_{Negative\ control}} \right) \times 100$$

Equation 14: The percentage nitrite formation inhibited (Waitumbi and Warburg, 1998).

Where Abs = absorbance; TC = test compounds; NO_2^- = nitrite; NO = Nitric oxide.

3.7. Whole organism lethality assays

The toxic effects of 8-OH and its derivatives were determined by means of the *Artemia franciscana* lethality assay and the *Anopheles arabiensis* larvicidal assay.

3.7.1. *Artemia* Lethality assay

The *Artemia* lethality assay was used to test the lethality of the compounds on the *Artemia* organism (*Ar. franciscana*). A modified method as described by Meyer *et al*, (1982) was used. A clearance certificate waiver (*Artemia*) 07-11-2017-O was obtained from the Animal Research Ethics Committee of the University of the Witwatersrand (Appendix A.3).

3.7.1.1. Hatching of nauplii

The *Artemia* eggs (Ocean Nutrition; 0.1 g; stored at 4°C) were hatched in a sea salt solution (Tropic Marin 2.6 M in deionised water) in a continuously aerated developing compartment. The *Artemia* eggs were placed under a lamp in order to provide the optimal light and heat (30°C) source for hatching within 18 hours (Meyer *et al.*, 1982; Fatope *et al*., 1993; Krishnaraju *et al.*, 2005). Subsequently, the *Artemia* were concentrated by decanting the water containing the shrimp into a rectangular plastic container and tilting it towards the lamp light for 30 minutes (Meyer *et al.*, 1982; Fatope *et al*., 1993; Krishnaraju *et al.*, 2005).

3.7.1.2. Treatment of nauplii with compounds

From the concentrate, 20 to 30 live nauplii (50 µL per well) were pipetted to a 48-well plate and sustained at 30°C. Salt water (197.5 µL) was added to each well, before the test compound (2.5 µL) was added to wells in triplicate (Meyer *et al.*, 1982; Fatope *et al*., 1993; Krishnaraju *et al.*, 2005). The negative control was nauplii in salt water and the positive control was nauplii in potassium dichromate (5.4 mM). At time points of 0, 24, 48 and 72 hours, the number of dead *Artemia* were counted microscopically (10X magnification), The *Artemia* were killed at 0, 24, 48 and 72 hours with 50% v/v acetic acid and the total number of *Artemia* per well were counted at 72 hours. The percentage mortality was calculated using Equation 15.

$$\% \text{ Mortality} = \frac{\text{Time}_{24 \text{ or } 48 \text{ hr}} - \text{Time}_{0 \text{ hr}}}{\text{Acetic acid}_{24 \text{ or } 48 \text{ hr}} - \text{Time}_{0 \text{ hr}}} \times 100$$

Equation 15: The percentage mortality of *Artemia* (Meyer *et al.*, 1982; Fatope *et al*., 1993; Krishnaraju *et al.*, 2005).

The median lethal dose (LD_{50}) values and 95% confidence intervals were determined using probit analysis.

3.7.1.3. The morphological effect of test compounds on *Artemia* nauplii

The morphological effects of the test compounds and the negative control were microscopically examined at 40X magnification (Venkateswara *et al.*, 2007) at a timepoint of 24, 48 and 72 hours. The test compounds and the negative control were compared, and the differences were noted using the Olympus CKX41 camera (Wirsam).

3.7.2. Larvicidal assay

The larvicidal assay was used to test the toxic effect the compounds/EOCs has on the dichlorodiphenyltrichloroethane (DDT) susceptible strain of *An. arabiensis* (KGB) malaria vector according to the methods described by WHO (2005). A clearance certificate *Anopheles* Waiver 07-11-2017-O was obtained from the Animal Research Ethics Committee of the

University of the Witwatersrand (Appendix A.4). The larvae and larvae food were acquired from the Botha de Meillon Insectary at the National Institute for Communicable Diseases, Johannesburg. To disposable plastic cups (173.2 cm^2) containing 25 ml of deionized water, 25 third to fourth instar larvae (male or female) were added and fed larvae food daily.

3.7.2.1. Treatment of larvae with compounds

Deionized water (25 mL) was placed in test cups and 250 µL of deionized water was replaced with 200 µM compound/EOC (250 µL). To the test cups, 20 larvae (3^{rd} or 4^{th} instar) were transferred using plastic pipette droppers (WHO, 2005). The negative control was DMSO (100%; 250 µL) and the positive control was DDT (0.5 µM; 250 µL). To each test cup, larvae food was added daily, and a net secured with an elastic band placed over each cup. The test cups were incubated for 24 to 48 hours at 25-28°C. After incubation, the larval mortality was recorded. The larvae were gently probed with a spatula to ensure whether they were dead or moribund (moribund larvae are incapable of rising to the surface and cannot show characteristic diving reaction when water is disturbed) were recorded (WHO, 2005). The pupae development was also recorded. The assay was repeated 5 times for each compound and control to obtain a total number of 100 larvae. The % survival and % mortality was calculated using Equations 16 and 17, respectively. The median lethal dose (LD_{50}) value was determined for compounds with a % mortality greater than 60% by screening the various concentrations and using IBM SPSS® (version 22) analysis to conduct a probit.

$$\% \text{ Survival} = \frac{\text{Number of alive larvae + No. of pupae}}{\text{Number of dead larvae + Number of moribund larvae}} \times 100$$

Equation 16: The percentage survival of larvae treated with test compounds/EOCs (WHO, 2005).

$$\% \text{ Mortality} = \frac{X-Y}{X} \times 100$$

Equation 17: The percentage mortality of larvae treated with test compounds/EOCs (WHO, 2005).

Where X was the percentage survival in the untreated control; Y was the percentage survival in the treated sample.

3.7.2.2. The morphological effect of test compounds on larvae

The morphological effects of the test compounds and the negative control were microscopically examined at 40X magnification. The test compounds and the negative control were compared, and the differences were noted using the Olympus CKX41 camera.

3.8. Drug combination assays

Compounds that demonstrate copper homeostasis and antimalarial activity were combined with chloroquine, quinine or TMB at varying ratios (Table 3.6) and their combined activity determined using the copper chelation, ferriprotoporphyrin biomineralization inhibition and pLDH assays from which eight to ten 1:2 serial dilutions were prepared. Isobolograms were constructed from the ratio values.

Table 3.6: The concentrations of the combination ratios used to construct the isobologram.

Combination solution	Ratio of the IC_{50} value of X to the IC_{50} value of Y	
	Compound X	Compound Y
1	10	0
2	7.5	0.25
3	5	1
4	2.5	1.5
5	2	2
6	1.5	2
7	1	2.5
8	0.5	5
9	0.25	7.5
10	0	10

The fractional inhibitory concentration (FIC) was calculated using Equation 18, where the FIC is the degree of the synergy of an interaction (Elion, Singer and Hitchings, 1954; Berenbaum, 1978). A synergistic interaction is when a combination of agents results in the total outcome of the effects of the agents are greater than the sum of the individual effects of each agent, an additive interaction is the resultant sum of the combination of the two agents and an antagonistic interaction is when the effect of one agent inhibits the effect of the other agent when in combination (Berenbaum, 1978).

$$\textbf{FIC50} = \frac{\textbf{IC}_{50}\ \textbf{value of ratio of}\ TC_X\ \textbf{in combination}}{\textbf{IC}_{50}\ \textbf{value of}\ TC_X\ \textbf{alone}}$$

Equation 18: The FIC_{50} values of the test compounds at each ration was determined using the IC_{50} values of the IC_{50} values in combination and the IC_{50} values of compounds alone X or T (Berenbaum, 1978).

Where TC = Test compound; CC = Control compound; X = ratio of test compound/EOC

Using the FIC values, the isobologram was constructed to determine whether the compounds had a synergistic, additive, or antagonistic interaction as depicted in Figure 3.13.

The degree of the interaction, which is equivalent to the sum of the FIC_{50} values (ΣFIC_{50}) for the two test compounds/control drug at each combination ratio (Table 3.6), was then calculated (Berenbaum, 1978). The cut-off points used to define the possible interactions differ amongst authors, therefore, for the purpose of this study a $\Sigma FIC_{50} < 0.75$ indicates synergism, a $0.75 < \Sigma FIC_{50} < 1.75$ indicates an additive relationship, and a $\Sigma FIC_{50} > 1.75$ indicates antagonism (Figure 3.13) (Fidock *et al*., 2004).

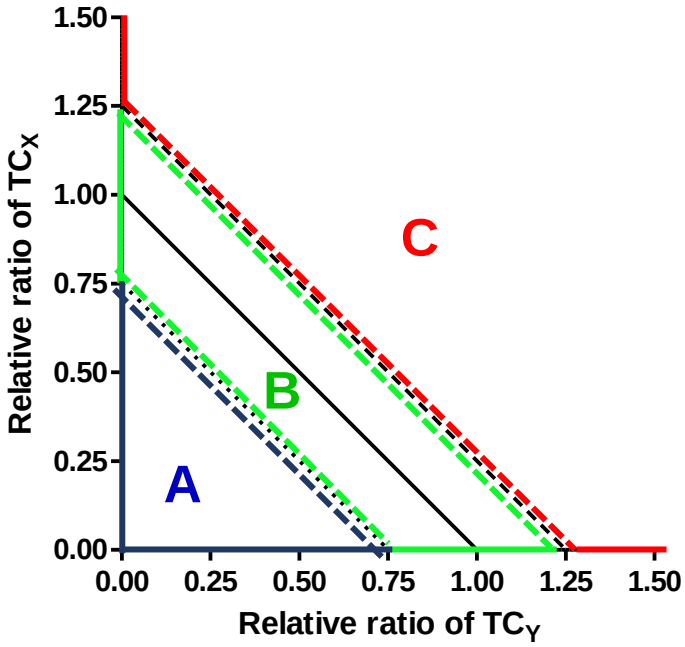

Figure 3.13: An isobologram showing the possible interactions between test compound X (TC_X) and test compound Y (TC_Y); where the points below 0.75, between 0.75 to 1.25 and above 1.25 depicted a synergistic (A), additive (B) and antagonist (C) interaction (Berenbaum, 1978).

3.9. Data analysis and statistics

Each assay was repeated at least in triplicate, with the compounds tested in triplicate per assay. For larvae, each compound was tested once per experiment and the experiment repeated five times to produce a mean and standard deviation. The student t-test statistical analysis was determined to examine variance to the controls using GraphPad Prism version 5.0. Differences were considered significant at $P < 0.05$.

Chapter 4. 8-Hydroxyquinoline Results

4.1.1. Copper Homeostasis

4.1.1.1. Metal complexation and copper chelation

The metal complexation and copper chelation of compounds were tested against both coppers - (I) and - (II). The peak wavelengths of the compounds with copper were determined by UV-spectral analysis of a range of absorbances (200 to 900 nm). The metal complexation assay determined the interaction of the compounds with copper in comparison to the wavelength at which the peak absorbance of the compound alone and copper alone occurred. The hydroxylamine standard curve (Figure 4.1) validates that the free copper ions that did not form chelates, were oxidized to copper (I) ions, and were detected using neocuproine. The results of the compounds that demonstrated copper chelation and metal ion complexation are reported in Table 4.1 and Table 4.2.

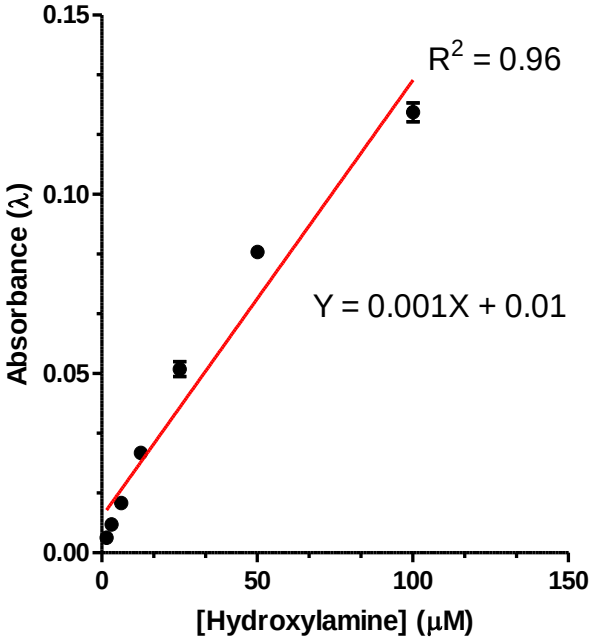

Figure 4.1: The hydroxylamine standard curve. An R squared value of 0.96, indicates that the hydroxylamine standard curve justifies the variability of the data around its mean (NCSS, 2020).

As shown in Table 4.1, several compounds displayed a higher copper (I) chelation activity in comparison to the control, TMB: 5,7-diiodo-8-OH > 5-nitro-8-OH > 5,7-dichloro-2-methyl-8-OH > 5,7-dichloro-8-OH > 5-HSO_3-7-iodo-8-OH > 5-chloro-7-iodo-8-OH > 5,7-dibromo-8-OH > N-butyl-2,2-imino-di-(8-OH) > 5-chloro-7-bromo-8-OH > 5-chloro-8-OH > 5,7-dimethyl-8-OH > 5-HSO_3-8-OH > 5-amino-8-OH.

Table 4.1: The copper chelation of compounds, where the chemical structures can be seen in Figure 3.1 and Table 3.2.

Compound	% Copper (I) Chelation [Significant difference to TMB control]	% Copper (II) Chelation [Significant difference to TMB control]
TMB	76.77 ± 1.32	84.77 ± 0.86
TET	38.15 ± 1.48 [Yes (P = 0.001)]	27.34 ± 5.96 Yes (P = 0.004)
D-Penicillamine	21.56 ± 1.28 [Yes (P < 0.0001)]	37.89 ± 0.09 Yes (P = 0.002)
5,7-Diiodo-8-OH	116.89 ± 5.22 [Yes (P = 0.01)]	45.54 ± 4.04 Yes (P = 0.004)
5-HSO_3-7-iodo-8-OH	107.14 ± 10.49 [Yes (P = 0.02)]	26.06 ± 6.67 Yes (P = 0.003)
5,7-Dichloro-8-OH	104.72 ± 17.39 [No (P = 0.08)]	30.92 ± 1.14 Yes (P = 0.0003)
5-Chloro-7-iodo-8-OH	102.90 ± 5.78 [Yes (P = 0.02)]	27.16 ± 5.77 Yes (P = 0.0020)
5,7-Dibromo-8-OH	102.30 ± 16.35 [No (P = 0.06)]	25.36 ± 3.26 Yes (P = 0.0006)
N-butyl-2,2-imino-di-(8-OH)	101.67 ± 9.26 [Yes (P = 0.04)]	117.80 ± 15.08 No (P = 0.80)
5-HSO_3-8-OH	100.50 ± 3.14 [Yes (P = 0.02)]	50.13 ± 1.72 Yes (P = 0.002)
5-Nitro-8-OH	99.85 ± 12.10 [No (P = 0.09)]	21.57 ± 1.53 Yes (P = 0.0005)
5,7-Dichloro-2-methyl-8-OH	98.74 ± 10.93 [No (P = 0.09)]	27.80 ± 5.52 Yes (P = 0.002)
5-Chloro-7-bromo-8-OH	95.97 ± 6.57 [Yes (P = 0.04)]	26.10 ± 3.97 Yes (P = 0.002)
5-Chloro-8-OH	94.11 ± 9.81 [No (P = 0.11)]	26.44 ± 2.69 Yes (P = 0.0003)
5,7-Dimethyl-8-OH	89.71 ± 13.57 [No (P = 0.21)]	35.45 ± 1.66 Yes (P = 0.0008)
5-Amino-8-OH	52.35 ± 8.79 [Yes (P = 0.04)]	24.85 ± 2.63 Yes (P = 0.001)
2-Amino-8-OH	29.79 ± 1.17 [Yes (P = 0.0004)]	27.54 ± 6.15 Yes (P = 0.003)
8-OH	23.90 ± 0.29 [Yes (P = 0.0003)]	24.42 ± 2.19 Yes (P = 0.0003)
2-Benzyl-8-OH	7.44 ± 2.01 [Yes (P < 0.0001)]	1.22 ± 0.21 Yes (P = 0.0006)
8-Chloro-2-OH	7.43 ± 0.88 [Yes (P < 0.0001)]	3.55 ± 1.88 Yes (P = 0.0004)
5-Carboxy-8-OH	7.33 ± 0.18 [Yes (P = 0.0001)]	3.95 ± 0.98 Yes (P = 0.0001)
8-Fluoro-4-OH	6.63 ± 0.57 [Yes (P = 0.0001)]	≤ 0.01
2-Methyl-8-OH	5.91 ± 0.56 [Yes (P = 0.0002)]	1.30 ± 1.20 Yes (P = 0.0009)
4-OH	5.72 ± 0.29 [Yes (P = 0.0001)]	≤ 0.01
Quinine	21.60 ± 0.16 [Yes (P = 0.0002)]	13.81 ± 0.57 Yes (P = 0.0001)

* Neocuproine was the colourmetric indicator in the assay therefore % copper chelation not determined.

The 8-OH derivatives chelated copper (I) more favourably than copper (II) (Table 4.1). N-butyl-2,2-imino-di-(8-OH) demonstrated notable copper (I) chelation activity (≥ 90%) which was greater than the TMB control and comparable to the activity that was demonstrated in the copper (II) chelation activity. 8-OH and 2-amino-8-OH showed comparable copper (I) and (II) chelation assay activity. A significant difference ($P \leq 0.05$) was shown between the compounds except for 5,7-dichloro-8-OH and 5,7-dibromo-8-OH and the TMB control, namely 8-chloro-2-OH, 2-benzyl-8-OH, 8-fluoro-4-OH, 2-methyl-8-OH, 4-OH and 5-carboxy-8-OH which demonstrated a copper (II) chelation activity that was less than 10%.

The IC_{50} values of the compounds in the copper chelation assay were determined and are shown in Figure 4.2. In Figure 4.2, N-butyl-2,2-imino-di-(8-OH) demonstrated an IC_{50} value that was approximately ten times more potent than that of the TMB control in the copper (I) chelation assay. N-butyl-2,2-imino-di-(8-OH) demonstrated an IC_{50} value that was comparable to the TMB control in the copper (II) chelation assay. In the copper (I) chelation assay, the IC_{50} value of N-butyl-2,2-imino-di-(8-OH) was significantly different ($P = 0.003$) to the TMB control. In the copper (II) chelation assay, the IC_{50} value of N-butyl-2,2-imino-di-(8-OH) was not significantly different ($P = 0.46$) to the TMB control.

For results showing percentages greater than 100% (Table 4.1, Table 4.5, Table 4.10 and Table 4.12), may be explained by the propagation of uncertainty effect of variables. Uncertainties arise as a result of one or more measurement limitations such as instrument precision, solution purity, liquid handling, transfer failures etc (Ellison and Williams, 2000). These uncertainties may affect the variables which are the 3 values that were obtained from the assay measurements. The uncertainty is shown using the standard deviation which quantifies the result and its error (Ellison and Williams, 2000). Therefore, the confidence limit (upper and lower limits of the standard deviation) of a value describes the region within which the true value of the variable may be found (Ellison and Williams, 2000).

N-butyl-2,2-imino-di-(8-OH) demonstrated the highest activity in copper (I) and –(II) metal complexation. This activity was significantly different for copper (I) metal complexation and not significantly different to the TMB control for copper (II) metal complexation (Table 4.2). 5-Chloro-7-iodo-8-OH, 5,7-diiodo-8-OH and 5-chloro-7-bromo-8-OH demonstrated a copper (I) metal complexation activity greater than 70%. 5-Nitro-8-OH and 5,7-dimethyl-8-OH demonstrated copper (I) metal complexation greater than 70%. 5-Amino-8-OH and 2-amino-8-OH had comparable copper (I) activity to one another (Table 4.2). 5-Carboxy-8-OH demonstrated a copper (II) metal complexation activity greater than 70% which was significantly different to the TMB control ($P = 0.002$). 5-Amino-8-OH and 5-HSO_3-7-iodo-8-OH

also demonstrated notable copper (II) metal complexation activity. The compounds demonstrated a more favourable activity to copper (I) than to copper (II) metal complexation.

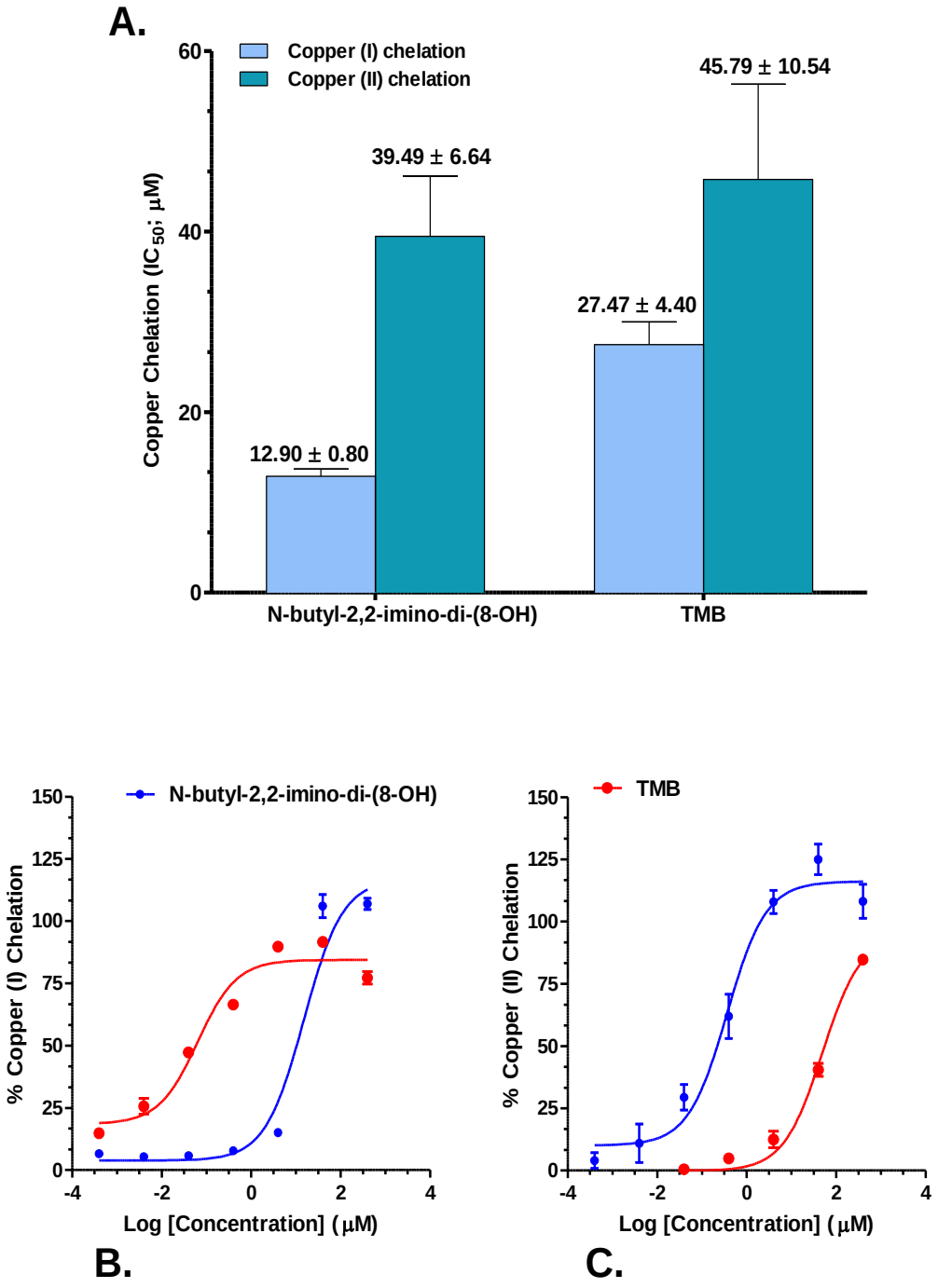

Figure 4.2: The IC_{50} values (A) and non-linear regression graphs (B and C) of N-butyl-2,2-imino-di-(8-OH) and TMB for copper (I)- and (II) chelation.

The IC_{50} value of N-butyl-2,2-imino-di-(8-OH) showed a stronger affinity than the TMB control in the copper (I) chelation assay and a similar action in the copper (II) chelation assay.

Table 4.2: The copper complexation effects of compounds.

Compound	% Copper (I) complexation	Significant difference to TMB control	% Copper (II) complexation	Significant difference to TMB control	Compound alone	Combination copper (I)	Combination copper (II)
					Peak wavelength (nm)		
TMB	59.41 ± 1.12	-	89.66 ± 0.27	-	350	350	350
Neocuproine	49.93 ± 7.10	No (P = 0.18)	27.30 ± 5.09	No (P = 0.12)	350	450	320
D-Penicillamine	26.44 ± 3.82	Yes (P = 0.004)	38.44 ± 1.98	Yes (P = 0.0005)	425	430	640
TET	15.26 ± 2.09	Yes (P = 0.0003)	28.81 ± 4.82	Yes (P = 0.002)	350	ND	350
Chloroquine	40.29 ± 3.17	Yes (P = 0.005)	39.27 ± 5.20	Yes (P = 0.004)	370	680	330
Quinine	33.17 ± 3.98	Yes (P = 0.004)	38.45 ± 9.27	Yes (P = 0.01)	360	320	340
N-butyl-2,2-imino-di-(8-OH)	91.53 ± 0.68	Yes (P = 0.001)	88.77 ± 1.74	No (P = 0.50)	365	340	330
5-nitro-8-OH	78.23 ± 5.28	Yes (P = 0.03)	57.14 ± 1.91	Yes (P = 0.002)	364	430	420
5-chloro-7-iodo-8-OH	75.58 ± 1.23	Yes (P = 0.01)	58.47 ± 4.37	Yes (P = 0.006)	320	410	470
5,7-diiodo-8-OH	73.84 ± 2.88	Yes (P = 0.002)	55.59 ± 3.77	Yes (P = 0.004)	330	410	340
5-chloro-7-bromo-8-OH	71.39 ± 1.69	Yes (P = 0.02)	49.72 ± 4.59	Yes (P = 0.004)	500	420	320
5,7-dimethyl-8-OH	70.14 ± 1.03	Yes (P = 0.001)	42.07 ± 5.11	Yes (P = 0.004)	320	425	330
8-chloro-2-OH	68.93 ± 9.80	No (P = 0.20)	11.46 ± 1.41	Yes (P = 0.007)	330	340	330
5,7-dichloro-8-OH	67.79 ± 1.97	Yes (P = 0.02)	53.75 ± 3.15	Yes (P = 0.002)	312	410	320
5,7-dichloro-2-methyl-8-OH	57.70 ± 0.89	No (P = 0.53)	63.07 ± 1.57	Yes (P = 0.001)	310	400	350
5,7-dibromo-8-OH	63.37 ± 8.28	No (P = 0.51)	55.58 ± 3.14	Yes (P = 0.002)	320	410	325
2-amino-8-OH	60.10 ± 6.31	No (P = 0.86)	55.59 ± 5.13	Yes (P = 0.008)	347	380	340
5-amino-8-OH	59.00 ± 4.45	No (P = 0.91)	65.93 ± 6.12	Yes (P = 0.02)	363	500	360
5-HSO_3-7-iodo-8-OH	57.85 ± 2.46	No (P = 0.52)	60.62 ± 9.02	Yes (P = 0.03)	313	316	380
5-carboxy-8-OH	56.88 ± 4.97	No (P = 0.55)	73.15 ± 4.30	Yes (P = 0.02)	325	360	370
5-HSO_3-8-OH	55.75 ± 2.09	No (P = 0.11)	46.86 ± 1.72	Yes (P = 0.0004)	362	397	317
5-chloro-8-OH	55.14 ± 1.23	Yes (P = 0.04)	43.04 ± 2.83	Yes (P = 0.001)	328	412	393
8-OH	52.36 ± 8.43	No (P = 0.33)	45.42 ± 7.04	Yes (P = 0.008)	342	400	380
2-methyl-8-OH	37.99 ± 2.32	No (P = 0.01)	46.12 ± 2.92	Yes (P = 0.001)	361	388	367
8-fluoro-4-OH	15.43 ± 3.25	Yes (P = 0.003)	3.22 ± 5.71	Yes (P = 0.001)	317	317	314
4-OH	8.49 ± 5.70	Yes (P = 0.003)	11.36 ± 3.42	No (P = 0.15)	332	332	324
2-benzyl-8-OH	4.24 ± 2.16	Yes (P = 0.0008)	7.85 ± 4.23	Yes (P = 0.0008)	322	322	322

The peak absorbance of the metal complexation of compounds were determined and the absorption spectra are shown in Figure 4.3, Figure 4.4, Figure 4.5, and Figure 4.6. In Figure 4.3, a spectral shift to the right and upwards can be seen when 5-nitro-8-OH was combined with copper (I) when compared to the spectrums of 5-nitro-8-OH and copper (I) alone. This demonstrates that an interaction between 5-nitro-8-OH and copper (I) occurred.

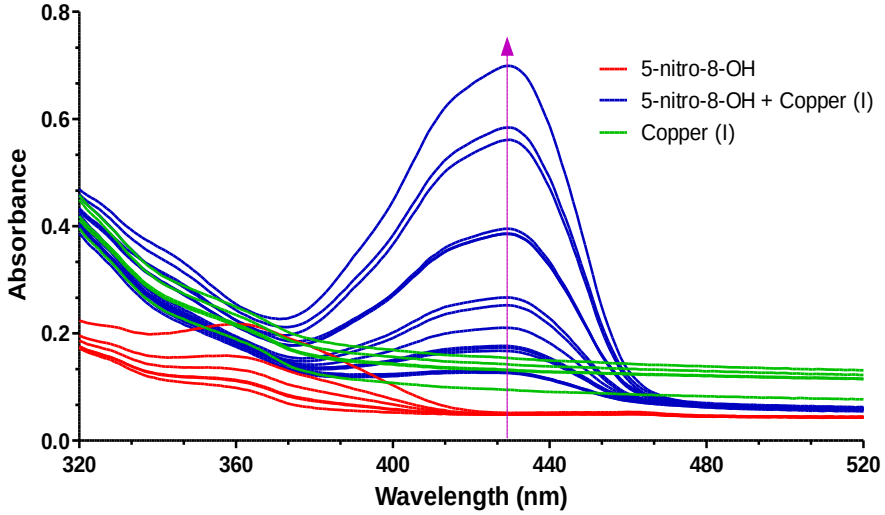

Figure 4.3: The absorption spectrum for copper (I) alone, 5-nitro-8-OH alone and in combination with copper (I).

The absorption spectrum and the peak wavelength (vertical violet line) of the compounds were determined starting at a concentration of 1 mM and diluted to 0.5, 0.25, 0.125, 0.0625, 0.03125 and 0.016 mM for both copper (I) and 5-nitro-8-OH where each line represents a different concentration. The peak wavelength of 5-nitro-8-OH/copper (I) metal complexation was determined to be approximately 430 nm.

In Figure 4.4, a spectral shift upwards can be seen when N-butyl-2,2-imino-di-(8-OH) was combined with copper (I) when compared to the spectrums of N-butyl-2,2-imino-di-(8-OH) and copper (I) alone. This shows that an interaction between N-butyl-2,2-imino-di-(8-OH) and copper (I) occurred.

In Figure 4.5, a spectral shift upwards and to the right was observed when 5-HSO_3-7-iodo-8-OH was combined with copper (II) when compared to the spectrums of 5-HSO_3-7-iodo-8-OH and copper (II) alone. This displays the interaction that occurred between 5-HSO_3-7-iodo-8-OH and copper (II).

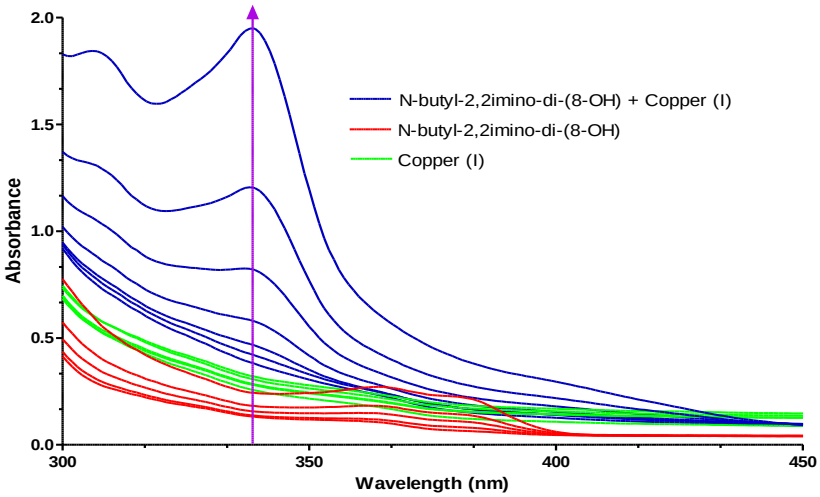

Figure 4.4: The absorption spectrum for copper (I) alone, N-butyl-2,2-imino-di-(8-OH) alone and in combination with copper (I).

The absorption spectrum and the peak wavelength (vertical violet line) of the compounds were determined starting at a concentration of 1 mM and diluted to 0.5, 0.25, 0.125, 0.0625, 0.03125 and 0.016 mM for both copper (I) and N-butyl-2,2-imino-di-(8-OH) where each line represents a different concentration. The peak wavelength of N-butyl-2,2-imino-di-(8-OH)/copper (I) metal complexation was determined to be approximately 340 nm.

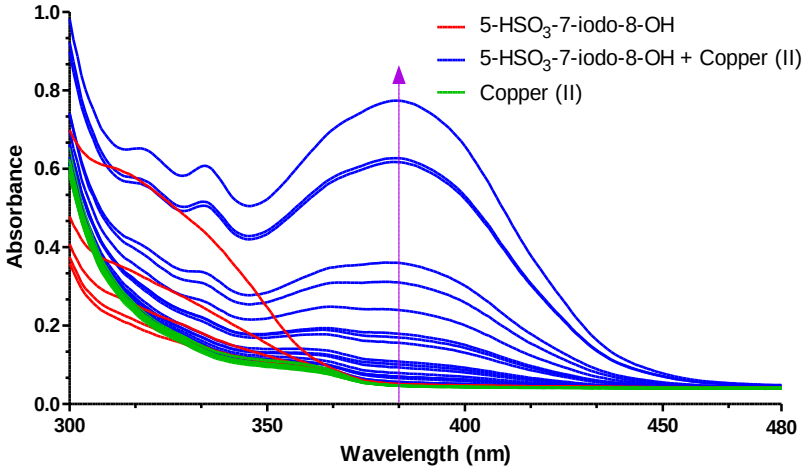

Figure 4.5: The absorption spectrum for copper (II) alone, 5-HSO_3-7-iodo-8-OH alone and in combination with copper (II).

The absorption spectrum and the peak wavelength (vertical violet line) of the compounds were determined starting at a concentration of 1 mM and diluted to 0.5, 0.25, 0.125, 0.0625, 0.03125 and 0.016 mM for both copper (II) and 5-HSO_3-7-iodo-8-OH where each line represents a different concentration. The peak wavelength of 5-HSO_3-7-iodo-8-OH /copper (II) metal complexation was determined to be approximately 380 nm.

In Figure 4.6, an elongation of the absorption spectrum upwards was observed when N-butyl-2,2-imino-di-(8-OH) was combined with copper (II) when compared to the spectrums of N-butyl-2,2-imino-di-(8-OH) and copper (II) alone. This showed the existence of an interaction between N-butyl-2,2-imino-di-(8-OH) and copper (II).

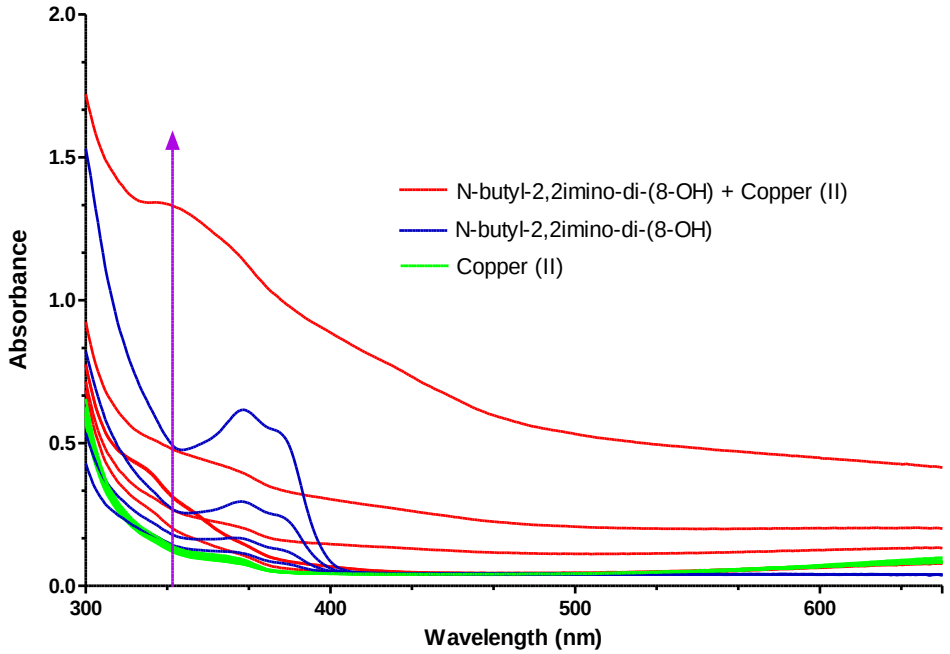

Figure 4.6: The absorption spectrum for copper (II) alone, N-butyl-2,2-imino-di-(8-OH) alone and in combination with copper (II).

The absorption spectrum and the peak wavelength (vertical violet line) of the compounds were determined starting at a concentration of 1 mM and diluted to 0.5, 0.25, 0.125, 0.0625, 0.03125 and 0.016 mM for both copper (II) and N-butyl-2,2-imino-di-(8-OH) where each line represents a different concentration. The peak wavelength of N-butyl-2,2-imino-di-(8-OH)/copper (II) metal complexation was determined to be approximately 380 nm.

4.1.1.2. Copper chelation combinations

The results for the copper chelation combinations of and N-butyl-2,2-imino-di-(8-OH) with quinine and TMB are shown in Figure 4.8. Based on the IC_{50} values in Figure 4.2, the most active compound, namely N-butyl-2,2-imino-di-(8-OH) was combined with TMB and quinine. The isobologram for the combinations of N-butyl-2,2-imino-di-(8-OH) with quinine or TMB were constructed using Table 3.6 and Table 4.3. The log sigmoidal dose response curves for the combinations are shown in Figure 4.7.

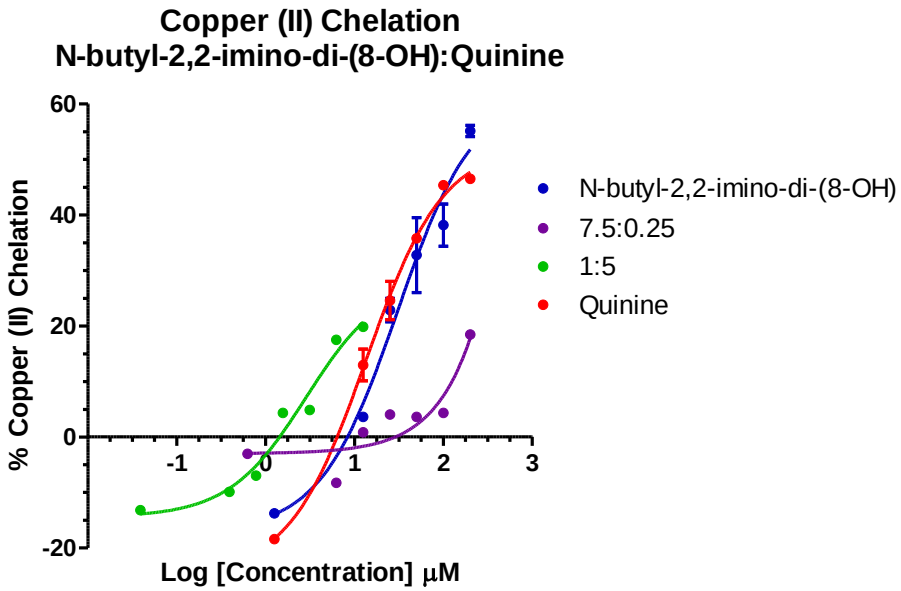

Figure 4.7: The log sigmoidal dose response curves of the combinations of N-butyl-2,2-imino-di-(8-OH) with quinine in the copper (II) chelation assay.

Table 4.3: The FIC_{50} values used to calculate the ΣFIC for the copper chelation assay.

FIC_{50} values				
Ratio N-butyl-2,2-imino-di-(8-OH): Control	**Copper (I)**		**Copper (II)**	
	N-butyl-2,2-imino-di-(8-OH): Quinine	**N-butyl-2,2-imino-di-(8-OH): TMB**	**N-butyl-2,2-imino-di-(8-OH): Quinine**	**N-butyl-2,2-imino-di-(8-OH): TMB**
7.5:0.25	0.13	0.03	0.03	0.50
5:1	0.14	0.12	0.007	0.78
2.5:1.5	0.44	0.31	0.25	0.22
2:2	0.56	0.04	0.38	0.19
1:5	0.34	0.17	0.63	0.17
0.25:7.5	0.68	0.25	0.06	0.07

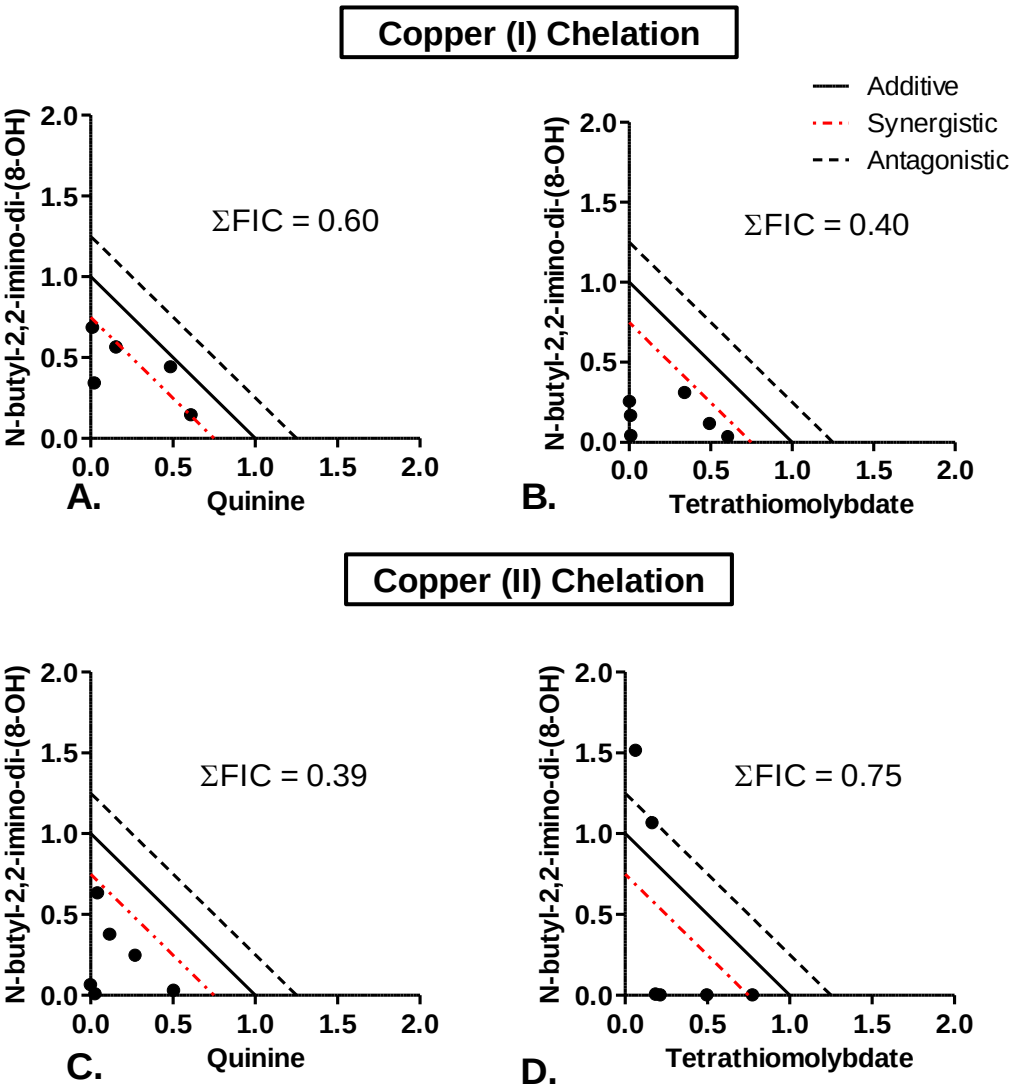

Figure 4.8: The combination copper chelation results of N-butyl-2,2-imino-di-(8-OH) and Quinine (A and C) and TMB (B and D).

N-butyl-2,2-imino-di-(8-OH) demonstrated a synergistic copper chelation interaction when combined with TMB (against copper (I)), N-butyl-2,2-imino-di-(8-OH) when combined with quinine against copper (I) and when combined with quinine (against copper (II)). An additive interaction was seen when N-butyl-2,2-imino-di-(8-OH) was combined with TMB against copper (II).

4.1.1.3. Copper reduction

The copper reduction assay measures the amount of copper (II) reduced to copper (I) as a marker of antioxidant activity (Section 3.2.3). The antioxidant activity or copper reduction activity of the test and control compounds at the equivalent concentration of the activity of Trolox™ starting at 200 µM are reported in Table 4.4. BHA is a known antioxidant and was used as a comparison to the test compounds. Activity of test compounds greater than 30% is shown in Table 4.4, along control compounds and the 8-OH parent compound for comparison.

The compounds did not show a significant difference to the BHA control (P > 0.05), whilst AA (P = 0.02) and EDTA (P = 0.0003) were significantly different to BHA. 2-Amino-8-OH and 2-methyl-8-OH had the highest TEAC value. The remaining compounds were active within the range of 2.75 to 14.94 µM (Appendix C.3, Table C.2).

Table 4.4: The Trolox™ equivalent antioxidant capacity, as determined by the copper reduction assay.

Compound	TEAC at 200 µM	Significant difference to BHA control (P < 0.05)
BHA	135.32 ± 18.73	-
TMB	371.39 ± 22.61	Yes (P = 0.001)
2-Methyl-8-OH	149.33 ± 18.47	No (P = 0.41)
2-Amino-8-OH	105.94 ± 10.18	Yes (P = 0.03)
Camptothecin	51.75 ± 2.14	Yes (P = 0.02)
Quinine	49.14 ± 3.60	Yes (P = 0.02)
Chloroquine	27.22 ± 3.32	Yes (P = 0.007)
5,7-Dimethyl-8-OH	32.31 ± 3.19	Yes (P = 0.01)
5-Amino-8-OH	32.02 ± 5.31	Yes (P = 0.02)
AA	22.39 ± 3.90	Yes (P = 0.01)
D-Penicillamine	14.31 ± 2.35	Yes (P = 0.004)
EDTA	6.05 ± 2.03	Yes (P = 0.001)
8-OH	3.06 ± 0.72	Yes (P = 0.007)

The TEAC values of 2-amino-8-OH and 2-methyl-8-OH (Figure 4.9) at several concentrations (200, 100, 50, 25, 12.5, 6.25 and 3.125 µM) were determined and was similar to the BHA and comparable to Trolox™. An R squared value of 0.99 for Trolox™, indicating that the curve justifies the variability of the data around its mean (Figure 4.9).

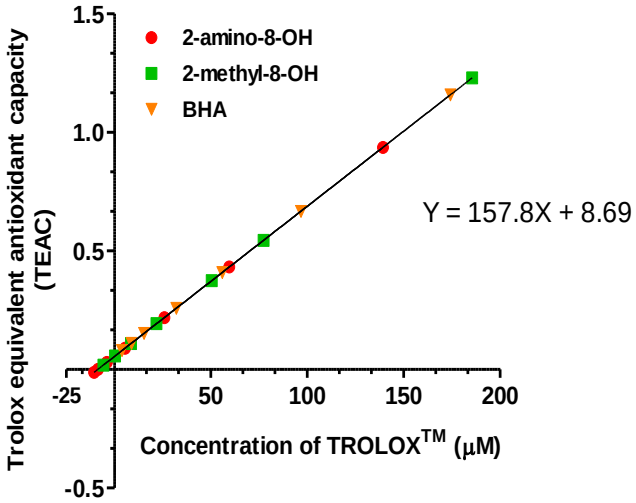

Figure 4.9: The linear regression curve showing the interpolated values for the compounds with the highest TEAC values and the negative control EDTA.

4.1.2. Anti-malarial investigations

4.1.2.1. Inhibition of *in vitro* malaria parasite growth

Compounds affecting copper homeostasis (Section 4.1.1) were tested for *in vitro* antimalarial activity (Table 4.5). Several 8-OH's inhibited parasite growth by more than 60% at a concentration of 200 µM, however, they were not as active as the chloroquine and quinine (Table 4.5). The 8-OH derivatives that demonstrated the highest percentage parasitaemia inhibition were 2-amino-8-OH, N-butyl-2,2-imino-di-(8-OH), 5,7-dibromo-8-OH, 2-benyzyl-8-OH, 8-OH, 8-chloro-2-OH, 5-amino-8-OH, 5-nitro-8-OH, 5-chloro-7-iodo-8-OH, 5,7-dichloro-8-OH and 5-HSO_3-7-iodo-8-OH (Table 4.5).

The IC_{50} values of those which inhibited greater than 50% parasite growth were determined (Figure 4.10). The compounds that demonstrated an IC_{50} value lower than 1 µM were: 5,7-dichloro-8-OH, BHA, N-butyl-2,2-imino-di-(8-OH) and bathocupriene (Table 4.5). 5,7-Dibromo-8-OH, 2-benzyl-8-OH, 8-chloro-2-OH and 5-chloro-7-iodo-8-OH all demonstrated a percentage parasitaemia inhibition greater than 70%, however the IC_{50} values that were determined for these compounds were greater than 100 µM. In contrast, 8-OH, 5,7-dimethyl-8-OH and 5-HSO_3-7-iodo-8-OH showed a percentage parasitaemia inhibited greater than 70%.

Table 4.5: The IC_{50} values of the compounds against the *P. falciparum* 3D7 malaria strain were determined for all the compounds that inhibited >60% of parasite growth an initial screen at 200 µM using the pLDH assay.

Compounds	IC_{50} value (µM) [% Parasite growth at 200 µM]	Significant difference to the IC_{50} value of chloroquine control
Chloroquine	0.07 ± 0.003	-
DHA	0.003 ± 0.0004	Yes (P = 0.0005)
Quinine	0.11 ± 0.02	No (P = 0.06)
5,7-Dichloro-8-OH	0.19 ± 0.04	No (P = 0.34)
BHA	0.23 ± 0.05	Yes (P = 0.01)
N-Butyl-2,2-imino-di-(8-OH)	0.58 ± 0.03	Yes (P = 0.004)
Bathocuproine	0.65 ± 0.12	Yes (P = 0.007)
TMB	1.30 ± 0.13	Yes (P = 0.002)
BHT	1.24 ± 0.22	Yes (P = 0.006)
Cupferron	3.22 ± 0.72	Yes (P = 0.009)
5-HSO_3-7-iodo-8-OH	5.82 ± 0.41	Yes (P = 0.0009)
2-Amino-8-OH	15.64 ± 1.49	Yes (P = 0.002)
5-Amino-8-OH	15.19 ± 3.59	Yes (P = 0.009)
5,7-Dimethyl-8-OH	22.33 ± 0.88	Yes (P = 0.0003)
8-OH	34.97 ± 2.75	Yes (P = 0.001)
D-Penicillamine	45.88 ± 0.86	Yes (P < 0.0001)
5,7-Dibromo-8-OH	>200 [87.33 ± 3.41%]	***
2- Benzyl-8-OH	>200 [78.98 ± 9.62%]	***
8-Chloro-2-OH	>200 [76.13 ± 9.01%]	***
5-Chloro-7-iodo-8-OH	>200 [74.55 ± 1.01%]	***
5-Nitro-8-OH	>200 [74.36 ± 2.98%]	***
5-Chloro-8-OH	>200 [63.88 ± 9.18%]	***
5,7-Diiodo-8-OH	>200 [56.59 ± 52.69%]	ND
5,7-Dichloro$_2$-2-CH_3-8-OH	>200 [53.26 ± 14.78%]	ND
5-Chloro-7-bromo-8-OH	>200 [47.32 ± 1.57%]	***
4-OH	>200 [45.35 ± 23.18%]	ND
2-Methyl-8-OH	>200 [44.00 ± 8.54%]	***
Neocuproine	>200 [42.18 ± 8.50%]	ND
5-HSO_3-8-OH	>200 [41.94 ± 21.87%]	***
8-Fluoro-4-OH	>200 [37.23 ± 31.37%]	ND
TET	>200 [32.94 ± 3.69%]	ND
5-carboxy-8-OH	[≤ 0.01%]	**

**Not determined as % parasite growth less than 50%; ***Could not determine IC_{50} value and P value due to non-convergence of nonlinear regression; ND = Not determined.

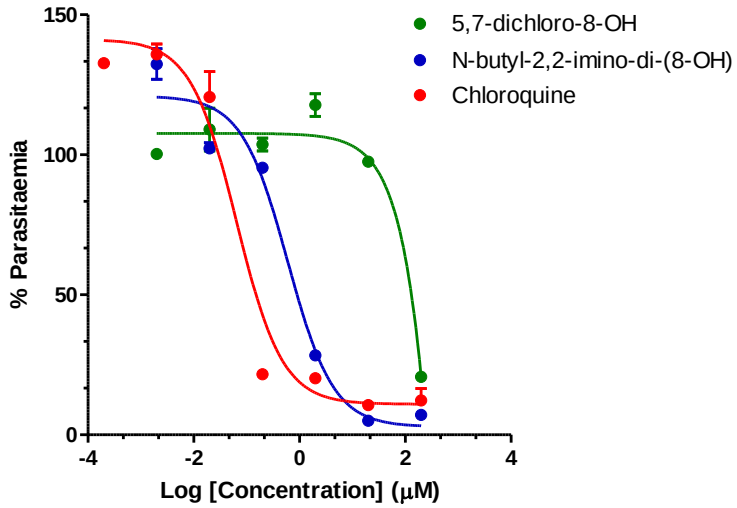

Figure 4.10: The sigmoidal log-dose response curve of the malaria parasite when exposed to 5,7-dichloro-8-OH, N-butyl-2,2-imino-di(8-OH) and chloroquine as determined by the pLDH assay.

4.1.2.1.1. The effect of the 8-OH derivatives on parasitic stage, parasitaemia and the morphology of the parasite

The 8-OH derivative, namely, N-butyl-2,2-imino-di-(8-OH) (Section 4.1.1) that showed considerable activity across the copper homeostasis assays namely, the copper chelation, metal complexation and the copper reduction assays, was incubated with synchronised parasites over 72 hours in comparison to quinine (Figure 4.11 and Table 4.6). The stages proceeded normally as rings, trophozoites and schizonts in a 48-hour cycle with gametocytes forming under stressful conditions (Table 4.6, Untreated controls, 36 hours).

In Table 4.6 and Figure 4.11, the following was observed at different timepoints:

- *0 to 6 hours:* No significant changes in morphology observed at this point however the parasitaemia of quinine and N-butyl-2,2-imino-di-(8-OH) are lower than that of the untreated control (Table 4.6). The total % parasitaemia (Figure 4.11, graph D) was at the highest point for the untreated control, N-butyl-2,2-imino-di-(8-OH) and quinine.
- *12 hours:* No changes in morphology was observed when comparing N-butyl-2,2-imino-di-(8-OH) and quinine to the untreated control. A decrease in the % parasitaemia in the rings (Figure 4.11, graph A) and increase in % parasitaemia in trophozoites (Figure 4.11, graph B) was observed as expected. The untreated control had a higher total % parasitaemia in comparison to N-butyl-2,2-imino-di-(8-OH) and quinine. N-butyl-2,2-imino-di-(8-OH) had a slightly higher total % parasitaemia in comparison to quinine. An approximated 2% decrease in total % parasitaemia was observed for quinine and 1% decrease for N-butyl-2,2-imino-di-(8-OH).

Table 4.6: The effect of N-butyl-2,2-imino-di-(8-OH) and quinine at the IC_{50} value concentrations on the parasitic stages and morphology over a 72-hour period in comparison to untreated *P. falciparum* parasites.

Time (hours)	Untreated control	N-butyl-2,2-imino-di-(8-OH) at 5.1 µM	Quinine (0.07 µM)
0 – 6 Ring stage			
12 Late rings - Early trophozoite stage	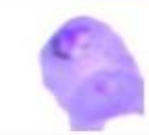	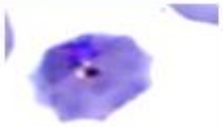	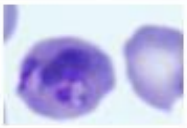
18 Trophozoite stage	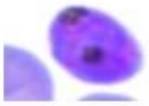		
24 Mid-Trophozoite stage		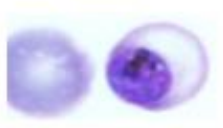	
30 Late Trophozoite – Early schizont stage		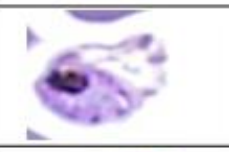	
36 Developing schizont stage		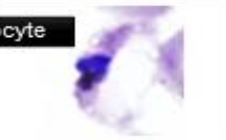	
48 New ring stage/late schizont stage			
54 Mid to late ring stage			
60 Late rings to trophozoites			
66 Late trophozoites to early schizonts	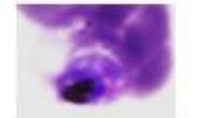		
72 Late schizont to early ring stage		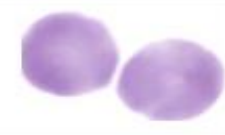	

- *18 hours:* Normal morphological trophozoite development was observed in the untreated control, N-butyl-2,2-imino-di-(8-OH) and quinine. Rings were still present in the untreated control. The total % parasitaemia for quinine and N-butyl-2,2-imino-di-(8-OH) was lower than the untreated control. An increase in schizonts (Figure 4.11, graph C) was observed in the untreated control and the total % parasitaemia increased for N-butyl-2,2-imino-di-(8-OH), quinine and the untreated control.
- *24 hours:* Trophozoites were present, the % parasitaemia of rings was 0% and the % trophozoites were decreasing for N-butyl-2,2-imino-di-(8-OH). The % trophozoites (Figure 4.11, graph B) were equal for N-butyl-2,2-imino-di-(8-OH) and the untreated control. The total % parasitaemia decreased for the untreated control and quinine.
- *30 hours:* Early schizonts were observed for N-butyl-2,2-imino-di-(8-OH) and the late trophozoites and early schizonts in the untreated control showing that the stages were progressing as expected. Stage progression was interrupted for quinine as it was showing predominately schizonts. No trophozoites were observed for quinine. The total % parasitaemia of the untreated increased while that of N-butyl-2,2-imino-di-(8-OH) showed a sharp decrease in % parasitaemia. The total % parasitaemia for quinine was steadily decreasing.
- *36 hours:* Schizonts were observed in the untreated control and mid to late rings/ early trophozoites were observed for N-butyl-2,2-imino-di-(8-OH) (Table 4.6). Rings were observed in the quinine control which suggested an alteration in the normal stage development of the parasite. The % parasitaemia of rings started to increase for quinine and the untreated control. The % parasitaemia of rings increased for N-butyl-2,2-imino-di-(8-OH). The untreated control and quinine demonstrated the highest % parasitaemia of schizonts at this time point. At the 36-hour mark; gametocyte formation was seen in the untreated control where trophozoites should be present. The presence of gametocytes may be due to environmental stressors as gametocyte development is expected after 7 days incubation. The gametocyte was identified as a male due to its crescent shape and nucleus with freely scattered chromatin.
- *48 hours:* Rings were observed in the untreated control and in N-butyl-2,2-imino-di-(8-OH). Few parasites were observed for quinine. An increase in the % parasitaemia of rings and a decrease in the % parasitaemia of trophozoites was observed for the untreated control and quinine. The % rings remained the same as seen at 36 hours was observed for N-butyl-2,2-imino-di-(8-OH) and the total % parasitaemia for the untreated control and quinine was shown to decrease.
- *54 hours:* Mid-rings were observed in N-butyl-2,2-imino-di-(8-OH) and mid-rings and trophozoites in the untreated control. The % rings increased for quinine and decreased

for N-butyl-2,2-imino-di-(8-OH) from the 48-hour timepoint. A decrease in the % rings was observed for the untreated control and N-butyl-2,2-imino-di-(8-OH) and a slight increase in % trophozoites was observed for quinine. No schizonts were observed for N-butyl-2,2-imino-di-(8-OH), quinine and the untreated control. The total % parasitaemia for N-butyl-2,2-imino-di-(8-OH) was at its lowest point at 54 hours and a slight increase in total % parasitaemia for quinine was observed. The total % parasitaemia for the untreated control was observed to be steadily decreasing.

- *60 hours:* Trophozoites were observed for the untreated control and N-butyl-2,2-imino-di-(8-OH) whereas no parasites were observed for quinine. The % trophozoite increased for the untreated control and N-butyl-2,2-imino-di-(8-OH) and no schizonts were present. A slight increase in total % parasitaemia was observed in N-butyl-2,2-imino-di-(8-OH) possible indicating a recovery of the parasites from initial treatment. No parasites were observed for quinine from this point.
- *66 hours:* Late trophozoites and schizonts were observed for the untreated control and N-butyl-2,2-imino-di-(8-OH). A slight decrease in total % parasitaemia was observed in the untreated control. No parasites were observed for quinine.
- *72 hours:* Rings were observed in the untreated control as well as an increase in the % trophozoites and schizonts. The % total parasitaemia decreased to 0% for N-butyl-2,2-imino-di-(8-OH) and remained unchanged for the untreated control.

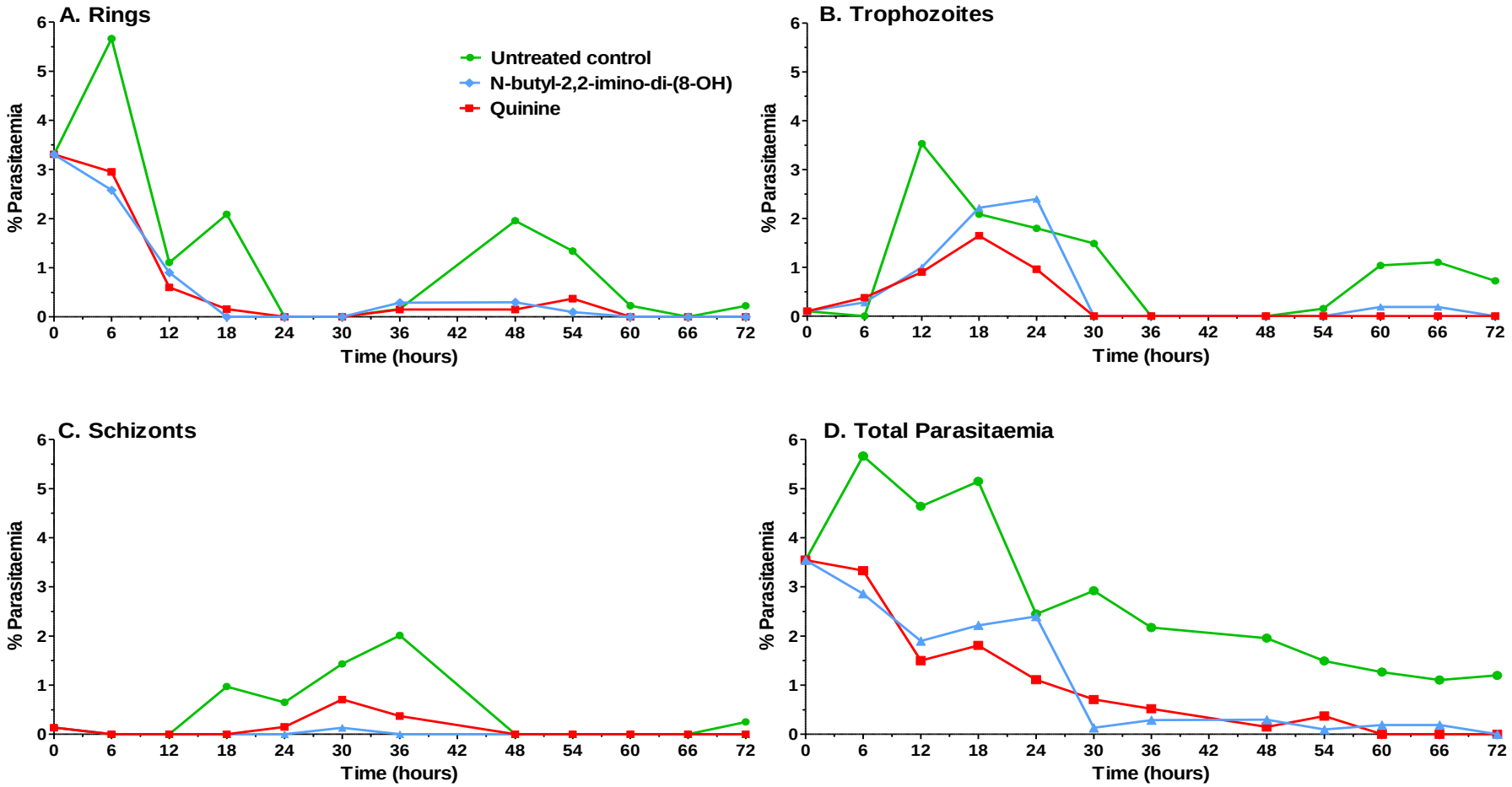

Figure 4.11: The comparison of the % parasitaemia over 72 hours of the ring (A), trophozoite (B), schizont (C) stages and the total % parasitaemia of the untreated control, N-butyl-2,2-imino-di-(8-OH) (5.1 µM) and the quinine (0.07 µM) control.

Parasites were treated with N-butyl-2,2-imino-di-(8-OH) and quinine at time point 0 hours and the parasites that were treated with N-butyl-2,2-imino-di-(8-OH) started to show signs of population recovery after 54 hours.

4.1.2.1.2. pLDH assay antimalarial combinations

The most active 8-OH, N-butyl-2,2-imino-di-(8-OH) was combined with the chloroquine to observe the resultant antimalarial activity of the combination (Figure 4.13). The combination demonstrated a synergistic interaction with only one outlier at x = 0.91; y = 0.0096, interacting in an additive manner. N-butyl-2,2-imino-di-(8-OH) demonstrated a potent antimalarial and copper homeostasis activity amongst the 8-OH derivatives with an IC_{50} value of 0.58 ± 0.03 µM (Table 4.5). Therefore, it was selected to examine its collective effect with chloroquine against *P. falciparum* using the pLDH assay (Figure 4.13). The combination demonstrated a synergistic effect with a sum (ΣFIC) value of 0.54. The IC_{50} values determined at the different ratios of the of N-butyl-2,2-imino-di-(8-OH) and chloroquine in combination are described in Table 4.7 and the sigmoidal log dose response curves of the ratios are shown in Figure 4.12.

Table 4.7: The FIC_{50} values used to calculate the ΣFIC in the pLDH assay.

FIC_{50} values		
Ratio N-butyl-2,2-imino-di-(8-OH): Chloroquine	**Chloroquine**	**N-butyl-2,2-imino-di-(8-OH)**
7.5:0.25	0.71	0.002
5:1	0.92	0.009
2.5:1.5	0.19	0.008
2:2	0.489	0.006
1.5:2	0.079	0.008
1:2.5	0.039	0.008
0.5:5	0.02	0.024
0.25:7.5	0.49	2.04

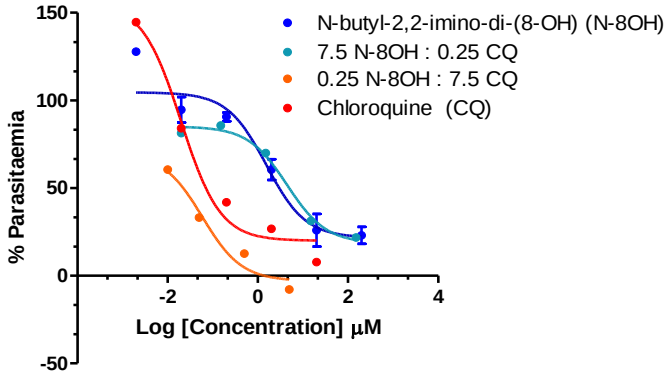

Figure 4.12: The sigmoidal log-dose response curves of the malaria parasite when exposed to combinations of N-butyl-2,2-imino-di(8-OH) and chloroquine at different ratios as determined by the pLDH assay.

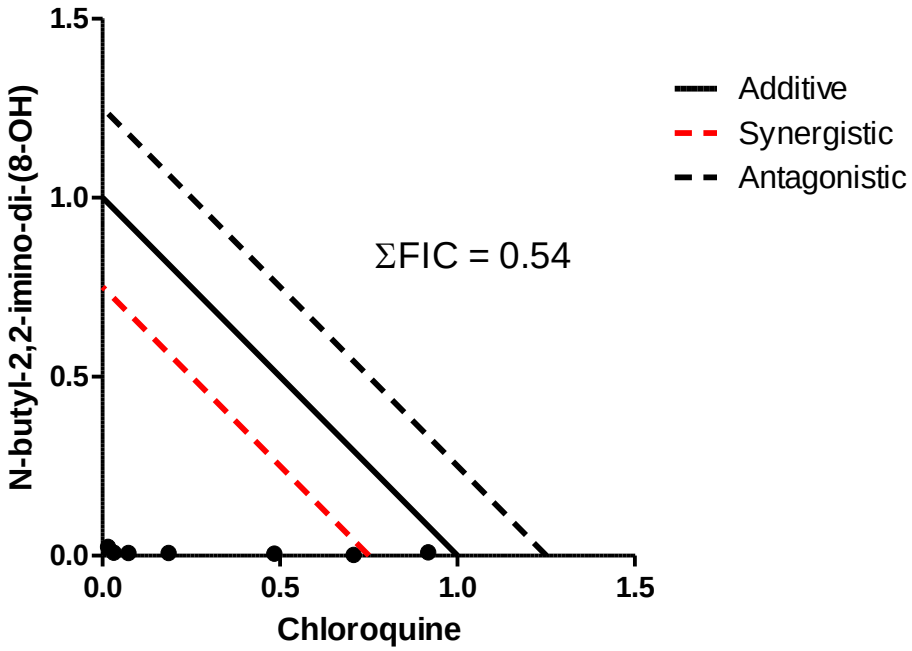

Figure 4.13: The combination assay of N-butyl-2,2-imino-di-(8-OH) and chloroquine in the pLDH assay, indicating a synergistic interaction where the ΣFIC was less than 0.75.

4.1.2.2. The ferriprotoporphyrin biomineralization inhibition assay

The inhibition of ferriprotoporphyrin biomineralization was determined and the percentage ferriprotoporphyrin biomineralization formation inhibited can be seen in Table 4.8. N-butyl-2,2-imino-di-(8-OH) showed the highest % FBIT and was comparable to the chloroquine positive control and higher than that of the quinine positive control. 5,7-diiodo-8-OH and 4-OH demonstrated a % FBIT greater than 80%. 5,7-Dichloro-8-OH demonstrated a % FBIT greater than 70% while 8-fluoro-4-OH and 5,7-dichloro-2-methyl-8-OH had a % FBIT greater than 70%.

N-butyl-2,2-imino-di-(8-OH) had the lowest IC_{50} value which was lower than the quinine positive control and comparable to the chloroquine control. 5,7-diiodo-8-OH, 4-OH and 5-chloro-7-iodo-8-OH demonstrated IC_{50} values lower than that of quinine. 5,7-Dichloro-8-OH, 8-fluoro-4-OH, 5,7-dichloro-2-methyl-8-OH and 5-HSO_3-8-OH had comparable IC_{50} values to that of quinine.

Table 4.8: The percentage ferriprotoporphyrin biomineralization inhibited by compounds at 200 µM.

Compounds	% FBIT at 200 µM	IC_{50} (µM)
Chloroquine	97.86 ± 0.48	22.91 ± 3.78
Quinine	83.52 ± 3.09	37.71 ± 3.63 Yes (P = 0.02
N-Butyl-2,2-imino-di-(8-OH)	96.94 ± 0.92	23.24 ± 4.46 No (P = 0.89
5,7-Diiodo-8-OH	80.28 ± 7.73	25.65 ± 4.21 No (P = 0.48)
4-OH	80.25 ± 2.77	25.89 ± 4.46 No (P = 0.48)
5,7-Dichloro-8-OH	72.51 ± 11.40	41.00 ± 0.28 Yes (P = 0.02)
5,7-Dichloro-2-CH_3-8-OH	63.60 ± 1.28	44.68 ± 1.81 Yes (P = 0.03)
8-Fluoro-4-OH	66.96 ± 1.08	40.91 ± 6.44 No (P = 0.08)
D-penicillamine	68.64 ± 6.50	53.47 ± 7.69 Yes (P = 0.005)
TMB	96.48 ± 0.72	26.34 ± 3.17
5-Chloro-7-iodo-8-OH	54.54 ± 4.78	27.66 ± 4.26 No (P = 0.25)
5-HSO_3-8-OH	40.03 ± 4.45	*
5,7-Dibromo-8-OH	39.68 ± 5.94	*
2-Benzyl-8-OH	37.41 ± 5.55	*
5-Amino-8-OH	38.60 ± 3.00	*
5-Chloro-8-OH	24.16 ± 3.61	*
8-OH	23.2 ± 4.3	*
2-Methyl-8-OH	21.13 ± 4.17	*
8-Chloro-2-OH	22.61 ± 1.88	*
5-HSO_3-7-iodo-8-OH	16.84 ± 2.14	*
2-Amino-8-OH	16.87 ± 0.45	*
5-Carboxy-8-OH	15.60 ± 1.16	*
5,7-Dimethyl-8-OH	12.89 ± 1.36	*
5-Chloro-7-bromo-8-OH	12.29 ± 1.67	*
BHA	12.0 ± 0.6	*
5-Nitro-8-OH	10.08 ± 0.85	*
Neocuproine	≤0.10 ± 0.10	*
EDTA	≤0.10 ± 0.1	*

* Not determined as % ferriprotoporphyrin biomineralization inhibited was not greater than 50%.

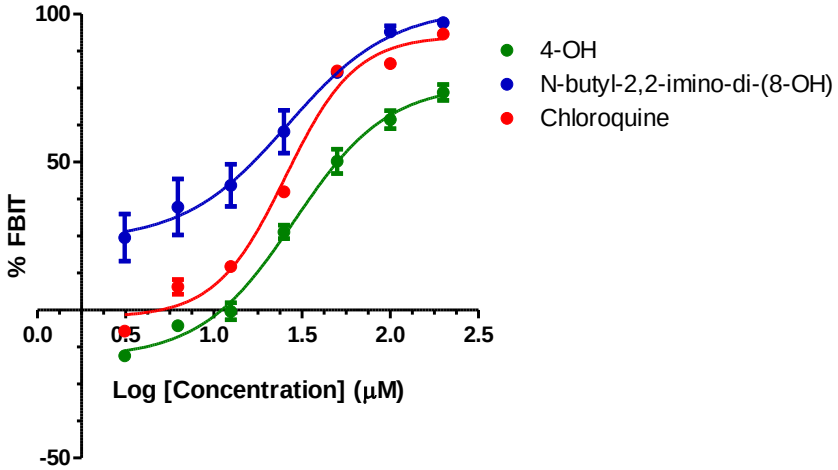

Figure 4.14: The log-dose response curve of 4-OH, N-butyl-2,2-imino-di-(8-OH) and chloroquine as determined by the FBIT assay, indicating the inhibition of ferriprotoporphyrin biomineralization in a dose dependant manner.

4.1.2.3. The biomineralization inhibition combination

N-butyl-2,2-imino-di-(8-OH) was combined with the chloroquine positive control and the ferriprotoporphyrin biomineralization inhibition activity of the combination was determined as shown in Figure 4.16. N-butyl-2,2-imino-di-(8-OH) demonstrated the most potent FBIT activity of all the 8-OH's derivatives with an IC_{50} value 23.24 ± 4.46 µM (Table 4.8). Therefore, it was selected to examine its collective FBIT effect with the chloroquine positive control as shown in Figure 4.16. The combination demonstrated a synergistic effect with a sum (ΣFIC) value of 0.38. N-butyl-2,2-imino-di-(8-OH) was combined with the chloroquine positive control and the ferriprotoporphyrin biomineralization inhibition activity of the combination was determined as shown in Figure 4.16. The IC_{50} values determined at the different ratios of the of N-butyl-2,2-imino-di-(8-OH) and chloroquine in combination are described in Table 4.9 and the sigmoidal log dose response curves of the ratios are shown in Figure 4.15.

Table 4.9: The FIC_{50} values used to calculate the ΣFIC in the FBIT assay.

FIC_{50} values		
Ratio	**Chloroquine**	**N-butyl-2,2-imino-di-(8-OH)**
7.5:0.25	0.79	0.15
5:1	0.82	0.23
2.5:1.5	0.31	0.25075
2:2	0.08	0.19
1.5:2	0.03	0.17
1:2.5	0.02	0.31
0.5:5	0.01	0.34
0.25:7.5	0.003	0.14

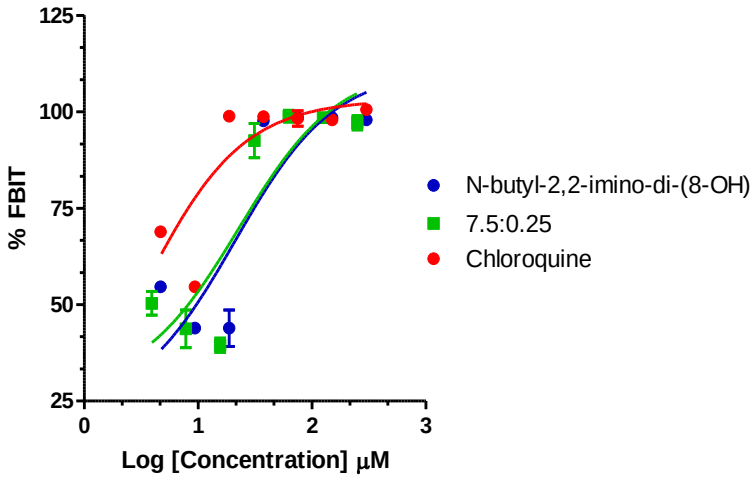

Figure 4.15: The sigmoidal log-dose response curves of N-butyl-2,2-imino-di(8-OH) and chloroquine at different ratios indicating the dose dependant manner in which ferriprotoporphyrin biomineralization was inhibited using the FBIT assay.

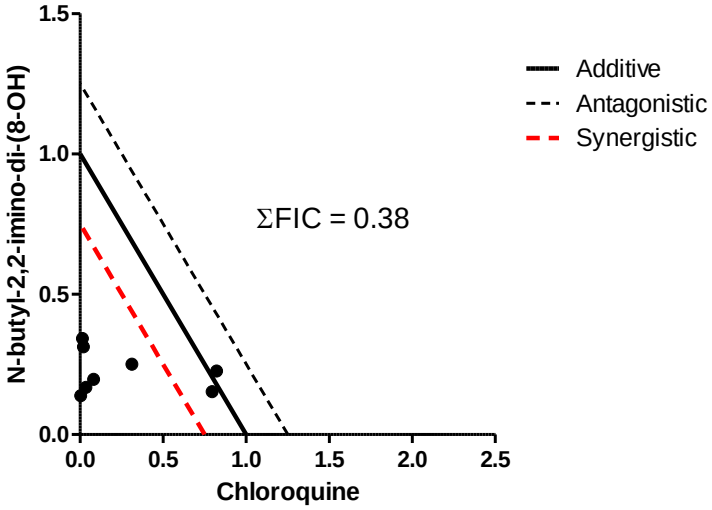

Figure 4.16: The combination assay of N-butyl-2,2-imino-di-(8-OH) and chloroquine in the ferriprotoporphyrin biomineralization inhibition.

The combination showed a synergistic outcome where the FBIT activity of the combination was greater than the sum of N-butyl-2,2-imino-di-(8-OH) and chloroquine FBIT activity individually.

4.1.3. The haemolytic effect of compounds

4.1.3.1. Red blood cell toxicity assay

The red blood cell toxicity assay was used to determine the haemolytic effect of the compounds at several different concentrations. The red blood cell toxicity assay was used to determine the haemolytic effect of the 8-OH derivatives at several different concentrations (Table 4.10). 8-OH derivatives with a percentage haemolysis greater than 30% are highly haemolytic and therefore have an unfavourable toxicological profile. 5-Chloro-7-iodo-8-OH, 5,7 dichloro-8-OH, 5,7-dibromo-8-OH, 2-benzyl-8-OH, 5-Chloro-7-bromo-8-OH, 5-amino-8-OH, 5,7-dichloro-2-CH_3-8-OH and 5,7-diiodo-8-OH demonstrated unfavourable haemolysis (≥ 20%). 4-OH and 8-fluoro-4-OH, 2-amino-8-OH, 5-carboxy-8-OH, 5-HSO_3-8-OH, 5-nitro-8-OH, N-butyl-2,2-imino-di-(8-OH) and 5-chloro-8-OH demonstrated a % haemolysis less than 10%. The 8-OH derivatives demonstrated p-values ranging between 0.0001 and 0.97.

4.1.3.2. Haemolytic protective effect of compounds against copper (I)

In comparison to the copper homeostasis results in Section 4.1.1, the protective effect of the active copper (I) chelating compounds (Section 4.1.1) were selected to determine their potential protective effect against copper (I) –induced haemolysis (Figure 4.17 and Figure 4.18). The haemolytic effect of the compounds with copper (I) differed from the compounds alone (Figure 4.17).

The 8-OH derivatives that demonstrated the greatest protective effect against copper (I) were: 2-benzyl-8-OH, 5-chloro-7-iodo-8-OH, 5,7-diiodo-8-OH, 8-fluoro-4-OH, 5-HSO_3-7-iodo-8-OH, 8-OH and N-butyl-2,2-imino-di-(8-OH). Whilst, 8-OH and N-butyl-2,2-imino-di-(8-OH) had comparable results to the copper (I) chelator, neocuproine. When incubated with copper (I), the following compounds showed an increase in haemolysis in comparison when incubated with RBCs alone. 5-HSO_3-8-OH, 5,7-dichloro-2-methyl-8-OH, 5,7-dimethyl-8-OH, 5-carboxy-8-OH, 5-chloro-8-OH, 2-amino-8-OH, 5-nitro-8-OH, 8-chloro-2-OH and 2-methyl-8-OH. demonstrated a large increase in haemolysis in comparison to the results in Table 4.10, as did chloroquine and quinine.

Table 4.10: The percentage haemolysis that was caused by test and control compounds at 200 µM. The significant difference of the compound compared to Chloroquine ($P < 0.05$) is shown in parentheses below the % haemolysis.

Compound	% Haemolysis at 200 µM	Compound	% Haemolysis at 200 µM
Copper (I)	*102.8 ± 6.6 [Yes (P = 0.003)]	**Copper (II)**	17.9 ± 14.0 [No (P = 0.97)]
Camptothecin	0.56± 0.13 [No (P = 0.34)]	**8-chloro-2-OH**	15.52 ± 1.34 [No (P = 0.10)]
4-OH	4.56 ± 0.70 [Yes (P = 0.001)]	**2-methyl-8-OH**	18.06 ± 0.47 [No (P = 0.70)]
8-Fluoro-4-OH	5.54 ± 0.75 [Yes (P < 0.0001)]	**Chloroquine**	18.32 ± 0.89
2-amino-8-OH	8.20 ± 1.56 [Yes (P = 0.004)]	**Neocuproine**	18.38 ± 0.23 [No (P = 0.94)]
5-carboxy-8-OH	8.92 ± 0.45 [Yes (P = 0.004)]	**Dihydroartemisinin**	18.48 ± 0.80 [No (P = 0.83)]
5-HSO_3-8-OH	9.37 ± 1.09 [Yes (P = 0.01)]	**Quinine**	18.93 ± 1.03 [No (P = 0.38)]
5-nitro-8-OH	9.52 ± 1.11 [No (P = 0.01)]	**D-penicillamine**	20.09 ± 1.79 [No (P = 0.28)]
TMB	9.55 ± 0.27 [Yes (P = 0.005)]	**5-Chloro-7-iodo-8-OH**	21.96 ± 1.45 [Yes (P = 0.02)]
N-butyl-2,2-imino-di-(8-OH)	9.78 ± 1.70 [Yes (P = 0.007)]	**5,7 dichloro-8-OH**	22.60 ± 0.16 [Yes (P = 0.02)]
5-chloro-8-OH	9.79 ± 1.41 [Yes (P = 0.01)]	**5,7-dibromo-8-OH**	22.82 ± 1.76 [Yes (P = 0.02)]
EDTA	10.19 ± 2.38 [Yes (P = 0.05)]	**2-benzyl-8-OH**	22.92 ± 2.29 [No (P = 0.05)]
5-HSO_3-7-iodo-8-OH	10.3 5 ± 1.27 [Yes (P = 0.02)]	**5-Chloro-7-bromo-8-OH**	24.07 ± 1.13 [No (P = 0.02)]
AA	11.10 ± 1.56 [Yes (P = 0.004)]	**5-amino-8-OH**	24.76 ± 0.12 [Yes (P = 0.006)]
5,7-dimethyl-8-OH	11.19 ± 0.58 [Yes (P = 0.007)]	**5,7-dichloro-2-CH_3-8-OH**	25.32 ± 2.56 [Yes (P = 0.002)]
8-OH	11.35 ± 0.27 [Yes (P = 0.003)]	**5,7-diiodo-8-OH**	29.74 ± 1.23 [Yes (P = 0.02)]

* Compounds with a percentage haemolysis greater than 30% are highly haemolytic and therefore have an unfavourable toxicological profile.

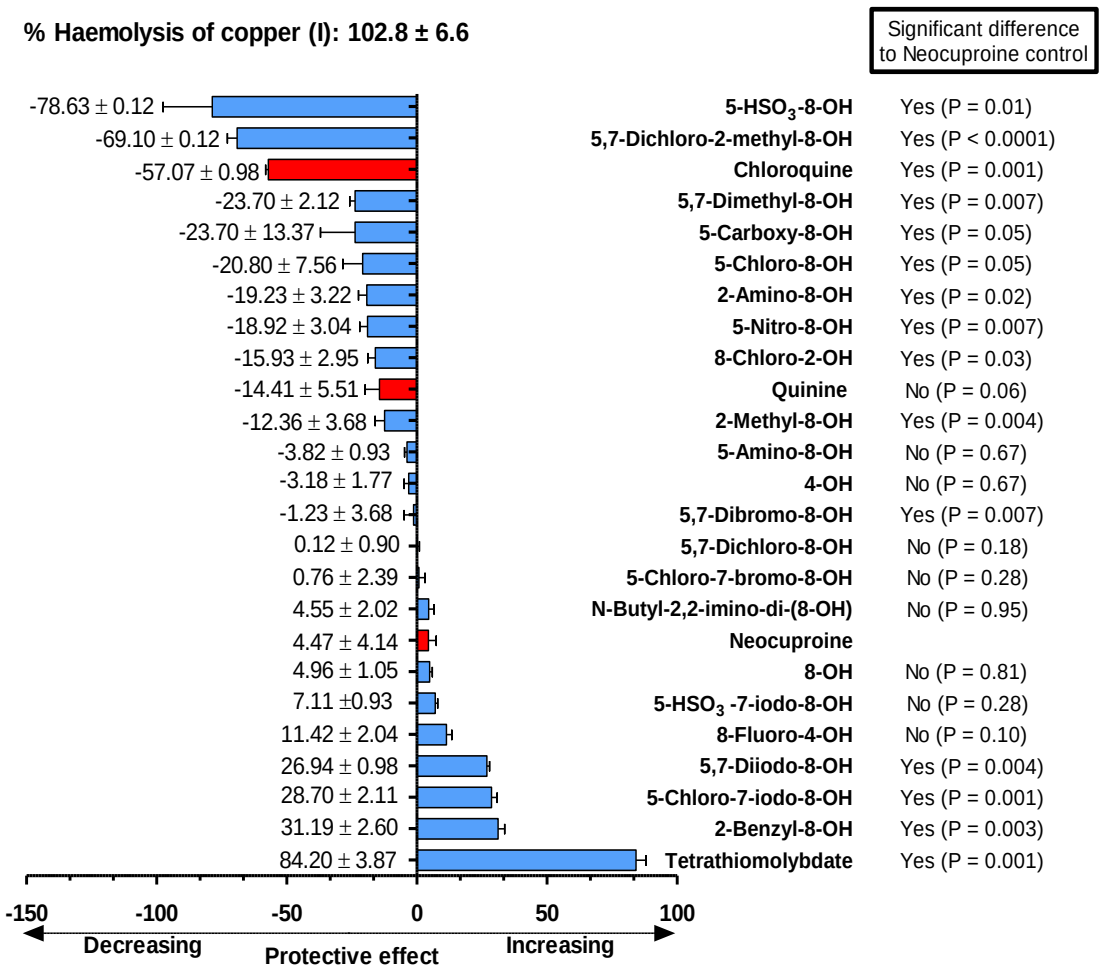

Figure 4.17: The protective effect of the compounds on red blood cells treated with Cu(I). The difference of the compound alone (at 200 µM) and the combination determined the protective effect of the compound against copper (I) (at 200 µM).

4.1.3.3. Haemolytic protective effect of compounds against copper (II)

When compared to the copper homeostasis results in Section 4.1.1 the protective effect was determined. Compounds that showed activity in the copper (II) chelation assay (Section 4.1.1) were selected to test whether they had a protective effect against copper (II) incubated with red blood cells. The difference and the haemolytic effect of the combinations are shown in Figure 4.18. The 8-OH derivatives that showed the greatest protective effect against copper (II) haemolysis were: 5-amino-8-OH and 2-methyl-8-OH. 5-Chloro-8-OH, quinine and D-penicillamine had comparable effect and demonstrated an increase in lysis when incubated with copper (II). N-butyl-2,2-imino-di-(8-OH) had a comparable negative haemolytic effect to chloroquine. TMB demonstrated a protective effect against copper (I) and (II) haemolysis. The 8-OH derivatives showed a greater affinity to prevent the haemolysis caused by copper (I) than that caused by copper (II). 2-Benzyl-8-OH, 5-chloro-7-iodo-8-OH, 5,7-diiodo-8-OH, 8-fluoro-4-OH, 5-HSO_3-7-iodo-8-OH, 8-OH and N-butyl-2,2-imino-di-(8-OH) selectively

demonstrated a protective effect against copper (I) haemolysis, but the lytic effect increased when incubated with copper (II) treated red blood cells.

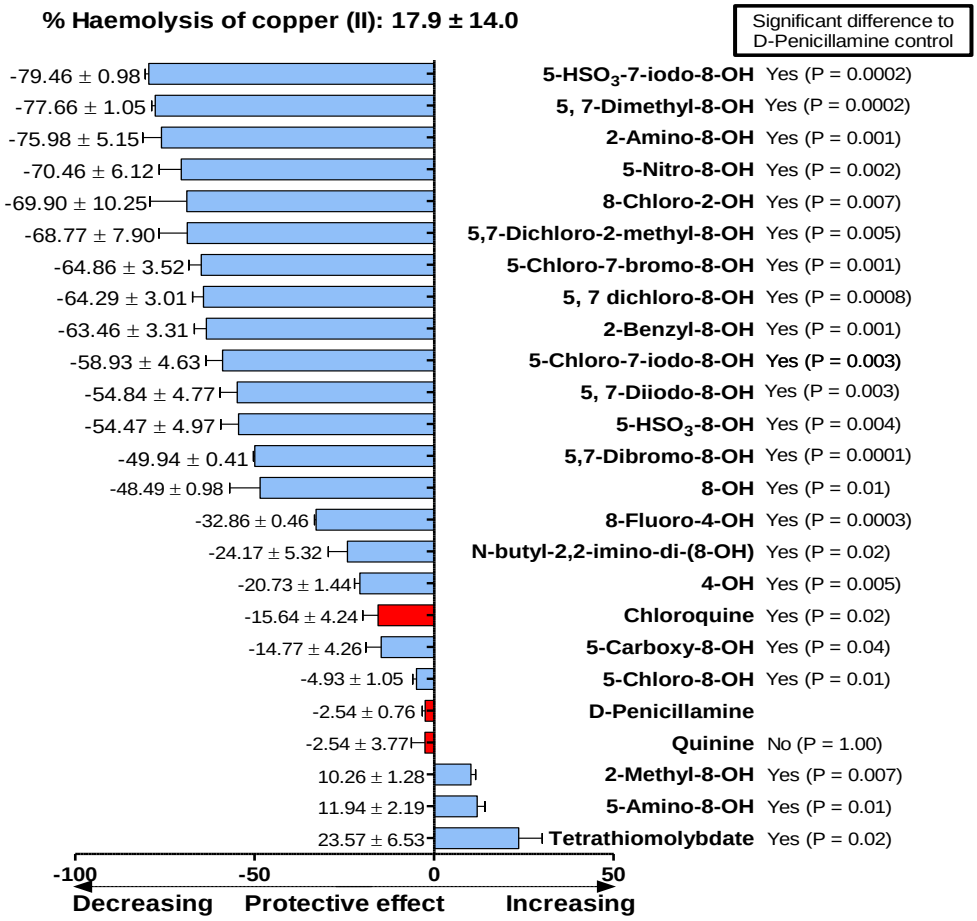

Figure 4.18: The protective effect of the compounds on red blood cells treated with Cu(II). The difference of the compound alone (at 200 µM) and the combination determined the protective effect of the compound against copper (II) (at 200 µM).

4.1.4. Effect of compounds on neuroblastoma cells

4.1.4.1. Cytotoxicity assay

The 8-OH derivatives demonstrated properties to inhibit cellular growth, with the majority resulting in cellular viability lower than 60% indicating toxicity (Table 4.11). The IC_{50} values for these compounds demonstrate the toxicity where the lower the IC_{50} value, the more toxic of the compound.

In Table 4.11, The IC_{50} values of 8-OH derivatives with cellular viability less than 50% were determined. 5,7-Dichloro-8-OH had the lowest IC_{50} value for the MTT assay and 5-amino-8-OH had the lowest IC_{50} values for the SRB assay. A greater cellular viability inhibition by the

8-OH derivatives was observed in the MTT assay overall than what was observed in the SRB assay. The two assays were measuring two different cellular inhibitory processes therefore they had different results that depended on the compounds specific mechanism of inhibitory action (Berenbaum, 1978; Lin, Hoult and Raman, 1999).

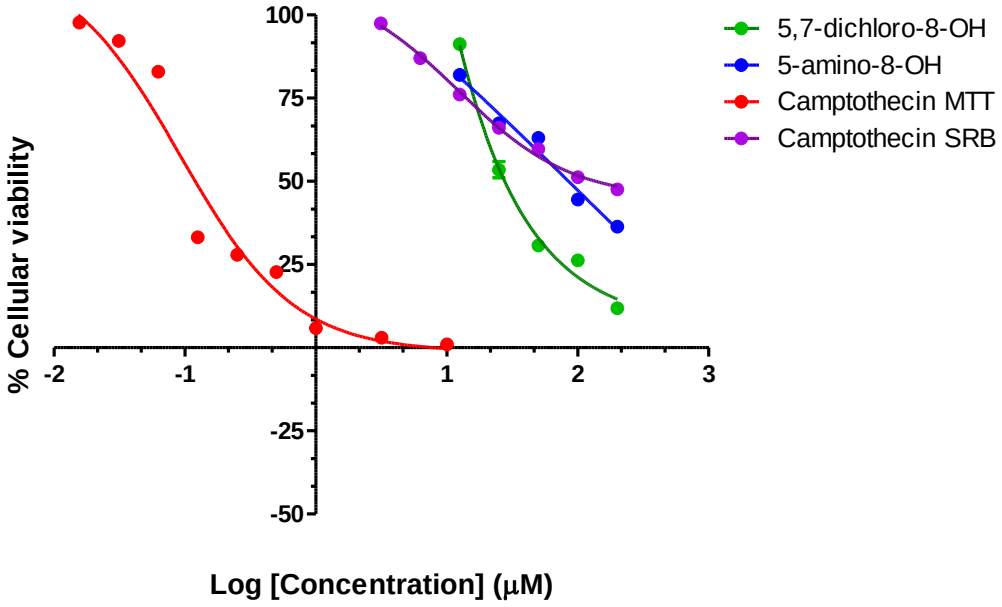

Figure 4.19: The sigmoid log-dose response curve of 5,7-dichloro-8-OH and camptothecin as determined by the MTT assay, and 5-amino-8-OH and camptothecin as determined by the SRB assay when exposed to the neuroblastoma cell line.

4.1.4.1.1. Adherent cell counting

The number of viable and non-viable cells was counted at 1, 24 and 48 hours and images taken using the Olympus microscope at 20X magnification to determine the effect of the compounds on the number of cells. The percentage change in cellular viability was determined and changes in cell shape, size and number were noted. The results not shown in Figure 4.20 can be seen in Appendix C, Section C.7, Table C.12.

Table 4.11: The IC_{50} values of the neuroblastoma cell line, as determined by the MTT and SRB assays.

Compound	MTT viability assay	SRB viability assay
	IC_{50} value (µM)	**IC_{50} value (µM)**
Copper (I)	7.8 ± 0.9	≥ 200
Copper (II)	24.1 ± 1.4	≥ 200
Camptothecin	13.8 ± 3.0	10.1 ± 2.0
Methotrexate	≥ 200	13.5 ± 4.9
5,7-Dichloro-8-OH	7.0 ± 0.7 [No (P = 0.1)]	≥ 200
N-Butyl-2,2-imino-di-(8-OH)	9.32 ± 1.4 [No (P = 0.05)]	22.8 ± 4.0 [Yes (P = 0. 03)]
5-Chloro-7-bromo-8-OH	9.8 ± 0.8 [No (P = 0.3)]	25.3 ± 1.1 [Yes (P = 0.01)]
5,7-Dichloro-2-CH_3-OH	12.1 ± 2.7 [No (P = 0.1)]	23.6 ± 5.0 [Yes (P = 0.04)]
5-Amino-8-OH	14.1 ± 2.6 [No (P = 0.6)]	11.6 ± 2.8 [No (P = 0.25)]
Quinine	≥ 200	≥ 200
8-OH	20.6 ± 1.4 [Yes (P = 0.04)]	≥ 200
5-Chloro-7-iodo-8-OH	21.2 ± 2.4 [Yes (P = 0.007)]	≥ 200
5-Nitro-8-OH	22.2 ± 2.7 [Yes (P=0.03)]	22.5 ± 2.6 [No (P = 0.002)]
5,7-Diiodo-8-OH	24.5 ± 5.6 [No (P = 0.05)]	≥ 200
2-Benzyl-8-OH	24.9 ± 0.7 [Yes (P=0.04)]	25.8 ± 4.7 [Yes (P = 0.004)]
5,7-Dibromo-8-OH	25.5 ± 3.4 [Yes (P=0.03)]	45.2 ± 7.3 [Yes (P = 0.03)]
TET	32.2 ± 1.7 [Yes (P = 0.001)]	≥ 200
5-Chloro-8-OH	≥ 200	29.7 ± 4.7 [Yes (P = 0.03)]
Chloroquine	44.0 ± 8.2 [Yes (P=0.06)]	≥ 200
D-Penicillamine	50.1 ± 4.4 [Yes (P = 0.009)]	10.0 ± 4.2 [No (P = 1.0)]
5-Carboxy-8-OH	≥ 200	≥ 200
2-Amino-8-OH	75.7 ± 5.6	28.4 ± 4.5 [Yes (P = 0.03)]
TMB	≥ 200	≥ 200
5,7-Dimethyl-8-OH	94.0 ± 6.9 [Yes (P = 0.003)]	27.1 ± 5.2 [Yes (P = 0.008)]
Neocuproine	≥ 200	≥ 200
5-HSO_3-8-OH	≥ 200	14.7 ± 0.9
5-HSO_3-7-iodo-8-OH	≥ 200	29.4 ± 4.0
4-OH	≥ 200	≥ 200
EDTA	≥ 200	≥ 200
Trolox™	≥ 200	≥ 200
BHA	≥ 200	≥ 200

4.1.4.2. Protective effect of compounds against copper

Copper (I) and copper (II) demonstrated significant toxicity against the neuroblastoma cell line in comparison to camptothecin (Figure 4.21; Table 4.11). While both had similar percentage cellular viabilities when compared to one another, copper (I) demonstrated a 3-fold higher potency than copper (II) in terms of IC_{50} values Table 4.11).

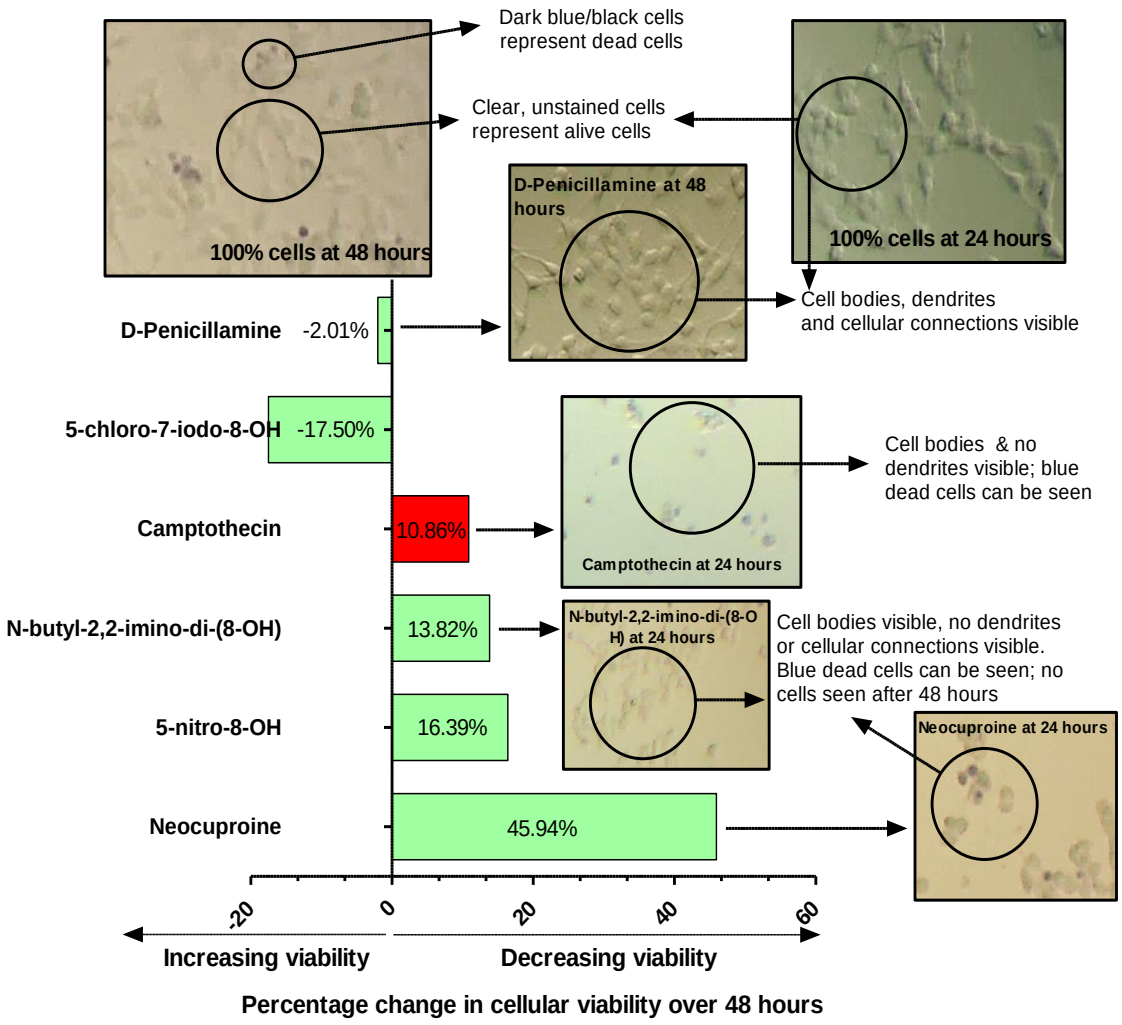

Figure 4.20: The percentage change in viability and morphology of viable cells over time when treated with compounds in neuroblastoma cells.

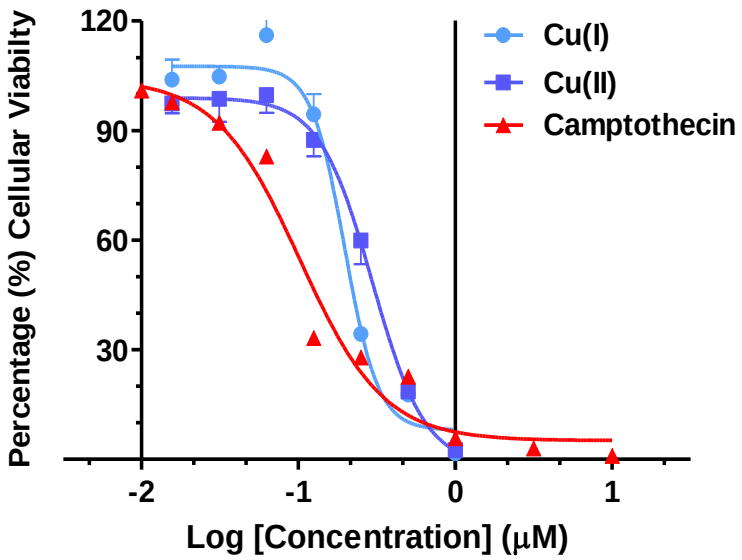

Figure 4.21: The log-sigmoid dose response curve of the neuroblastoma cell line when exposed to copper (I), copper (II), and camptothecin as determined by the MTT assay.

4.1.4.2.1. Protective effect of compounds against copper (I)

The percentage viability of the compounds incubated in the presence of excess copper (I) indicated that 5-amino-8-OH, 5,7-diiodo-8-OH, N-butyl-2,2-imino-di-(8-OH), 8-fluoro-4-OH, 5,7-dichloro-2-methyl-8-OH, 5,7-dibromo-8-OH, 5-chloro-7-iodo-8-OH, 8-chloro-2-OH, 5-carboxy-8-OH, 5,7-dichloro-8-OH, 5,7-dimethyl-8-OH, 2-methyl-8-OH, 2-amino-8-OH and 2-benzyl-8-OH all demonstrated a protective effect against the cytotoxic activity of copper (I) (Figure 4.22). The potency of the positive control, camptothecin decreased when incubated with copper (I). The compounds showed a protective effect against copper (I) cytotoxicity.

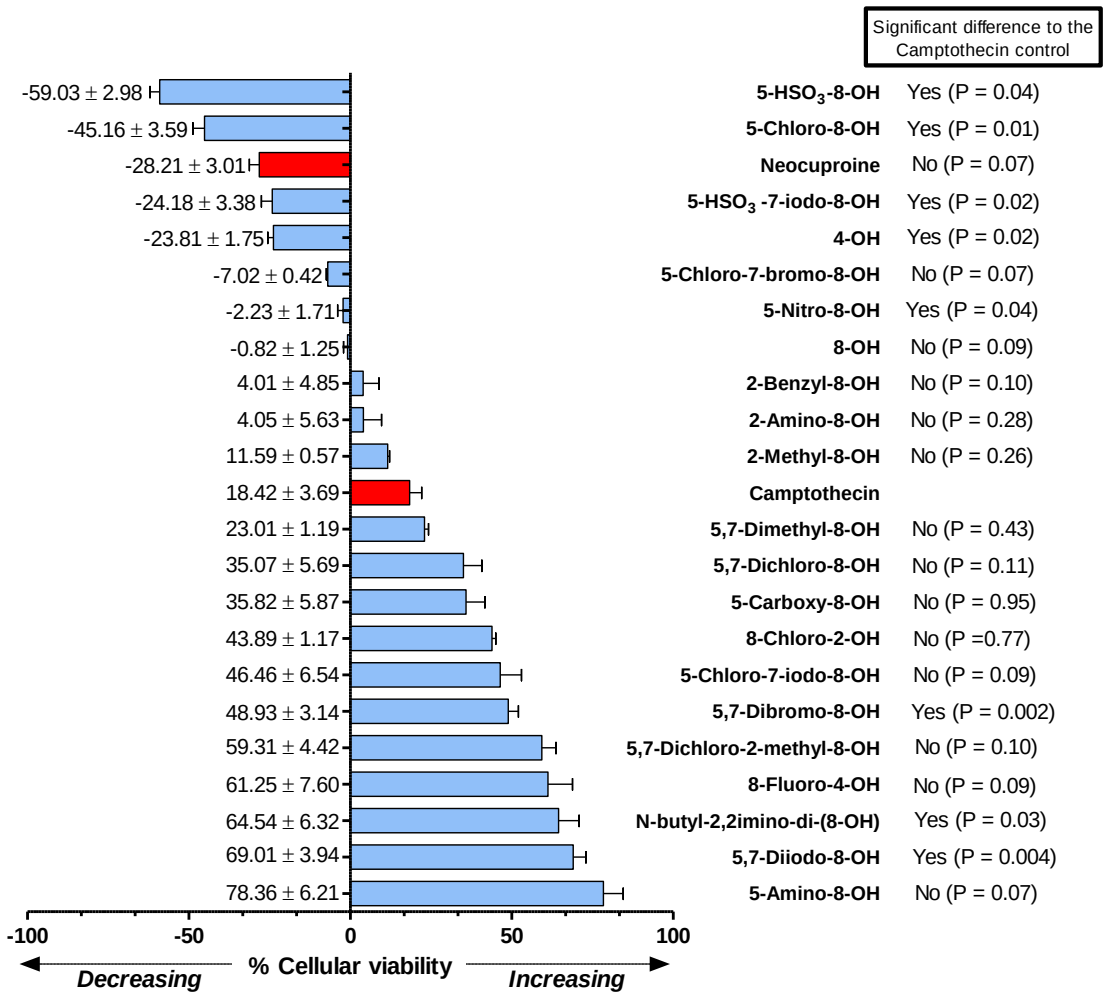

Figure 4.22: The effect of incubation with copper (I) and compounds on percentage cellular viability

In the presence of copper (I) (200 µM), the compounds at 200 µM showed a change in cellular viability in comparison to when they were incubated alone.

4.1.4.2.2. Protective effect of compounds against copper (II)

In Figure 4.23 the percentage viability of the compounds and copper (II) incubation are presented. 5-Amino-8-OH, 5,7-dichloro-8-OH, N-butyl-2,2-imino-di-(8-OH), 5,7-dibromo-8-OH, 5,7-diiodo-8-OH, 8-fluoro-4-OH, 5-HSO_3-7-iodo-8-OH, 2-benzyl-8-OH, 8-OH, 5,7-dichloro-2-methyl-8-OH, 5-chloro-7-iodo-8-OH, 2-methyl-8-OH, 2-amino-8-OH and 5,7-dimethyl-8-OH demonstrated a protective effect when incubated with copper (II) and neuronal cells. Camptothecin and D-penicillamine showed a protective effect – 4-fold less than the most active compound 5-amino-8-OH.

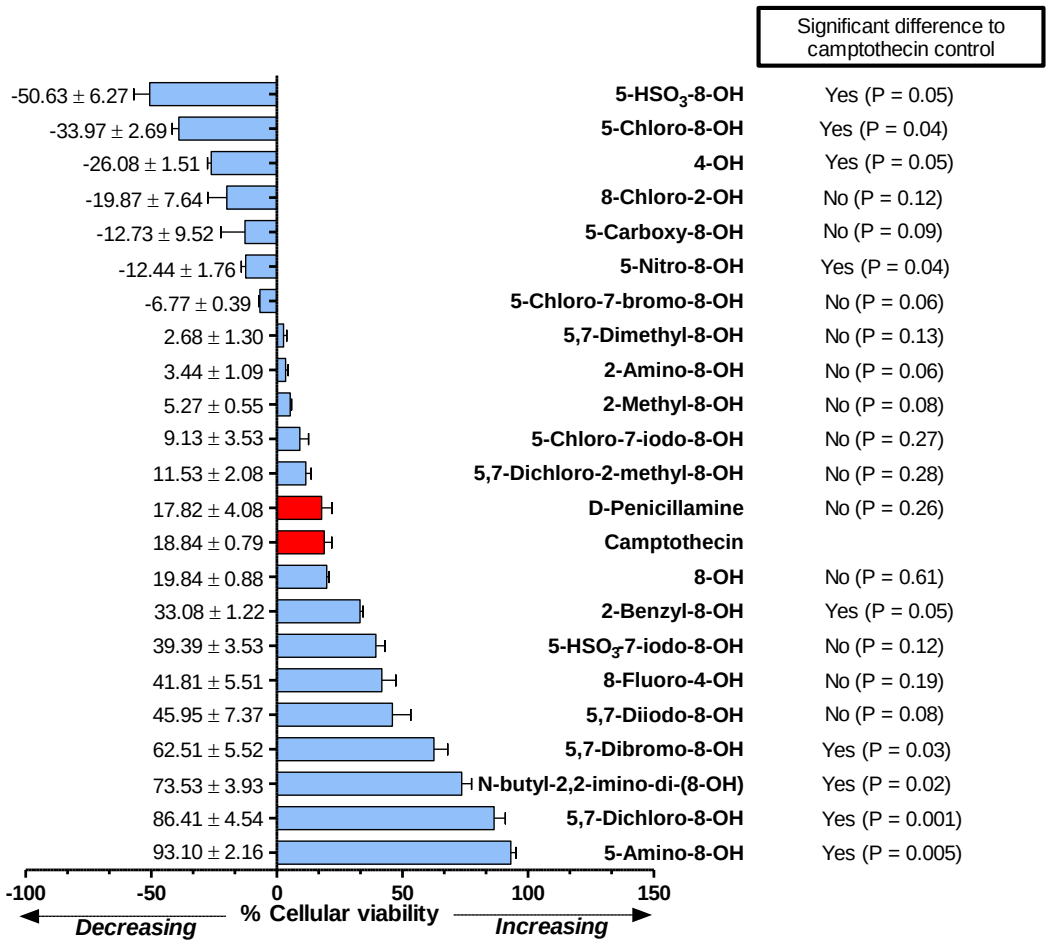

Figure 4.23: The effect of incubation with copper (II) and compounds on percentage cellular viability.

In the presence of copper (II) (200 µM), the compounds at 200 µM exhibited an adjustment in cellular viability as compared to when they were incubated alone.

4.1.4.2.3. Effect of compounds and copper on the structure of neuronal cells

N-butyl-2,2-imino-di-(8-OH) was selected along with the copper chelating control compounds, neocuproine and D-penicillamine to visualise the effect of copper (I) and (II) on the SH-SY5Y cell line (Figure 4.24). When N-butyl-2,2-imino-di-(8-OH) was compared to the copper treated controls and the untreated controls, no copper (in both the copper (I) and –(II) treated cells) were detected in the neuronal cells. Similarly, copper was not detectable in D-penicillamine-treated cells and brick red copper deposits were visible in the neocuproine treated cells (Figure 4.24).

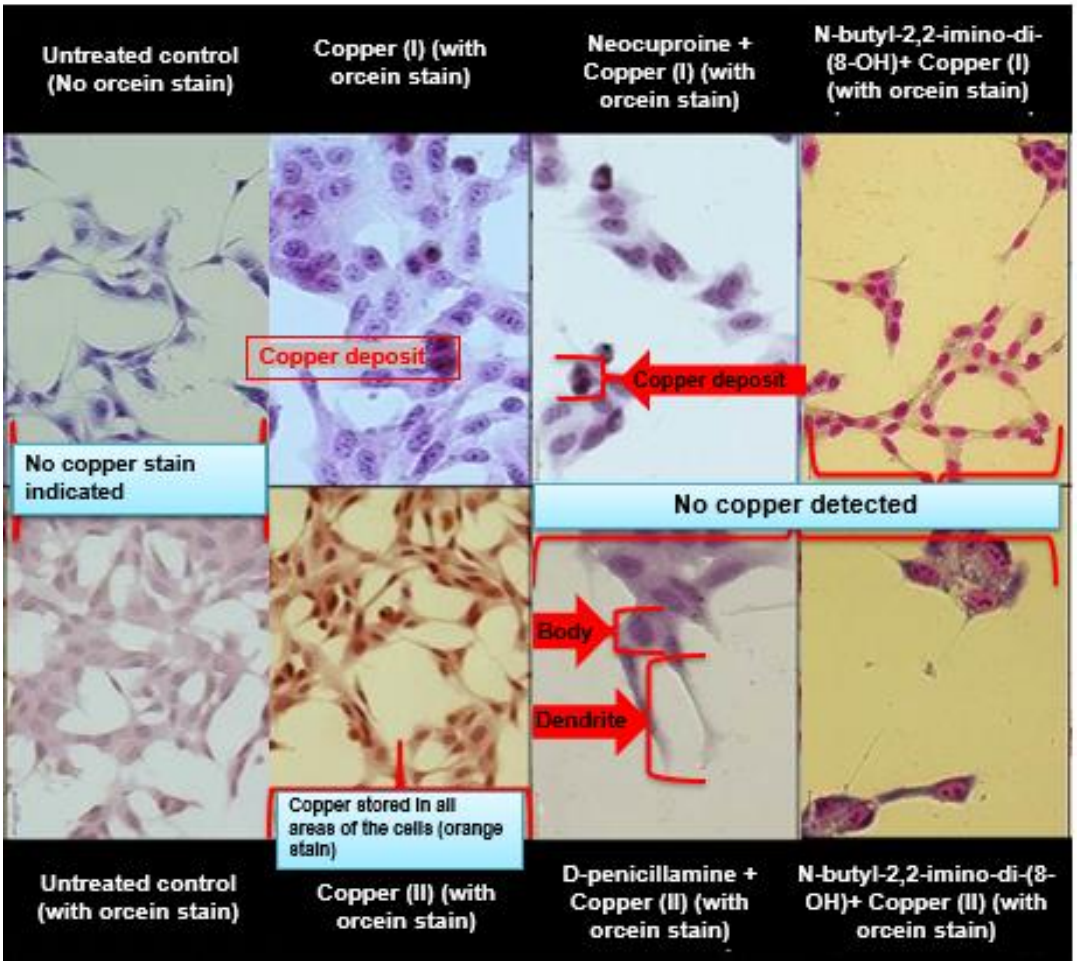

Figure 4.24: The neuronal cell staining without copper, with coppers (I) and (II) and control and test compounds in combination with copper.

Copper (I) deposits were clearly visible in the copper (I) and –(II) treated cells, as well as in the neocuproine treated cells.

4.1.5. Antioxidant activity of compounds

4.1.5.1. DPPH• assay

Of all the compounds tested, TMB was the most potent free radical scavenger (Table 4.12) and 2-fold more active than Trolox™ (Table 4.13). 5,7-Dimethyl-8-OH and 5-amino-8-OH demonstrated potent free radical scavenging activity that was comparable to that of the Trolox™ control, but less so than AA and BHA (Table 4.12). In contrast, 8-chloro-2-OH, 2-benzyl-8-OH and 8-fluoro-4-OH were the compounds with the poorest antioxidant activity . The IC_{50} values of those compounds that demonstrated activity greater than 60% are shown in Table 4.12 and Figure 4.25.

Table 4.12: The percentage free radical scavenged by test and control compounds.

Compound	IC_{50} value (µM)	Significant difference to IC_{50} value of Trolox™ control (P < 0.05)
Trolox™	10.89 ± 3.1	-
BHA	37.20 ± 0.85	Yes (P = 0.0007)
AA	22.87 ± 1.88	No (P = 0.14)
TMB	5.92 ± 0.13	Yes (P = 0.002)
5-Amino-8-OH	12.54 ± 1.55	No (P = 0.86)
5,7-Dimethyl-8-OH	16.33 ± 3.54	No (P = 0.16)
2-Amino-8-OH	33.73 ± 5.67	Yes (P = 0.005)
N-butyl-2,2-imino-di-(8-OH)	64.56 ± 18.58	Yes (P = 0.04)

*ND = not determined

In Table 4.12, 5,7-diiodo-8-OH, 2-methyl-8-OH, 5,7-dichloro-8-OH, 5,7-dichloro-2-CH_3-8-OH, 5,7-dibromo-8-OH, 5-chloro-7-iodo-8-OH, 5-chloro-7-bromo-8-OH, 5-chloro-8-OH, 5-HSO_3-7-iodo-8-OH, 5-HSO_3-8-OH, 5-carboxy-8-OH, 5-nitro-8-OH, 4-OH, 8-chloro-2-OH, 2-benzyl-8-OH and 8-fluoro-8-OH all demonstrated an IC_{50} value ≥ 200 µM.

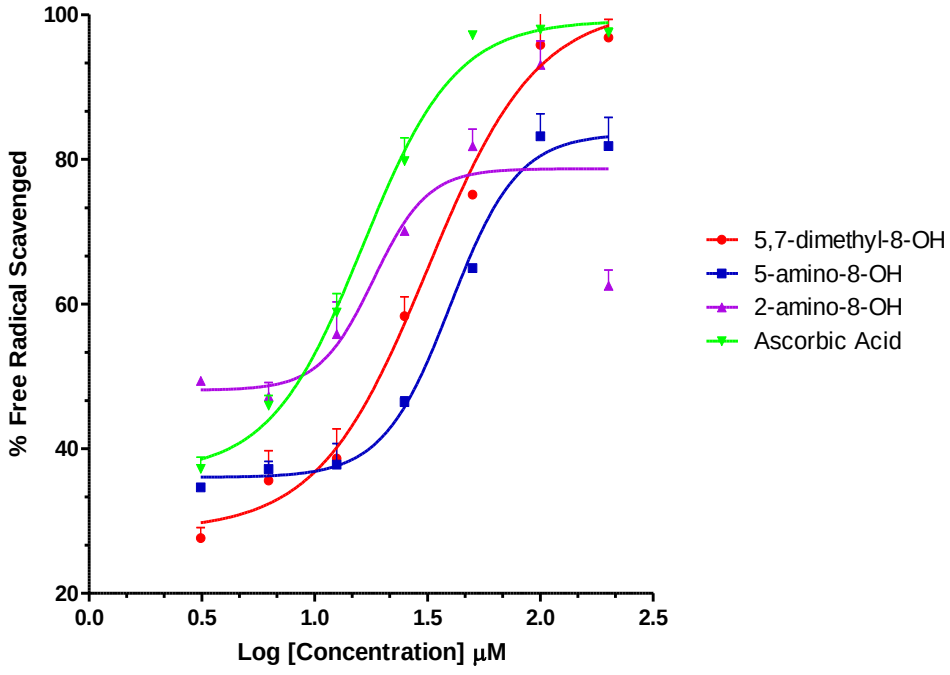

Figure 4.25: The log-sigmoid dose response curve of the free radical scavenging activity of the most active 8-OHs compared to that of AA, Trolox and BHA.

4.1.5.2. Lipid peroxidation inhibition assay

This assay determined whether the compounds inhibited or induced the formation of lipid peroxidation. Overall, the compounds demonstrated a low inhibitory ability to prevent lipid peroxidation (Table 4.13).

No compounds demonstrated a higher % lipid peroxidation inhibition than the BHA control. Of the 8-OH derivatives, 5-carboxy-8-OH showed the greatest lipid peroxidation activity and 5-chloro-8-OH showed the highest potency in inhibiting the formation of lipid peroxidation amongst the compounds (Table 4.13). The IC_{50} value of those compounds with a % lipid peroxidation inhibition greater than 40% is shown in Table 4.13 and Figure C.1.

Table 4.13: The lipid peroxidation inhibition activity as determined by the lipid peroxidation inhibition assay.

Compound	% Lipid peroxidation inhibition [IC_{50} value (µM)]	Compound	% Lipid peroxidation inhibition [IC_{50} value (µM)]
AA	88.12 ± 1.94 [34.37 ± 3.32]	**4-OH**	32.07 ± 0.76
Trolox™	68.79 ± 1.75 [15.19 ± 3.58]*	**8-Chloro-2-OH**	30.69 ± 2.33
5-Carboxy-8-OH	54.54 ± 1.35	**2-Amino-8-OH**	30.11 ± 1.01
TMB	45.53 ± 5.79	**2-Benzyl-8-OH**	29.80 ± 2.32
5-Chloro-8-OH	39.78 ± 0.95	**5,7-Dichloro-2-CH_3-8-OH**	29.42 ± 0.80
5,7-Dichloro-8-OH	33.83 ± 1.08	**5-HSO_3-8-OH**	29.29 ± 0.63
5-Chloro-7-bromo-8-OH	35.33 ± 0.79	**5,7-Dibromo-8-OH**	29.16 ± 1.39
5-Chloro-7-iodo-8-OH	34.32 ± 0.53	**5,7-Diiodo-8-OH**	27.78 ± 0.39
8-OH	40.19 ± 0.92	**N-butyl-2,2-imino-di-(8-OH)**	24.66 ± 3.51
5-HSO_3-7-iodo-8-OH	40.03 ± 1.93	**8-Fluoro-4-OH**	24.37 ± 1.72
5,7-Dimethyl-8-OH	32.41 ± 0.37	**5-Amino-8-OH**	23.78 ± 1.89
2-Methyl-8-OH	32.55 ± 0.98	**5-Nitro-8-OH**	1.88 ± 0.45

*P = 0.01

4.1.5.3. Griess reagent assay

This assay determined whether the compounds inhibited the formation nitrite as a measure of nitric oxide which is a reactive molecule that may mediate oxidative effects (Table 4.14). In comparison to the AA and gallic acid positive controls, the 8-OH derivatives did not possess any significant ability to inhibit nitrite production.

N-butyl-2,2-imino-di-(8-OH) was the most active of the tested compounds and was significantly different to the gallic acid control (P = 0.0009). The compounds showed different activities to one another with a mean result of 23.03 ± 2.04%. TMB demonstrated comparable nitrite production inhibition in comparison to AA and gallic acid (P = 0.24).

Table 4.14: The percentage nitrite in the media of SHSY5Y cells treated with compounds as determined by the Griess reagent assay.

Compounds	% Nitrite	Significant difference to Gallic acid control (P < 0.05)
AA	84.58 ± 4.43	Yes (P = 0.04)
Gallic acid	78.29 ± 2.57	-
TMB	64.79 ± 11.36	No (P = 0.24)
N-butyl-2,2-imino-di-(8-OH)	30.26 ± 4.84	Yes (P = 0.0009)
5-Amino-8-OH	25.39 ± 1.66	Yes (P = 0.0004)
Cupral	24.68 ± 1.99	Yes (P = 0.002)
5-Carboxy-8-OH	24.50 ± 2.93	Yes (P < 0.0001)
5-HSO_3-8-OH	23.56 ± 2.79	Yes (P = 0.0001)
8-OH	23.51 ± 1.66	Yes (P < 0.0001)
2-Benzyl-8-OH	23.43 ± 2.81	Yes (P < 0.0001)
2-Methyl-8-OH	23.31 ± 4.61	Yes (P < 0.0006)
8-Chloro-2-OH	23.30 ± 3.32	Yes (P = 0.0001)
5-Chloro-7-iodo-8-OH	23.10 ± 4.75	Yes (P = 0.0009)
5-Chloro-8-OH	23.06 ± 3.26	Yes (P = 0.0001)
5,7-Dichloro-8-OH	23.02 ± 2.79	Yes (P = 0.0002)
5,7-Dimethyl-8-OH	21.87 ± 2.10	Yes (P = 0.0002)
5-Nitro-8-OH	20.76 ± 2.45	Yes (P = 0.0001)
5-Chloro-7-bromo-8-OH	22.59 ± 3.87	Yes (P = 0.0005)
2-Amino-8-OH	22.51 ± 2.14	Yes (P = 0.0002)
4-OH	21.13 ± 2.38	Yes (P < 0.0001)
5-HSO_3-7-iodo-8-OH	20.87 ± 4.37	Yes (P = 0.0006)
5,7-Dichloro-2-CH_3-8-OH	22.40 ± 4.11	Yes (P = 0.0004)
5,7-Dibromo-8-OH	20.72 ± 3.56	Yes (P = 0.0007)
5,7-Diiodo-8-OH	21.74 ± 3.45	Yes (P = 0.0002)
8-Fluoro-4-OH	22.51 ± 1.40	Yes (P = 0.0002)

4.1.6. *Artemia* lethality assay

4.1.6.1. Effect of 8-OH derivatives on *Artemia* mortality

Several 8-OH derivatives demonstrated unfavourable toxicity against *Artemia franciscana* nauplii, where 2-benzyl-8-OH, 5,7-dimethyl-8-OH and N-butyl-2,2-imino-di-(8-OH) caused more than 80% mortality after 24 hours and ≥ 90% mortality after 48 and 72 hours exposure (Table 4.15). These compounds showed a similar activity to the positive control, potassium dichromate. After 24 hours exposure, 5-HSO_3-7-iodo-8-OH, 5,7-dichloro-2-CH_3-8-OH, 2-methyl-8-OH, 5,7-dibromo-8-OH and 5-chloro-8-OH demonstrated a % mortality of ≤ 10% which increased from 25 to 35% after 72 hours.

Table 4.15: The inhibitory effect of compounds on the viability of *Artemia* nauplii at time points of 24, 48 and 72 hours.

Time (hrs)	24 Hr	48 Hr	72 Hr	Significant difference to potassium dichromate control (P < 0.05)
Compound	**% Mortality at 200 µM**			
Potassium dichromate	90.37 ± 19.26	96.12 ± 7.76	96.61 ± 6.78	-
2-Benzyl-8-OH	90.65 ± 11.14	96.12 ± 6.76	100 ± 0.00	No (P = 0.28)
N-butyl-2, 2imino-di-(8-OH)	88.09 ± 6.74	95.27 ± 9.45	96.23 ± 7.55	No (P = 0.18)
5, 7-Dimethyl-8-OH	89.53 ± 2.70	99.69 ± 0.62	100 ± 0.00	No (P = 0.27)
8-Chloro-2-OH	10.94 ± 2.45	12.05 ± 2.87	13.48 ± 3.72	No (P = 0.06)
5,7 Dichloro-8-OH	8.07 ± 1.77	17.09 ± 7.00	22.62 ± 12.51	No (P = 0.06)
5-Chloro-8-OH	5.52 ± 1.76	24.81 ± 5.40	32.82 ± 6.89	No (P = 0.06)
2-Amino-8-OH	6.20 ± 1.01	16.39 ± 4.28	23.59 ± 11.14	No (P = 0.06)
5-Chloro-7-iodo-8-OH	4.98 ± 1.10	48.52 ± 6.86	55.58 ± 9.03	No (P = 0.09)
4-OH	4.13 ± 0.85	6.98 ± 2.24	11.89 ± 1.53	No (P = 0.06)
8-Fluoro-4-OH	4.10 ± 0.86	5.91 ± 2.86	5.91 ± 2.86	No (P = 0.06)
5-HSO_3-7-iodo-8-OH	4.37 ± 0.35	16.59 ± 6.18	32.40 ± 6.88	No (P = 0.06)
5-Amino-8-OH	4.19 ± 0.47	7.09 ± 3.09	9.19 ± 3.61	No (P = 0.06)
5,7-Dichloro-2-CH_3-8-OH	3.28 ± 0.51	17.69 ± 3.42	27.92 ± 5.77	No (P = 0.06)
5-HSO_3-8-OH	3.22 ± 0.53	3.63 ± 1.36	4.78 ± 2.57	No (P = 0.06)
2-Methyl-8-OH	2.73 ± 0.89	28.36 ± 4.65	31.37 ± 3.31	No (P = 0.06)
5-Nitro-8-OH	2.37 ± 0.81	4.45 ± 1.82	7.53 ± 1.90	No (P = 0.06)
5,7-Diiodo-8-OH	2.16 ± 0.53	5.51 ± 2.34	5.83 ± 2.17	No (P = 0.06)
8-OH	1.42 ± 0.17	5.34 ± 2.23	7.48 ± 1.85	No (P = 0.06)
5,7-Dibromo-8-OH	0.68 ± 0.79	17.24 ± 2.90	25.47 ± 7.41	No (P = 0.06)
5-Chloro-7-bromo-8-OH	0.00 ± 0.00	15.36 ± 8.76	23.91 ± 11.73	No (P = 0.06)

Several 8-OH derivatives demonstrated low toxicity that was not significantly different to potassium dichromate ($P > 0.05$). These include 8-chloro-2-OH, 5-amino-8-OH, 4-OH, 8-fluoro-4-OH, 5-HSO_3-8-OH, 5-nitro-8-OH, 5,7-diiodo-8-OH and 8-OH.

The LD_{50} values of 5,7-Dimethyl-8-OH and N-butyl-2,2-imino-di-(8-OH) were approximately two-fold more potent than that of potassium dichromate, thereby indicating that these compounds were more toxic towards the *Artemia* nauplii (Table 4.16).

Table 4.16: The LD_{50} values of compounds with a high % mortality against *Artemia* nauplii

Compounds	LD_{50} value	95% Confidence Interval	
	(µM)	Lower	Upper
Potassium dichromate	99.44	20.52	482.01
N-butyl-2,2-imino-di-(8-OH)	43.68	18.29	104.30
5,7-Dimethyl-8-OH	49.56	15.36	159.89
2-Benzyl-8-OH	166.66	38.56	720.25

4.1.6.2. Effect of 8-OH derivatives on *Artemia* morphology

The effect of the positive potassium dichromate control on the morphology of the brine shrimp was compared to the untreated control. Growth was arrested in early stage of nauplii (hatchling) at 24 hours in those that were exposed to potassium dichromate (Figure 4.26B) and noticeable deformities in the ocellus, sensorial antennules, swimming appendages, thorax and cercapod was observed when compared to the untreated control (Figure 4.26A).

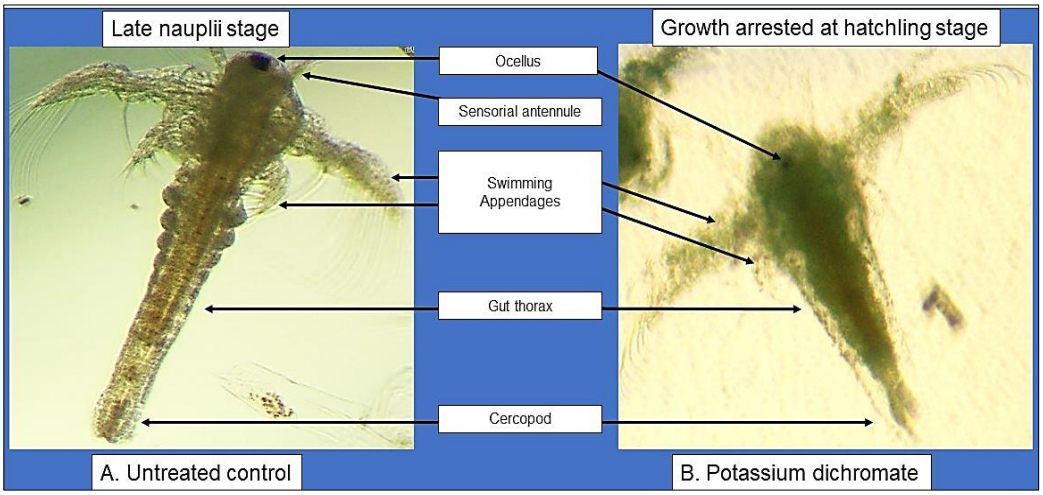

Figure 4.26: The comparison of the morphology of the untreated control vs the potassium dichromate positive control for the brine shrimp lethality assay.
The effect of the potassium dichromate control at 200 µM after 24 hours of exposure on the anatomy of brine shrimp nauplii.

In contrast, 5-chloro-7-iodo-8-OH demonstrated a degradative effect on the swimming appendages and cercapod of the nauplii (Figure 4.27A). 2-Benzyl-8-OH showed that the growth of the nauplii was halted early in development and looked similar to the nauplii that were exposed to potassium dichromate (Figure 4.27B). The effect of 5,7-dimethyl-8-OH exposure on the *Artemia* nauplii was seen throughout the entire organism (Figure 4.27C). All structures of the brine shrimp nauplii appeared to have been damaged by the exposure. N-butyl-2,2-imino-di-(8-OH) did not seem to halt the growth of the nauplii (Figure 4.27D), however the thorax seemed underdeveloped in comparison to the untreated control.

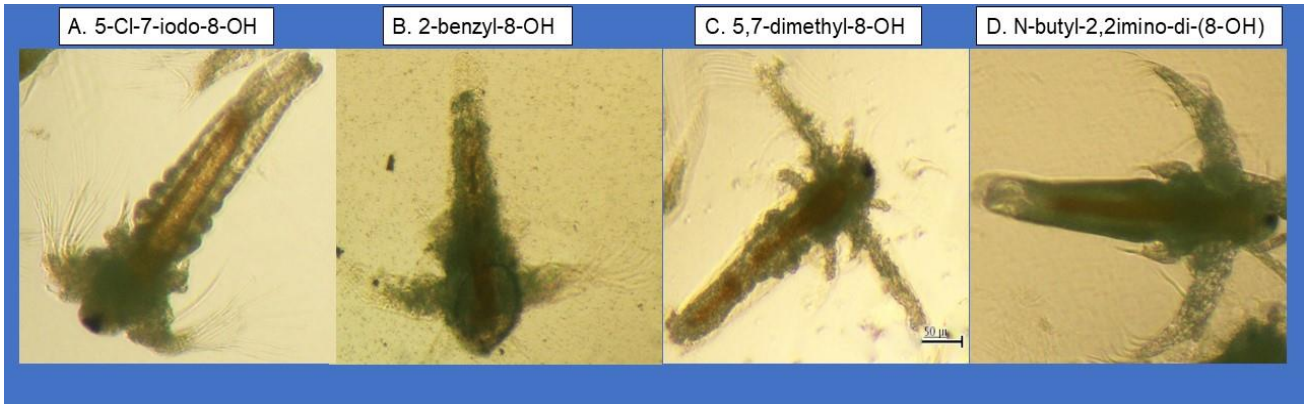

Figure 4.27: The effect of compounds on the anatomy of brine shrimp nauplii.
The effects of the 5-chloro-7-iodo-8-OH, 2-benzyl-8-OH, 5,7-dimethyl-8-OH and N-butyl-2,2-imino-di-(8-OH) at 200 µM after 24 hours of exposure on the anatomy of brine shrimp nauplii.

4.1.7. Larvicidal assay

4.1.7.1. Effect of 8-OH derivatives on larvae mortality

The larvicidal assay evaluated the inhibitory effect of 8-OH derivatives against the larvae of *An. arabiensis* (Table 4.17). 2-Benzyl-8-OH, 5,7-dichloro-2-CH_3-8-OH and 5-chloro-7-bromo-8-OH were found to be the most active larvicidal agents with activity greater than 90%. Whilst 5-Nitro-8-OH, 5,7-dichloro-8-OH and 5,7-dibromo-8-OH inhibited >80%, and N-butyl-2, 2imino-di-(8-OH) and 5-chloro-7-iodo-8-OH was > 60%. The remainder of the 8-OH derivatives demonstrated larvicidal activity in the range of 12 to 53%. The 8-OH derivatives inhibited the *Anopheles* larvae in a time-dependant manner (Table 4.17). The 8-OH derivatives did not show favourable LD_{50} values with large upper and lower confidence intervals (Table 4.18).

Table 4.17: The % mortality of larvae exposed to 8-OH derivatives.

Compound	% Mortality at 200 µM	Significant difference to DDT (P < 0.05)
DDT	100.00 ± 0.00	-
2-Benzyl-8-OH	99.00 ± 2.24	No (P = 1.00)
5,7-Dichloro-2-CH_3-8-OH	95.00 ± 5.00	No (P = 0.21)
5-Chloro-7-bromo-8-OH	94.00 ± 10.84	No (P = 0.54)
5-Nitro-8-OH	83.00 ± 5.70	Yes (P = 0.01)
5,7 Dichloro-8-OH	83.00 ± 8.37	Yes (P = 0.01)
5,7-Dibromo-8-OH	83.00 ± 8.37	Yes (P = 0.01)
N-butyl-2, 2imino-di-(8-OH)	77.00 ± 5.70	Yes (P = 0.01)
5-Chloro-7-iodo-8-OH	66.00 ± 8.94	Yes (P = 0.01)
5, 7-Dimethyl-8-OH	53.00 ± 14.40	No (P = 0.008)
8-OH	41.00 ± 9.62	No (P = 0.008)
5-HSO_3-7-iodo-8-OH	39.00 ± 8.94	Yes (P = 0.01)
8-Fluoro-4-OH	38.00 ± 7.58	Yes (P = 0.01)
8-Chloro-2-OH	30.00 ± 6.12	Yes (P = 0.01)
5,7-Diiodo-8-OH	28.00 ± 6.71	Yes (P = 0.01)
2-Methyl-8-OH	24.00 ± 4.18	Yes (P = 0.01)
5-HSO_3-8-OH	23.00 ± 5.70	Yes (P = 0.01)
4-OH	18.00 ± 2.74	Yes (P = 0.01)
2-Amino-8-OH	15.00 ± 3.54	Yes (P = 0.01)
5-Chloro-8-OH	15.00 ± 3.54	Yes (P = 0.01)
5-Amino-8-OH	12.00 ± 2.74	Yes (P = 0.01)

Table 4.18: The LD_{50} values of active compounds against larvae.

Compounds	LD_{50} value	95% Confidence Interval	
	µM	Lower	Upper
DDT	0.20	0.039	1.04
2-Benzyl-8-OH	174.53	72.20	421.92
5,7-Dichloro-2-CH_3-8-OH	353.79	101.77	1229.86
5,7-Dibromo-8-OH	565.14	114.24	2795.71
N-butyl-2,2-imino-di-(8-OH)	806.87	349.36	1863.52

4.1.7.2. Effect of 8-OH derivatives on larvae morphology

Physical structures of the larvae that are clearly shown in the untreated control such as the mouth brushes, imaginal eye, cardia, intestinal tract, comb scales and dorsal brush, are not as easily to distinguish in the DDT exposed larvae (Figure 4.28).

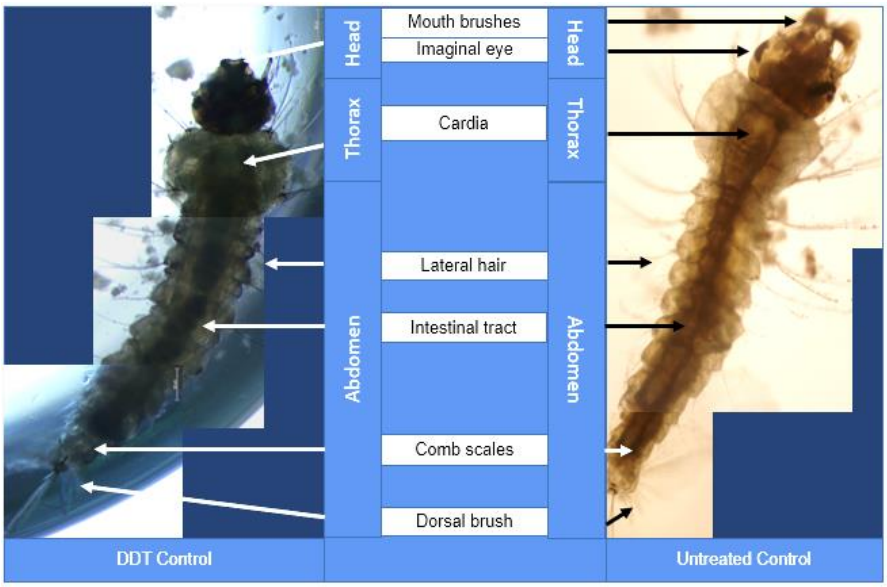

Figure 4.28: The morphological effects of the widely used insecticide, DDT (200 µM) after 24 hours of exposure on *An. arabiensis* larvae, in comparison to the untreated larvae.

Both N-butyl-2,2-imino-di-(8-OH) and 5,7-dichloro-CH_3-8-OH demonstrated adverse effects on the morphology of the *An. arabiensis* larvae (Figure 4.29). N-butyl-2,2-imino-di-(8-OH) (Figure 4.29A) appeared to cause significant internal damage to the larvae as the internal structures are visibly distorted. Similarly, 5,7-dichloro-2-CH_3-8-OH (Figure 4.29D) resulted in damage to the intestinal tract and internal structures of the larvae. The anatomical structures of larvae exposed to 2-benzyl-8-OH (Figure 4.29B) and 5,7-dibromo-8-OH (Figure 4.29C) were not visibly different to the untreated control (Figure 4.28).

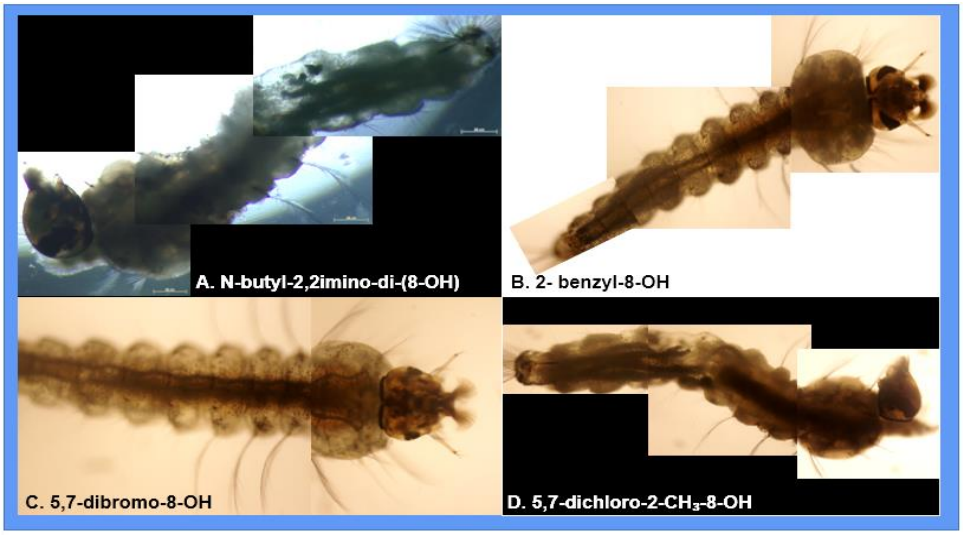

Figure 4.29: The effects of the N-butyl-2,2-imino-di-(8-OH), 2-benzyl-8-OH, 5,7-dibromo-8-OH and 5,7-dichloro-2-methyl-8-OH (200 µM) after 24 hours of exposure to *Anopheles* larvae.

Chapter 5. Essential Oil Constituents Results

5.1.1 Copper Homeostasis

5.1.1.1 Copper chelation

The copper chelation of the EOCs were tested against both copper(I) and copper(II) (Table 5.1). The hydroxylamine standard curve (Chapter 4, Figure 4.1) validated that the free copper ions that did not form metal chelates were oxidized to copper (I) ions and could be detected using neocuproine. The inactive EOCs displayed ranges for copper (I) chelation between 4.92 to 18.86% and for copper (II) chelation between 1.64 to 39.41% (Appendix C, Sections C.1 and C.2).

Table 5.1: The copper chelation effects of EOCs at 200 µM [Significant difference to TMB control, ($P < 0.05$)].

EOC/Compound	% Copper (I) Chelation	% Copper (II) Chelation
TMB	76.77 ± 1.32	84.77 ± 0.86
Neocuproine	*	*
D-Penicillamine	21.56 ± 1.28 [Yes ($P < 0.0001$)]	37.89 ± 0.09 [Yes ($P = 0.002$)]
Quinine	21.60 ± 0.16 [Yes ($P = 0.0002$)	13.81 ± 0.57 [Yes ($P < 0.0001$)]
(±)-Menthone	29.42 ± 3.52 Yes ($P < 0.0001$)	30.97 ± 0.64 Yes ($P = 0.02$)
TET	38.15 ± 1.48 [Yes ($P = 0.001$)]	27.34 ± 5.96 [Yes ($P = 0.004$)]
2-Mercaptothiazoline	13.23 ± 1.10 [Yes ($P < 0.0001$)]	12.62 ± 2.28 [Yes ($P = 0.0003$)]
Eugenol	9.39 ± 2.17 [Yes ($P = 0.0001$)]	7.76 ± 1.25 [Yes ($P < 0.0001$)]
Citral	8.82 ± 1.95 [Yes ($P < 0.0001$)]	5.32 ± 1.76 [Yes ($P = 0.0003$)]
(-)-α-Pinene	6.94 ± 1.45 [Yes ($P = 0.0005$)]	≤ 0.01 [Yes ($P < 0.0001$)]
(+)-α-Pinene	6.87 ± 1.04 [Yes ($P = 0.0003$)]	≤ 0.01 [Yes ($P < 0.0001$)]
Thymol	5.86 ± 1.40 [Yes ($P < 0.0001$)]	3.25 ± 0.20 [Yes ($P < 0.0001$)]
(S)-(-)-β-Citronellol	4.65 ± 0.41 [Yes ($P < 0.0001$)]	2.77 ± 0.28 [Yes ($P < 0.0001$)]

*Reagent in the assay therefore % copper chelation not determined.

The order of the EOCs that demonstrated the most activity in the copper (I) and-(II) chelation assay were as follows: (±)-menthone, 2-mercapthothiazoline and eugenol (Table 5.1). The TMB control demonstrated the highest copper (I) chelation at 200 µM; whilst D-penicillamine had comparable percentage copper (I) chelation to quinine at 200 µM.

The highest copper (II) chelation at 200 µM was TMB, followed by D-penicillamine and (±)-menthone. The percentage copper (II) chelation for TET and (±)-menthone was comparable,

as was quinine and 2-mercapthothiazoline (Table 5.1). D-penicillamine and TMB demonstrated a higher percentage copper (II) chelation in comparison to that of copper (I) chelation at a one to one ratio (Chelate: Cu(I)); however they were more specific for copper (I) chelation. (±)-Menthone showed no significant difference when its percentage copper (I) chelation was compared to that of its copper (II) chelation; although it had a two-fold preference for copper (I) over copper (II), when considering the IC_{50} values. A significant difference ($P < 0.05$) was observed for the percentage copper (I) and copper (II) chelation of the following: quinine, chloroquine and (S)-(-)-β-citronellol. The EOCs showed a significant difference to TMB, D-penicillamine and neocuproine ($P < 0.05$) in the copper chelation assay.

5.1.1.2 Copper complexation

The complexation assay determined the interaction of the EOCs with copper when added in a 1:1 ratio and showed variable activity (Table 5.2). A significant difference ($P < 0.05$) was observed when the percentage copper (I) and copper (II) complexation were compared for the following EOCs: 2-mercapthothiazoline, eugenol, thymol, (S)-(-)-β-citronellol and citral. The copper (II) complexation sigmoidal log dose response curve for thymol, (±)-menthone, and TMB is shown in Figure 5.1.

The control compounds demonstrated favourability towards copper (II) in the metal complexation assay, namely D-penicillamine, TMB and TET (Table 5.2). EOCs such as (±)-menthone, thymol and citral showed preference towards copper (II) complexation; while 2-mercapthothiazoline, eugenol, (-)-α-pinene, (+)-α-pinene favoured copper (I). The EOCs showed a significant difference to the TMB, D-penicillamine and neocuproine ($P < 0.05$) in the copper chelation and copper complexation assays.

5.1.1.3 Copper chelation combinations

The most active EOC, namely (±)-menthone (Table 5.1) was combined with TMB and quinine (Table 5.2, Table 5.3 and Figure 5.2). Synergistic interactions were observed between (±)-menthone with quinine (Figure 5.3A) to chelate copper (I) and (±)-menthone with quinine to chelate copper (II) (Figure 5.3C); as well as (±)-menthone and TMB to chelate copper (II) (Figure 5.3D). An additive interaction was seen between (±)-menthone and TMB to chelate copper (I) (Figure 5.3B). The isobologram for the combinations of (±)-menthone with quinine or TMB were constructed using Table 3.6 and Table 5.3.

Table 5.2: The copper complexation effects of EOCs [Significant difference to TMB control, ($P < 0.05$)].

EOC/Compound	% Copper (I) complexation	% Copper (II) complexation	IC_{50} value copper (I) complexation (µM)	IC_{50} value copper (II) complexation (µM)
TMB	59.41 ± 1.12	89.66 ± 0.27	≥ 100	25.80 ± 2.92
Neocuproine	40.66 ± 16.82 [No (P = 0.15)]	27.30 ± 5.09 [Yes (P = 0.002)]	**	**
D-Penicillamine	26.44 ± 3.82 [Yes (P = 0.004)]	38.44 ± 1.98 [Yes (P = 0.0005)]	**	**
TET	15.26 ± 2.09 [Yes (P = 0.0003)]	28.81 ± 4.82 [Yes (P = 0.002)]	**	**
Chloroquine	40.29 ± 3.17 [Yes (P = 0.005)]	39.27 ± 5.20 [Yes (P = 0.004)]	**	**
Quinine	33.17 ± 3.98 [Yes (P = 0.004)]	38.45 ± 9.27 [Yes (P = 0.01)]	**	**
(±)-Menthone	46.35 ± 3.18 [Yes (P = 0.02)]	91.12 ± 7.43 [Yes (P < 0.0001)]	**	10.78 ± 2.00
Thymol	13.35 ± 1.95 [Yes (P = 0.001)]	79.04 ± 1.62 [Yes (P = 0.01)]	**	20.04 ± 0.27
(-)-α-Pinene	29.55 ± 2.77 [Yes (P = 0.02)]	3.26 ± 0.94 [Yes (P < 0.0001)]	**	**
Citral	12.80 ± 1.52 [Yes (P = 0.0002)]	41.33 ± 4.52 [Yes (P = 0.01)]	**	**
2-Mercaptothiazoline	22.14 ± 2.86 [Yes (P = 0.002)]	6.36 ± 1.30 [Yes (P = 0.0001)]	**	**
Eugenol	14.18 ± 2.16 [Yes (P = 0.002)]	5.05 ± 1.30 [No (P < 0.0001)]	**	**
(S)-(-)-β-Citronellol	10.76 ± 4.29 [Yes (P = 0.003)]	10.12 ± 2.51 [Yes (P = 0.0004)]	**	**
(+)-α-Pinene	12.92 ± 2.40 [Yes (P = 0.002)]	6.15 ± 0.30 [Yes (P < 0.0001)]	**	**

** not determined as the EOC/compound did not demonstrate activity greater than 60%

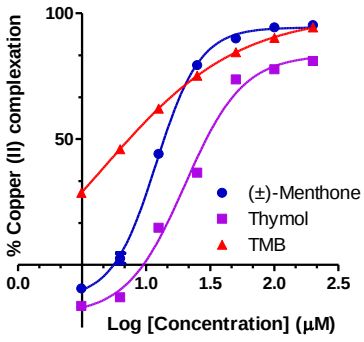

Figure 5.1: The log-dose response curve of the copper (II) complexation activity of (±)-menthone, thymol and TMB.

The various concentrations used in the combination studies from which the resultant IC_{50} values were determined for each compound using the copper chelation assay. The IC_{50} values were used to calculate the relative ratio (=FIC value) to construct the isobologram (Figure 5.3) and the average ΣFIC used to determine the type of interaction.

Table 5.3: The FIC_{50} values used to calculate the ΣFIC used to construct the isobologram for the copper chelation assay.

FIC_{50} values				
Ratio (±)-Menthone: Control	**Copper (I)**		**Copper (II)**	
	(±)-Menthone: Quinine	**(±)-Menthone: TMB**	**(±)-Menthone: Quinine**	**(±)-Menthone: TMB**
7.5:0.25	0.05	0.06	0.02	0.88
5:1	0.07	0.18	0.14	0.77
2.5:1.5	0.17	0.39	0.22	0.38
2:2	0.13	0.54	0.21	0.23
1:5	0.20	0.91	0.41	0.21
0.25:7.5	0.81	1.06	0.73	0.05

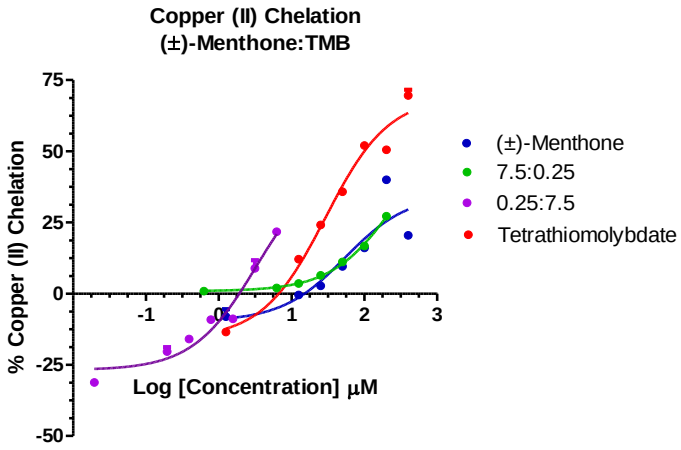

Figure 5.2: The log dose response curves of the combinations of (±)-menthone with TMB in the copper (II) chelation assay.

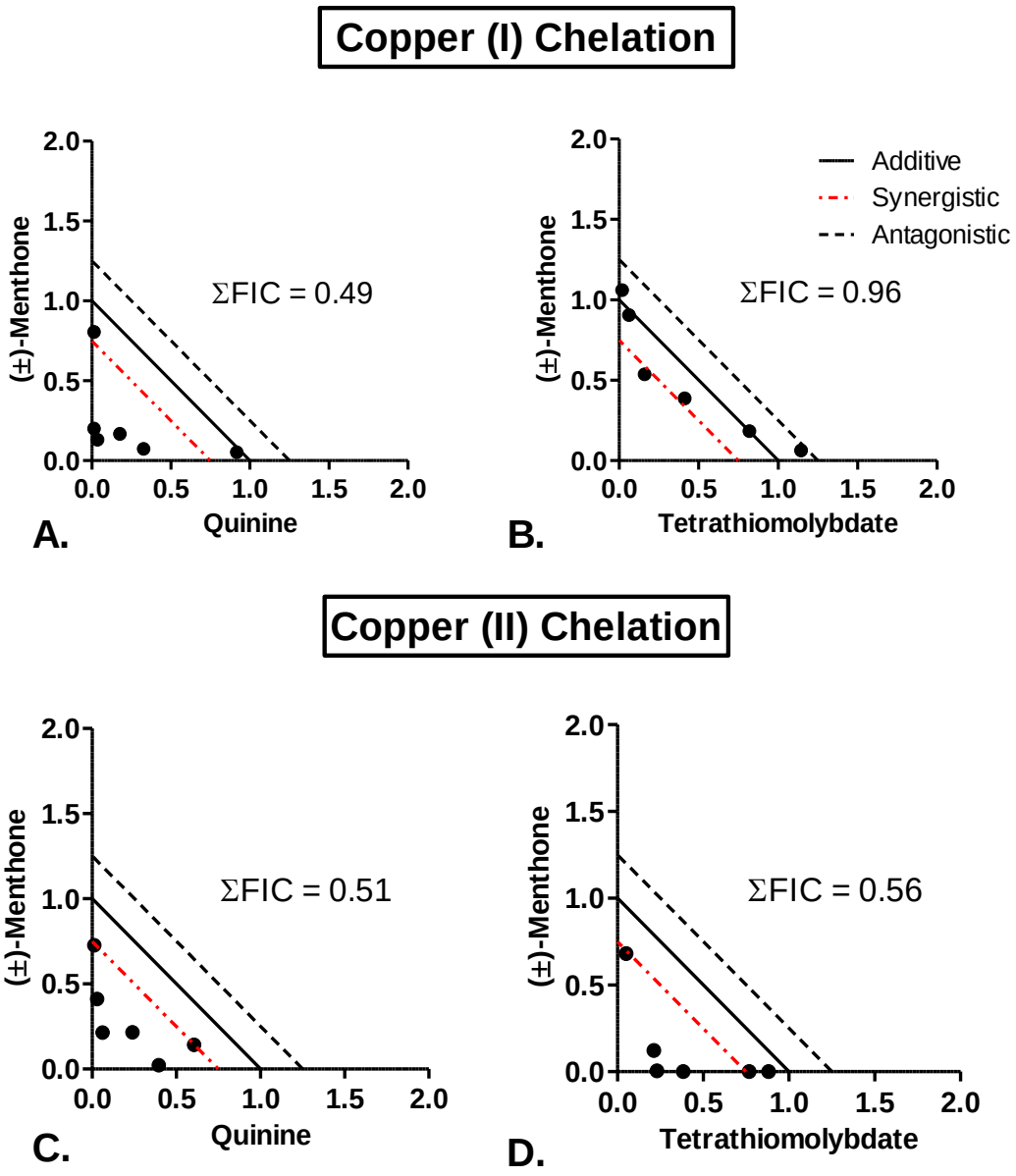

Figure 5.3: The combination copper chelation interactions of (±)-menthone and quinine (A and C) and TMB (B and D).

5.1.1.4 Copper reduction

All EOCs were screened at 200 µM and those that demonstrated activity greater than 60% were plotted in a linear regression (Figure 5.4). The copper reduction activity of the EOCs at the equivalent concentration of the activity of Trolox™ starting at 200 µM are shown in Table 5.4. Eugenol demonstrated the highest TEAC amongst the EOCs. Eugenol had comparable activity to the BHA control. (±)-Menthone had a two-fold higher TEAC to that of the known antioxidant AA, while 2-mercaptothiazoline had comparable activity to AA activity. The inactive EOCs (activity <60%) demonstrated activity ranging between 2.07 to 8.88 µM (Appendix C, Section C.3, Table C.3).

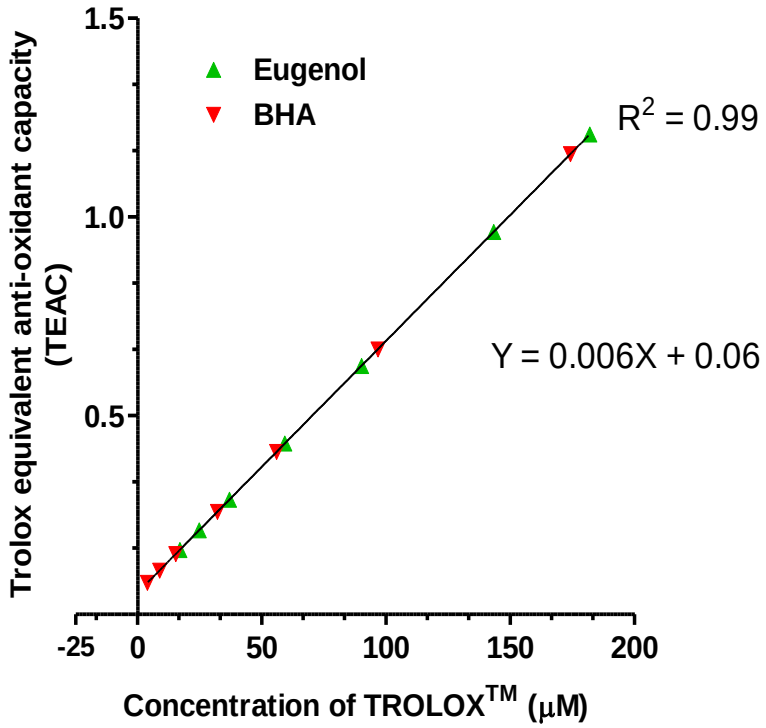

Figure 5.4: The linear regression curve showing the interpolated values for eugenol and BHA (The r^2 value for Trolox was 0.99).

The TEAC values at several concentrations for eugenol was determined and found to be similar to Trolox™.

Table 5.4: The Trolox™ equivalent antioxidant capacity, as determined by the copper reduction assay.

EOCs/Compound	TEAC at 200 µM	Significant difference to BHA control (P < 0.05)
BHA	135.32 ± 18.73	-
AA	22.39 ± 3.90	Yes (P = 0.01)
Eugenol	139.01 ± 18.45	No (P = 0.29)
(±)-Menthone	43.55 ± 8.11	Yes (P = 0.007)
2-Mercaptothiazoline	27.20 ± 0.64	Yes (P = 0.01)
(R)-(+)-Limonene	12.38 ± 2.80	Yes (P = 0.008)
Carvacrol	11.97 ± 2.36	Yes (P = 0.01)
Citral	11.09 ± 1.60	Yes (P = 0.008)
Farnesol	10.68 ± 0.53	Yes (P = 0.007)
(+)-Carvone	10.33 ± 1.95	Yes (P = 0.007)
***Cis*-geraniol**	10.29 ± 0.73	Yes (P = 0.008)
EDTA	6.05 ± 2.03	Yes (P = 0.006)

5.1.2 Antimalarial investigations

5.1.2.1 Inhibition of *in vitro* malaria parasite growth

EOCs showing activity in the copper chelation and reduction assays (Table 5.1 and Table 5.4) were tested and the IC_{50} values also determined for those inhibiting more than 60% parasite growth. Several EOCs demonstrated favourable inhibitory properties but were not as active as chloroquine and quinine (Table 5.5; IC_{50} values).

The EOC that demonstrated the highest percentage parasitaemia inhibition at 200 µM was α-humulene while the least active EOC was (-)-camphor. The percentage parasite growth inhibited for (±)-camphor was less than 0.01% (Not shown in Table 5.5). When considering the IC_{50} values, (+)-α-pinene was found to be more active as an antimalarial compared to quinine and chloroquine although its IC_{50} value was three-fold higher than that of DHA. Similarly (±)-camphorquinone demonstrated potent antimalarial activity with an IC_{50} value of 0.069 µM. Eugenol demonstrated a low ability to inhibit parasite growth at 200 µM, its interaction with copper warranted further investigation (Section 5.1.1.4, Table 5.4). The IC_{50} values of several of the EOCs showed a significant difference to chloroquine control ($P < 0.05$).

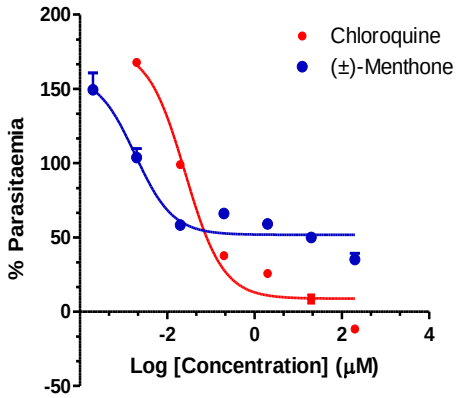

Figure 5.5: The log-dose response curve of the antimalarial activity of (±)-menthone and chloroquine in the pLDH assay.

5.1.2.2 The effect of the EOCs on parasitic stage, parasitaemia and the morphology of the parasite

Due to the promising activity of (±)-menthone to chelate and reduce copper (Section 5.1.1) its effect on synchronised parasites over a 72-hour period was determined in comparison to quinine (Table 5.6 and Figure 5.6). In Figure 5.6 and Table 5.6, the effect of (±)-menthone and control compounds on the parasitic stage over time is shown. In the untreated control, the stages proceed normally as rings, trophozoites and schizonts in a 48-hour cycle with gametocytes forming under stressful conditions.

Table 5.5: The percentage parasite growth inhibited at 200 µM and IC_{50} values of the EOCs against the *P. falciparum* 3D7 malaria strain, as determined by the pLDH assay [Significant difference to Chloroquine control (P < 0.05)].

EOCs/Compounds	IC_{50} value (µM) [% Parasite growth at 200 µM]	Significant difference to chloroquine control	EOCs/Compounds	IC_{50} value (µM) [% Parasite growth at 200 µM]
DHA	0.003 ± 0.0004	Yes (P = 0.0005)	***Trans*-geraniol**	≥200 [39.35 ± 0.87]
Chloroquine	0.07 ± 0.003	-	**(±)-Linalool**	≥200 [40.42 ± 1.71]
Quinine	0.11 ± 0.02	No (P = 0.06)	**(S)-(-)-Limonene**	≥200 [40.09 ± 1.94]
(+)-α-Pinene	0.009 ± 0.002	Yes (P = 0.002)	**α-Bisabolol**	≥200 [39.87 ± 0.13]
Eugenol	≥200	ND	**(+)-Carvone**	≥200 [38.43 ± 2.20]
(±)-Camphorquinone	0.069 ± 0.0001 [87.77 ± 6.50]	No (P = 0.25)	**(±)-Menthol**	≥200 [38.34 ± 0.10]
Citral	≥200	ND	**(-)-Bornyl acetate**	≥200 [37.92 ± 7.32]
Myrcene	6.53 ± 0.89 [84.78 ± 1.46]	Yes (P = 0.003)	**(-)-Linalool**	≥200 [37.18 ± 1.51]
(±)-Lavandulol acetate	12.33 ± 2.17 [91.28 ± 0.22]	Yes (P = 0.005)	***Trans*-nerolidol**	≥200 [37.78 ± 0.12]
Artemisia ketone	12.43 ± 2.79 [97.29 ± 1.92]	Yes (P = 0.008)]	**(-)-Pulegone**	≥200 [35.56 ± 2.09]
Ocimene	12.58 ± 0.16 [95.42 ± 0.64]	Yes (P < 0.0001)	**1,4 Cineole**	≥200 [35.29 ± 5.06]
α-Humulene	18.54 ± 2.73	Yes (P = 0.004)	**(-)-Terpinen-4-ol**	≥200 [35.31 ± 0.46]
(±)-α-β-Thujone	23.17 ± 4.19	Yes (P = 0.005)	**1,8-Cineole**	≥200 [35.10 ± 4.38]
2-Mercaptothiazoline	14.24 ± 0.01	Yes (P < 0.0001)	**Carvacrol**	≥200 [34.45 ± 4.58]
Thymol	18.92 ± 3.53 [90.38 ± 4.92]	Yes (P = 0.006)	**(+)-Terpinen-4-ol**	≥200 [33.66 ± 1.20]
(+)-*Trans*-caryophyllene	24.23 ± 0.97 [68.61 ± 0.84]	Yes (P = 0.0003)	**(-)-Citronellal**	≥200 [32.32 ± 0.14]
(S)-(-)-β-Citronellol	≥200 [47.46 ± 6.44]	ND	**(+)-β-Pinene**	≥200 [33.63 ± 18.82]
(±)-Menthone	≥200	ND	**(-)-Fenchone**	≥200 [31.72 ± 1.19]
(-)-Caryophyllene oxide	≥200 [82.12 ± 1.79]	ND	**(+)-Borneol**	≥200 [30.52 ± 6.63]
(-)-β-Pinene	≥200 [67.60 ± 8.07]	ND	**(-)-Borneol**	≥200 [29.75 ± 5.68]
(1S)-(+)-Camphorquinone	≥200 [77.15 ± 4.43]	ND	**(+)-Fenchone**	≥200 [28.36 ± 4.58]
(-)-α-Thujone	≥200 [65.57 ± 1.94]	ND	**(+)-Pulegone**	≥200 [28.25 ± 2.70]
(-)-α-Pinene	≥200 [63.47 ± 4.21]	ND	**(R)-(+)-Limonene**	≥200 [26.65 ± 1.83]
***Cis*-nerolidol**	≥200 [49.48 ± 1.64]	ND	**Farnesol**	≥200 [24.83 ± 1.99]
ρ-Cymene	≥200 [48.02 ± 7.71]	ND	**(1R)-(+)-Camphor**	≥200 [23.93 ± 3.80]
***Cis*-geraniol**	≥200 [45.72 ± 5.13]	ND	**(1R)-(-)-Camphorquinone**	≥200 [23.65 ± 0.19]
Geranyl acetate	≥200 [42.43 ± 1.98]	ND	**(-)-Carvone**	≥200 [18.62 ± 0.43]
Linalyl acetate	≥200 [42.36 ± 2.14]	ND	**(-)-Camphor**	≥200 [6.32 ± 0.25]

In Table 5.6 and Figure 5.6, the following was observed at different timepoints:

- *0 to 6 hours:* Expected early ring stage. No significant changes in morphology observed at this point, however the ring % parasitaemia of quinine and (±)-menthone are lower than that of the untreated control (Table 5.6). The total % parasitaemia for all parasitic stages (Figure 5.6D) was at the highest point for the untreated control, (±)-menthone and quinine.
- *12 hours:* Expected late rings and early trophozoites. No changes in morphology was observed when comparing (±)-menthone and quinine to the untreated control. A decrease in the % parasitaemia in the rings (Figure 5.6A) and increase in % parasitaemia in trophozoites (Figure 5.6B) was observed as expected. The untreated control had a higher total % parasitaemia in comparison to (±)-menthone and quinine. (±)-Menthone had a higher total % parasitaemia in comparison to quinine. A 2% decrease in total % parasitaemia was observed for (±)-menthone and quinine.
- *18 hours:* Expected Trophozoite stage. Normal morphological trophozoite development was observed in the untreated control, (±)-menthone and quinine. Late stage rings were still present in the untreated control. The % parasitaemia was lowest for quinine and (±)-menthone was lower than the untreated control (Figure 5.6D). An increase in schizonts (Figure 5.6C) was observed in the untreated control and the total % parasitaemia increased for (±)-menthone, quinine and the untreated control.
- *24 hours:* Expected trophozoite stage. Trophozoites were present, the % parasitaemia of rings was 0% and the % schizonts were increasing for (±)-menthone, quinine and the untreated control. The total percentage parasitaemia decreased for the untreated control and quinine while the total % parasitaemia increased for (±)-menthone.
- *30 hours:* Expected late trophozoite/early schizont stage. Late trophozoite and early schizonts were observed for (±)-menthone and the untreated control showed that the stages progressed as expected. Trophozoites were seen in the (±)-menthone and untreated control. The total % parasitaemia of the untreated control increased. The total % parasitaemia for quinine was steadily decreasing.
- *36 hours:* Expected schizont stage. Schizonts were observed in the untreated control and (±)-menthone (Table 5.6). Rings were observed in the quinine control, which suggested an alteration in the normal stage development of the parasite. The % parasitaemia of rings started to increase for quinine and the untreated control. The % parasitaemia of trophozoites increased to 1% for (±)-menthone compared to 2% in the untreated control. The untreated control, quinine and (±)-menthone all demonstrated the highest % parasitaemia of schizonts at this time point, which is as expected.

- *48 hours:* Expected early ring stage. Rings were observed in the untreated control and (±)-menthone (Table 5.6). An increase in the % parasitaemia of rings and a decrease in the % parasitaemia of trophozoites was observed for the untreated control, quinine and (±)-menthone. An increase in the % schizonts was observed for (±)-menthone and the total % parasitaemia for the untreated control, quinine and (±)-menthone was observed.
- *54 hours:* Expected mid-ring stage. Mid-rings and trophozoites were observed in (±)-menthone and the untreated control (Table 5.6). The trophozoites appeared smaller when compared to those observed at the 6-hour timepoint, indicating a possible change in morphology due to stressful conditions. The % rings increased for quinine and no change in % rings was observed for (±)-menthone from the previous 48-hour timepoint. A decrease in the % rings was observed for the untreated control and a slight increase in % trophozoites was observed for quinine and (±)-menthone. The total % parasitaemia for (±)-menthone was at its lowest point at 54 hours and a slight increase in total % parasitaemia for quinine was observed. The total % parasitaemia for the untreated control was observed to be steadily decreasing.
- *60 hours:* Expected late rings to trophozoite stage. Trophozoites were observed for the untreated control and (±)-menthone, whereas no parasites were observed for quinine. The % trophozoites increased for the untreated control. A slight increase in total % parasitaemia was observed in (±)-menthone possible indicating a recovery of the parasites from initial treatment.
- *66 hours*: Expected late trophozoites and schizonts Late trophozoites and schizonts were observed for (±)-menthone. An increase in % rings and a decrease in % schizonts was observed in (±)-menthone.
- *72 hours:* Expected early rings. Rings were observed for both (±)-menthone and the untreated control as well as an increase in the % trophozoites and schizonts. The % total parasitaemia continued to increase in (±)-menthone and remained unchanged for the untreated control. No parasites were observed for quinine.

Table 5.6: The effect of (±)-menthone and quinine at the IC_{50} value concentrations on the parasitic stages and morphology over a 72-hour period in comparison to untreated *P. falciparum* parasites.

Time (hours)	Untreated control	(±)-Menthone (6.4 µM)	Quinine (0.07 µM)
0 – 6 Ring stage	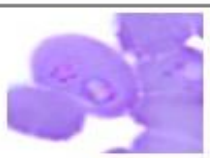	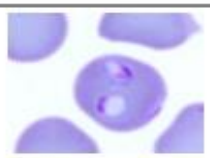	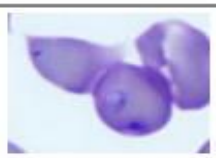
12 Late rings - Early trophozoite stage	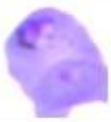	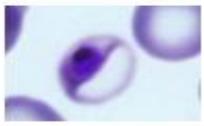	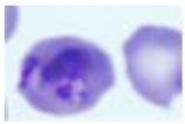
18 Trophozoite stage	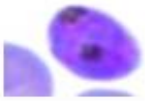		
24 Mid-Trophozoite stage			
30 Late Trophozoite – Early schizont stage			
36 Developing schizont stage			
48 New ring stage		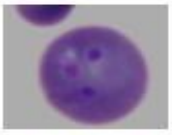	
54 Mid to late ring stage			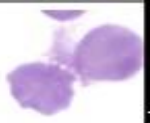
60 Late rings to early trophozoite			
66 Late trophozoites to early schizonts			
72 Late schizont to early ring stage			

No Parasites

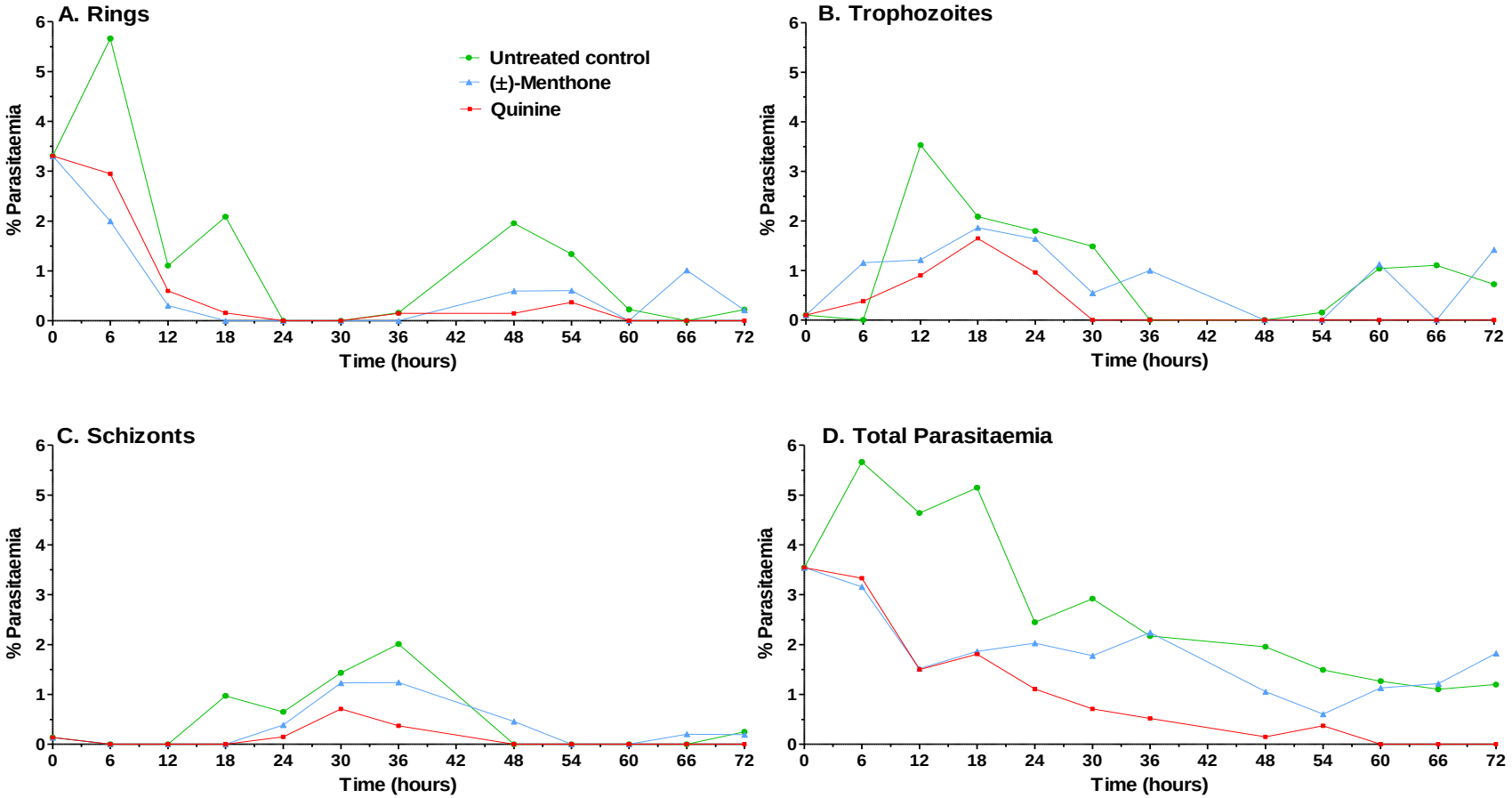

Figure 5.6: The comparison of the % parasitaemia over 72 hours of the ring (A), trophozoite (B), schizont (C) stages and the total % parasitaemia of the untreated control, (±)-menthone (6.4 µM) and the quinine (0.07 µM) control.

Parasites were treated with (±)-menthone and quinine at timepoint 0 hours and the parasites that were treated with (±)-menthone started to show signs of population recovery after 54 hours.

5.1.2.3 *In vitro* antimalarial combinations

(+)-α-Pinene demonstrated the most potent antimalarial activity of all the EOCs with an IC_{50} value of 0.009 ± 0.002 µM (Table 5.5), therefore, it was selected to examine its collective effect with chloroquine against the *P. falciparum* malaria parasite (Figure 5.8). The combination demonstrated a synergistic effect with an average ΣFIC value of 0.45 as verified by the points below the red 'synergistic' line in the isobologram. The IC_{50} values determined at the different ratios of the of (+)-α-pinene and chloroquine in combination are described in Table 5.7 and the sigmoidal log dose response curves of the ratios are shown in Figure 5.7.

Table 5.7: The FIC_{50} values used to calculate the ΣFIC in the pLDH assay.

FIC_{50} values		
Ratio	**Chloroquine**	**(+)-α-pinene**
7.5:0.25	0.72	0.008
5:1	0.56	0.02
2.5:1.5	0.68	0.09
2:2	0.0002	0.0007
1.5:2	0.35	0.12
1:2.5	0.05	0.04
0.5:5	0.08	0.28
0.25:7.5	0.06	0.59

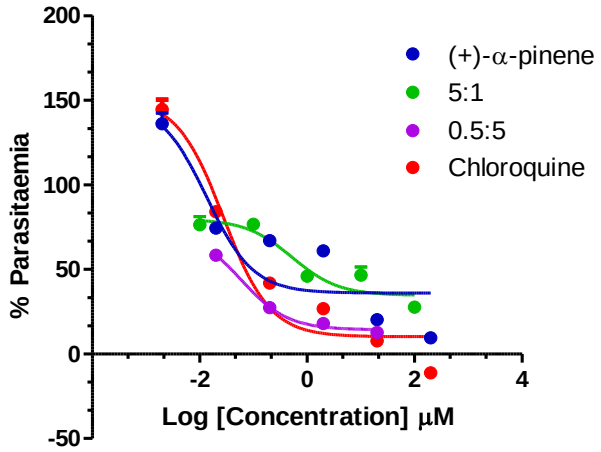

Figure 5.7: The sigmoidal log-dose response curves of the malaria parasite when exposed to combinations of (+)-α-pinene and chloroquine at different ratios as determined by the pLDH assay.

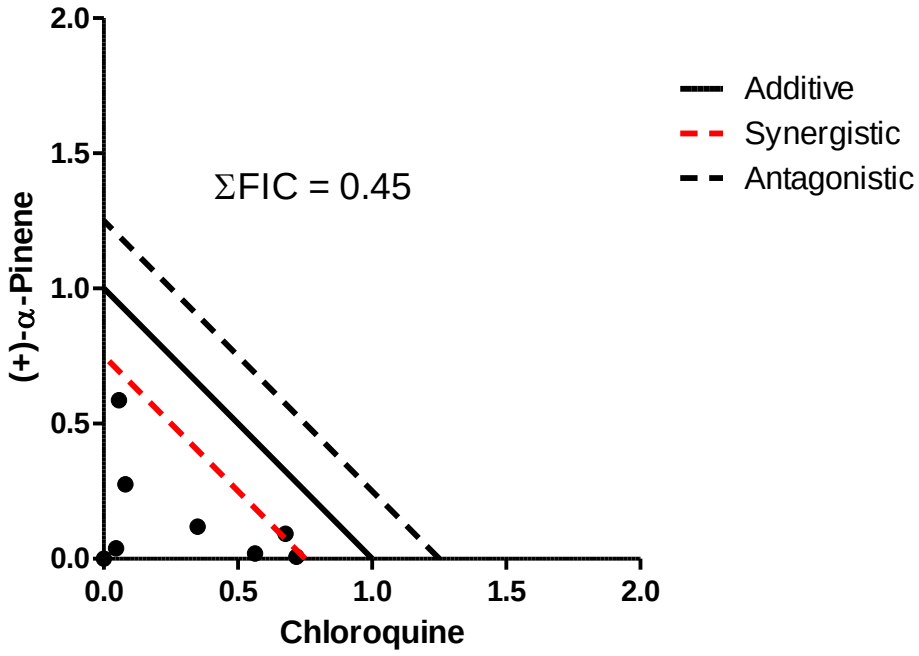

Figure 5.8: The synergistic interaction of (+)-α-pinene and chloroquine on the *in vitro* growth of *P. falciparum* growth as determined in the pLDH assay, indicating a synergistic interaction where the ΣFIC was less than 0.75.

5.1.2.4 The ferriprotoporphyrin biomineralization inhibition assay

Several EOCs (200 µM) displayed no inhibitory properties on β-haematin synthesis with an activity range of 1.25 to 30.44% (Appendix C, Section C.4, Table C.4). (+)-Pulegone and (-)-pulegone had the highest ability to inhibit biomineralization and were comparable to chloroquine and quinine (Table 5.8). Similarly, the following EOCs demonstrated a high % FBIT: (+)-Terpinen-4-ol > citral > myrcene > (-)-citronellol > (+)-α-pinene. Due to the slope of the log sigmoid dose response curve, (S)-(-)-(β)-citronellol was found to be the most potent of the EOCs. All active (%FBIT ≥ 60%) EOCs demonstrated IC_{50} values lower than quinine (Table 5.8 and Figure 5.9)

Table 5.8: The percentage ferriprotoporphyrin biomineralization inhibited by EOCs at 200 µM.

EOCs/Compounds	% FBIT at 200 µM	IC_{50} (µM)	EOCs/Compounds	% FBIT at 200 µM
Chloroquine	97.86 ± 0.48	22.91 ± 3.78	**(+)-*Trans*-caryophyllene**	40.59 ± 5.35 [No (P = 0.003)]
Quinine	83.52 ± 3.09 [Yes (P = 0.02)]	37.71 ± 3.63 [Yes (P = 0.009)]	**Carvacrol**	40.37 ± 0.91 [Yes (P = 0.0002)]
(S)-(-)-β-Citronellol	64.48 ± 4.97 [Yes (P = 0.008)]	19.80 ± 3.21 [No (P = 0.23)]	**(-)-Terpinen-4-ol**	39.39 ± 2.58 [Yes (P = 0.0008)]
(+)-α-Pinene	82.16 ± 2.70 [Yes (P = 0.01)]	23.09 ± 1.91 [No (P = 0.151)]	**2-Mercaptothiazoline**	38.37 ± 3.64 [Yes (P = 0.001)]
Citral	90.31 ± 2.49 [Yes (P = 0.04)]	23.09 ± 3.91 [No (P = 0.52)]	**(-)-Borneol**	37.91 ± 7.14 [No (P = 0.008)]
(+)-Terpinen-4-ol	92.55 ± 2.01 [Yes (P = 0.03)]	25.80 ± 5.22 [No (P = 0.68)]	**(±)-Menthol**	37.73 ± 9.23 [No (P = 0.18)]
(-)-Linalool	70.06 ± 1.36 [Yes (P = 0.002)]	26.59 ± 4.21 [No (P = 0.29)]	**(-)-Camphor**	37.63 ± 2.67 [Yes (P = 0.0009)]
(-)-Citronellal	86.27 ± 7.55 [No (P = 0.12)]	26.83 ± 3.15 [No (P = 0.31)]	***Cis*-geraniol**	37.63 ± 7.83 [Yes (P = 0.006)]
Myrcene	90.08 ± 5.79 [No (P = 0.13)]	28.87 ± 4.17 [No (P = 0.34)]	***Cis*-nerolidol**	36.20 ± 12.22 [Yes (P = 0. 001)]
(+)-Pulegone	96.78 ± 1.08 [No (P = 0.33)]	34.01 ± 3.41 [Yes (P = 0.02)]	***Trans*-geraniol**	36.31 ± 4.77 [No (P = 0.002)]
(-)-Pulegone	96.44 ± 1.47 [No (P = 0.33)]	33.17 ± 5.37 [No (P = 0.06)]	**(S)-(-)-Limonene**	31.75 ± 1.80 [Yes (P = 0.0002)]
(-)-α-Thujone	46.94 ± 10.64 [Yes (P = 0.02)]	*	**(±)-Lavandulol acetate**	30.86 ± 2.98 [No (P = 0.0005)]
(1R)-(+)-Camphor	46.79 ± 9.65 [No (P = 0.01)]	*	**(±)-Menthone**	10.31 ± 1.46 [Yes (P = 0.0001)]
Artemisia ketone	41.67 ± 2.69 [Yes (P = 0.0005)]	*	**EDTA**	≤0.10 ± 0.1 [Yes (P = 0.004)]
(±)-α-β-Thujone	40.92 ± 6.92 [No (P = 0.006)]	*		

* not determined

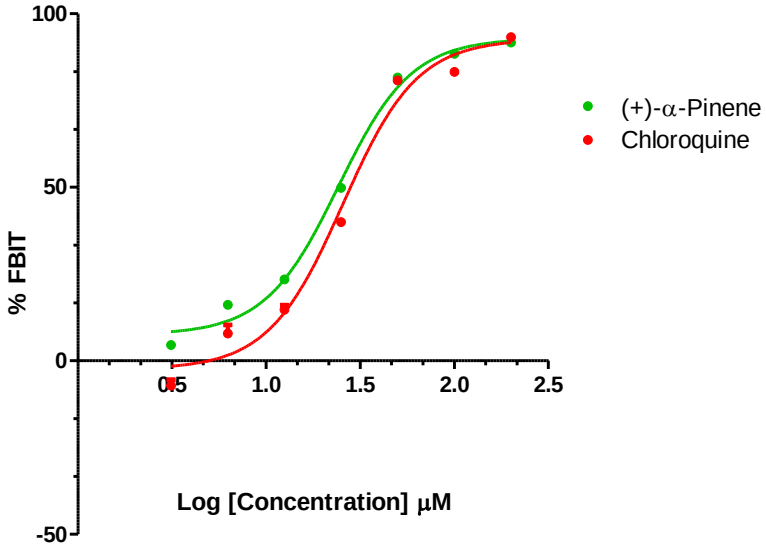

Figure 5.9: The log-dose response curve of (+)-α-pinene and chloroquine as determined by the FBIT assay.

5.1.2.5 The antimalarial haematin inhibition combination

(S)-(-)-β-Citronellol demonstrated the most potent FBIT activity of all the EOCs with an IC_{50} value 19.80 ± 3.21 µM (Table 5.8), and when combined with the IC_{50} value of chloroquine in several ratios resulted in a synergistic interaction with a sum (ΣFIC) value of 0.64 (Figure 5.10 and Figure 5.11). The IC_{50} values determined at the different ratios of the of (S)-(-)-β-Citronellol and chloroquine in combination are described in Table 5.9 and the sigmoidal log dose response curves of the ratios are shown in Figure 5.10.

Table 5.9: The FIC_{50} values used to calculate the ΣFIC in the FBIT assay.

FIC_{50} values		
Ratio	**Chloroquine**	**(S)-(-)-β-citronellol**
7.5:0.25	0.65	0.21
5:1	0.36	0.33
2.5:1.5	0.07	0.37
2:2	0.04	0.62
1.5:2	0.01	0.55
1:2.5	0.65	0.21
0.5:5	0.36	0.33
0.25:7.5	0.07	0.37

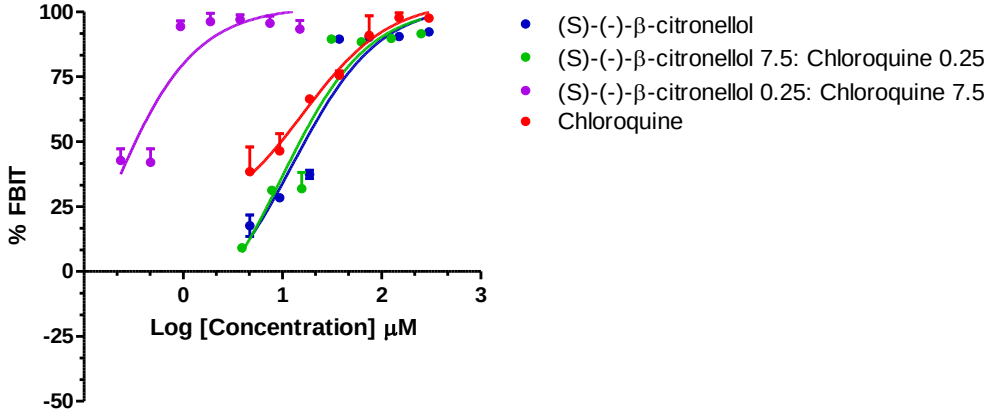

Figure 5.10: The sigmoidal log-dose response curves of (S)-(-)-β-citronellol and chloroquine at different ratios indicating the dose dependant manner in which ferriprotoporphyrin biomineralization was inhibited using the FBIT assay..

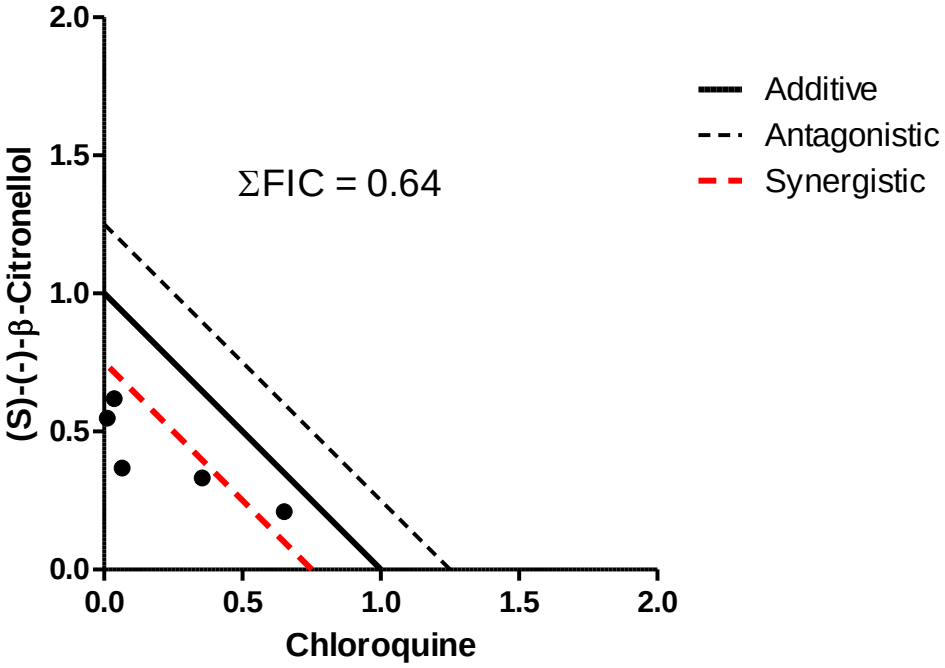

Figure 5.11: The combination assay of (S)-(-)-β-citronellol and chloroquine in the ferriprotoporphyrin biomineralization inhibition assay.

The combination showed a synergistic outcome where the FBIT activity of the combination was greater than the sum of (S)-(-)-β-citronellol and chloroquine FBIT activity individually.

5.1.3 The haemolytic effect of essential oil constituents

5.1.3.1 Red blood cell toxicity assay

The red blood cell toxicity assay was used to determine the haemolytic effect of the EOCs at several different concentrations (Table 5.10). Myrcene and carvacrol both demonstrated unfavourable haemolysis (≥ 20%); in contrast, (-)-α-pinene, thymol, (+)-β-pinene and ocimene demonstrated lower haemolytic effects (≤ 2%). All EOCs demonstrated a % haemolysis greater than that of chloroquine and quinine. The EOCs demonstrated p-values ranging between 0.0001 and 0.38.A % haemolysis of greater than 30% is considered to be highly haemolytic.

5.1.3.2 Protective effect of EOCs against copper (I)-induced haemolysis

The EOCs that demonstrated the greatest protective effect against copper (I) induced lysis were: carvacrol, eugenol and (+)-carvone. 1,8-cineole, (-)-terpinen-4-ol, (±)-linalool and (±)-menthone had comparable results to the copper (I) chelator, neocuproine (% haemolysis = 18.38 ± 0.23). (+)-α-Pinene demonstrated a large increase in haemolysis when incubated with copper (I), as did chloroquine and quinine (Figure 5.12).

5.1.3.3 Haemolytic protective effect of EOCs against copper (II)

The EOCs that showed the greatest protective effect against copper (II)-induced haemolysis included: carvacrol, eugenol, (±)-linalool, (-)-terpinen-4-ol and (+)-carvone (Figure 5.13). (±)-Menthone and D-penicillamine had comparable effect and demonstrated an increase in lysis when incubated with copper (II). (+)-α-Pinene had a 2-fold greater lytic effect than quinine; whilst (±)-menthol had a comparable haemolytic effect to chloroquine.

Table 5.10: The percentage haemolysis that was induced by EOCs.

EOCs/Compound	% Haemolysis at 200 µM	EOCs	% Haemolysis at 200 µM
Chloroquine	18.32 ± 0.89		
Quinine	18.93 ± 1.03 [No (P = 0.38)]	**(S)-(-)-β-Citronellol**	5.28 ± 0.96 [Yes (P = 0.0006)]
Myrcene	40.27 ± 6.29 [Yes (P = 0.003)]	**(S)-(-)-Limonene**	4.93 ± 1.11 [Yes (P = 0.001)]
Carvacrol	27.53 ± 5.72 [No (P = 0.11)]	**(+)-Fenchone**	3.96 ± 0.93 [Yes (P = 0.008)]
Eugenol	8.21 ± 1.14 [No (P = 0.08]	**(±)-Camphorquinone**	3.52 ± 0.24 [Yes (P = 0.006)]
1,8-Cineole	8.04 ± 1.24 [Yes (P = 0.02)]	**α-Humulene**	3.02 ± 0.27 [Yes (P = 0.003)]
1,4 Cineole	8.39 ± 1.07 [Yes (P = 0.02)]	**Artemisia ketone**	2.85 ± 0.23 [Yes (P = 0.01)]
(±)-Linalool	8.67 ± 0.99 [Yes (P = 0.001)]	**ρ-Cymene**	2.74 ± 0.42 [Yes (P = 0.003)]
(-)-Terpinen-4-ol	7.91 ± 1.08 [Yes (P = 0.006)]	**α-Bisabolol**	2.49 ± 1.06 [Yes (P = 0.005)]
***Cis*-nerolidol**	7.60 ± 1.30 [Yes (P = 0.001)]	**(-)-Caryophyllene oxide**	2.48 ± 0.47 [Yes (P = 0.002)]
(+)-Carvone	6.94 ± 1.00 [Yes (P = 0.001)]	**(1R)-(-)-Camphorquinone**	2.46 ± 0.28 [Yes (P = 0.003)]
(-)-Linalool	6.63 ± 1.32 [Yes (P = 0.002)]	**(+)-*Trans*-caryophyllene**	2.44 ± 0.37 [Yes (P = 0.002)]
(±)-Menthol	6.19 ± 0.63 [Yes (P = 0.0004)]	**(1S)-(+)-Camphorquinone**	2.41 ± 0.24 [Yes (P = 0.004)]
(+)-Terpinen-4-ol	6.16 ± 0.70 [Yes (P = 0.0003)]	**(-)-Borneol**	2.38 ± 0.77 [Yes (P = 0.003)]
(±)-Lavandulol acetate	6.14 ± 0.35 [Yes (P = 0.003)]	**(+)-Borneol**	2.37 ± 1.14 [Yes (P = 0.005)]
(-)-Carvone	6.05 ± 0.97 [Yes (P = 0.0004)]	**2-Mercaptothiazoline**	2.33 ± 0.13 [Yes (P = 0.003)]
***Trans*-nerolidol**	6.02 ± 0.58 [Yes (P = 0.0004)]	**(-)-Bornyl acetate**	2.28 ± 0.47 [Yes (P = 0.002)]
(-)-Pulegone	6.01 ± 1.05 [Yes (P = 0.0004)]	**(-)-α-Thujone**	2.22 ± 0.48 [Yes (P = 0.002)]
(-)-Menthone	5.93 ± 0.85 [Yes (P = 0.002)]	**(-)-β-Pinene**	2.19 ± 0.27 [Yes (P = 0.0002]
Geranyl acetate	5.89 ± 1.08 [Yes (P = 0.003)]	**(±)-α-β-Thujone**	2.18 ± 0.04 [Yes (P = 0.001)]
Farnesol	5.82 ± 0.40 [Yes (P = 0.001)]	**(+)-α-Pinene**	2.16 ± 0.36 [Yes (P = 0.002)]
(-)-Citronellal	5.81 ± 0.95 [Yes (P = 0.0004)]	**(±)-Camphor**	2.15 ± 0.45 [Yes (P = 0.002)]
Linalyl acetate	5.78 ± 1.02 [Yes (P = 0.001)]	**(1R)-(+)-Camphor**	2.14 ± 0.08 [Yes (P = 0.001)]
(R)-(+)-Limonene	5.62 ± 1.18 [Yes (P = 0.0002)]	**(-)-Fenchone**	2.06 ± 0.14 [Yes (P = 0.003)]
(+)-Pulegone	5.58 ± 1.04 [Yes (P = 0.0008)]	**(-)-Camphor**	2.03 ± 0.40 [Yes (P = 0.0005)]
***Trans*-geraniol**	5.51 ± 0.65 [Yes (P = 0.0001)]	**Ocimene**	1.95 ± 0.45 [Yes (P = 0.004)]
***Cis*-geraniol**	5.21 ± 0.56 [Yes (P = 0.0003)]	**(+)-β-Pinene**	1.85 ± 0.12 [Yes (P = 0.0007)]
Citral	5.37 ± 0.79 [Yes (P < 0.0001)]	**Thymol**	1.84 ± 0.33 [Yes (P = 0.001)]
(±)-Menthone	5.36 ± 0.97 [Yes (P < 0.0001)]	**(-)-α-Pinene**	1.65 ± 0.28 [Yes (P = 0.002)]

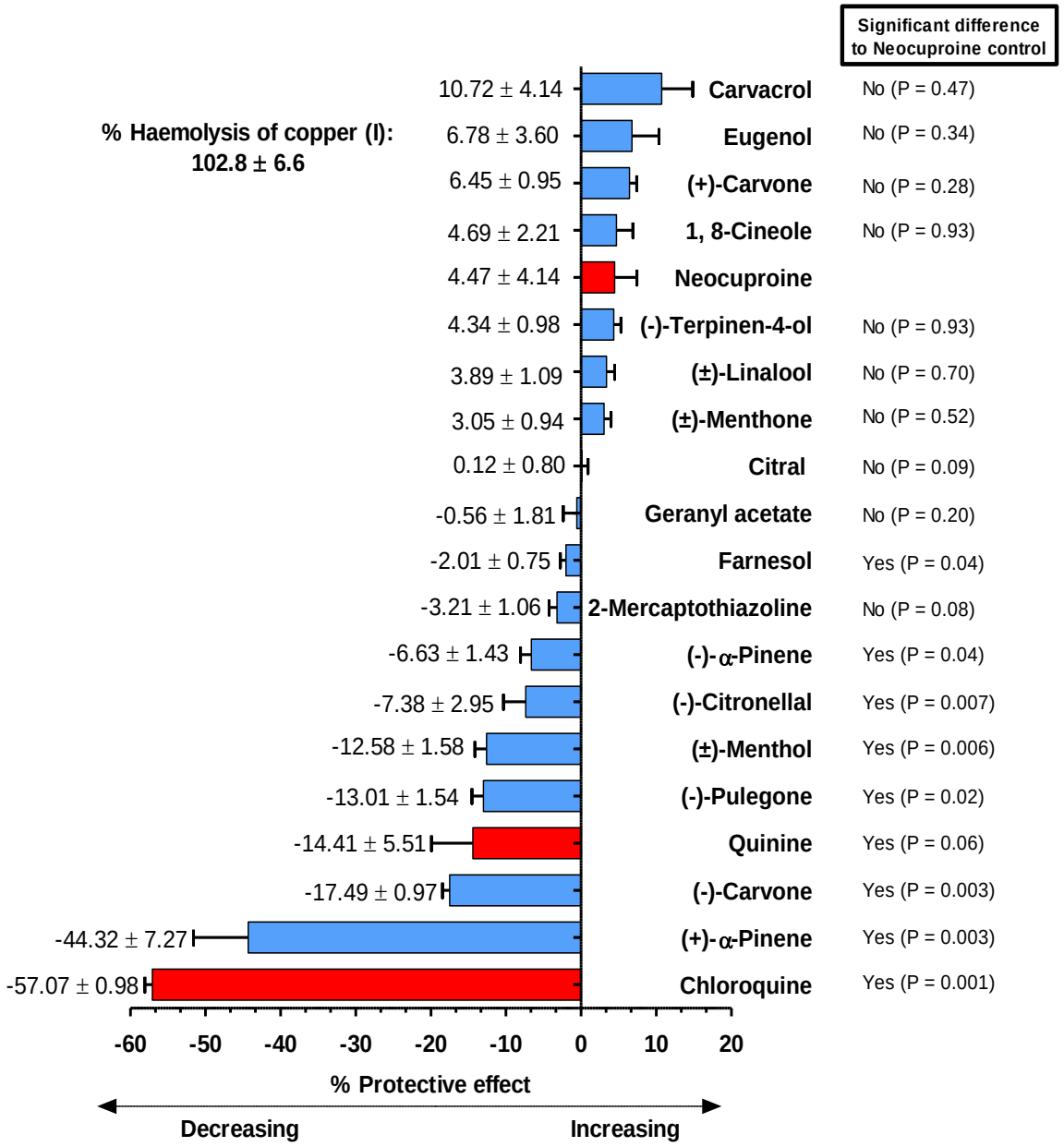

Figure 5.12: The protective effect of the EOCs on red blood cells treated with copper (I). The difference of the EOCs alone (at 200 µM) and the combination determined the protective effect of the EOCs against copper (I) (at 200 µM).

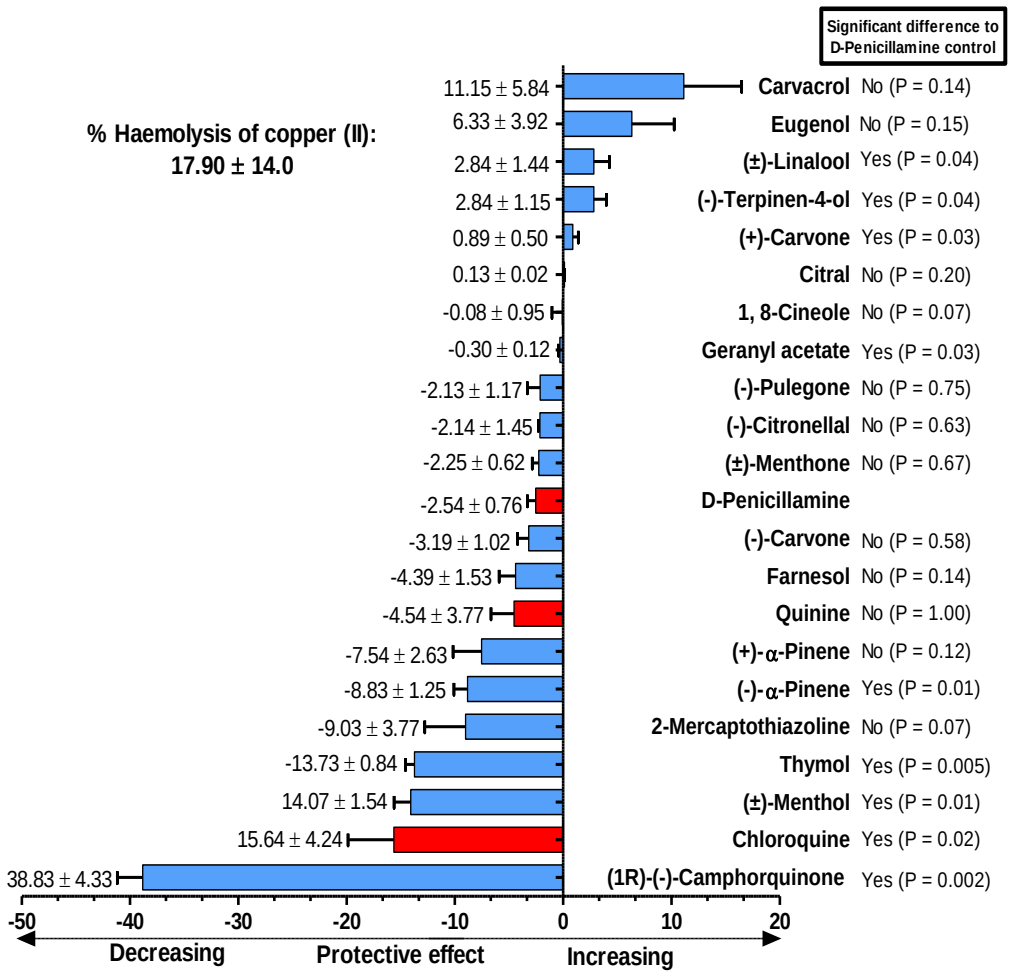

Figure 5.13: The protective effect of the EOCs on red blood cells treated with copper (II). The difference of the EOC alone (at 200 µM) and the combination determined the protective effect of the EOC against copper (II) (at 200 µM).

5.1.4 Effect of essential oils on neuroblastoma cells

5.1.4.1 Cytotoxicity assay

The following EOCs exhibited a cellular viability (≥ 80%) against the neuroblastoma cells as determined by the MTT assay: (±)-menthol, (1R)-(+)-camphor, (1R)-(-)-camphorquinone, carvacrol, 2-mercaptothiazoline, artemisia ketone, (+)-fenchone and (-)-bornyl acetate (Table 5.11). In contrast, the majority of the EOCs, i.e. 89% of those evaluated, displayed a cellular viability of ≥ 60% growth as evaluated by the SRB assay. The two assays were measuring two different cellular inhibitory processes therefore they had different results that depended on the compounds specific mechanism of inhibitory action (Berenbaum, 1978; Lin, Hoult and Raman, 1999). The results excluded were recorded in Appendix C, Section C.5, Table C.5.

Table 5.11: The percentage cellular viability and IC_{50} values of the EOC, copper ions and controls (200 µM) on the neuroblastoma cell line. When compared to camptothecin, a P value > 0.05 was considered not significant (NS).

EOCs	MTT viability assay	SRB viability assay
	IC_{50} value (µM)	IC_{50} value (µM)
Copper (I)	7.8 ± 0.9 Yes (P = 0.02)	≥200
Copper (II)	24.1 ± 1.4 No (P = 0.12)	≥200
Camptothecin	13.8 ± 3.0	10.1 ± 2.0
(-)-α-Pinene	9.18 ± 1.01 Yes (P = 0.04)	≥200
(1S)-(+)-Camphorquinone	9.26 ± 2.40 Yes (P = 0.03)	≥200
Geranyl acetate	12.97 ± 1.09 Yes (P = 0.02)	≥200
Eugenol	14.43 ± 1.24 No (P = 0.46)	≥200
(+)-α-Pinene	15.67 ± 0.49 Yes (P = 0.04)	≥200
(±)-Linalool	15.33 ± 1.04 No (P = 0.14)	≥200
Linalyl acetate	22.24 ± 2.18 No (P = 0.11)	≥200
(-)-Citronellal	24.59 ± 2.52 No (P = 0.10)	≥200
(-)-Pulegone	27.64 ± 1.64 No (P = 0.10)	≥200
(S)-(-)-(β)-Citronellol	46.07 ± 5.21 No (P = 0.09)	≥200
Methotrexate	≥200	13.5 ± 4.9 No (P = 0.44)

2-Mercaptothiazoline was the only EOC to exhibit some degree of toxicity where the cellular viability was less than 60% for the SRB assay. Whilst ten EOCs were observed to be more cytotoxic with the cellular viability less than 40% when assessed via the MTT assay: (+)-α-Pinene, (±)-linalool, (-)-α-pinene, (±)-camphorquinone, eugenol, geranyl acetate, linalyl acetate, (-)-pulegone, (S)-(-)-(β)-citronellol and (-)-citronellal.

From the log sigmoid dose response curves, (-)-α-pinene was the most toxic of the EOCs as determined by the MTT assay (Table 5.11). The EOCs selectively inhibited the neuroblastoma cells in the MTT assay as compared to the SRB assay.

5.1.4.2 Protective effect of EOCs against copper

The results excluded from Figure 5.12 and Figure 5.13 were recorded in Appendix C, Section C.5, Table C.9. The effect of the EOCs when incubated with neuroblastoma in the presence of a copper excess was determined for both copper (I) and copper (II).

5.1.4.2.1. Protective effect of EOCs against copper (I)

Neuroblastoma cells were incubated with copper (I) for 24 hours, thereafter with the addition of the EOCs, the effect on cellular viability was recorded (Figure 5.14). Eugenol, (+)-α-pinene, (-)-citronellal and farnesol all demonstrated a protective effect against the cytotoxic activity of copper (I) (Figure 5.14). Camptothecin decreased the cytotoxic effects of copper (I), whilst the EOCs did not protect the cells against copper (I) cytotoxicity.

5.1.4.2.2. Protective effect of EOCs against copper (II)

Neuroblastoma cells were incubated with copper (II) for 24 hours, thereafter with the addition of the EOCs, the effect on cellular viability was recorded (Figure 5.15). Eugenol and (+)-α-pinene mimicked the protective effects of camptothecin and D-penicillamine when incubated with copper (II) and neuronal cells (Figure 5.15). The majority of EOCs demonstrated an increase in cytotoxicity and did not protect the cells against the cytotoxic effect of copper (II). In contrast, eugenol and (+)-α-pinene both demonstrated a protective effect against both copper (I) and –(II) cytotoxic activity (Figure 5.15). .

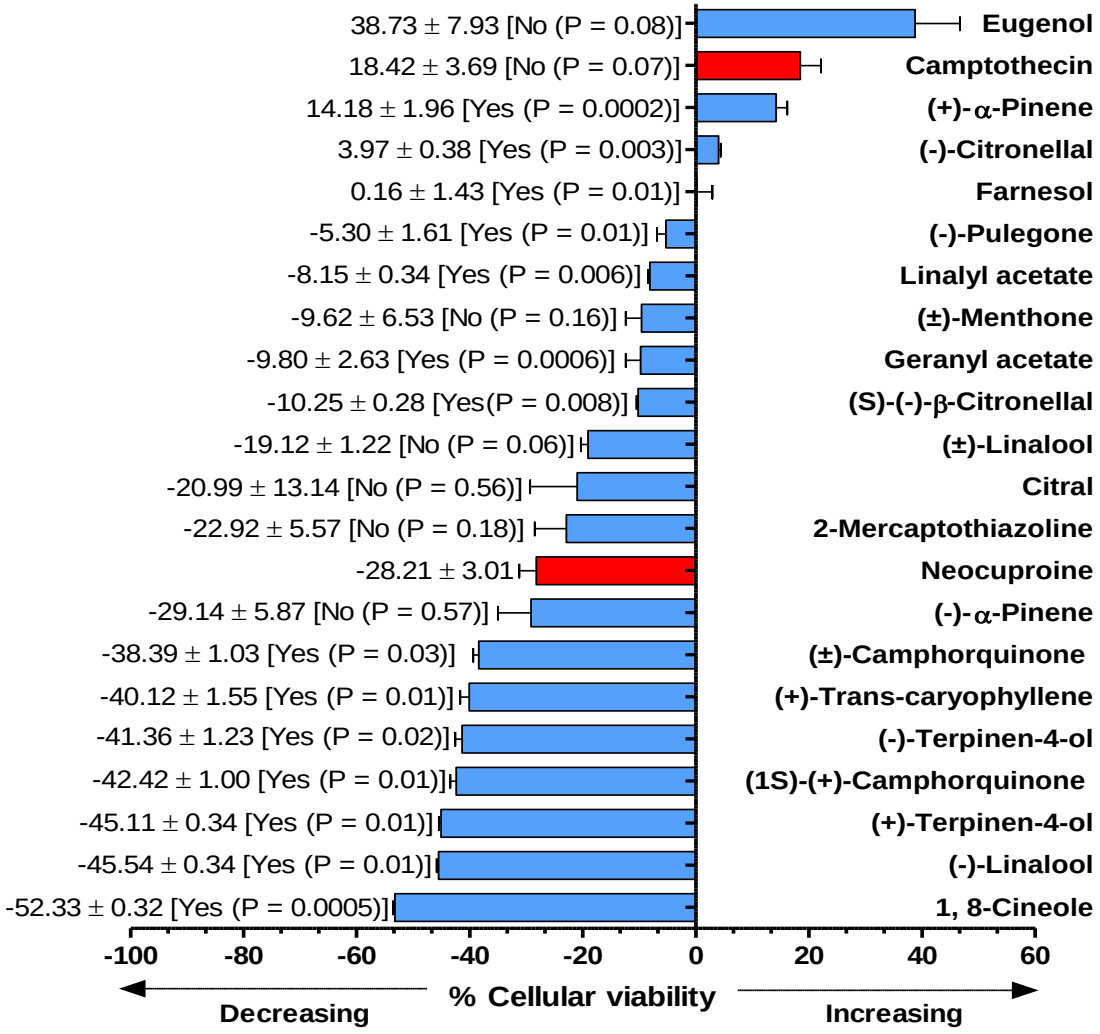

Figure 5.14: The effect of incubation with copper (I) and EOCs on percentage cellular viability.

When incubated with copper (I) (200 µM), EOCs at 200 µM showed a change in cellular viability in comparison to when incubated alone..

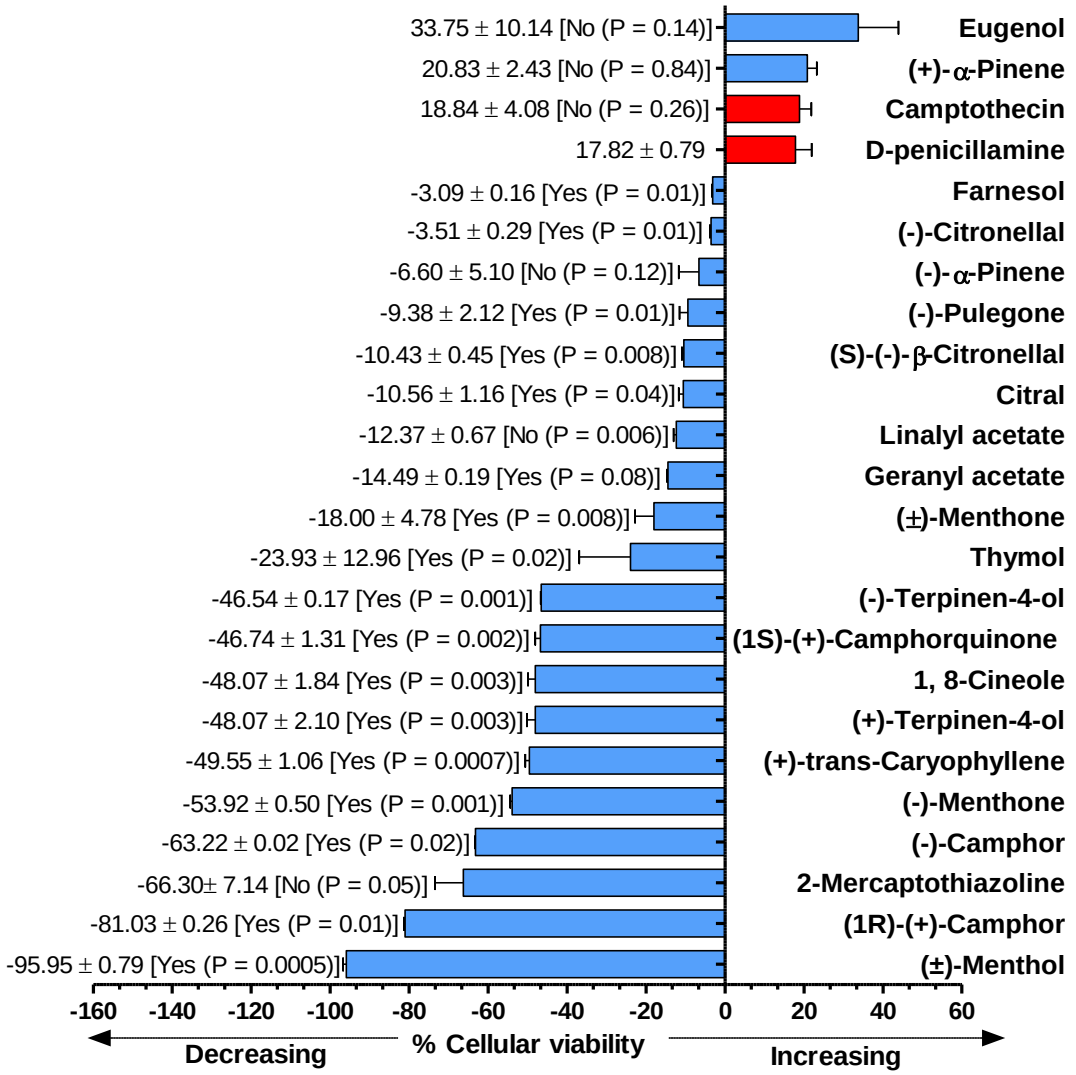

Figure 5.15: The effect of incubation with copper (II) and EOCs on percentage cellular viability.

When incubated with copper (II) (200 µM), EOCs at 200 µM showed a change in cellular viability in comparison to when incubated alone. The EOCs showed no significant difference to the D-penicillamine control with a P = 0.10 and for (-)-citronellal (P = 0.08); (-)-camphor, geranyl acetate, citral, (-)-α-pinene and 2-mercaptothiazoline (P = 0.20).

5.1.4.3 Effect of EOCs and copper on the structure of neuronal cells

(±)-Menthone, was selected along with copper control compounds: neocuproine and D-penicillamine to visualise the effect of copper (I) and (II) on the SH-SY5Y cell line (Figure 5.16). No copper (in both the copper (I) and –(II) treated cells) was observed in the neuroblastoma cells that were treated with (±)-menthone. Copper was not detectable in D-

penicillamine-treated cells; whilst brick red copper deposits were visible in the neocuproine treated cells (Figure 5.16).

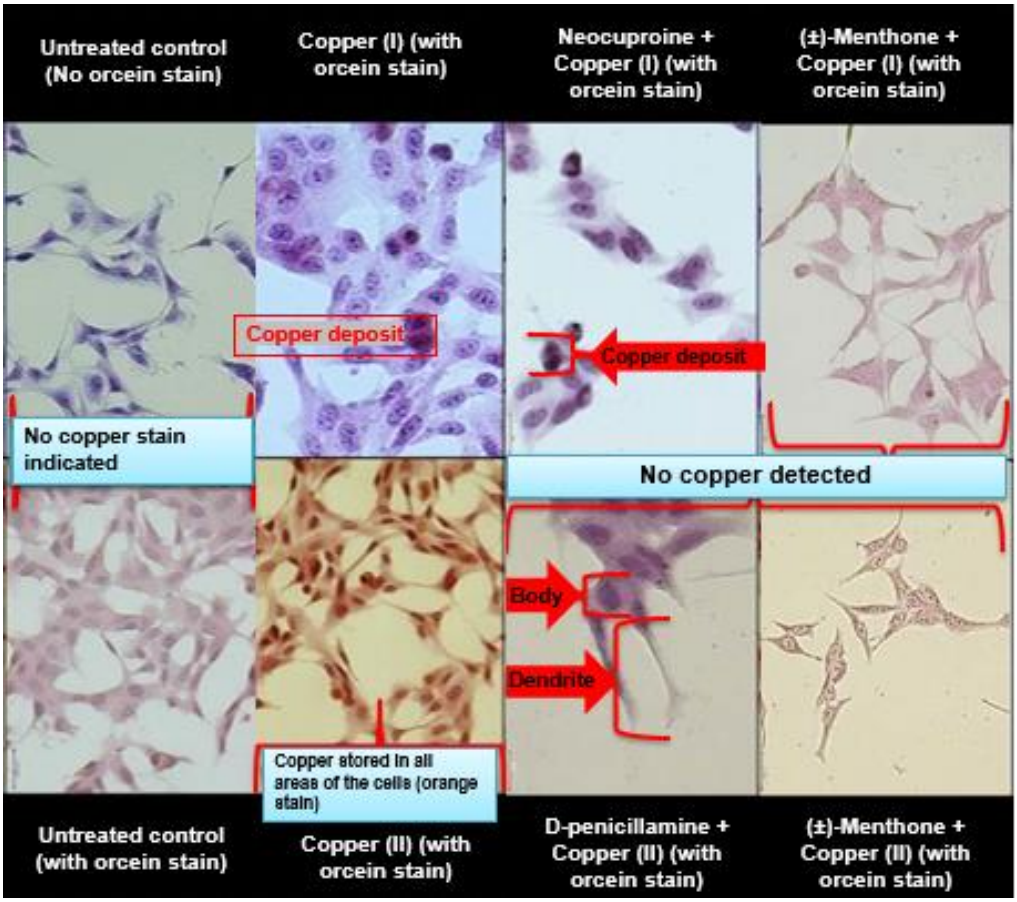

Figure 5.16: The neuronal cell staining without copper, with coppers (I) and (II) and control and EOCs in combination with copper.

Copper (I) deposits were clearly visible in the copper (I) and –(II) treated cells, as well as in the neocuproine treated cells.

5.1.5 Antioxidant activity of essential oils constituents

5.1.5.1 DPPH$^{\bullet}$ free radical scavenging activity

The IC_{50} values for the most active EOCs were determined and compared to the Trolox™ control. EOCs that demonstrated a high percentage free radical scavenging activity did not necessarily have consistent IC_{50} values. EOCs that did not demonstrate activity in this assay were included in Appendix C, Section C, Table C.10).

Eugenol had comparable % free radical scavenging activity to Trolox™, BHA and AA, with the IC_{50} values indicating that eugenol was less potent than Trolox™; and more potent than BHA and AA (Table 5.12 and Figure 5.17). Overall, the EOCs did not demonstrate strong free

radical scavenging activity (Appendix C., Section C.6, Table C.10). Eugenol did not have significantly higher antioxidant activity in comparison to the Trolox™ (Table 5.12).

Table 5.12: The percentage free radical scavenged by the EOC's and control compounds.

EOCs/Compound	% Free radical scavenged at 200 µM	IC_{50} value (µM)	Significant difference to Trolox™ control
Trolox™	96.30 ± 1.00	10.89 ± 3.1	-
BHA	91.90 ± 6.10	37.20 ± 0.85	Yes (P = 0.0007)
AA	96.20 ± 1.80	22.87 ± 1.88	No (P = 0.14)
Eugenol	92.80 ± 4.40	13.22 ± 1.65	No (P = 0.15)
(-)-β-Pinene	22.96 ± 2.48	ND	ND
Thymol	14.71 ± 3.30	ND	ND
(-)-Bornyl acetate	6.01 ± 1.03	ND	ND
Geranyl acetate	5.76 ± 1.20	ND	ND
(+)-Carvone	4.03 ± 1.35	ND	ND
α-Bisabolol	4.03 ± 0.74	ND	ND
(±)-Linalool	3.23 ± 0.19	ND	ND
Carvacrol	3.13 ± 0.62	ND	ND
(-)-Pulegone	3.10 ± 0.15	ND	ND
(±)-Lavandulol acetate	3.04 ± 0.64	ND	ND
***Cis*-nerolidol**	3.03 ± 0.68	ND	ND
(S)-(-)-β-Citronellol	3.01 ± 0.52	ND	ND
(-)-Carvone	3.01 ± 0.50	ND	ND
(±)-Menthone	2.94 ± 0.30	ND	ND
***Trans*-nerolidol**	2.88 ± 0.79	ND	ND
Farnesol	2.74 ± 0.42	ND	ND
(-)-Menthone	2.73 ± 0.39	ND	ND
Artemisia ketone	2.52 ± 0.61	ND	ND
Ocimene	2.49 ± 0.52	ND	ND
(+)-α-Pinene	2.44 ± 0.29	ND	ND
(±)-α-β-Thujone	2.35 ± 0.56	ND	ND
(-)-Fenchone	2.31 ± 0.40	ND	ND
Citral	2.26 ± 0.22	ND	ND
(-)-α-Pinene	1.43 ± 0.31	ND	ND
EDTA	0.01 ± 0.01	ND	ND

*ND = not determined

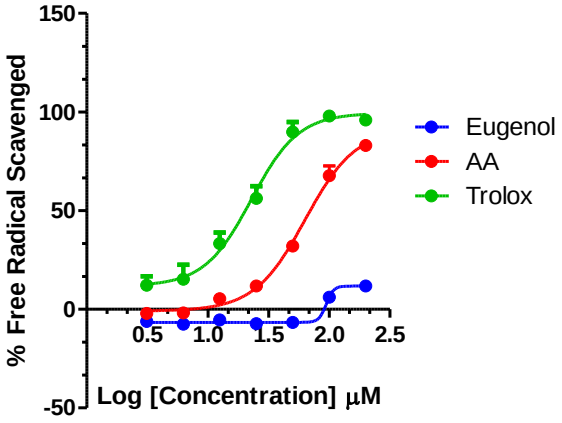

Figure 5.17: The log-sigmoid dose response curve of the free radical scavenging activity of eugenol compared to that of AA and Trolox.

5.1.5.2 Lipid peroxide inhibition and inducing assay

Overall, the EOCs demonstrated low inhibition of lipid peroxidation (Figure 5.18). Thymol, eugenol, 2-mercapotothiazoline, (±)-menthone, 1,4-cineole, 1,8-cineole, (±)-camphorquinone, (1S)-(+)-camphorquinone and (-)-β-pinene demonstrated a higher % lipid peroxidation inhibition than BHA (Figure 5.18). However, their activity was significantly ($P < 0.05$) lower than that of AA. Thymol and (±)-menthone had the greatest potency in inhibiting the formation of lipid peroxidation amongst the EOCs. Citral, linalyl acetate, (-)-citronellal and (1R)-camphorquinone, (-)-linalool and (-)-menthone all induced lipid peroxidation, consequently showing that they were not effective antioxidants. The results for EOCs that did not demonstrate activity in this assay are included in Appendix C, Section C.6, Table C.11 and Table C.12.

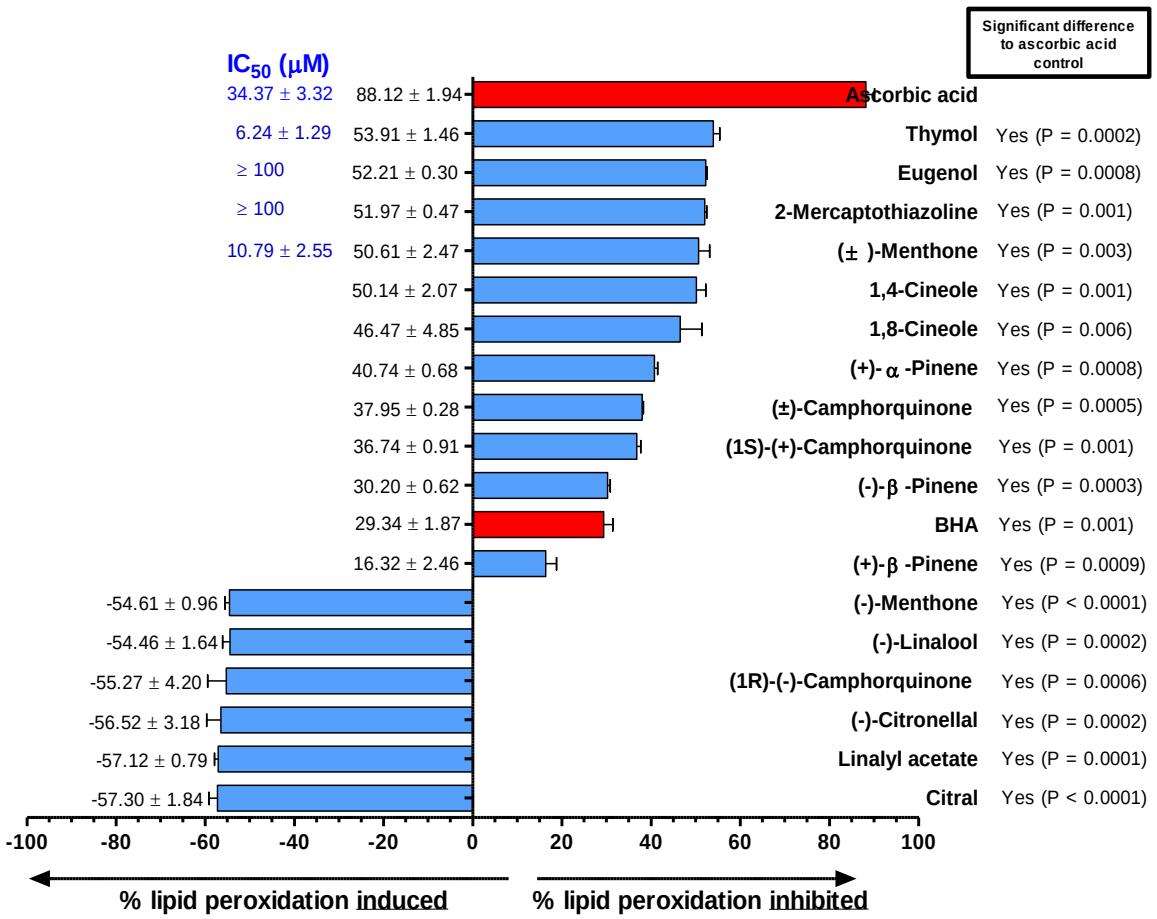

Figure 5.18: The percentage lipid peroxidation inhibited or induced by EOCs.
The EOCs (at 200 µM) did not show a significant difference in activity to the AA control.

5.1.5.3 Inhibition of nitrite formation

In comparison to AA and gallic acid, the EOCs demonstrated a very low ability to inhibit nitrite production (Table 5.13). Citral and *cis*-geraniol demonstrated an activity greater than 30% and were significantly different to AA ($P < 0.05$). The EOCs showed similar activities to one another with a mean result of 22.93 ± 2.83%. The results for EOCs that did not demonstrate activity in this assay are included in Appendix C, Section C.6, Table C.13.

Table 5.13: The percentage nitrite released by SHSY5Y cells treated with EOCs and known antioxidants (AA and gallic acid) as determined by the Griess reagent assay. Significant difference to AA control (P < 0.05).

Compound/EOCs	% Nitrite	Compound/EOCs	% Nitrite
AA	84.58 ± 4.43	**Carvacrol**	23.82 ± 4.82 [Yes (P = 0.0002)]
Gallic acid	78.29 ± 2.57 [Yes (P = 0.009)]	**(+)-α-Pinene**	22.63 ± 3.98 [Yes (P < 0.0001)]
Citral	33.60 ± 3.98 [Yes (P = 0.006)]	**(±)-Lavandulol acetate**	22.55 ± 2.94 [Yes (P < 0.0001)]
***Cis*-geraniol**	33.44 ± 3.86 [Yes (P = 0.001]	**(S)-(-)-Limonene**	22.48 ± 4.76 [Yes (P = 0.0002)]
Geranyl acetate	26.55 ± 3.24 [Yes (P = 0.0002)]	**(±)-Camphor**	22.48 ± 3.03 [Yes (P = 0.0002)]
(-)-Citronellal	25.88 ± 5.27 [Yes (P = 0.0003)]	**(-)-Menthone**	22.40 ± 2.17 [Yes (P = 0.0002)]
Farnesol	25.78 ± 4.48 [Yes (P = 0.0004)]	**(-)-Bornyl acetate**	22.32 ± 2.85 [Yes (P = 0.0002)]
(R)-(+)-Limonene	25.06 ± 4.01 [Yes (P < 0.0001)]	***(+)-Trans*-caryophyllene**	22.26 ± 3.63 [Yes (P = 0.0001)]
***Trans*-geraniol**	25.02 ± 5.84 [Yes (P = 0.0004]	***Cis*-nerolidol**	22.20 ± 2.40 [Yes (P = 0.0002)]
(-)-Linalool	24.79 ± 5.87 [Yes (P = 0.0005]	**(-)-Fenchone**	22.10 ± 3.66 [Yes (P = 0.0002)]
Eugenol	24.55 ± 4.74 [Yes (P = 0.0001]	**(±)-α-β-Thujone**	22.06 ± 4.20 [Yes (P = 0.0003)]
(S)-(-)-β-Citronellol	24.45 ± 5.23 [Yes (P = 0.0003]	**(-)-Borneol**	22.03 ± 3.71 [Yes (P = 0.0001)]
Linalyl acetate	24.31 ± 5.33 [Yes (P = 0.0002]	**(-)-β-Pinene**	21.69 ± 1.62 [Yes (P = 0.0005)]
(±)-Menthone	24.29 ± 5.60 [Yes (P = 0.0003]	**(-)-α-Thujone**	21.54 ± 3.78 [Yes (P = 0.0001)]
(-)-Carvone	24.15 ± 5.70 [Yes (P = 0.0004]	**(-)-Caryophyllene oxide**	21.42 ± 2.86 [Yes (P < 0.0001)]
(+)-Pulegone	24.03 ± 4.73 [Yes (P = 0.0002]	**Ocimene**	21.42 ± 4.18 [Yes (P = 0.002)]
1,8-Cineole	23.70 ± 4.98 [Yes (P = 0.0001]	**(±)-Linalool**	21.24 ± 3.10 [Yes (P = 0.0002)]
Thymol	23.90 ± 4.92 [Yes (P = 0.0003]	**(±)-Menthol**	21.18 ± 5.00 [Yes (P = 0.0003)]
(-)-Terpinen-4-ol	23.88 ± 4.32 [Yes (P = 0.0001]	**(1S)-(+)-Camphorquinone**	21.13 ± 2.72 [Yes (P = 0.0002)]
***Trans*-nerolidol**	23.68 ± 4.41 [Yes (P < 0.0001]	**(-)-Camphor**	20.90 ± 3.09 [Yes (P < 0.0001)]
(+)-Terpinen-4-ol	23.58 ± 4.47 [Yes (P < 0.0001)]	**(1R)-(-)-Camphorquinone**	20.84 ± 3.69 [Yes (P = 0.0001)]
(+)-Fenchone	23.44 ± 3.60 [Yes (P < 0.0001)]	**(1R)-(+)-Camphor**	20.84 ± 2.56 [Yes (P = 0.0002)]
(-)-α-Pinene	23.33 ± 3.51 [Yes (P < 0.0001)]	**(+)-Carvone**	20.66 ± 1.73 [Yes (P = 0.0006)]
(+)-β-Pinene	23.25 ± 4.29 [Yes (P < 0.0001)]	**2-Mercaptothiazoline**	20.03 ± 2.14 [Yes (P = 0.001)]

5.1.6 Larvicidal activity

Carvacrol, (-)-carvone, (-)-linalool and linalyl acetate were the most active larvicides with activity greater than 90% (Table 5.14). (S)-(-)-β-Citronellol, (+)-pulegone, (-)-menthone, (+)-carvone, *cis*-nerolidol, *trans*-geraniol, *cis*-geraniol and (±)-menthone were also highly active to inhibit the *Anopheles* larvae (70-80% lethality). The remainder of the EOCs demonstrated larvicidal activity in the range of 7% to 47%. EOCs with an activity less than 18% are shown in Appendix C, Section C.7, Table C.14.

Table 5.14: The larvicidal activity of EOCs compared to DDT after 24 hours.

EOCs	% Mortality	EOCs	% Mortality
DDT	100.00 ± 0.0	**Eugenol**	36.00 ± 4.20 [Yes (P < 0.0001)]
Carvacrol	93.00 ± 5.7 [No (P = 0.05)]	**(-)-Borneol**	34.00 ± 11.40 [Yes (P < 0.0001)]
(-)-Carvone	91.00 ± 4.2 [Yes (P = 0.02)]	**(1R)-(+)-Camphor**	32.00 ± 7.60 [Yes (P < 0.0001)]
(-)-Linalool	90.00 ± 6.10 [Yes (P = 0.02)]	**(±)-Camphorquinone**	32.00 ± 6.70 [Yes (P < 0.0001)]
Linalyl acetate	92.00 ± 5.70 Yes (P = 0.03)]	**ρ-Cymene**	32.00 ± 5.70 [Yes (P < 0.0001)]
(S)-(-)-β-Citronellol	85.00 ± 3.50 [Yes (P = 0.0007)]	**(-)-Camphor**	32.00 ± 4.50 [Yes (P < 0.0001)]
(+)-Pulegone	85.00 ± 6.10 [Yes (P = 0.005)]	**(-)-Citronellal**	31.00 ± 7.40 [Yes (P < 0.0001)]
(-)-Menthone	82.00 ± 5.70 [Yes (P = 0.002)]	**(+)-Borneol**	30.00 ± 7.90 [Yes (P < 0.0001)]
(+)-Carvone	80.00 ± 3.50 [Yes (P = 0.0002)]	**Citral**	30.00 ± 7.90 [Yes (P < 0.0001)]
***Cis*-nerolidol**	80.00 ± 3.50 [Yes (P = 0.0002)]	**(1S)-(+)-Camphorquinone**	30.00 ± 7.10 [Yes (P = 0.01)]
***Trans*-geraniol**	79.00 ± 7.40 [Yes (P = 0.0032)]	**(-)-Terpinen-4-ol**	30.00 ± 3.50 [Yes (P < 0.0001)]
***Cis*-geraniol**	79.00 ± 6.50 [Yes (P = 0.002)]	**α-Bisabolol**	30.00 ± 3.50 [Yes (P < 0.0001)]
(±)-Menthone	73.00 ± 5.70 [Yes (P = 0.0005)]	**(-)-β-Pinene**	28.00 ± 5.70 [Yes (P < 0.0001)]
1,8-Cineole	47.00 ± 5.70 [Yes (P < 0.0001)]	**(1R)-(-)-Camphorquinone**	27.00 ± 8.40 [Yes (P = 0.01)]
***Trans*-nerolidol**	42.00 ± 5.70 [Yes (P < 0.0001)]	**Geranyl acetate**	27.00 ± 4.50 [Yes (P < 0.0001)]
(+)-α-Pinene	41.00 ± 6.50 [Yes (P < 0.0001)]	**Farnesol**	25.00 ± 5.00 [Yes (P < 0.0001)]
(-)-α-Pinene	40.00 ± 5.00 [Yes (P < 0.0001)	**(±)-Linalool**	23.00 ± 2.70 [Yes (P < 0.0001)]
1,4 Cineole	38.00 ± 5.70 [Yes (P < 0.0001)	**(±)-Lavandulol acetate**	22.00 ± 10.40 [Yes (P < 0.0001)]
(S)-(-)-Limonene	38.00 ± 10.40 [Yes (P = 0.0002)]	**(+)-β-Pinene**	22.00 ± 4.50 [Yes (P < 0.0001)]
(+)-Terpinen-4-ol	38.00 ± 7.60 [Yes (P < 0.0001)]	**(R)-(+)-Limonene**	22.00 ± 2.70 [Yes (P < 0.0001)]
(-)-Fenchone	38.00 ± 5.70 [Yes (P < 0.0001)]	**(+)-Fenchone**	19.00 ± 9.60 [Yes (P < 0.0001)]
(-)-Pulegone	37.00 ± 6.70 [Yes (P < 0.0001)]	**Thymol**	19.00 ± 9.60 [Yes (P < 0.0001)]

Chapter 6. Discussion

The copper ion is an essential component of several proteins, enzymes that maintain biological processes and biochemical pathways such as signalling, cell growth, propagation, and energy production in micro-organisms and humans (Acuña-Castillo, Morales and Huidobro-Toro, 2000; Sadiq *et al.*, 2012; Fu, Chang and Giedroc, 2014; Gaetke, Chow-Johnson and Chow, 2014; Ladomersky and Petris, 2015; Angelé-Martínez *et al.*, 2017; Alghobashy *et al.*, 2018). Targeting copper for the management of diseases such as prolonged inflammation, cancer, neurodegenerative disorders, infection, and Wilson's disease has been suggested (Brown, 2010; Manto, 2014; Sun *et al.*, 2014; Bandmann, Weiss and Kaler, 2015; Liu *et al.*, 2016; Blockhuys and Wittung-Stafshede, 2017; Neumann, Gulati and Nolan, 2017; Wiemann *et al.*, 2017). Therefore, compounds that show promise in treating copper excess and the subsequent generation of free radicals are needed for the treatment of these diseases.

Copper levels have been shown to be raised in infections and copper homeostasis is thus affected by the presences of microbial organisms (Culbertson *et al.*, 2020). Copper is an important cofactor in the biochemistry and function of the malaria parasite and a potential chemotherapeutic target (Asahi *et al.*, 2014). The malaria parasite is reliant on copper for its normal metabolic functioning (Rasoloson *et al.*, 2004; Asahi *et al.*, 2013, 2014). Copper chelation has led to the inhibition of parasite function including inhibition of the asexual stages, fertility, normal growth, and the expression of genes that encode parasitic copper-binding proteins (Rasoloson *et al.*, 2004; Asahi *et al.*, 2011, 2013, 2014; Asahi, 2012; Kenthirapalan *et al.*, 2014). Cerebral malaria is the primary cause of death in children infected with severe *P. falciparum* (Becker *et al.*, 2004). The presence of toxic free haem and FPIX as by-products of the malaria parasite metabolism causes the generation of ROS and damage to the host cellular membranes and proteins (Tilley, Loria and Foley, 2001; Becker *et al.*, 2004). Compounds that treat both the oxidative stress and the malaria infection would prove useful. The emergence of resistance against traditional antimalarials and insecticides is a constant threat to eliminating malaria and it is therefore recommended by the WHO that combination treatments are used in treating malaria to prevent resistance (WHO, 2019). Since copper chelators have shown antimalarial properties, compounds that can bind to copper and restrict its uptake or use by parasitic enzymes and proteins would prevent the disease progression of malaria.

Compounds that chelate metal ions and reduce their oxidant effect are needed to prevent the pathogenesis of an imbalance in copper homeostasis, specifically copper excess. The need for novel antimalarial treatments that interrupt the metabolism of the parasite is paramount to

controlling this disease. Novel compounds also need to demonstrate efficacy and an advantageous safety profile. As such the rationale for the testing the copper homeostasis properties of the 8-OH derivatives and EOCs was to provide alternative treatments for malaria or alter copper homeostasis in neuronal cells.

6.1. The 8-OH derivatives

The 8-OH compound and its derivatives have been shown to be metal ion chelators (Figure 6.1) (Zheng *et al.*, 2005; Martín Santos *et al.*, 2013); where they have shown promise in the treatment of Alzheimer's, Parkinson's, certain cancers and malaria (Table 4.5 and Table 4.11) (Scheibel and Adler, 1980; Scheibel and Stanton, 1986; Viola-Rhenals, Rieber and Rieber, 2006; Li *et al.*, 2010; Singh *et al.*, 2019; Choroba *et al.*, 2020). 5-Chloro-7-iodo-8-OH (clioquinol) is used as an effective anti-amoebic, antiprotozoal and antibiotic agent and is still used topically as an antibacterial and antifungal agent (Takeda *et al.*, 2010; Rosenthal, 2015; Rossiter and Blockman, 2020). It was associated with inducing subacute myelo-optic neuropathy through the mechanism of decreasing vitamin B_{12} levels (Benvenisti-Zarom, Chen and Regan, 2005). It was theorised that 5-chloro-7-iodo-8-OH formed chelates with the cobalt ion within the vitamin B_{12} cyanocobalamin molecule thereby rendering the molecule inactive (Bareggi and Cornelli, 2012). In this study, of the twenty-one 8-OH derivatives tested, with greatest overall effect in binding/chelating both copper (I) and –(II) was N-butyl-2,2-imino-di-(8-OH) whilst other examples of active compounds included 5,7-diiodo-8-OH and 5-HSO_3-7-iodo-8-OH. (Table 4.1; Section 6.1.1). 8-OH derivatives with functional groups at the 5 and 7 position on the 8-OH ring showed copper chelation activity with 5-chloro-7-iodo-8-OH showing the widest range of activity (Section 6.1.2).

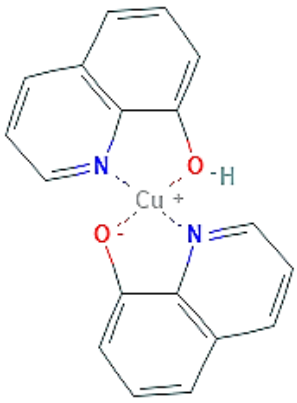

Figure 6.1: The copper chelation structure of 8-OH (Pubchem, 2020b).

6.1.1. N-Butyl-2,2-imino-di-(8-OH)

6.1.1.1. Copper homeostasis and antioxidant activity

Intracellular copper excess has led to the advancement of several disorders including cancer, diabetes, cardiac hypertrophy, and neurodegenerative diseases. The pathogenesis of these diseases are further progressed by chronic inflammation caused by the generation of ROS by free copper ions (Balsano, Porcu and Sideri, 2018). The copper chelation control used in this study was TMB demonstrated potent copper -(I) and -(II) chelation activity as well as powerful antioxidant activity (Table 4.1, Figure 4.2, and Table 4.12). TMB is able to chelate copper *in vivo* and decrease inflammation in the joints of a rat model for the inflammatory disease, rheumatoid arthritis (Omoto *et al.*, 2005). Similarly, 8-OH derivatives inhibited janus kinase (JAK) which is one of the components believed to be responsible for the inflammation cascade in rheumatoid arthritis (Kiss *et al.*, 2016). Derivatives of 8-OH have previously been shown to possess metal ion chelation activity against copper (II), zinc (II), platinum (II) and gallium (III) (Pape *et al.*, 2018).

In the current study, copper homeostasis activity of N-butyl-2,2-imino-di-(8-OH) was assessed to determine the copper chelation, complexation, and *in vitro* complexation activity of the compound; and was shown to possess a wide range of promising activity (Figure 6.2). N-butyl-2,2-imino-di-(8-OH) was a significantly more potent copper (I) chelator compared to the TMB control ($P = 0.04$), with an IC_{50} value that was approximately 2-fold more potent (Figure 4.2). The spectral shifts observed in Figure 4.4 and Figure 4.6 indicated that an interaction between N-butyl-2,2-imino-di-(8-OH) and copper ions occurred. The chelating ability was also observed when N-butyl-2,2-imino-di-(8-OH) had an increased protective effect against copper (I) ion induced haemolysis (Figure 4.17). When the functional groups of heterocyclic compounds were substituted at different positions on the phenolic ring, the antimicrobial activity of the compound changed (Dave and Rahatgaonkar, 2016). Combining a nitro- and a halogen group resulted in the compounds inhibiting *S. aureus* when it was inactive before the derivatisation (Dave and Rahatgaonkar, 2016). Therefore, it was shown that the activity of the compounds was dependent on the functional groups substituted or added to the heterocyclic ring (Dave and Rahatgaonkar, 2016). The activity of N-butyl-2,2-imino-di-(8-OH) may be attributed to the large imino functional groups and the two 8-OH rings present on N-butyl-2,2-imino-di-(8-OH). Correspondingly, a tetradentate 8-OH derivative containing two 8-OH rings demonstrated an increase in prevention of β-amyloid aggregation in comparison to 8-OH and 5-chloro-7-iodo-8-OH (Deraeve *et al.*, 2007).

N-butyl-2,2-imino-di-(8-OH) synergistically chelated copper (I) when combined with TMB (Figure 4.8); whilst the interaction of N-butyl-2,2-imino-di-(8-OH) and quinine against copper

(I) and -(II) was synergistic (Figure 4.8). This was also observed for the interaction with N-butyl-2,2-imino-di-(8-OH) and TMB against copper (II). A synergistic interaction resulted in the combination of the two compounds having a higher activity than the compounds alone (Bell, 2005). Therefore, the activity of the combination of N-butyl-2,2-imino-di-(8-OH) and TMB demonstrates that they would be effective copper (I) and –(II) chelators. It would be vital to further investigate this combination. Several copper chelators have demonstrated synergistic and additive interactions in combination against cancer cells. The combination of TMB and D-penicillamine synergistically inhibited colorectal, ovarian and cervical carcinoma cells with the mechanism of action being proposed as the enhancement of hCTR1 activity (Liang *et al.*, 2009, 2012; Ishida *et al.*, 2010). This combination has also enhanced the activity of cisplatin against ovarian cancer cells (Fu *et al.*, 2012). Similarly, the combination of BCS and TMB enhanced the activity of the anti-cancer agent, oxaliplatin against colorectal cancer cells (Cui *et al.*, 2017).

Raised serum copper levels have been detected in cancer patients and is believed to contribute to the pathogenesis of the disease (Wang, Hsia and Shieh, 2016). The combination of TMB with chloroquine was shown to induce cell autophagy in pancreatic cancer cells. This combination also decreased oxidative stress and it was proposed that the combination chelated copper that was needed for mitochondrial function in the pancreatic cancer cells (Yu *et al.*, 2019). Since the combination of N-butyl-2,2-imino-di-(8-OH) and TMB was synergistic, it could be advantageous to consider the combination for future studies involving carcinogenesis and copper excess. N-butyl-2,2-imino-di-(8-OH) was more selective for copper (I) chelation than for copper (II) chelation and demonstrated free radical scavenging activity. This chemo-selectivity may be advantageous when specifically targeting copper (I) ions as they are more likely to form oxidants than copper (II) (Saito *et al.*, 2019). Removal of copper (I) ions may reduce the possibility of the chronic oxidant stress induced by copper excess seen in diseases such as diabetes mellitus, obesity, amylotrophic lateral sclerosis, and Wilson's disease. The chelation of free copper ions by the 8-OH derivative, tacrine-7-hydroxycoumarin prevented copper breakdown of H_2O_2, a significant decrease in oxidative stress, the inhibition of acetylcholinesterase and amyloid aggregation reduction in an Alzheimer's disease model (Hamulakova *et al.*, 2016). Since N-butyl-2,2-imino-di-(8-OH) displayed copper chelation/complexation (Table 4.1 and Table 4.2) and antioxidant properties (Table 4.12) in this study, it may have the potential of hindering the excess metal ions and ROS in diseases like Wilson's, cancer, diabetes, and Alzheimer's.

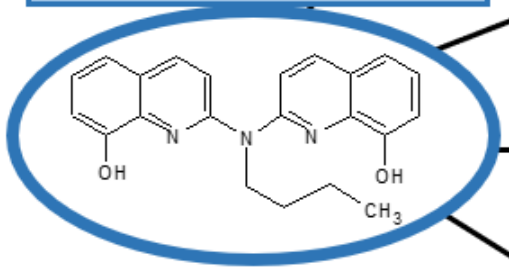

COPPER HOMEOSTASIS

Copper (I) chelation	Copper (II) chelation
101.67 ± 9.26% IC_{50}: 12.90 ± 0.80 µM Synergistic interaction with quinine (ΣFIC=0.60) and TMB (ΣFIC=0.40)	117.80 ± 15.08% IC_{50}: 44.37 ± 10.54 µM Synergistic interaction with quinine (ΣFIC=0.39) Additive interaction with TMB (ΣFIC=0.75)
Copper (I) complexation	**Copper (II) complexation**
91.53 ± 0.68%	88.77 ± 1.74%

ANTIMALARIAL INVESTIGATIONS

Parasite growth inhibited	FBIT	Larvicidal (Mortality)
89.81 ± 14.25% IC_{50}: 0.58 ± 0.03 µM Synergistic interaction with Chloroquine (ΣFIC=0.54)	96.94 ± 0.92% 23.24 ± 4.46 µM Synergistic interaction with Chloroquine (ΣFIC = 0.38)	77.00 ± 5.70%

ANTIOXIDANT ACTIVITY

DPPH• (FRS)	Lipid peroxidation inhibition	Griess reagent assay (% Nitrite)
62.36 ± 3.77%	24.66 ± 3.51%	30.26 ± 4.84%

TOXICITY

Haemolysis	Neuronal cells (% cellular viability)	*Artemia* lethality assay (Mortality)
9.78 ± 1.70% Cu (I):↑ Protective effect Cu (II):↓ Protective effect	MTT: 14.8 ± 1.9; IC_{50}: 9.32 ± 1.4 µM SRB: 12.9 ± 0.4%; IC_{50}: 22.8 ± 4.0 µM Cu (I): ↑ Protective effect Cu (II): ↑ Protective effect	24 hrs: 88.09 ± 6.74% 48 hrs: 95.27 ± 9.45% 72 hrs: 96.23 ± 7.55% LD50: 43.68 µM

Figure 6.2: The summary of activity for N-buty-2,2-imino-di-(8-OH).

The activity of N-butyl-2,2-imino-di-(8-OH) across this study and divided into its copper homeostasis, antimalarial, antioxidant activity and toxicity.

6.1.1.2. Antimalarial activity

N-butyl-2,2-imino-di-(8-OH) demonstrated a potent antimalarial activity which was less than chloroquine, quinine and the DHA controls (Table 4.5).

N-butyl-2,2-imino-di-(8-OH) did not affect the permeability of the RBC membrane (Table 4.10) as such the effect was directed to the intracellular parasite. N-butyl-2,2-imino-di-(8-OH) had 2-fold greater activity (IC_{50} value) than the copper (I) and (II)-chelator TMB (Figure 4.2) and an 80-fold higher antimalarial activity (IC_{50} value) than the copper (II) chelator, D-penicillamine (Table 4.5). TMB directly targeted the schizont stage of the *P. falciparum* parasite and caused significant inhibition of the parasite that may have been due to the binding of intracellular copper or inhibition of copper proteins (Asahi *et al.*, 2014). Since the copper metabolism of *P. falciparum* is not yet fully understood, the compounds may have an effect on one or more of the enzymes and proteins involved in the cellular transport of copper, including ATPase and COX17 (Figure 2.1) (Rasoloson *et al.*, 2004; Choveaux, Przyborski and Goldring, 2012). In this study the copper (I) chelator, neocuproine was a weak inhibitor of parasite growth of the 3D7 strain of *P. falciparum* (Table 4.5; % parasitaemia inhibited: 42.18 ± 8.50 µM). Asahi *et al.,* (2014) showed that neocuproine (IC_{50} value: 0.13 ± 0.06 µM) inhibited the *P. falciparum* FCR3 strain at all stages of the lifecycle. It was proposed that interrupting copper metabolic processes caused the inhibition of *P. falciparum* and that copper is an important factor in the development of *P. falciparum* parasite (Asahi *et al.*, 2014). In the current study TMB was 2-fold less potent than N-butyl-2,2-imino-di-(8-OH) and neocuproine demonstrated a weak antimalarial activity (Table 4.5). Since the 8-OH derivatives have been shown to chelate iron, the antimalarial activity of N-butyl-2,2-imino-di-(8-OH) may be enhanced in comparison to TMB and neocuproine (Chobot *et al.*, 2018; Yang *et al.*, 2018). N-Butyl-2,2-imino-di-(8-OH) decreased the percentage parasitaemia at the trophozoite stage in comparison to the untreated control and therefore had an effect on parasitic stage development (Table 4.6 and Figure 4.11). Further studies are required to assess the effect of these potent copper chelators on the identified copper-containing enzymes/proteins.

To potentiate the effect of active compounds, the WHO recommends that combination therapy be used in the treatment of *P. falciparum* malaria. This strategy established that the combination therapy is more effective in treating malaria and preventing resistance emergence (WHO, 2019). As such N-butyl-2,2-imino-di-(8-OH) was combined with chloroquine with a synergistic interaction observed (Figure 4.13). This could be due to the inhibition of complementary pathways to cause parasite death. One such target could be metal homeostasis where metal chelators that have the ability to not only chelate copper but also iron depending on their affinity for the metal. These include the iron chelators, desferrioxamine

and 8-OH derivatives which have been shown to inhibit iron-dependant DNA polymerase, resulting in parasite death (Gordeuk, Thuma and Brittenham, 1994; Cabantchik, Moody-Haupt and Gordeuk, 1999; Mabeza *et al.*, 1999). The potent antimalarial activity of bis-thiosemicarbazone derivatives was attributed to their ferric ion chelation ability (Akladios *et al.*, 2019).

Another potential target and mechanism of action of the individual N-butyl-2,2-imino-di-(8-OH) or combination with chloroquine could involve the inhibition of haemozoin (Figure 6.3) (Tilley, Loria and Foley, 2001). N-Butyl-2,2-imino-di-(8-OH) demonstrated the most potent ability of the tested 8-OH derivative to inhibit β-haematin formation that was similar to the chloroquine control (1.2-fold difference in activity) (Table 4.8). In addition, N-butyl-2,2-imino-di-(8-OH) was found to be ineffective in inhibiting lipid peroxidation (Table 4.13), thereby not interfering with the lytic mechanism of action of the chloroquine-haem complex. Due to the ability of N-butyl-2,2-imino-di-(8-OH) to inhibit the formation of β-haematin (Table 4.8) and ability to inhibit the malaria parasite, it can be proposed that it does so in a similar way to chloroquine by preventing inert haemozoin formation and the accumulation of lytic compound-haem complexes.

Chloroquine inhibits the malaria parasite at the trophozoite stage by preventing the breakdown of haem to the inert haemozoin thereby causing a toxic build-up of haem and oxidative stress within the parasite (Figure 6.3) (Blasco, Leroy and Fidock, 2017). The lytic chloroquine-haem complex damages the membrane of the malarial food vacuole via lipid peroxidation, causing the contents to leak into extracellular fluid that impairs the mitochondrial membrane, leading to oxidative stress and parasite death (Ch'Ng *et al.*, 2011). Although the malaria parasite has a tightly controlled redox stabilizing system that protects the parasite from the oxidative storm that it produces in the host cell, it is dependent on the host red blood cell for SOD and other catalase enzymes (Kavishe, Koenderink and Alifrangis, 2017). Therefore, compounds such as chloroquine and quinine could overwhelm this fine balance by the induction of free radicals, as well as target the metabolic processes that reduce or prevent oxidative stress within the parasite (Mavondo *et al.*, 2019). Quinine has been proposed to inhibit haemozoin formation to a lesser extent to chloroquine (Table 4.8), but the interaction of N-butyl-2,2-imino-di-(8-OH) with quinine may be a favourable interaction to complement this therapeutic agent used in the treatment of malaria. Alternatively, N-butyl-2,2-imino-di-(8-OH) could bind and chelate iron within the haem ring thereby preventing the cross-linking of the haem units to form haemozoin. A similar effect was reported for the ferrous chelator 2,2'-bipyridyl inhibiting haemozoin formation (Van Zyl *et al.*, 1993). The synergistic interaction of N-butyl-2,2-imino-di-(8-OH) with chloroquine (Figure 4.16) to inhibit β-haematin formation, which indicates that the combination of N-butyl-2,2-imino-di-(8-OH) with a quinoline possesses a favourable inhibitory effect and

combinations of N-butyl-2,2-imino-di-(8-OH) with either TMB or quinine may warrant further investigation into novel combination therapy against malaria.

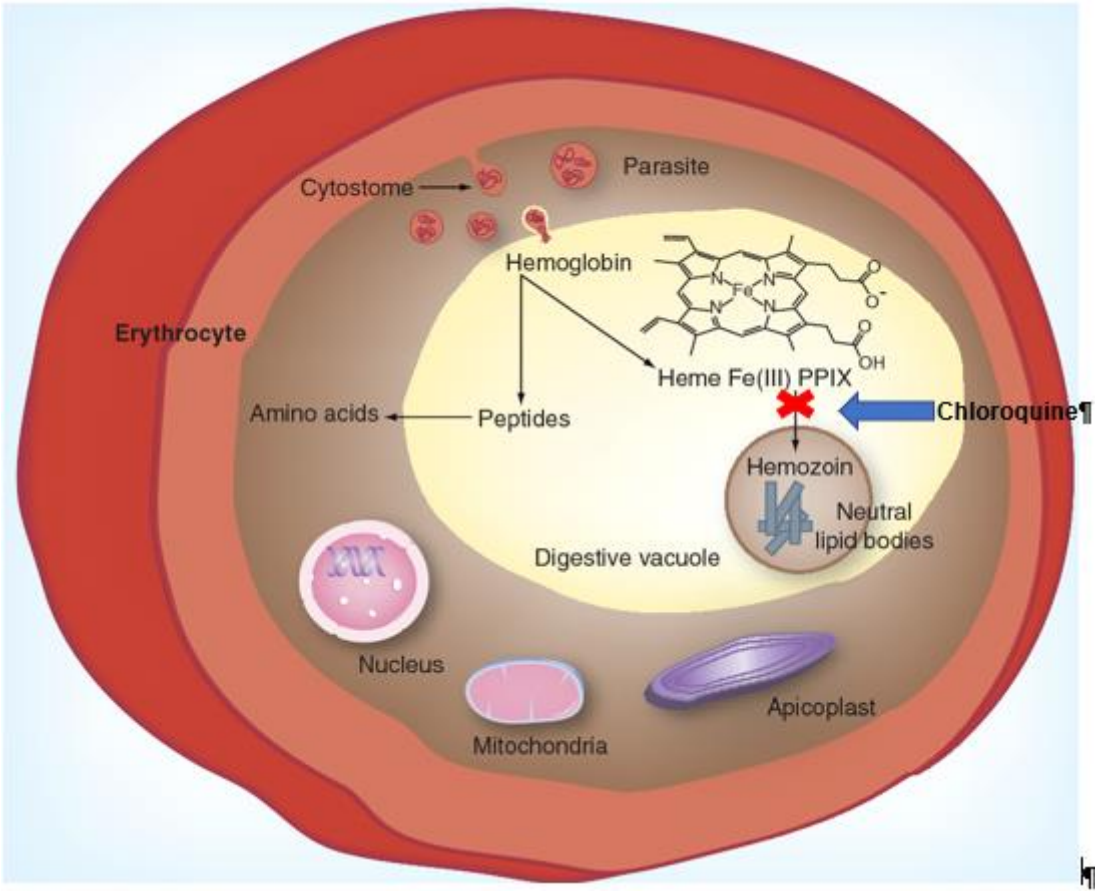

Figure 6.3: The inhibition of parasitic metabolic breakdown of haemoglobin by chloroquine (Fong and Wright, 2013).

When enzymes and proteins responsible for copper regulation malfunction, this leads to pro-oxidant activities and the generation of free radicals that damage sensitive cellular organelles (De Luca *et al.*, 2019). Copper is an important element in metabolic redox reactions; where it generates electrons by fluctuating between its Cu(I/II) states (De Luca *et al.*, 2019). This redox activity allows free copper ions to catalyse oxidative reactions such as the Haber-Weiss reaction (Figure 2.4) by generating ROS by interacting with O_2^- and H_2O_2 (Halliwell and Gutterridge, 1990). The generation of ROS leads to the damage of important biological molecules such as lipids and proteins (Manzl *et al.*, 2004).

N-butyl-2,2-imino-di-(8-OH) demonstrated a 2-fold lower (P = 0.007) haemolytic activity than chloroquine (Table 4.10) which may be favourable as the haemolysis leads to the release of intracellular components that increase oxidative stress and can potentiate the clinical symptoms (Sharma and Singh, 2019). Furthermore, N-butyl-2,2-imino-di-(8-OH) scavenged

free radicals (greater than 60%) but was 1.5-fold lower than the ascorbic acid control and had an IC_{50} value that demonstrated no potency (Table 4.12). In addition, N-butyl-2,2-imino-di-(8-OH) was the most potent inhibitor of nitrite of the 21 tested 8-OH derivatives but was 2.8-fold less active than the ascorbic acid control (Table 4.14). Together this indicates that N-butyl-2,2-imino-di-(8-OH) may prevent the formation of redox species and being an antioxidant with the potential to protect the host against oxidative stress which is a concern in the malaria-infected patient. Since the malaria parasite stimulates the production of inflammatory species molecules like superoxide and H_2O_2 within the host RBCs and causes an oxidative stress cycle that can overwhelm the host leading to RBC destruction and cellular death, these metal chelators may be beneficial (Mavondo *et al.*, 2019). Metal chelators have shown some benefit in the clinical patient and warrants consideration as adjuvant supportive therapy (Gordeuk, Thuma and Brittenham, 1994; Cabantchik, Moody-Haupt and Gordeuk, 1999; Mabeza *et al.*, 1999). It has previously been shown that the addition of iron chelators not only target the parasite by withholding iron but also by forming extracellular iron complexes that are able to enter the RBC and produce toxic free radical mediated reaction on the parasite (Mabeza *et al.*, 1999). As such, the dose being administered and the mechanism of action of N-butyl-2,2-imino-di-(8-OH) could be essential in malaria infection management. Agents that inhibit the parasite by metal chelation and protect the host from oxidative stress, possibly in combination with chloroquine that accumulates within the parasite, would be beneficial in the management of malaria.

6.1.1.3. Larvicidal activity

N-Butyl-2,2-imino-di-(8-OH) demonstrated potent *An. gambiae* larvicidal activity (Table 4.17) and caused considerable degradation of the morphological structure of the larvae (Figure 4.29). Since N-butyl-2,2-imino-di-(8-OH) has been established to be a potent copper ion modulator it may cause a copper deficiency within the larvae. N-Butyl-2,2-imino-di-(8-OH) possibly interacts with important copper-dependent enzymes within the larvae by disrupting homeostatic processes. One such enzyme could be the multicopper oxidase, laccase found in *An. gambiae* species. It is believed to function as cuticle sclerotization and as a protectant against oxidation from toxic haem after a blood meal (Lang, Kanost and Gorman, 2012; Peng *et al.*, 2014). Cuticle sclerotization is the stabilization and strengthening process of an insect's exoskeleton and is vital for movement (Riddiford, 2009). Copper is needed in order for laccase to carry out its function (Upadhyay, Torres and Lin, 2013). By inhibiting the gene that codes for a multicopper oxidase protein, the researchers found that the development of the larvae of *An. gambiae* was completely inhibited (Peng *et al.*, 2014). The supplementation of copper in the laccase of *Fusarium oxysporum* fungi resulted in the increase in the enzymatic activity

(Hernández-Monjaraz *et al.*, 2018). Therefore, complexation formation with copper ions meant for laccase activities may disrupt the metabolism of the mosquito and provide a new mechanism of action to manage the malaria vector. N-Butyl-2,2-imino-di-(8-OH) decreased the rigid appearance of the larvae morphology and caused the degradation of the thorax and abdomen (Figure 4.29). The destabilization of the larvae morphology may be due to the inhibition of the larval laccase. Further studies are needed where the molecular mechanism of larval inhibition by N-butyl-2,2-imino-di-(8-OH) is investigated.

6.1.1.4. N-butyl-2,2-imino-di-(8-OH) toxicity

Copper levels have been reported to be higher in several cancers found in the brain, breast, prostate and ovary. It is believed that the copper chelator dextran-catechin formed copper conjugates in neuroblastoma cells, thereby decreasing the growth of the cancer cells and prevented copper binding to glutathione allowing this important antioxidant to prevent oxidative stress (Vittorio *et al.*, 2016). Angiogenesis promotes the growth and spread of cancer, with copper being an important factor in activating stimulants of angiogenesis such as fibroblast growth factor (Brewer, 2017). TMB has been shown to inhibit angiogenesis without causing a copper deficiency in the patient (Brewer, 2017). Similarly, TMB was effective in inhibiting the neuroblastoma SH-SY5Y cell line in this study (Table 4.11) with N-butyl-2,2-imino-di-(8-OH) being 3-fold more effective than TMB and only 1.7-fold less cytotoxic than the camptothecin control (Table 4.11; $P = 0.05$). The inhibition of cancerous cells demonstrates that the properties and potential anti-cancerous effect of N-butyl-2,2-imino-di-(8-OH) should be further investigated to determine if it is due to its copper interaction especially since it showed *in vitro* copper protection in the neuroblastoma cells (Table 4.11).

Conversely, the haemolysis that was induced by N-butyl-2,2-imino-di-(8-OH) is concerning as this could lead to serious adverse events in individuals using this as a treatment. Compounds should demonstrate both safety and efficacy to be considered a valuable treatment for diseases (Tamargo, Le Heuzey and Mabo, 2015). N-butyl-2,2-imino-di-(8-OH) had a high lethality towards the *A. franciscana* nauplii and caused a delay in morphologic development, which was also observed for the potassium dichromate control (Figure 4.27). Glyphosate is a divalent cation chelating herbicide used to control unwanted plants causes the unintentional death of *Artemia*, amphibians and fish (Rahnama, Tulaby Dezfuly and Alishahi, 2018). Consequently, the use of N-butyl-2,2-imino-di-(8-OH) as a novel larvicide may not be viable due to its toxicity in *Artemia* and caution should be taken when considering the compound for use in distribution to spray larval breeding sites and in the vicinity of mammals. Further extensive tests need to be done to ascertain the safety profile of the compound.

Due to the promising effects of N-butyl-2,2-imino-di-(8-OH) on copper homeostasis and the inhibitory effects on haemozoin synthesis in the malarial parasite and larvicidal activity, further derivatisation of this 8-OH chelator is warranted to decrease the potential toxicity profile of N-butyl-2,2-imino-di-(8-OH) against a larger toxicity panel before considering its use in the management of malaria or copper overload diseases.

6.1.2. Activity of 8-OH derivatives influenced by functional groups

6.1.2.1. Compounds with a functional group at the 5 and 7 position of the 8-OH ring

5-Chloro-7-iodo-8-OH has functional groups at the 5 and 7 position on the 8-OH ring, its structure contributes to its various actions (Figure 6.5). 8-OH derivatives showing notable copper ion activity contained functional groups at the 5 and 7 positions on the 8-OH ring, namely 5,7-dichloro-8-OH (Figure D.11), 5,7-diiodo-8-OH (Figure D.12), 5,7-dibromo-8-OH (Figure D.13), 5,7-dimethyl-8-OH (Figure D.14), 5-chloro-7-iodo-8-OH, 5-HSO_3-7-iodo-8-OH (Figure D.15) and 5-chloro-7-bromo-8-OH (Figure D.16) in comparison to the TMB control (Table 4.1 and Table 4.2). 5-Chloro-7-iodo-8-OH has been found to reallocate divalent metal ions such as iron, copper and zinc within cells (Mot and Crouch, 2017) and its anticancer activity is proposed to be due to the inhibition of angiogenesis and the activation of pathways that inhibit the growth signals of cancer cells through its metal ion chelating action (Khan *et al.*, 2020).

Those compounds with halogen functional groups at the 5 and 7 position (5,7-diiodo-8-OH, 5-chloro-7-iodo-8-OH and 5,7-dichloro-8-OH) exhibited copper (I)- and copper-(II) chelation activity (Figure 6.4). Interestingly, the compounds seem to favour chelation of copper (I) ions compared to the chelation of copper (II) ions (Table 4.1). When comparing these compounds to the parent compound, 8-OH, several derivatives such as 5,7-dichloro-8-OH, 5,7-diiodo-8-OH, 5,7-dibromo-8-OH, 5,7-dimethyl-8-OH, 5-chloro-7-iodo-8-OH, 5-HSO_3-7-iodo-8-OH and 5-chloro-7-bromo-8-OH showed approximately a 4-fold increase in copper (I) chelating activity. Derivatives with an iodo functional group displayed a higher copper (I) chelation activity in comparison to the other halogenated 8-OH derivatives with those containing a chloro group also demonstrating advantageous activity Figure 6.4.

D-Penicillamine and TET have a binding affinity for Cu^{2+} ions, while neocuproine selectively binds Cu^{1+} ions (Ding, Xie and Kang, 2011) therefore the chelation of compounds would also be dependent on the state of the transition metal ion and may favour binding of metal ions with lower or higher transitional states. Copper (I) ions have a higher redox activity than copper (II) ions leading to greater ROS generation, as such, specifically targeting these ions would provide an increase in protection against oxidants (Saito *et al.*, 2019).

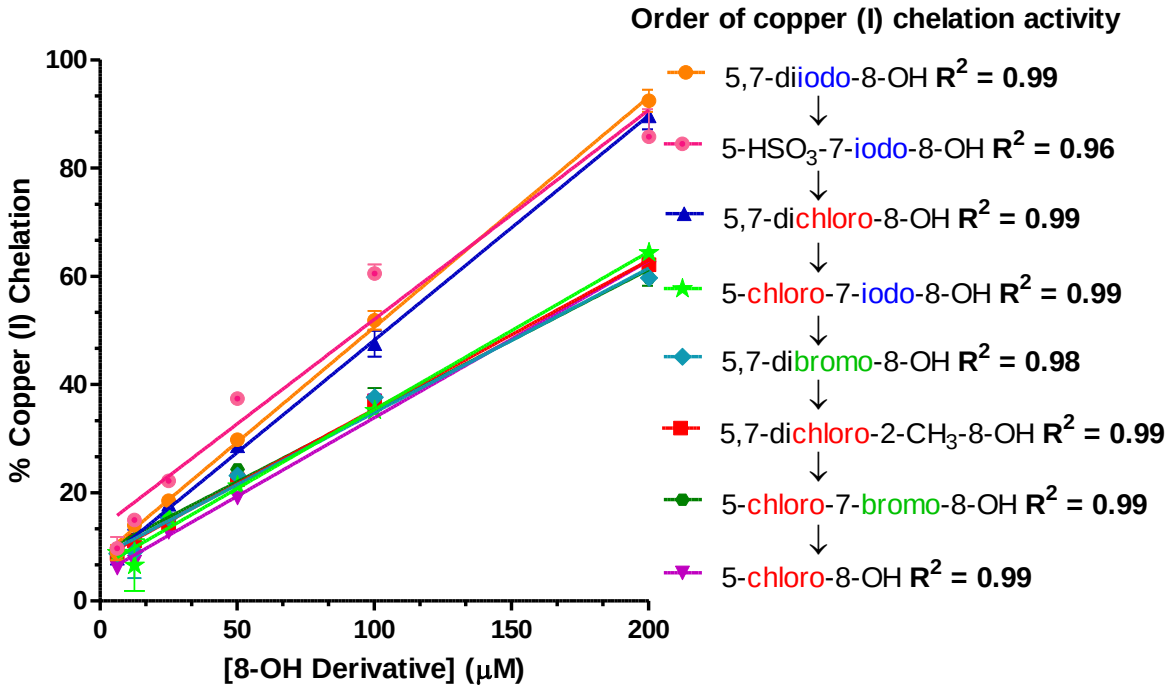

Compound	R^2 value	Linear regression equation
5,7-diiodo-8-OH	0.9977	y = 2.352x + (-19.02)
5-HSO_3-7-iodo-8-OH	0.9572	y = 2.587x + (-34.67)
5,7-dichloro-8-OH	0.9971	y = 2.409x + (-16.13)
5-chloro-7-iodo-8-OH	0.9863	y = 3.43x + (-21.31)
5,7-dibromo-8-OH	0.9809	y = 3.75x + (-30.57)
5,7-dichloro-2-CH_3-8-OH	0.9968	y = 3.629x + (-28.52)
5-chloro-7-bromo-8-OH	0.9888	y = 2.409x + (-34.17)
5-chloro-8-OH	0.9932	y = 3.447x + (-16.73)

Figure 6.4: The linear regression of halogenated 8-OH derivatives and the order of activity in the copper (I) chelation assay.

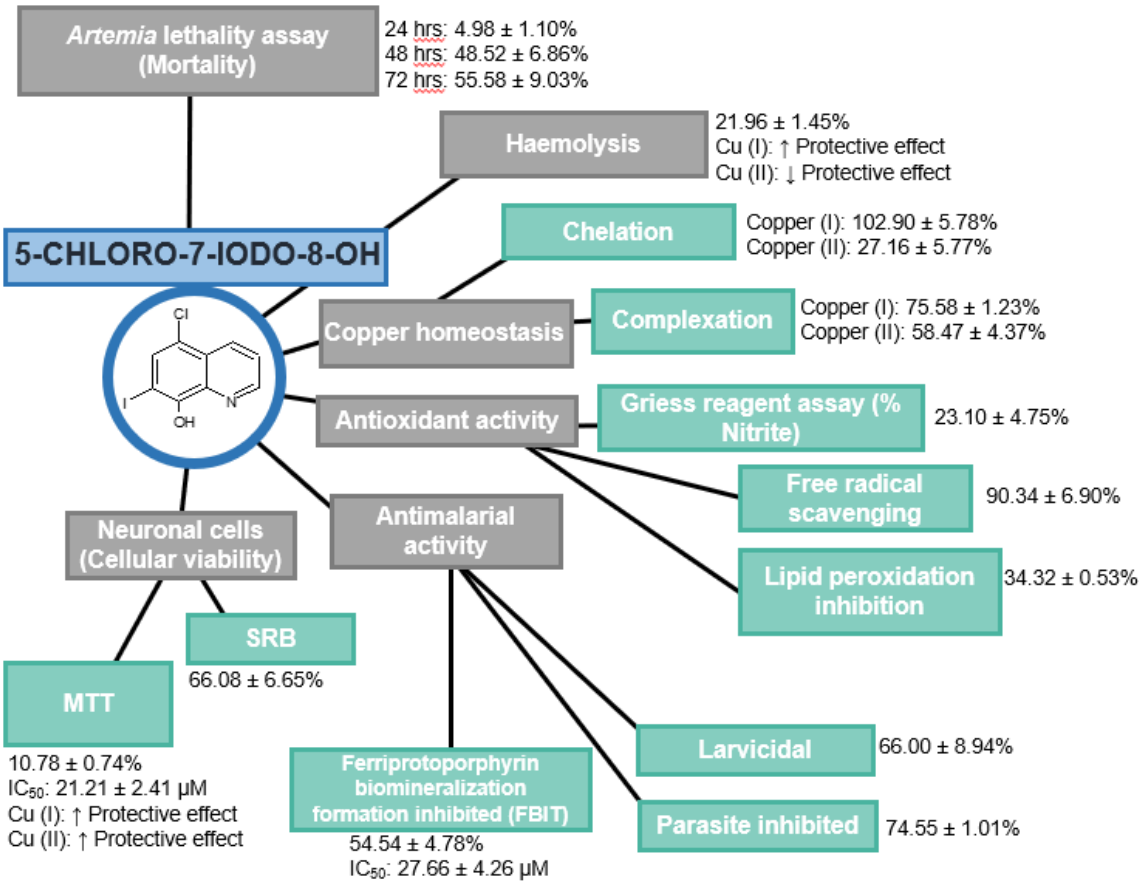

Figure 6.5: The summary of pharmacological activity for 5-chloro-7-iodo-8-OH.

5-Chloro-7-iodo-8-OH and the 8-OH derivative, 5,7-dichloro-2-[(dimethylamino)methyl]quinolin-8-ol (PBT2) form complexes with the divalent transition metal rich aggregates, resulting in low molecular weight and harmless complexes that modulate the formation of Alzheimer's disease amyloid fibrils and suppress pre-existing aggregates (Ryan *et al.*, 2015). The complexity of compound PBT2s' functional groups contributed to its ability to bind large toxic Aβ peptides. Where compound PBT2 contains two chloro-functional groups at positions 5 and 7 and a dimethylamino group at position 2 on the 8-OH ring (Ryan *et al.*, 2015). Therefore, the position of the functional group contributed to the activity of the compounds, the functional group itself also influenced the activity of the compound. 5-Chloro-7-iodo-8-OH has demonstrated potent lipophilicity and chelated divalent metal ions such as cobalt (Yassin *et al.*, 2000). Further to this, 5-chloro-7-iodo-8-OH chelated metal ions and caused a decrease of vitamin B_{12} in the brain tissue of mice. Therefore, this compound was able to accumulate in brain tissue and chelate metal ions (Yassin *et al.*, 2000). This inhibition of vitamin B_{12} absorption further demonstrates that 5-chloro-7-iodo-8-OH was responsible for the incidences of subacute myelo-optic neuropathy in 1970 and it may prove favourable for patients to receive vitamin B_{12} supplements if they are treated with this medicine (Yassin *et al.*, 2000; Chen *et al.*, 2007). The neurotoxic effects of 5-chloro-7-iodo-8-OH still affected

patients 32 years after treatment with many exhibiting symptoms such as loss of vision, difficulty walking, urinary and bowel disturbances and nerve damage (Konagaya *et al.*, 2004). Moreover, clioquinol demonstrated toxicity in dorsal root ganglion cells and decreased the axon ability to potentiate signals (Toyoshima, 2017). The synthesis of a derivative or a targeted delivery system of 5-chloro-7-iodo-8-OH may prove advantageous in decreasing its neurotoxicity. In order to improve targeted delivery, encapsulating 5-chloro-7-iodo-8-OH in mesoporous nanoparticles was shown to increase intracellular levels as well as prevent Aβ-induced oxidative stress in pheochromocytoma cells (Oliveri *et al.*, 2014). The suggested that the mechanisms of action of 5-chloro-7-iodo-8-OH was competitive chelation of zinc and copper ions within the amyloid and the promotion of movement of metal ions from extracellular location into intracellular spaces, which decreased free ion redox reactions and corrected the excess metal ions (Adlard *et al.*, 2008; Barnham and Bush, 2014). This beneficial effect could be of great advantage to increase the antimalarial or anticancer effects of these chelators. It has been proposed that the limited access of the metal chelators reduced the accumulation of the chelator into the parasite, which reflected in the higher concentration of compound that is required to kill the parasite or cell (Alves *et al.*, 2015). As such, increasing the lipophilicity of the chelator encapsulated in the nanoparticles could achieve the resultant inhibitory effect at lower concentrations (Alves *et al.*, 2015).

Substitution with methyl groups at positions 5 and 7 on the 8-OH ring has previously been shown to increase the cytotoxic potency against HL60 leukaemia cells (Havrylyuk *et al.*, 2018). The authors suggested that the possible mechanism of action is the inhibition of protein synthesis (Havrylyuk *et al.*, 2018). Similarly, 5,7-dimethyl-8-OH was cytotoxic against the neuroblastoma cells in the SRB assay comparably to the camptothecin control ($P = 0.008$). Lipophilic metal chelators such as the 8-OH derivatives are nitrogen-donors that bind to copper ions (Tardito *et al.*, 2011, 2012). The complex moves across the cellular membrane and triggers the build-up of copper ions within cancerous cells (Tardito *et al.*, 2011, 2012). The authors also found 5,7dimethyl-8-OH and its copper complex to be highly lipophilic and cytotoxic against HeLa carcinoma cells (Tardito *et al.*, 2011, 2012). Correspondingly, 8-OH has acted as an iron ionophore that inhibits the DNA of cancerous cells (Schraufstatter *et al.*, 1986). 8-OH has demonstrated iron chelation and it was proposed that the 8-OH-iron complex degrades the phosphodiester backbone of DNA in cancerous cells leading to the inhibition of these cells (Hecht, 1987). Furthermore, this complex may cause cellular membrane impairment that causes calcium loss from the cell and signals endonucleases to cleave DNA leading to apoptosis (Leanderson and Tagesson, 1996). In the current study methyl groups at positions 5 and 7 also resulted in considerable copper(I) chelation as seen for 5,7-dimethyl-8-OH (Figure D.14), and when neuronal cells were exposed to increased copper levels, a

neuroprotective effect against both copper(I) and copper(II) exposure was noted (Table 4.11 and Figure 4.22 and Figure 4.23). This effect may be of importance in Wilson's disease to protect the cells from toxic effects of elevated levels of copper. Copper concentrations have been shown to be 850% higher than normal in the post-mortem cerebrospinal fluid of patients with neuropsychiatric Wilson's disease (Kodama *et al.*, 1988). Effective copper chelators that prevent this toxic accumulation of copper may prevent the severe pathogenesis and death in this disease. The safety index is an important factor to consider for therapeutic application where the copper complexing effects of 5,7-dimethyl-8-OH may speak to its inhibition of the neuroblastoma cells; however the dose would need to be optimised to protect the cells if this compound is to be used in the management of the copper excess seen in Wilson's disease.

Metal ion imbalance can modulate cellular proteins and cause excessive oxidative reactions leading to cellular damage (Singh *et al.*, 2019). Compounds with metal ion complexation and antioxidant activity could prevent these reactions. Namely, 5,7-dichloro-8-OH, 5,7-diiodo-8-OH, 5,7-dibromo-8-OH, 5,7-dimethyl-8-OH, 5-chloro-7-iodo-8-OH, 5-chloro-7-bromo-8-OH and 5,7-dichloro-2-methyl-8-OH were all free radical scavengers and had comparable activity to known antioxidants, such as Trolox™, ascorbic acid and BHA (Table 4.12). A modelling study of 5,7-dichloro-2-methyl-8-OH (Cherdtrakulkiat *et al.*, 2020) (Figure D.17) concluded this highly nucleophilic molecule possessed oxidant potential. 5-Chloro-7-iodo-8-OH and 5,7-dichloro-8-OH (Figure D.11) were also shown to effectively scavenge oxidants (Cherdtrakulkiat *et al.*, 2020). Thiourea derivatives of 8-OH were found to bind phospholipase A2, an enzyme that produces oxidants as a breakdown by-product of fatty acid formation in a modelling study which indicated that they had the potential to be antioxidants (Kalaiyarasi *et al.*, 2019). This was shown *ex vitro* to be correct in this study (Table 4.13), where 5-carboxy-8-OH, 5-chloro-8-OH, 5,7-dichloro-8-OH, 5-chloro-7-bromo-8-OH and 5-chloro-7-iodo-8-OH were the most active.

Malaria-infected patients have been found to have significantly higher levels of ROS in comparison to uninfected subjects (Ebrahim and Gnanasekaran, 2019). This was in part due to the patient's own immune system being activated by the presence of parasites (Cabrales *et al.*, 2011; Ebrahim and Gnanasekaran, 2019). Macrophages and neutrophils generate ROS to prompt oxidative stress and cell death in the malaria parasite. However, this increase in ROS damages the host cells (Percário *et al.*, 2012). Metabolic processes of the parasite such as haemoglobin degradation in the parasitic vacuole to produce the by-product, FPIX, contributes to the increase in ROS through the Fenton reaction (Postma *et al.*, 1996; Egan *et al.*, 2002). Metal ion chelators, as well as antioxidants could prove useful in managing both the parasitic infection and the subsequent oxidative stress from the immune response. 5,7-

Dichloro-8-OH, 5,7-dibromo-8-OH, 5,7-dimethyl-8-OH, 5-HSO_3-7-iodo-8-OH, and 5-chloro-7-iodo-8-OH showed a percentage parasitaemia inhibition that was comparable to the DHA control (Table 4.5). Modelling studies to determine new antimalarial molecular targets revealed that 5-chloro-7-iodo-8-OH could possibly inhibit *P. falciparum* via protease inhibition of the parasitic enzymes responsible for haem production and it was found that the compound inhibited the W2 strain of *P. falciparum in vitro* (Nunes *et al.*, 2019). The derivative of 8-OH, 1-1-(thiophene-2-carbonyl)-3-(quinolin-8-yl)thiourea was able to bind to pLDH (enzyme that is important in the glycolysis pathway in *P. falciparum* parasites) more readily than the control antimalarial, mefloquine (Kalaiyarasi *et al.*, 2019). In addition, 5-Chloro-7-iodo-8-OH and 5,7-dichloro-8-OH may be a possible malaria parasite dehydrogenase inhibitor (Sureshkumar *et al.*, 2020). Since 5,7-dichloro-8-OH, 5,7-dibromo-8-OH, 5,7-dimethyl-8-OH, 5-HSO_3-7-iodo-8-OH and 5-chloro-7-iodo-8-OH showed activity in the pLDH assay they may inhibit the malaria parasite by inhibition of the pLDH enzyme. Furthermore, 5,7-dichloro-8-OH, 5,7-diiodo-8-OH and 5,7-dichloro-2-methyl-8-OH favourably inhibited the formation of β-haematin in a manner that was comparable to the chloroquine control (Table 4.8). Hence, it may be possible that the mechanism of parasite inhibition by 5,7-dichloro-8-OH was a combination of copper chelation, antioxidant activity and inhibition of β-haematin formation. The metal chelation and parasitic inhibition activity of 8-OH derivatives were found to be directly associated with each other (Scheibel and Adler, 1982). Derivatives of 8-OH with a chloro functional group at the 5 and/or 7 position demonstrated an increase in lipophilicity and metal ion chelation which did not correlate with an increase in antimalarial activity (Scheibel and Adler, 1982). This lipid permeability has resulted in the inhibition of intracellular parasitic metalloprotein oxidase enzymes by 8-OH by interfering with amino and sulfhydryl functional groups (Scheibel and Adler, 1980, 1981).

Management of malaria transmission may lie in the inhibition of the malaria vector at the larval stage. In order to reduce the occurrence of malaria and to achieve vector control, an efficient and eco-friendly inhibitor of *Anopheles* is needed (Benelli and Beier, 2017). The following 5,7 derivatives of 8-OH demonstrated larvicidal activity greater than 60%: 5,7-dichloro-8-OH, 5,7-dibromo-8-OH, 5-chloro-7-iodo-8-OH, 5-chloro-7-bromo-8-OH and 5,7-dichloro-2-methyl-8-OH, which was comparable to DDT (Table 4.17). DDT inhibits the closing of the insect neuronal sodium ion channels resulting in increased nerve activity, sodium leakage, membrane disruption, and ultimately death (Coats, 1990). Furthermore, DDT and pyrethroids cause oxidative stress in *An. arabiensis* and it was determined that the larvae may obtain resistance overtime by improving how they deal with oxidative stress (Oliver and Brooke, 2016). Therefore, the mechanism of larvicidal activity of these derivatives could possibly be through some other pathway and not due to their antioxidant activity. Glyphosate is a metal

chelating herbicide that inhibits pathogens by restricting their uptake of essential nutrients and causing a deficiency of metal ions (Mertens *et al.*, 2018). Glyphosate chelates copper in soil and has been shown to bind several other metal ions including Cadmium and Zn (Tsui, Wang and Chu, 2005; Zhou *et al.*, 2013). Glyphosate has also shown to not be a selective inhibitor of organisms and causes toxicity in aquatic organisms (Rahnama, Tulaby Dezfuly and Alishahi, 2018). Exposure of *Anopheles* larvae to glyphosate induced the development of resistance to the herbicide in the adult vector (Oliver and Brooke, 2018). To combat this resistance to commercially available insecticides, novel compounds such as the 8-OH derivatives that selectively inhibit malaria larvae and cause metal ion deficiency may prove effective. Metal ion chelators such as the 8-OH derivatives (Table 4.17) have inhibited the metabolic activity of the multicopper oxidases present in larvae (Dittmer and Kanost, 2010). When the copper dependent enzyme, laccase loses functionality, it results in an insect with a malformed cuticle and is lethal (Arakane *et al.*, 2005; Andersen, 2012). Furthermore, compounds that inhibit acetylcholinesterase have demonstrated larvicidal activity, since derivatives of 8-OH have been found to inhibit acetylcholinesterase and chelate copper in humans, they should be further studied to determine whether this is a possible mechanism of larvicidal action (Fernández-Bachiller *et al.*, 2010; Pradeepa *et al.*, 2016). Restricting copper from this enzyme through chelation would be a novel larvicidal approach.

5,7-Dichloro-8-OH, 5,7-diiodo-8-OH, 5,7-dibromo-8-OH, 5-chloro-7-bromo-8-OH, 5-HSO_3-7-iodo-8-OH and 5,7-dichloro-2-methyl-8-OH induced a low mortality rate of *Artemia* that incrementally increased over 72 hours (Table 4.15). Their toxicity may only be targeted for the *anopheles'* larvae and they may prove to be eco-friendly larvicides. Further studies of the toxicity of these compounds on other aquatic organisms should be conducted since these compounds were non-toxic towards *Artemia*. These derivatives could be used to selectively inhibit the larvae of the malaria vector while not harming other organisms.

6.1.2.2. Compounds with a single functional group on the 8-OH ring

Simple derivatives of 8-OH were able to inhibit resistant bacteria such as *S. aureus* and *Klebsiella pneumoniae* by inhibiting metal binding sites on bacterial enzymes and inhibiting nitric oxide production (Srisung *et al.*, 2013). Similarly, 8-OH itself inhibited 10 strains of *P. falciparum in vitro* comparably to chloroquine (Biswas, 2003). This antimicrobial and antimalarial activity by enzyme inhibition may provide a mechanism of action for 8-OH and its derivatives with single functional groups. 5-Chloro-8-OH, 5-HSO_3-8-OH (Figure D.7), and 5-nitro-8-OH both demonstrated copper (I) chelation of greater than 90% and inhibited the *P. falciparum* parasite comparably to the DHA control (Table 4.1 and Table 4.5). The copper (I) chelation activity of 5-chloro-8-OH and 5-nitro-8-OH (Figure D.6) may contribute to the mechanism of antimalarial action by chelating copper (I) ions from enzymes responsible for

metabolic processes in the parasite. RBCs contain copper within Cu/Zn SOD, when *Plasmodium* invades the RBCs it utilizes the host copper for its own metabolism. The copper (I) chelator, neocuproine, inhibited the malaria parasite by chelating copper from the Cu/Zn SOD (Rasoloson *et al.*, 2004). 8-OH (Figure D.1) has also been shown to be a potent inhibitor of the anaerobic protozoal parasite, *Trichomonas vaginalis,* through the breakdown of this parasites apicoplasts (Rossiter and Blockman, 2020) and (Chellan, Sadler and Land, 2017). Apicoplasts are important elements for parasitic metabolic pathways that include the synthesis of fatty acids and stores iron and haem. It is also linked to the functioning of the parasitic mitochondria and is crucial for *P. falciparum* functioning (Kalanon and McFadden, 2010). Thus, 8-OH and its derivatives could potentially target the apicoplasts of *P. falciparum.* The chelating aspect of these compounds could also prove useful in causing a metal ion deficiency in *P. falciparum* or the toxic accumulation of a metal ion complex within the parasitic cell (Scheibel and Adler, 1980). Scheibel and Adler (1981) found that two 8-OH molecules with substitutions at the 5th position on the quinoline group inhibited *P. falciparum* growth by approximately 25%, demonstrating that these compounds have antimalarial activity.

Artemisinin derivatives are generally well-tolerated in the treatment of malaria; however they have caused acute haemolytic anaemia which may result in the death of patients (Rehman *et al.*, 2014). Compounds with a favourable effect on RBCs are needed. These compounds also demonstrated a low haemolytic effect in comparison to chloroquine control (Table 4.10) and a low lethality in the *Artemia* nauplii (Table 4.15). Thereby their favourable toxicity profile in addition to their selective copper (I) chelation may be useful in the management of copper excess diseases.

5-Chloro-8-OH (Figure D.6) and 5-nitro-8-O both (Figure D.8) displayed cytotoxicity towards the neuroblastoma cells (Table 4.11). Both of these compounds have a functional group at the 5-position on the 8-OH ring and were less cytotoxic than those compounds with a functional group at the 7-position. The anticancer activity of 5-nitro-8-OH was compared to 5-chloro-7-iodo-8-OH and it was found to be more potent than 5-chloro-7-iodo-8-OH against lymphoma, leukaemia and pancreatic cancer cell lines (Jiang *et al.*, 2011). 5-Nitro-8-OH was also shown to be a copper ionophore, inhibited angiogenesis and it did not possess the neurotoxicity of 5-chloro-7-iodo-8-OH (Jiang *et al.*, 2011). In this study the cytotoxic activity against the neuroblastoma cells of 5-chloro-7-iodo-8-OH was 4.7-fold higher than 5-nitro-8-OH (Table 4.11). Thereby showing that the anticancer activity of these compounds may be specific for different cell lines. 8-OH derivatives were shown to be metal ion ionophores that disrupt the membrane permeability of cancerous cells leading to calcium ion loss and cell death (Leanderson and Tagesson, 1996; Ding *et al.*, 2005; Lind, Park and Drexler, 2009; Yu *et al.*,

2009). Since these compounds demonstrated properties to increase membrane permeability and inhibited the metabolism and protein content of neuroblastoma cells, further investigation is needed to determine their effect on other cell lines and metal ions.

2-Benzyl-8-OH (Figure D.4) had no activity in the copper homeostasis and antioxidant assays however it demonstrated neuroblastoma inhibition (Table 4.11), antimalarial (Table 4.5) and larvicidal (Table 4.17) activity. It also induced increased mortality of *Artemia* to an equivalent efficacy to that of the potassium dichromate control; (Table 4.15) and was found to induce lysis of the red blood cell membrane (Table 4.10). 2-Benzyl-8-OH demonstrated promising copper (I/II) protective effects in the neuroblastoma cells and the red blood cells (Figure 4.17, Figure 4.22and Figure 4.23). Since this derivative had a less than 5% activity in the copper chelation/complexation and antioxidant assays (Table 4.1, Table 4.2 and Table 4.12), its protective effect against copper excess was through some other type of mechanism of action. The probable mechanism of action for this compound could not be determined in this study, however it seems to possess non-selective toxicity towards the *Anopheles* larvae and *Artemia* nauplii. As such, pesticides with non-selective toxicity are not ideal candidates to inhibit the malaria vector in a fresh water environment (Rahnama, Tulaby Dezfuly and Alishahi, 2018).

Antioxidants have protective effects against oxidative stress and have been previously considered to possibly assist in the management of neurological impairment (Neves Carvalho *et al.*, 2017). In order to be effective, antioxidants would need to cross the blood brain barrier to prevent oxidative stress within neuronal cells (Neves Carvalho *et al.*, 2017). 8-OH and its derivatives have been shown to cross the blood brain barrier and decrease the production of ROS (Barnham *et al.*, 2004). *P. falciparum* induced cerebral malaria results in a high level of ROS within the neuronal cells of patients. This leads to seizures, coma and death (Vanka *et al.*, 2020). Those patients that do survive demonstrate cognitive injury even after recovering from the infection. The continued cognitive impairment is believed to be as a result of inflammation in neurological cellular sites (Vanka *et al.*, 2020). Compounds with both antioxidant and antimalarial activities could aide in managing both the malarial infection and the subsequent oxidative inflammatory response. 5-Amino-8-OH and 2-amino-8-OH were both shown to be antioxidants with comparable activity to the ascorbic acid control (Table 4.12). Both compounds also effectively inhibited the malaria parasite (Table 4.5) and demonstrated a low lethality in the *Artemia* lethality assay (Table 4.15). 5-Amino-8-OH (Figure D.9) showed potent superoxide scavenging activity as well as antimicrobial activity against methicillin-resistant *Staphylococcus aureus* (Cherdtrakulkiat *et al.*, 2020). Consequently, this compound may have a broad range of antimicrobial activity. Both of these compounds have an amino functional group on the 8-OH ring, and this may be the reason for both the

antioxidant and antimalarial activity. Furthermore, 5-amino-8-OH and 2-amino-8-OH (Figure D.5) were cytotoxic against neuroblastoma cells (Table 4.11). The combination of antimalarial, antioxidant and anticancer activity of these amino derivatives should be further investigated.

2-Methyl-8-OH (Figure D.3) was shown to be a powerful antioxidant and therefore protected the membranes of erythrocytes (Table 4.4, Table 4.12 and Table 4.10). Furthermore, it demonstrated a protective effect against copper (II) haemolysis (Figure 4.18) and excess copper (I/II) in neuroblastoma cells (Figure 4.22 and Figure 4.23). 2-Methyl-8-OH demonstrated low activity (44.00 ± 8.54%) when compared to the DHA control (Table 4.5). In contrast, a computational model of 2-methyl-8-OH suggested that it could induce oxidation with potential to inhibit potently malarial dehydrogenase enzymes (Sureshkumar *et al.*, 2020). A derivative of 2-methyl-8-OH that consisted of two 2-methyl-8-OH rings demonstrated potent antioxidant, copper (II), zinc (II) and nickel (II) chelation and chelated copper (II) from Aβ proteins thereby preventing aggregation (Safadi *et al.*, 2017). The joining of the two rings seemingly augmented the activity of 2-methyl-8-OH. Ascorbic acid is a recognised antioxidant that is also known to induce oxidant reactions with the generation of ROS species (Tu, Njus and Schlegel, 2017). In the current study it was not determined whether 2-methyl-8-OH could induce pro-oxidant activity and the results did not support any evidence that 2-methyl-8-OH could produce oxidants. Therefore, assays to determine the pro-oxidant effects of 2-methyl-8-OH should be completed to determine if it has similar activity to ascorbic acid.

5-Carboxy-8-OH (Figure D.10) demonstrated lipid peroxidation inhibition (Table 4.13) but was inactive in all other assays. It may therefore have a potential use in preventing oxidative reactions that cause damage to sensitive lipid membranes. Conversely, 5-carboxy-8-OH was shown to be an iron chelator that moved iron ions across cellular membranes and inhibited the oxoglutarate oxygenase enzyme which is a potentiator of cancer, anaemia, and ischaemic diseases (Hopkinson *et al.*, 2013). The authors attributed the iron translocation to the compound being a small molecule (Hopkinson *et al.*, 2013). It may be possible that the 5-carboxy-8-OH is a selective iron ion chelator and its basic structure could have caused it to be less active in the antioxidant, antimalarial and cytotoxic assays in comparison to the other 8-OH derivatives. Bisphenolic derivatives of 8-OH are complex molecules which had significant antibacterial, antifungal, free radical scavenging and metal ion reducing activity with the derivative containing two 8-OH rings being the most potent in comparison to the parent compound (Indira *et al.*, 2019). Consequently, compounds with complex functional groups are more likely to show a diverse range of properties. Thereby, the lack of activity across all assays of 8-chloro-2-OH, 8-fluoro-4-OH and 4-OH (Figure D.2 and Figure D.18) may be due to their simple structure.

The 8-OH derivatives were shown to be copper ion modulators with several demonstrating antioxidant, anticancer, antimalarial and larvicidal activity. The activity of these compounds may lie in their molecular structure and it seems that their activity is dictated by the position of the functional group, the functional group itself and the size of the molecule. The toxicity of these compounds would need further study to determine their potential therapeutic applications. To truly elucidate the mechanisms of actions of the 8-OH derivatives further studies determining possible enzymes induced/inhibited are needed.

6.2. EOCs

EOCs are volatile, aromatic compounds that have shown promise in the treatment of inflammatory conditions such as cancer, atherosclerosis, and cardiovascular conditions (Baptista-Silva *et al.*, 2020). Several EOCs, such as (±)-menthone, and eugenol displayed antioxidant activity by scavenging free radicals (Table 5.12), inhibiting lipid peroxidation (Figure 5.18), and prevented the formation of nitrogen oxygen species (Table 5.13). (+)-α-Pinene was able to activate immune system cytokines and is able to alter the actions of the immune system (Kedzia *et al.*, 1998; Bae *et al.*, 2011). This immune system activation is useful in fighting disease progress of certain cancers and chronic inflammation (Edris, 2007; Pan *et al.*, 2009). The EOCs in this study also displayed anticancer properties against the neuroblastoma cells (Table 5.11). Of the 55 EOCs evaluated in this study, the one that showed the widest range of activity was (±)-menthone. It possessed copper (I/II) chelation activity, *in vitro* copper chelation, had a synergistic copper chelation with quinine and reduced copper, while able to inhibit lipid peroxidation. It also demonstrated antimalarial action and larvicidal activity (Figure 6.6). (+)-α-Pinene was the EOC that demonstrated the most potent activity against the malaria parasite, with a synergistic interaction with chloroquine and also had effective antioxidant activity (Table 5.12).

6.2.1. (±)-Menthone

(±)-Menthone (Figure 6.6), which is a phenolic EOC present in the essential oil from *Calamintha incana* for example, demonstrated the widest range of activity for the EOCs across the assays conducted in this study (Božović and Ragno, 2017). Copper is thought to play an essential role in cancer cell angiogenesis, which is essential for the growth and survival of cancer cells (Finney *et al.*, 2009). TMB has been reported to inhibit angiogenesis through its binding of copper, thereby restricting the stimulation of the angiogenic process (Doñate *et al.*, 2008). Copper and metal ion complexation would be a useful tool in the management of diseases like cancer.

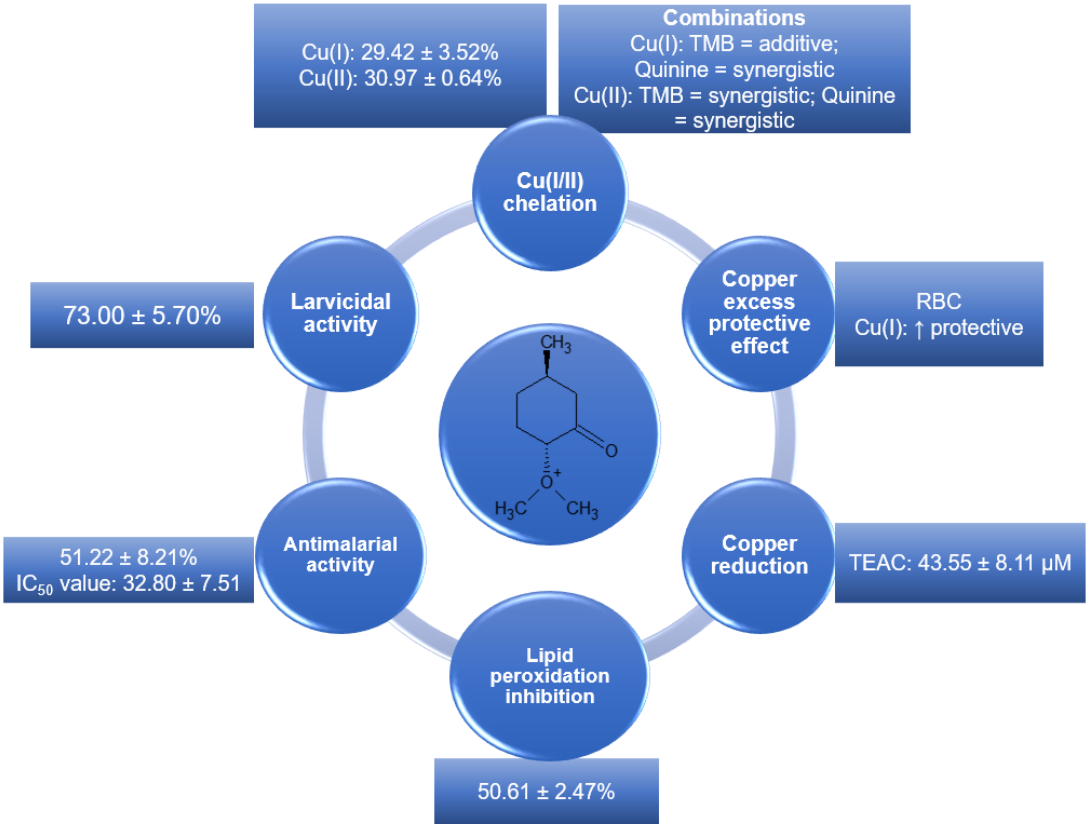

Figure 6.6: The molecular structure and summary of activity of (±)-menthone (Pubchem, 2020a).

This essential oil was found in this study to possess moderate antioxidant activity (Figure 5.18) compared to the potent activity reported by Popović-Djordjević (2019); which was complemented by the powerful copper and iron reducing and some ferrous ion chelation properties (Popović-Djordjević *et al.*, 2019). The metal ion chelation activity of menthone is not well documented, therefore the copper chelation activity was determined in this study. (±)-Menthone demonstrated the highest copper chelation activity amongst all the EOCs, which was considerably lower in comparison to the TMB control (Table 5.1; Cu(I): P = 0.0001; Cu(II): P = 0.02). It also demonstrated favourable copper complexation activity that was comparable to the TMB control and was found to be more selective for copper (II) than copper (I) (Table 5.2). (±)-Menthone synergistically chelated both copper (I) as well as copper (II) when cobined with quinine, with a similar synergistic chelation of copper (II) in combination with TMB (Figure 5.3). The anti-angiogenic effect of TMB was as a result of the molecule causing a copper deficiency in copper-dependent enzymes that promote the angiogenic process (Alvarez *et al.*, 2010). TMB was also found to induce dormancy in cancerous tumours (Pan *et al.*, 2009). As such the additive and synergistic copper chelation interaction between (±)-menthone and TMB may enhance the anti-angiogenic properties of TMB. TMB was also found to induce dormancy in cancerous tumours (Pan *et al.*, 2009). Therefore, the combination of (±)-menthone and TMB

should be further studied in several different cancer cell lines. Inflammatory processes have been linked to the worsening of diseases like cancer by inducing tumour development (Pan *et al.*, 2009). Safe and effective immune system modulators that prevent and manage chronic inflammation are needed to mitigate cancer disease progression (Coussens and Werb, 2002).

EOCs have demonstrated antioxidant, anticancer and anti-inflammatory properties (Edris, 2007). In this study, (±)-menthone demonstrated moderate antioxidant activity by reducing copper (II) ions and inhibiting lipid peroxidation formation (Table 5.4 and Figure 5.18) and it was cytotoxic against neuroblastoma cells (Table 5.11). Thereby, this compound may have potential to be used in the management of oxidative stress and cancer. A study found that in combination with ascorbic acid, menthone potently decreased acyclovir-induced apoptosis in the sperm cells of rats by decreasing the action of caspase 3 (Toghiani *et al.*, 2016).

Menthone selectively inhibited COX-2 in comparison to aspirin which is an important mediator of the inflammatory process (Kawata, Kameda and Miyazawa, 2008). It also decreased the allergy mediating levels of IL-13 *in vivo* and boosted the number of cells that yield antibodies thereby increasing the activity of the immune system (Raphael and Kuttan, 2003). (±)-Menthone is a powerful antioxidant that is able to modulate the immune response, which could be a useful property in the search for new treatments for inflammatory diseases. (±)-Menthone had a protective effect against gastric ulcers in rat models. The authors attributed this property to possible modulation of the proton pump inhibitors in gastric cells and to menthones antioxidant activity (Nazer, Darvishi and Qolampour, 2018). (±)-Menthone had a favourable toxicity profile as it demonstrate a low haemolytic activity that was 5-fold higher than the chloroquine control (Table 5.10). Therefore, due to its copper protective, antioxidant, and low haemolytic effect; (±)-menthone may be used as a chemoprotective agent.

As a result of the breakdown of haemoglobin in the food vacuole of *Plasmodium,* oxidant generating compounds like FPIX are produced (Postma *et al.*, 1996). FPIX that is not detoxified into haemozoin is released into the cytoplasm of the host cells where the free Fe^{3+} ions of this by-product interacts with membranes leading to the destabilization of these membranes and lipid peroxidation (Fitch *et al.*, 1982; Famin, Krugliak and Ginsburg, 1999; Zhang, Krugliak and Ginsburg, 1999; Egan *et al.*, 2002; Singh *et al.*, 2017). This leads to the release of cytoplasm into extracellular sites and the activation of the host immune system. Immune system mediators such as TNF-α generates an inflammatory response that produces ROS that is meant to overwhelm and inhibit the malaria parasite with oxidants (Figueiredo *et al.*, 2007). The production of the excess oxidants results in the malaria patient experiencing oxidative stress which leads to increase risk of haemolysis, metabolic acidosis and difficulty

breathing (Becker *et al.*, 2004; Kavishe, Koenderink and Alifrangis, 2017). One of the mechanisms of action for artemisinin-based combination therapy is believed to be inducing oxidative stress within the parasite which may also lead to further oxidative damage within the host (Kavishe, Koenderink and Alifrangis, 2017). Compounds that possess both antimalarial and antioxidant properties may prove useful in both treating the malaria infection and the consequential oxidative stress in the host. (±)-Menthone had a similar percentage parasitaemia inhibition in comparison to the DHA control. Malaria parasites showed a recovery in parasitaemia 60 hours after (±)-menthone treatment. Since the antimalarial activity of (±)-menthone was not that potent, the potential of combining it with an antioxidant such as ascorbic acid may prove beneficial (Figueiredo *et al.*, 2007). In addition, due to its potentially important antioxidant activity, further studies are needed to determine whether it would be useful in the management of the oxidative stress that the pathogenesis of malaria produces. (±)-Menthone did not have an effect on the malaria parasite stages or on its morphology when compared to the untreated control and that of quinine. The antimalarial activity of (±)-menthone does not meet the selection criteria to be an effective antimalarial because its IC_{50} value was above 1 µM (Katsuno *et al.*, 2015).

Therefore, determining the activities of (±)-menthone against other microorganisms such as bacteria may be advantageous in finding novel treatments. Menthone inhibited several strains of bacteria namely: *B. cereus*, *S. epidermidis*, *K. pneumoniae* and *P. aeruginosa* which was attributed to its cyclic monoterpenoid structure (Ben Haj Yahia *et al.*, 2019). *Mentha piperita* oil is comprised of menthol and menthone, demonstrated potent antiviral effects against *Herpes simplex* virus-1 and -2 and both of these EOCs demonstrated respectable antibacterial activity against *Staphylococcus epidermidis, S. aureus, Micrococcus luteus, Escherichia coli, Listeria monocytogenes, Enterococcus faecalis, P. aeruginosa, and Salmonella typhimurium* (Schuhmacher, Reichling and Schnitzler, 2003; Hajlaoui *et al.*, 2008).

(±)-Menthone may not exhibit favourable antimalarial activity, but it may prove to be an effective insecticide against the *Anopheles* malaria vector. (±)-Menthone is a constituent of the *Mentha* plant species, several studies have shown that the essential oil of the *Mentha* peppermint plant has an effective, long lasting and wide range of repellent activity against several types of *Anopheles* mosquitos (Ansari *et al.*, 2000; Amer and Mehlhorn, 2006; Sritabutra *et al.*, 2011). Menthone has been found to be a 2.51% component of the essential oil from *Mentha arvensis* L., which exhibits both repellent and larvicidal activity against *Aedes aegypti* malaria vector mosquito (Manh and Tuyet, 2020). The essential oil from *Mentha spicata*, which menthone is a component (1.15.%), demonstrated potent larvicidal properties against the mosquito vectors *An. stephensi* (83.20 ± 1.80%), *Culex quinquefasciatus* (96.80 ±

1.20%) and *Ae. aegypti* (98.10 ± 1.20%) (Govindarajan *et al.*, 2012). Menthone is the main component (22.00%) of the essential oil *Mentha aquatica* demonstrated potent larvicidal activity (LD_{50} value = 0.76 µM) against the mosquito *C. quinquefasciatus* (Pavela, Kaffkova and KUMŠTA, 2014). In this study, (±)-menthone demonstrated a strong larvicidal activity (73.00 ± 5.70%) that was significantly lower than the DDT control (Table 5.14; P = 0.0001). The effect of this compound on another aquatic species like *Artemia* should be determined to ensure selective inhibition of the malaria larvae if it was to be considered as a larvicidal environmental spray. Therefore, (±)-menthone is an EOC with copper chelating, antioxidant, anticancer, antimalarial and larvicidal properties with a favourable toxicity in RBCs. Its distinctive properties warrant further investigation.

6.2.2. (+)-α-Pinene

The development of resistance to antimalarial agents by *P. falciparum* has initiated an intensive search for novel treatments and management strategies (Egan, 2015). Agents like artemisinin and quinine were originally sourced from plants to be used as antimalarial agents (Kaur *et al.*, 2009). As such, the solution for malaria control could lie in plant-derived compounds such as the EOCs. (+)-α-Pinene is classified as an aromatic, polyphenolic terpene (Figure 6.7) and is a constituent of plants such as *Ocimum basilicum* (basil), *Mentha* (mint) and *Cinnamomum camphora* (camphor) and has exhibited antimalarial activity (Zhou *et al.*, 2004; Van Zyl *et al.*, 2006; Pérez G *et al.*, 2011).

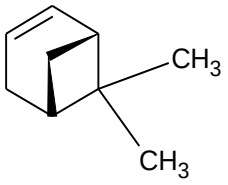

Figure 6.7: The molecular structure of (+)-α-pinene (Pubchem, 2020a).

The antimicrobial mechanism of action of (+)-α-pinene was proposed to be through the inhibition of microbial phospholipases when evaluated against *Candida albicans* and methicillin-resistant *Staphylococcus aureus* (Da Silva *et al.*, 2012). It also demonstrated a synergistic antimicrobial activity against *C. albicans, Cryptococcus neoformans, Rhizopus oryzae* and methicillin-resistant *S. aureus* when used in combination with amphotericin B and this combination also showed a decrease in toxicity to murine macrophages (Da Silva *et al.*, 2012). α-Pinene as a component of eucalyptus oil was shown to be possess strong antimalarial activity against chloroquine-sensitive and chloroquine-resistant strains of *P. falciparum* at the trophozoite stage (Su *et al.*, 2008; Sebei *et al.*, 2015). This antimalarial

activity was demonstrated in this study, where (+)-α-pinene demonstrated an IC_{50} value that was lower than the chloroquine control against the 3D7 chloroquine-sensitive strain(Table 5.5). (+)-α-Pinene has previously been reported to be a more potent antimalarial than quinine against the chloroquine-resistant FCR-3 strain of *P. falciparum* (Van Zyl *et al.*, 2006). Its mechanism of action against malaria could be proposed to be by inhibiting haemozoin formation in the parasite as was shown in the β-haematin formation inhibition assay (Table 5.8). Since both (+)-α-pinene and chloroquine have similar mechanisms of action (Figure 6.3) and comparable activity and this was shown to be an advantage as demonstrated by the resultant synergistic interaction (Figure 5.8).

The impact of isomeric differences on the pharmacological activity of drugs is well known and essential to be evaluated (Chhabra, Aseri and Padmanabhan, 2013). (+)-α-Pinene has been shown to have a far more potent antimalarial activity than its structural isomer (+)-β-pinene against the FCR-3 and 3D7 *P*. *falciparum* strains (Van Zyl *et al.*, 2006), whilst it was ineffective against the NF54 strain (Van Zyl *et al.*, 2006; Mustapha, 2017). This strain specific observation has previously been reported for the standard antimalarial agents such as chloroquine and quinine, where their targets are well characterised, as well as mechanisms of resistance. Similarly, the strain specific effect has been reported for investigatory compounds, such as amantadine and iron chelating agents, desferrioxamine and 2,2'-bipyridyl (Evans and Havlik, 1993, 1994; Van Zyl *et al.*, 1993). Where parasite sensitivity to the test compound could be affected by parasite target alterations, indicating that the more strains should be evaluated to ensure (+)-α-pinene will inhibit the majority of *P. falciparum* stains. Moreover, the promising synergistic interaction with chloroquine should be further investigated to determine if the combination could be feasible in the management of a malaria infection.

α-(+)-Pinene demonstrated a weak free radical scavenging activity (Table 5.12) and showed a 2-fold lower ability to inhibit lipid peroxidation compared to ascorbic acid (Figure 5.18). Conversely, (-)-β-pinene demonstrated the second highest free radical scavenging activity amongst the EOCs (Table 5.12). A study on the activity of enantiomers of pinene showed that the positive enantiomers demonstrated greater antibacterial activity than the negative enantiomers (Lis-Balcnin *et al.*, 1999). Enantiomer differences in antibacterial activity have also been seen with limonene and menthol (Lis-Balcnin *et al.*, 1999; Ozek *et al.*, 2010). α-Pinene was shown to be an immunostimulant, which may be useful in defending the host system from various pathogens (Kedzia *et al.*, 1998; Bala, Singha and Patra, 2019). It also modulated the activity of natural killer cells and activated lymphocytes (Standen, Connellan and Leach, 2006). Furthermore, α-pinene inhibited leukotriene production and has the potential to be used as an anti-inflammatory agent (Ahn *et al.*, 2001).

α-Pinene inhibits the growth of hepatic carcinoma cells and encouraged apoptotic death of ovarian cancer cells by modulating the immune response through caspase stimulation (Chen *et al.*, 2014; Hou *et al.*, 2019). (+)-α-Pinene had low haemolytic activity and showed a high cellular viability in the SRB assay (Table 5.10 and Table 5.11). Therefore, it was non-toxic to RBCs and did not affect neuroblastoma protein content. Conversely, it had a high cytotoxic effect as determined by the MTT assay in comparison to the camptothecin control with an increasing copper protective effect against copper(I) and –(II) in neuroblastoma cells which may be due to its copper complexation activity (Table 5.2, Figure 5.13 and Figure 5.14). Further studies are needed to determine its precise mechanism of action in malaria.

6.2.3. (S)-(-)-β-Citronellol

Citronellol is found in the oils of *Geranium*, *Java citronella* and *Eucalyptus citriodora* but the majority of citronellol is obtained from pinene oil (Bedoukian, 1986; Chadwick, 1988). It is widely used in fragrances and citrus flavourings of sweets, chewing gum and ice cream, and was found to be non-toxic in animal studies (Chadwick, 1988; Lewis *et al.*, 1994; Millenium Specialty Chemicals, 1995). (S)-(-)-β-Citronellol is a linear structure (Figure 6.8) with antibacterial and antioxidant as well as immune system altering effects (Su *et al.*, 2010; Jagdale *et al.*, 2015; Lopez-Romero *et al.*, 2015).

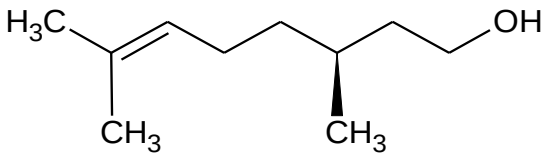

Figure 6.8: The molecular structure of (S)-(-)-β-citronellol (Pubchem, 2020a).

Citronellol inhibited nitric oxide synthase enzymatic activity that in turn decreased levels of nitric oxide and PGE2 synthesis (Su *et al.*, 2010). (S)-(-)-β-Citronellol moderately prevented the formation of nitrogen oxygen species (Table 5.13) It interacted with the COX-2 protein and the expression of mRNA expression, thereby inhibiting nitric oxide production and stimulating immune responses of macrophages (Su *et al.*, 2010). Immune system modifiers may induce responses that are beneficial in the treatment of certain cancers. Citronellol has been observed to inhibit non-small cell lung cancer cells *in vitro* by stimulating the TNF-α immune system pathway that increased the generation of ROS leading to necroptosis of the cancer cells. Correspondingly, (S)-(-)-β-citronellol demonstrated potent cytotoxic activity against the neuroblastoma SH-SY5Y cell line and found to be comparable to the inhibitory

activity of camptothecin, a known anticancer agent (Table 5.11). Further investigation into the possible mechanism of action of (S)-(-)-β-citronellol in neuroblastoma cell inhibition is needed.

(S)-(-)-β-Citronellol did not demonstrate promising malaria inhibition (Table 5.5), as such does not meet the criteria for a good antimalarial agent (Katsuno *et al.*, 2015). This activity on the whole parasite, does not correlate to the potent ability to inhibit haemozoin formation, which was even to a greater degree than chloroquine (Table 5.5). Although (S)-(-)-(β)-citronellol is a lipophilic compound, it did not appear to accumulate to a high enough concentration within the food vacuole, to potently inhibit haemozoin formation and subsequently be effective in inhibiting parasite growth at a low IC_{50} value, as observed for chloroquine. To improve upon the overall inhibitory effect, it could be proposed that the effect could be enhanced by combining these two compounds as indicated by the synergistic interaction to prevent haemozoin formation (Figure 5.11). In addition, the lack of haemolysis and potentially promising safety profile of (S)-(-)-(β)-citronellol warrants further investigation. Structural alterations or linking chloroquine to (S)-(-)-(β)-citronellol could improve the overall inhibitory effect on the whole parasite whilst retaining its ability to inhibit haemozoin formation.

The control of the *Anopheles* malaria vector would be useful in containing the spread of malaria. (S)-(-)-β-Citronellol is a component of the essential oil *Zingiber nimmonii*, which has demonstrated larvicidal activity against *An. stephensi* and *Ae. aegypti,* while not causing toxicity in the control organisms. It has been hypothesised that the use of this oil would also provide a vector control method that is both effective and eco-friendly (Govindarajan *et al.*, 2016). Furthermore, (S)-(-)-β-citronellol inhibited the activity of the larvae of *Aedes albopictus*, *Ae. aegypti* and *Culex pipiens pallens* mosquitos by inhibiting the action of acetylcholinesterase (Lee and Ahn, 2013). In the present study, (S)-(-)-β-citronellol demonstrated larvicidal activity that was greater than 80% and comparable to the DDT control. This further establishes this compound as a potential element in the management of malaria distribution.

6.2.4. Eugenol

The inflammatory response by the immune system is generally a defensive reaction of the body to invasive organisms or cellular injury and is in place to stimulate recovery (Ferrero-Miliani *et al.*, 2007; De Cássia Da Silveira E Sá, Andrade and De Sousa, 2013). When inflammation becomes chronic, it stimulates prolonged cellular damage and the prolonged release of cytokines (Ferrero-Miliani *et al.*, 2007; Nizamutdinova *et al.*, 2016). Eugenol is a phenolic EOC component (Figure 6.9) of clove oil, soybeans, cinnamon, basil and coffee (Charalambous, 1981; Marotti, Piccaglia and Giovanelli, 1996; Lee and Shibamoto, 2000;

Zhang *et al.*, 2013), that has demonstrated potent antioxidant activity, as demonstrated in this study (Figure 5.4and Figure 5.18; Table 5.4 and Table 5.12) (Seatlholo, 2007; Nagababu *et al.*, 2010; Gülçin, 2011; Zhang *et al.*, 2013).

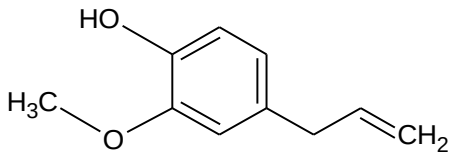

Figure 6.9: The molecular structure of eugenol (Pubchem, 2020a).

Eugenol has anti-inflammatory properties where it supressed iron mediated lipid peroxidation, and had both iron and copper reducing properties (Nagababu *et al.*, 2010; Gülçin, 2011). Eugenol demonstrated the greatest antioxidant activity amongst the EOCs by scavenging free radicals (IC_{50} value: 13.22 µM) and reducing copper (IC_{50} value: 16.06 µM) (Table 5.12 and Table 5.4) (Gülçin, 2011). This further establishes its antioxidant actions.

Eugenol has been shown to inhibit various cancer cell lines such as melanoma, leukemic, hepatocellular carcinoma and colon carcinoma *in vitro* (Ghosh *et al.*, 2005; Yoo *et al.*, 2005), as well as a potent activity against the neuroblastoma cells in this study (Table 5.11). The proposed mechanism of anti-cancer action was the induction of apoptosis and activation of cytokines that cause cytotoxicity within the cancer cell (Yoo *et al.*, 2005). The inhibitory effect of eugenol against cancerous cells has also been shown to be due to the disruption of the permeability of the membrane leading the leakage of cellular contents and cell death (Yoo *et al.*, 2005). Eugenol demonstrated moderate cytotoxicity against a normalised human kidney epithelial (HEK293) cells and this may show that it could have unfavourable toxicity (Mustapha, 2017). Therefore, eugenol has the potential to be used in the management of certain cancers and further studies to determine its activity in normal cell lines would need to be carried out to determine its effectiveness.

The anti-inflammatory and immune system modulation activity of eugenol may also contribute to its effect on microorganisms *in vitro*. Eugenol has antimicrobial activity, it has inhibited both resistant and sensitive strains of *Helicobacter pylori*, *E.coli* and *Pseudomonas* (Ali *et al.*, 2005). It was further discovered that eugenol inhibited *H. pylori* in an acidic environment which may be advantageous to inhibit the malaria with the parasite acidic vacuole function as a target (Ali *et al.*, 2005). Eugenol demonstrated low antimalarial activity against the 3D7 strain (Table 5.5), while showing moderate antimalarial activity against the FCR-3 and NF54 strains of *P. falciparum* (Van Zyl *et al.*, 2006; Mustapha, 2017) .

In modelling studies, it was shown that the probable inhibitory molecular target of eugenol was the octopamine receptor in *Ae. aegypti* mosquito which would inhibit synaptic growth within the insect (Khanikor *et al.*, 2013). Correspondingly, eugenol demonstrated moderate larvicidal activity in this study (Table 5.14) and the effect of this compound against the octopamine receptor in *An. gambiae* should be determined. In addition, the ability to inhibit acetylcholinesterase could also be a potential target of eugenol in the malaria vector (Osanloo *et al.*, 2018).

6.2.5. EOCs with antimalarial and larvicidal activity

Increased resistance to artemisinin-based combination treatment is categorised by prolonged parasite clearance especially at the asexual parasite ring stage (White, 2008; Flegg *et al.*, 2011). An alternative treatment to combat resistance is needed if *P. falciparum* is to be eliminated. This study showed the effects of compounds against the *P. falciparum* asexual stages. The EOCs that demonstrated the highest percentage parasitaemia inhibition in the pLDH antimalarial assay were α-humulene, (±)-α-β-thujone, 2-mercaptothiazoline, artemisia ketone, ocimene, (±)-lavandulol acetate, thymol, (±)-camphorquinone, myrcene, (-)-caryophyllene oxide, (-)-β-pinene and (-)-α-pinene (Table 5.5). However, the IC_{50} values of these EOCs (with the exception of (±)-camphorquinone) did not meet the criteria for an effective antimalarial (IC_{50} value < 1 µM) (Katsuno *et al.*, 2015). (±)-Camphorquinone showed inhibition greater than 80% and had a potent IC_{50} value that was lower than that of quinine and comparable to chloroquine (Table 5.5). Camphorquinone is a component of several essential oils including *Artemisia annua* and *Cinnamomum camphora. C. camphora* has traditionally been used as an analgesic and to provide relief from haemorrhoids, as well as being an antiseptic, aphrodisiac, contraceptive and anticonvulsant (Sikka and Bartolome, 2018). Camphorquinone stimulates the production of ROS and thereby the release of cytokines that resulted in the production of PGE2, cytotoxicity and apoptosis in non-cancerous dental pulp cells. Its pro-oxidant activity may also be present when it inhibits the malaria parasite (Chang *et al.*, 2015). *P. falciparum* treated with EOCs that contained linear structures with an alcohol functional group, like nerolidol, *cis*-nerolidol, *trans*-nerolidol, citral, farnesol and citronellal, inhibited the isoprenoid pathway responsible for the synthesis of coenzyme Q and this has a negative effect on parasitic growth in the intra-erythrocytic stages (de Macedo *et al.*, 2002). Further to this, it was found that terpene EOCs such as farnesol, limonene, and linalool inhibited the isoprenoid synthesis through the inhibition of Ras and Rap proteins, which lead to interruptions at the ring and schizont stage (Moura *et al.*, 2001; Holstein and Hohl, 2003; Goulart *et al.*, 2004). This pathway may be the potential mechanism of antimalarial action of these linear structured EOCs. (-)-Linalool and (+)-pulegone had promising properties to inhibit β-haematin or haemozoin formation that was comparable to chloroquine and quinine

(Table 5.8). They also demonstrated a favourable low haemolysis indicating a low toxicity profile (Table 5.10); however, they did not demonstrate *in vitro* antimalarial activity (Table 5.5). These EOCs should be tested against another strain of malaria to determine if they possess strain selective antimalarial properties.

Pesticides such as pyrethroids and organophosphates are widely used to control pests such as mosquitoes targeting both the adult and larval stages (Srinivasan *et al.*, 2008; Chauhan *et al.*, 2016). These chemicals have been continuously used and are detrimental to the health of humans and animals, as well as harmful to the environment (Pimentel, 1995; Aktar, Sengupta and Chowdhury, 2009). In addition, mosquitoes have developed resistance to the insecticides, compromising the eradication of malaria (Liu, 2015). As such, alternative novel vector controls that are not harmful to the environment are needed and the EOCs may provide the solution (Pavela, Vrchotová and Tříska, 2009). Furthermore, the control of malaria through inhibition of the vector larvae would be effective in limiting the spread of the parasite by restricting the development of adult mosquitos (Zahran and Abdelgaleil, 2011). Monoterpene EOCs such as carvone, limonene, geraniol, menthol, and thymol demonstrated potent larvicidal activity and prevented the progression to adult mosquito of the *Culex pipiens* L. mosquito, which is the carrier of the West Nile virus, St Louis encephalitis virus and avian malaria (Zahran and Abdelgaleil, 2011; Ewing *et al.*, 2019). Carvacrol, (-)-linalool, linalyl acetate, (+)-pulegone, (-)-menthone, (+)-carvone, *cis*-nerolidol, *trans*-geraniol, and *cis*-geraniol demonstrated a larvicidal activity greater than 70% (Table 5.14), but did not demonstrate notable activity in any other assay. The inhibition of acetylcholinesterase could be proposed as a possible mechanism of insecticidal action for monoterpenoids and the action against this enzyme by the EOCs should be investigated (Miyazawa and Yamafuji, 2005).

The EOC constituents in this study were shown to be antioxidants with some showing potent antimalarial activity as well as possible anticancer effects against neuroblastoma. Several of these compounds also have the potential to be used in the management of malaria vector larvae control.

Chapter 7. Conclusions, limitations of the study and recommendations for further research

7.1. Conclusion

As the disease burden increases, the need for novel medicinal agents with the potential of using copper as a targeted mechanism of action should be considered. Compounds like 5-chloro-7-iodo-8-OH, (±)-menthone, (+)-α-pinene and derivatives of N-butyl-2,2-imino-di-(8-OH), have the diversity to be effective in various pathologies, such as conditions with copper excess (Wilson's, Parkinson's and Huntington's), chronic inflammation, certain cancers and to restrict copper availability in malaria parasite and the larvae of the malaria vector. The conclusions of this study are supported by previous work on similar compounds (Brown, 2010; Manto, 2014; Sun *et al.*, 2014; Bandmann, Weiss and Kaler, 2015; Liu *et al.*, 2016; Blockhuys and Wittung-Stafshede, 2017; Neumann, Gulati and Nolan, 2017; Wiemann *et al.*, 2017).

The properties of the 8-OH derivatives that demonstrated copper homeostasis, antioxidant, antimalarial, anticancer and larvicidal activity were dictated by the position of the functional group on the 8-OH ring and the functional group itself. N-butyl-2,2-imino-di-(8-OH) has two 8-OH rings and showed the widest range of activity across all assays. It demonstrated selective copper (I) chelation, copper reduction and antioxidant activity and it synergistically chelated copper in combination with TMB. It had a synergistic interaction with chloroquine against malaria, therefore derivatives of this compound potentially could be used in combination therapy. As such, combination studies should be conducted with antimalarials such as mefloquine, lumefantrine and DHA. Compounds with a functional group at positions 5 and 7 on the 8-OH ring also demonstrated a broad scope of activity and their actions differed dependent on their functional group. Compounds with single functional groups were less active than those with complex or multiple functional groups. Possible mechanisms of actions of these compounds include selective metal ion chelation/interaction (copper (I)), anti-oxidant/pro-oxidant effects, anticancer effects, inhibition of the malaria parasite through the prevention of haem conversion into inert haemozoin and the inhibition of larvae through the possible restriction of copper. Several 8-OH derivatives demonstrated unfavourable toxicity against *Artemia* and haemolytic properties and it would be useful to further determine the full toxicity profile of these compounds by testing the toxicity of the compounds against other aquatic organisms such as zebra fish (*Danio rerio*), rainbow trout (*Oncorhynchus mykiss*) or mussels (*Mytilus galloprovincialis*) and normal cell lines such as the neuronal LUHMES. Therefore, the metal ion and antioxidant/pro-oxidant properties of 8-OH derivatives warrant further study.

The EOCs demonstrated antioxidant, anticancer, low haemolytic, antimalarial, and larvicidal abilities, with (±)-menthone demonstrating the widest range of activity across all assays used in this study. EOCs with phenolic structures demonstrated a wider range of activity in comparison to those with a linear structure. A possible mechanism of antimalarial action for (±)-menthone is its ability to activate the immune system response (Section 6.2.1; (Nazer, Darvishi and Qolampour, 2018). Due to the potent antioxidant actions, it could be used in conjunction with a standard antimalarial to treat the symptoms and malaria-induced oxidative stress. The inhibition of neuroblastoma cells by (±)-menthone may be due to its moderate copper chelation activity and the anti-angiogenic properties of TMB (Doñate *et al.*, 2008) may be further enhanced when in combination with (±)-menthone (Figure 5.3). Since the larvicidal activity of (±)-menthone in this study was favourable, the effect of this compound on other freshwater aquatic species should be investigated to determine if it specifically inhibits larvae.

(+)-α-Pinene is a polyphenolic terpene which inhibited the malaria parasite *in vitro* and inhibited the formation of β-haematin. Thereby its mechanism of antimalarial action could be through the inhibition of haem degradation to inert haemozoin which causes toxicity within the malaria parasite. Furthermore, the synergistic interaction combination between (+)-α-pinene and chloroquine shows that combinations with other antimalarials that do not have widespread resistance such as lumefantrine or DHA should be studied to determine the potential to be used in the management of a malaria infection. In this study, the isomeric differences between (+)-α-pinene and (+)-β-pinene resulted in (+)-α-pinene having a greater range of activity (Section 6.2.2). The antimalarial activity of (+)-α-pinene was also shown to be strain specific and therefore further studies should be carried out to determine the activity of (+)-α-pinene against other strains of malaria. The antimalarial, antioxidant action, anticancer effects of α-(+)-pinene are promising and further studies are needed to determine its possible mechanism of action.

In this study, (S)-(-)-β-citronellol demonstrated the most potent inhibition of β-haematin formation of the EOCs and had a synergistic interaction when in combination with chloroquine. Due to the widespread resistance of *P. falciparum* parasite to chloroquine, further combination studies with (S)-(-)-β-citronellol should be conducted with other antimalarials like artemisinin derivatives (Sidhu, Verdier-Pinard and Fidock, 2002). Eugenol also demonstrated *in vitro* antimalarial activity that may be due to its possible antioxidant/pro-oxidant effects (Bezerra *et al.*, 2017). Several EOCs were larvicidal with a possible mechanism of action being the inhibition of larval acetylcholinesterase (Section 6.2.5) and if their toxicity against other freshwater aquatic organisms is determined to be favourable, they may prove to be options for malaria vector control. Further studies to determine whether (±)-menthone and (+)-α-

pinene induce or inhibit pathways critical for malaria parasite function should be conducted in order to elucidate their possible mechanisms of antimalarial action.

Both groups of compounds demonstrated an interaction with copper and antioxidant potential which could lead to the management of copper excess diseases and the subsequent oxidative stress. The copper chelation of the 8-OH derivatives could be the root of their antimalarial activity and it would be prudent to determine whether these compounds inhibit important malarial metabolic elements. The antioxidant activity of both groups of compounds would be favourable in the management of oxidative stress whether induced by diseases of copper ion excess or malaria.

7.2. Limitations

On consideration the following limitations of the study were identified and need to be taken into consideration for similar studies in the future.

- This study was limited to determining the antimalarial activity of the twenty-one 8-OH and fifty-five EOCs against the 3D7 strain of *P. falciparum* and did not determine the effect of the compounds against other drug-resistant strains of *P. falciparum* or other strains of malaria such as *P. vivax.*
- 5,7-Dichloro-2-CH_3-8-OH, 5,7-diiodo-8-OH, 5,7-dichloro-8-OH, 5-chloro-7-bromo-8-OH, (-)-citronellal, (S)-(-)-(β)-citronellol, (-)-pulegone and eugenol demonstrated cytotoxicity against the neuroblastoma and the anticancer actions of these compounds against other cancer cell lines were not determined in this study.
- Furthermore, the cytotoxic action against a comparative normal non-cancerous neuronal cell line was not determined for 5,7-dichloro-2-CH_3-8-OH, 5,7-diiodo-8-OH, 5,7-dichloro-8-OH, 5-chloro-7-bromo-8-OH, (-)-citronellal, (S)-(-)-(β)-citronellol, (-)-pulegone and eugenol, and it is not known if the cytotoxicity is selective for cancerous cells or if these compounds are non-selective in their toxicity.
- Copper excess effects other organs other than the brain in the human body such as the liver, kidney, and cornea. In this study the effect of 5,7-diiodo-8-OH, 5-HSO_3-7-iodo-8-OH, 5,7-dichloro-8-OH, 5-chloro-7-iodo-8-OH, 5,7-dibromo-8-OH, N-butyl-2,2-imino-di-(8-OH) and (±)-menthone against copper excess was only determined in the neuroblastoma cell line as an initial starting point.
- Since the 8-OH derivatives are known iron chelators and the EOCs are metal ion reducers, the interaction of 5,7-diiodo-8-OH, 5-HSO_3-7-iodo-8-OH, 5,7-dichloro-8-OH, 5-chloro-7-iodo-8-OH, 5,7-dibromo-8-OH, N-butyl-2,2-imino-di-(8-OH) and (±)-menthone metal ions such as iron and zinc should have been further explored.

- The toxic effects of the fifty-five EOCs against *Artemia* were not determined due to time constraints.
- There has been some promising chemical properties determined with the chelates of 8-OH derivatives (Turnaturi, Oliveri and Vecchio, 2016). The activity and toxicity of copper chelates of 5,7-diiodo-8-OH, 5-HSO_3-7-iodo-8-OH, 5,7-dichloro-8-OH, 5-chloro-7-iodo-8-OH, 5,7-dibromo-8-OH, and N-butyl-2,2-imino-di-(8-OH) was not determined.
- The effect of 2-amino-8-OH, 5,7-dichloro-8-OH, 5-HSO_3-7-iodo-8-OH, 5,7-diiodo-8-OH, (±)-camphorquinone, (+)-α-pinene, eugenol and derivatives of N-butyl-2,2-imino-di-(8-OH) against the gametocyte stages of the malaria parasite was not determined. Inhibition of the sexual stages of the parasite would decrease the malaria transmission.

7.3. Recommendations

Due to the volume of compounds tested and the number of assays undertaken, numerous interesting results were determined which need further elaboration or undertaking.

- Non-toxic derivatives of N-butyl-2,2-imino-di-(8-OH) should be synthesized to determine their copper homeostasis, antimalarial and anticancer activity.
- To have a larger understanding of the effect of 2-amino-8-OH, 5,7-dichloro-8-OH, 5-HSO_3-7-iodo-8-OH, 5,7-diiodo-8-OH, (±)-camphorquinone, (+)-α-pinene, eugenol and derivatives of N-butyl-2,2-imino-di-(8-OH) against malaria and the potential variability against drug-resistant strains, the activity against other strains such as *P. falciparum* GB4 should be investigated.
- In order to determine if the anti-cancer activity of 5,7-dichloro-2-CH_3-8-OH, 5,7-diiodo-8-OH, 5,7-dichloro-8-OH, 5-chloro-7-bromo-8-OH, (-)-citronellal, (S)-(-)-(β)-citronellol, (-)-pulegone and eugenol was selective for neuroblastoma or could be more active/selective against other forms of cancer, the activity of the compounds against other cancerous cell lines from organs known be rich in metal ions such as Hep G2 (liver cancer cell line), HCM-BROD-0051-C64 (kidney cancer cell line) or Toledo (non-Hodgkin's B cell lymphoma) should be determined.
- The cytotoxic action against a comparative non-cancerous neuronal cell line such as LUHMES (mid-brain) should be determined for 5,7-dichloro-2-CH_3-8-OH, 5,7-diiodo-8-OH, 5,7-dichloro-8-OH, 5-chloro-7-bromo-8-OH, (-)-citronellal, (S)-(-)-(β)-citronellol, (-)-pulegone and eugenol.
- Further investigation should be conducted against kidney (OAT1 HEK 293T/17) and liver (THLE-3) cell lines to determine if 5,7-diiodo-8-OH, 5-HSO_3-7-iodo-8-OH, 5,7-dichloro-8-OH, 5-chloro-7-iodo-8-OH, 5,7-dibromo-8-OH, N-butyl-2,2-imino-di-(8-OH) and (±)-

menthone would prevent copper excess in these cells and whether they would be detrimental to the functioning of the organ.

- To determine the antimalarial mechanism of action, studies to evaluate the inhibitory effects of 2-amino-8-OH, 5,7-dichloro-8-OH, 5-HSO_3-7-iodo-8-OH, 5,7-diiodo-8-OH, (±)-camphorquinone, (+)-α-pinene, eugenol and derivatives of N-butyl-2,2-imino-di-(8-OH) on the copper-dependent malarial enzymes and proteins should be undertaken.
- The chelation activity of 5,7-diiodo-8-OH, 5-HSO_3-7-iodo-8-OH, 5,7-dichloro-8-OH, 5-chloro-7-iodo-8-OH, 5,7-dibromo-8-OH, derivatives of N-butyl-2,2-imino-di-(8-OH) and (±)-menthone should be determined against a larger range of metal ions especially ones that are implicated in oxidative reactions.
- In addition, to better understand the full extent of the antioxidant potency of eugenol, (-)-β-pinene, thymol, 5,7-Dicloro-2-CH_3-8-OH, 5,7-diiodo-8-OH, 5,7-dichloro-8-OH 5-chloro-7-iodo-8-OH and 5,7-dimethyl-8-OH further targets in the oxidative pathway should be evaluated using assays such as the ferric reducing antioxidant assay, the hydroxyl radical antioxidant assay, the oxygen radical antioxidant capacity assay and the total antioxidant capacity assay.
- The toxic effects of the fifty-five EOCs against *Artemia* should be investigated to ensure a more complete understanding of the compounds on the viability of a whole organism.
- The activity and toxicity of copper chelates of 5,7-diiodo-8-OH, 5-HSO_3-7-iodo-8-OH, 5,7-dichloro-8-OH, 5-chloro-7-iodo-8-OH, 5,7-dibromo-8-OH, and N-butyl-2,2-imino-di-(8-OH) should be investigated to determine their bioactivity.
- The favourable antimalarial activity of 2-amino-8-OH, 5-chloro-7-iodo-8-OH, 5,7-dichloro-8-OH, 5-HSO_3-7-iodo-8-OH, 5,7-diiodo-8-OH, (±)-camphorquinone, (+)-α-pinene, eugenol and derivatives of N-butyl-2,2-imino-di-(8-OH) warrants further testing against other in other protozoal microorganisms such as *Trypanosoma cruzi, Leishmania major, Acanthamoeba* species or *Naelgleria* species.
- The effect of 2-amino-8-OH, 5,7-dichloro-8-OH, 5-chloro-7-iodo-8-OH, 5-HSO_3-7-iodo-8-OH, 5,7-diiodo-8-OH, (±)-camphorquinone, (+)-α-pinene, eugenol and derivatives of N-butyl-2,2-imino-di-(8-OH) against the gametocyte stages of the *P. falciparum* malaria parasite should be determined.

References

Abou Zeid, C. and Kaler, S. G. (2019) 'Chapter 2 - Normal Human Copper Metabolism', in Weiss, K. H. and Schilsky, M. B. T.-W. D. (eds). Academic Press, pp. 17–22. doi: https://doi.org/10.1016/B978-0-12-811077-5.00002-5.

Acuña-Castillo, C., Morales, B. and Huidobro-Toro, J. P. (2000) 'Zinc and copper modulate differentially the P2X4 receptor', *Journal of Neurochemistry*, 74(4), pp. 1529–1537. doi: 10.1046/j.1471-4159.2000.0741529.x.

Adlard, P. A. *et al.* (2008) 'Rapid Restoration of Cognition in Alzheimer's Transgenic Mice with 8-Hydroxy Quinoline Analogs Is Associated with Decreased Interstitial Abeta', *Neuron*, 59(1), pp. 43–55.

Ahn, G. . *et al.* (2001) 'Essential oil component having inhibition activity of leukotriene production', *KR 2001086473*.

Ajjuri, R. R. and O'Donnell, J. M. (2013) 'Novel Whole-tissue Quantitative Assay of Nitric Oxide Levels in *Drosophila* Neuroinflammatory Response.', *Journal of visualized experiments : JoVE*, (82), pp. 1–10. doi: 10.3791/50892.

Akladios, F. N. *et al.* (2019) 'The Evaluation of Metal Co-ordinating Bis-Thiosemicarbazones as Potential Anti-malarial Agents', *Medicinal Chemistry*, pp. 51–58. doi: http://dx.doi.org/10.2174/1573406414666180525132204.

Aktar, W., Sengupta, D. and Chowdhury, A. (2009) 'Impact of pesticides use in agriculture: their benefits and hazards', *Interdisciplinary toxicology*, 2(1), pp. 1–12.

Ala, A. *et al.* (2007) 'Wilson ' s disease', *Lancet*, 397, pp. 397–408.

Alghobashy, A. A. *et al.* (2018) 'Trace elements and oxidative stress in children with type 1 diabetes mellitus', *Diabetes, metabolic syndrome and obesity: targets and therapy*, 11, p. 85.

Ali, S. M. *et al.* (2005) 'Antimicrobial activities of Eugenol and Cinnamaldehyde against the human gastric pathogen *Helicobacter pylori*', *Annals of Clinical Microbiology and Antimicrobials*, 4(1), p. 20. doi: 10.1186/1476-0711-4-20.

Alvarez, H. M. *et al.* (2010) 'Tetrathiomolybdate Inhibits Copper Trafficking Proteins Through Metal Cluster Formation', *Science*, 327(5963), pp. 331–334. doi: 10.1126/science.1179907.

Alves, E. *et al.* (2015) 'Encapsulation of metalloporphyrins improves their capacity to block the viability of the human malaria parasite *Plasmodium falciparum*', *Nanomedicine: Nanotechnology, Biology and Medicine*, 11(2), pp. 351–358. doi: https://doi.org/10.1016/j.nano.2014.09.018.

Amer, A. and Mehlhorn, H. (2006) 'Repellency effect of forty-one essential oils against *Aedes, Anopheles*, and *Culex* mosquitoes', *Parasitology Research*, 99(4), p. 478.

Andersen, S. O. (2012) 'Cuticular sclerotization and tanning', in *Insect Molecular Biology and Biochemistry*. Elsevier, pp. 167–192.

Angelé-Martínez, C. *et al.* (2017) 'Reactive oxygen species generation by copper (II) oxide nanoparticles determined by DNA damage assays and EPR spectroscopy', *Nanotoxicology*, 11(2), pp. 278–288.

Ansari, M. A. *et al.* (2000) 'Larvicidal and mosquito repellent action of peppermint (*Mentha piperita*) oil', *Bioresource technology*, 71(3), pp. 267–271.

Arakane, Y. *et al.* (2005) 'Laccase 2 is the phenoloxidase gene required for beetle cuticle tanning', *Proceedings of the National Academy of Sciences of the United States of America*, 102(32), pp. 11337 LP – 11342. Available at: http://www.pnas.org/content/102/32/11337.abstract.

Arciello, M. *et al.* (2011) 'Copper depletion increases the mitochondrial-associated SOD1 in neuronal cells', *BioMetals*, 24(2), pp. 269–278. doi: 10.1007/s10534-010-9392-3.

Arnal, N. *et al.* (2010) 'Clinical utility of copper, ceruloplasmin, and metallothionein plasma determinations in human neurodegenerative patients and their first-degree relatives', *Brain Research*, 1319, pp. 118–130.

Asahi, H. *et al.* (2011) 'Differing effects of nonesterified fatty acids and phospholipids on intraerythrocytic growth of *Plasmodium falciparu*m in serum-free medium', *Experimental Parasitology*, 127(3), pp. 708–713.

Asahi, H. (2012) 'Intraerythrocytic *Plasmodium falciparum* growth in serum-free medium with an emphasis on growth-promoting factors', *Malaria Parasites*, 73, p. 90.

Asahi, H. *et al.* (2013) 'Molecular factors that are associated with early developmental arrest of intraerythrocytic *Plasmodium falciparum*', *Canadian Journal of Microbiology*, 59(7), pp. 485–493.

Asahi, H. *et al.* (2014) 'Perturbation of copper homeostasis is instrumental in early developmental arrest of intraerythrocytic *Plasmodium falciparum*', *BioMed Central Microbiology*, 14, p. 167.

Asili, E. *et al.* (2019) 'A Mathematical Model for Amyloid-? Aggregation in the Presence of Metal Ions: A Timescale Analysis for the Progress of Alzheimer Disease', *Bulletin of Mathematical Biology*, 81(6), pp. 1943–1964.

Atzori, L. *et al.* (2011) 'D-penicillamine elastosis perforans serpiginosa: Description of two cases and review of the literature', *Dermatology Online Journal*, 17(4), p. 3.

Bae, G.-S. *et al.* (2011) 'Piperine ameliorates the severity of cerulein-induced acute pancreatitis by inhibiting the activation of mitogen activated protein kinases', *Biochemical and Biophysical Research Communications*, 410(3), pp. 382–388.

Bakkali, F. *et al.* (2008) 'Biological effects of essential oils - A review', *Food and Chemical Toxicology*, 46(2), pp. 446–475.

Bala, E., Singha, S. and Patra, S. (2019) 'Chapter 25 - Polysaccharides from leafy vegetables: chemical, nutritional and medicinal properties', in Hasnain, M. S. and Nayak, A. K. B. T.-N. P. in D. D. and B. A. (eds). Academic Press, pp. 567–588.

Balamurugan, K. and Schaffner, W. (2006) 'Copper homeostasis in eukaryotes: Teetering on a tightrope', *Biochimica et Biophysica Acta - Molecular Cell Research*, 1763(7), pp. 737–746.

Baloch, S. *et al.* (2011) 'Determination of Trace Metals Abnormalities in Patients with Vivax Malaria', *Iranian Journal of Parasitology*, 6(2), pp. 54–59.

Baloch, S. (2012) 'Metabolic Abnormalities in Patients with Malaria and Cerebral Malaria', in *International Conference on Biological and Medical Applications*. Dubai, pp. 1–4.

Balsano, C., Porcu, C. and Sideri, S. (2018) 'Is copper a new target to counteract the progression of chronic diseases?', *Metallomics*, 10(12), pp. 1712–1722.

Banci, L. *et al.* (2007) 'Human Sco1 functional studies and pathological implications of the P174L mutant', *Proceedings of the National Academy of Sciences of the United States of America*, 104(1), pp. 15–20.

Bandmann, O., Weiss, K. H. and Kaler, S. G. (2015) 'Wilson's disease and other neurological copper disorders', *The Lancet Neurology*, 14(1), pp. 103–113.

Baptista-Silva, S. *et al.* (2020) 'The progress of essential oils as potential therapeutic agents: a review', *Journal of Essential Oil Research*, pp. 1–17.

Bareggi, S. R. and Cornelli, U. (2012) 'Clioquinol: Review of its Mechanisms of Action and Clinical Uses in Neurodegenerative Disorders', *Central Nervous System Neuroscience &*

Therapeutics, 18(1), pp. 41–46.

Barnham, K. J. *et al.* (2004) 'Tyrosine gated electron transfer is key to the toxic mechanism of Alzheimer's disease β-amyloid', *The Federation of American Societies for Experimental Biology Journal*, 18(12), pp. 1427–1429.

Barnham, K. J. and Bush, A. I. (2014) 'Biological metals and metal-targeting compounds in major neurodegenerative diseases', *Chemical Society Reviews*, 43(19), pp. 6727–6749. doi: 10.1039/C4CS00138A.

Bartoloni, A. and Zammarchi, L. (2012) 'Clinical Aspects of Uncomplicated and Severe Malaria', *Mediterranean Journal of Hematology and Infectious Diseases*, 4(1), p. e2012026. doi: 10.4084/MJHID.2012.026.

Basco, L. K. *et al.* (1995) '*Plasmodium falciparum* and *Plasmodium vivax:* lactate dehydrogenase activity and its application for in vitro drug susceptibility assay', *Experimental Parasitology*, 80. doi: 10.1006/expr.1995.1032.

Becker, K. *et al.* (2004) 'Oxidative stress in malaria parasite-infected erythrocytes: host–parasite interactions', *International Journal for Parasitology*, 34(2), pp. 163–189. doi: https://doi.org/10.1016/j.ijpara.2003.09.011.

Bedoukian, P. Z. (1986) 'Perfumery and flavoring synthetics'. Allured Publishing Cooperation, IL, USA.

Bell, A. (2005) 'Antimalarial drug synergism and antagonism: Mechanistic and clinical significance', *FEMS Microbiology Letters*, 253(2), pp. 171–184. doi: 10.1016/j.femsle.2005.09.035.

Benelli, G. and Beier, J. C. (2017) 'Current vector control challenges in the fight against malaria', *Acta Tropica*, 174, pp. 91–96. doi: https://doi.org/10.1016/j.actatropica.2017.06.028.

Benvenisti-Zarom, L., Chen, J. and Regan, R. F. (2005) 'The oxidative neurotoxicity of clioquinol', *Neuropharmacology*, 49(5), pp. 687–694.

Berenbaum, M. C. (1978) 'A Method for Testing for Synergy with Any Number of Agents', *The Journal of Infectious Diseases*, 137(2), pp. 122–130. doi: 10.1093/infdis/137.2.122.

Bertinato, J. and L'Abbé, M. R. (2004) 'Maintaining copper homeostasis: Regulation of copper-trafficking proteins in response to copper deficiency or overload', *Journal of Nutritional Biochemistry*, 15(6), pp. 316–322.

Bezerra, D. P. *et al.* (2017) 'The Dual Antioxidant/Prooxidant Effect of Eugenol and Its Action in Cancer Development and Treatment', *Nutrients*, 9(12), p. 1367. doi: 10.3390/nu9121367.

Bhalerao, S. and Clandinin, T. R. (2012) 'Vitamin K2 Takes Charge', *Science*, 336(6086), pp. 1241–1242. doi: 10.1126/science.1223812.

Biamonte, M. A., Wanner, J. and Le Roch, K. G. (2013) 'Recent advances in malaria drug discovery', *Bioorganic and Medicinal Chemistry Letters*, 23(10), pp. 2829–2843.

Bischoff, K. B. *et al.* (1971) 'Methotrexate pharmacokinetics', *Journal of pharmaceutical sciences*, 60(8), pp. 1128–1133.

Biswas, S. (2003) '8-Hydroxyquinoline inhibits the multiplication of *Plasmodium falciparum* in vitro.', *Annals of Tropical Medicine and Parasitology*, 97(5), pp. 527–530. doi: 10.1179/000349803235002425.

Blasco, B., Leroy, D. and Fidock, D. A. (2017) 'Antimalarial drug resistance: linking *Plasmodium falciparum* parasite biology to the clinic', *Nature Medicine*, 23(8), pp. 917–928. doi: 10.1038/nm.4381.

Blincoe, C. (1993) 'Computer Simulation of Normal and Pathological Copper Metabolism in Man', 23(Table I), pp. 49–55.

Blockhuys, S. and Wittung-Stafshede, P. (2017) 'Roles of copper-binding proteins in breast cancer', *International Journal of Molecular Sciences*, 18(4), p. 871.

Bloland, P. B. (2001) 'Drug resistance in malaria', *World Health Organisation*. doi: 10.1007/978-1-4613-1267-3.

Blumberg, L. H. (2015) 'Recommendations for the treatment and prevention of malaria: Update for the 2015 season in South Africa', *South African Medical Journal*, 105(3), pp. 175–178.

Boll, M. C. *et al.* (2008) 'Free copper, ferroxidase and SOD1 activities, lipid peroxidation and NOx content in the CSF. A different marker profile in four neurodegenerative diseases', *Neurochemical Research*, 33(9), pp. 1717–1723.

Boucher, I. W. *et al.* (2006) 'The crystal structure of superoxide dismutase from *Plasmodium falciparum*', *BioMed Central Structural Biology*, 6(20), pp. 1–10.

Božović, M. and Ragno, R. (2017) 'Calamintha nepeta (L.) Savi and its Main Essential Oil Constituent Pulegone: Biological Activities and Chemistry', *Molecules* . doi: 10.3390/molecules22020290.

Braga, Cássio Braga e *et al.* (2015) 'Side Effects of Chloroquine and Primaquine and Symptom Reduction in Malaria Endemic Area (Mâncio Lima, Acre, Brazil)', *Interdisciplinary Perspectives on Infectious Diseases*, 2015, pp. 1–7.

Braidy, N. *et al.* (2019) 'The Precursor to Glutathione (GSH), γ-Glutamylcysteine (GGC), Can Ameliorate Oxidative Damage and Neuroinflammation Induced by Aβ40 Oligomers in Human Astrocytes', *Frontiers in Aging Neuroscience*, p. 177.

Bremner, I. and Beattie, J. H. (1990) 'Metallothionein and the Trace Minerals', *Annual Review of Nutrition*, 10(1), pp. 63–83.

Brewer, G. J. (2002) 'Control of Copper in Wilson's Disease and Diseases of Neovascularization, such as Cancer', in Massaro, E. J. (ed.) *Handbook of Copper Pharmacology and Toxicology*. New Jersey: Humana Press, pp. 443–460.

Brewer, G. J. (2003) 'Copper in medicine', *Current Opinion in Chemical Biology*, 7(2), pp. 207–212.

Brewer, G. J. *et al.* (2009) 'Treatment of Wilson's disease with tetrathiomolybdate: V. control of free copper by tetrathiomolybdate and a comparison with trientine', *Translational Research*, 154(2), pp. 70–77.

Brewer, G. J. (2015) 'The Modern Treatment of Wilson's Disease', *Journal of Gastrointestinal & Digestive System*, 05(04).

Brewer, G. J. (2017) 'Chapter 10 - Copper in Wilson's and Alzheimer's Diseases, Copper-Lowering Therapy in Cancer and Other Diseases, and Copper Deficiency', in Collins Genetic, and Nutritional Aspects of Major and Trace Minerals, J. F. B. T.-M. (ed.). Boston: Academic Press, pp. 115–129.

Brock, R., Hamelers, I. H. L. and Jovin, T. M. (1999) 'Comparison of fixation protocols for adherent cultured cells applied to a GFP fusion protein of the epidermal growth factor receptor', *Cytometry*, 35(4), pp. 353–362.

Brooks, G. F. *et al.* (2013) 'Medical Parasitology', in Brooks, G. F. et al. (eds) *Jawetz, Melnick, & Adelberg's Medical Microbiology*. 27th edn. New York, NY: McGraw-Hill Education. Available at: http://accesspharmacy.mhmedical.com/content.aspx?aid=1114739107.

Brown, D. R. (2010) 'Metalloproteins and neuronal death', *Metallomics*, 2(3), pp. 186–194.

Byrns, M. and Penning, T. (2011) 'Environmental Toxicology: Carcinogens and Heavy Metals', in Hilal-Dandan, R. and Brunton, L. L. (eds) *Goodman and Gilman's Manual of Pharmacology and Therapeutics*. 2nd edn. New York, NY: McGraw-Hill Education. Available at:

http://accesspharmacy.mhmedical.com/content.aspx?aid=1127555628.

Cabantchik, Z. I., Moody-Haupt, S. and Gordeuk, V. R. (1999) 'Iron chelators as anti-infectives; malaria as a paradigm', *FEMS Immunology and Medical Microbiology*, 26, pp. 289–298. doi: 10.1016/S0928-8244(99)00153-4.

Cabrales, P. *et al.* (2011) 'Nitric oxide protection against murine cerebral malaria is associated with improved cerebral microcirculatory physiology', *The Journal of infectious diseases*, 203(10), pp. 1454–1463.

Camarda, G. *et al.* (2019) 'Antimalarial activity of primaquine operates via a two-step biochemical relay', *Nature Communications*, 10(1), p. 3226.

De Cássia Da Silveira E Sá, R., Andrade, L. N. and De Sousa, D. P. (2013) 'A review on anti-inflammatory activity of monoterpenes', *Molecules*, 18(1), pp. 1227–1254.

Ch'Ng, J.-H. *et al.* (2011) 'Drug-induced permeabilization of parasite's digestive vacuole is a key trigger of programmed cell death in *Plasmodium falciparum*', *Cell Death & Disease*, 2(10), pp. e216–e216.

Chadwick, S. S. (1988) 'Ullmann's encyclopedia of industrial chemistry', *Reference Services Review*.

Chami, N. *et al.* (2005) 'Study of anticandidal activity of carvacrol and eugenol in vitro and in vivo', *Oral Microbiology and Immunology*, 20(2), pp. 106–111.

Chang, H. *et al.* (2013) 'Long-term effects of a combination of D-penicillamine and zinc salts in the treatment of Wilson's disease in children', *Experimental and Therapeutic Medicine*, 5(4), pp. 1129–1132.

Chang, M.-C. *et al.* (2015) 'Effects of Camphorquinone on Cytotoxicity, Cell Cycle Regulation and Prostaglandin E2 Production of Dental Pulp Cells: Role of ROS, ATM/Chk2, MEK/ERK and Hemeoxygenase-1', *PloS one*, 10, p. e0143663.

Charalambous, G. (ed.) (1981) *The Quality of Foods and Beverages V1: Chemistry and Technology*. 1st edn. Academic Press.

Chauhan, N. *et al.* (2016) 'Larvicidal potential of essential oils against Musca domestica and Anopheles stephensi', *Parasitology Research*, 115(6), pp. 2223–2231.

Chaulya, C. N., Haldar, P. K. and Mukherjee, A. (2010) 'In vitro free radical scavenging activity of methanol extract of rhizome of Cyperus tegetum roxb. (Cyperaceae)', *International Journal of Current Pharmaceutical Research*, 2(3), pp. 39–43.

Chellan, P., Sadler, P. J. and Land, K. M. (2017) 'Recent developments in drug discovery against the protozoal parasites Cryptosporidium and Toxoplasma', *Bioorganic & Medicinal Chemistry Letters*, 27(7), pp. 1491–1501.

Chen, D. B. *et al.* (2012) 'Penicillamine increases free copper and enhances oxidative stress in the brain of toxic milk mice', *PLoS ONE*, 7(5).

Chen, P., Miah, M. R. and Aschner, M. (2016) 'Metals and Neurodegeneration', *F1000Research*, 5, p. 366.

Chen, W.-H. *et al.* (2007) 'Clioquinol and vitamin B_{12} (cobalamin) synergistically rescue the lead-induced impairments of synaptic plasticity in hippocampal dentate gyrus area of the anesthetized rats in vivo', *Neuroscience*, 147(3), pp. 853–864.

Chen, W. *et al.* (2014) 'Inhibitory Effects of α-Pinene on Hepatoma Carcinoma Cell Proliferation', 15, pp. 3293–3297.

Cherdtrakulkiat, R. *et al.* (2020) 'Discovery of novel halogenated 8-hydroxyquinoline-based anti-MRSA agents: In vitro and QSAR studies', *Drug Development Research*, 81(1), pp. 127–135.

Chhabra, N., Aseri, M. L. and Padmanabhan, D. (2013) 'A review of drug isomerism and its significance', *International journal of applied & basic medical research*, 3(1), pp. 16–18. doi: 10.4103/2229-516X.112233.

Chobot, V. *et al.* (2018) 'Antioxidant properties and the formation of iron coordination complexes of 8-hydroxyquinoline', *International journal of molecular sciences*, 19(12), p. 3917.

Choroba, K. *et al.* (2020) 'In vitro antiproliferative effect of vanadium complexes bearing 8-hydroxyquinoline-based ligands – the substituent effect', *Dalton Transactions*, 49, pp. 6596–6606.

Choveaux, D. L., Przyborski, J. M. and Goldring, J. P. D. (2012) 'A *Plasmodium falciparum* copper-binding membrane protein with copper transport motifs', *Malaria journal*, 11, p. 397.

Coats, J. R. (1990) 'Mechanisms of toxic action and structure-activity relationships for organochlorine and synthetic pyrethroid insecticides', *Environmental health perspectives*, 87, pp. 255–262. doi: 10.1289/ehp.9087255.

Coussens, L. M. and Werb, Z. (2002) 'Inflammation and cancer', *Nature*, 420(6917), pp. 860–867.

Crisponi, G. *et al.* (2010) 'Copper-related diseases: From chemistry to molecular pathology', *Coordination Chemistry Reviews*, 254(7–8), pp. 876–889.

Cui, H. *et al.* (2017) 'Copper transporter 1 in human colorectal cancer cell lines: Effects of endogenous and modified expression on oxaliplatin cytotoxicity', *Journal of Inorganic Biochemistry*, 177, pp. 249–258. doi: https://doi.org/10.1016/j.jinorgbio.2017.04.022.

Culbertson, E. M. *et al.* (2020) 'Changes in mammalian copper homeostasis during microbial infection', *Metallomics*, 12(3), pp. 416–426.

D'Alessandro, S. *et al.* (2013) 'A *Plasmodium falciparum* screening assay for anti-gametocyte drugs based on parasite lactate dehydrogenase detection', *Journal of Antimicrobial Chemotherapy*, 68(9), pp. 2048–2058.

Dave, S. S. and Rahatgaonkar, A. M. (2016) 'Syntheses and anti-microbial evaluation of new quinoline scaffold derived pyrimidine derivatives', *Arabian Journal of Chemistry*, 9, pp. S451–S456.

Dell'Agli, M. *et al.* (2012) 'Anti-plasmodial and insecticidal activities of the essential oils of aromatic plants growing in the Mediterranean area', *Malaria Journal*, 11(1), p. 219.

Deraeve, C. *et al.* (2007) 'Bis-8-hydroxyquinoline ligands as potential anti-Alzheimer agents', *New Journal of Chemistry*, 31(2), pp. 193–195. doi: 10.1039/b616085a.

Desai, V. and Kaler, S. G. (2008) 'Role of copper in human neurological disorders', *The American Journal of Clinical Nutrition*, 88(3), pp. 855S-858S. doi: 10.1093/ajcn/88.3.855S.

Desjardins, R. E. *et al.* (1979) 'Quantitative assessment of antimalarial activity in vitro by a semiautomated microdilution technique', *Antimicrobial Agents and Chemotherapy*, 16(6), pp. 710–718.

Diaz, S. A. *et al.* (2014) '*Plasmodium falciparum* aldolase and the C-terminal cytoplasmic domain of certain apical organellar proteins promote actin polymerization', *Molecular and biochemical parasitology*, 197(1–2), pp. 9–14.

Dienes, H. P. and Schirmacher, P. (2019) 'Chapter 12 - Liver Pathology of Wilson Disease', in Weiss, K. H. and Schilsky, M. B. T.-W. D. (eds) *Wilson Disease: Pathogenesis, Molecular Mechanisms, Diagnosis, Treatment and Monitoring*. Academic Press, pp. 139–144. doi: 10.1016/B978-0-12-811077-5.00012-8.

Ding, W.-Q. *et al.* (2006) 'Clioquinol and docosahexaenoic acid act synergistically to kill tumor cells.', *Molecular cancer therapeutics*, 5(7), pp. 1864–1872.

Ding, W. *et al.* (2005) 'Anticancer Activity of the Antibiotic Clioquinol Anticancer Activity of the Antibiotic Clioquinol', pp. 3389–3395. doi: 10.1158/0008-5472.CAN-04-3577.

Ding, X., Xie, H. and Kang, Y. J. (2011) 'The significance of copper chelators in clinical and experimental application', *Journal of Nutritional Biochemistry*, 22(4), pp. 301–310.

Dittmer, N. T. and Kanost, M. R. (2010) 'Insect multicopper oxidases: diversity, properties, and physiological roles', *Insect biochemistry and molecular biology*, 40(3), pp. 179–188.

DoHRSA (2020) *Malaria Prevention*, *Department of Health: Republic of South Africa*. Available at: http://www.health.gov.za/index.php/malaria-prevention-treatment-advice (Accessed: 14 May 2020).

Doñate, F. *et al.* (2008) 'Identification of biomarkers for the antiangiogenic and antitumour activity of the superoxide dismutase 1 (SOD1) inhibitor tetrathiomolybdate (ATN-224)', *British Journal of Cancer*, 98(4), p. 776—783.

Donnelly, P. S., Xiao, Z. and Wedd, A. G. (2007) 'Copper and Alzheimer's disease', *Current Opinion in Chemical Biology*, 11(2), pp. 128–133.

Ebrahim, A. and Gnanasekaran, N. (2019) 'Oxidative Stress and Diminished Total Antioxidant Capacity in Malaria Patients Correspond to Increased Parasitemia and Severity of the Disease', *Reactive Oxygen Species*, 8(23), pp. 287–296.

Edris, A. E. (2007) 'Pharmaceutical and therapeutic potentials of essential oils and their individual volatile constituents: a review', *Phytotherapy Research*, 21(4), pp. 308–323.

Efferth, T. *et al.* (2007) 'Molecular Target-Guided Tumor Therapy with Natural Products Derived from Traditional Chinese Medicine', *Current Medicinal Chemistry*, pp. 2024–2032.

Egan, T. J. *et al.* (2002) 'Fate of haem iron in the malaria parasite *Plasmodium falciparum*', *The Biochemical Journal*, 365(2), pp. 343–347.

Egan, T. J. (2015) 'Drug-resistant *Plasmodium falciparum*: are recent advances a cause for optimism?', *Future microbiology*, 10(8), pp. 1261–1263.

Elion, G. B., Singer, S. and Hitchings, G. H. (1954) 'MICROBIOLOGICAL EFFECTS OF 6-MERCAPTOPURINE', *Annals of the New York Academy of Sciences*, 60(2), pp. 200–206.

Ellison, S. L. R. and Williams, A. (2000) 'Eurachem/CITAC guide: quantifying uncertainty in analytical measurement', *EURACHEM/CITAC*.

Evans, S. G. and Havlik, I. (1993) '*Plasmodium falciparum*: effects of amantadine, an antiviral, on chloroquine-resistant and -sensitive parasites *in vitro* and its influence on chloroquine activity', *Biochemical Pharmacology*, 45(5), pp. 1168–1170. doi: https://doi.org/10.1016/0006-2952(93)90264-W.

Evans, S. G. and Havlik, I. (1994) '*In vitro* drug interaction between amantadine and classical antimalarial drugs in *Plasmodium falciparum* infections', *Transactions of the Royal Society of Tropical Medicine and Hygiene*, 88(6), pp. 683–686.

Ewing, D. A. *et al.* (2019) 'Uncovering mechanisms behind mosquito seasonality by integrating mathematical models and daily empirical population data: Culex pipiens in the UK', *Parasites & Vectors*, 12(1), p. 74. doi: 10.1186/s13071-019-3321-2.

Falcone, E. *et al.* (2020) 'Acrolein and Copper as Competitive Effectors of α-Synuclein', *Chemistry - A European Journal*, 26(8), pp. 1871–1879. doi: 10.1002/chem.201904885.

Famin, O., Krugliak, M. and Ginsburg, H. (1999) 'Kinetics of inhibition of glutathione-mediated degradation of ferriprotoporphyrin IX by antimalarial drugs', *Biochemical Pharmacology*, 58(1), pp. 59–68. doi: https://doi.org/10.1016/S0006-2952(99)00059-3.

Fatope, M. O., Ibrahim, H. and Takeda, Y. (1993) 'Screening of higher plants reputed as pesticides using the brine shrimp lethality assay', *Pharmaceutical Biology*, 31(4), pp. 250–254.

doi: 10.3109/13880209309082949.

Ferenci, P. (2004) ‘Pathophysiology and clinical features of Wilson disease’, *Metabolic Brain Disease*, 19(3–4), pp. 229–239. doi: 10.1023/B:MEBR.0000043973.10494.85.

Ferenci, P. (2019) ‘Chapter 16 - Chelation Therapy: d-Penicillamine’, in Weiss, K. H. and Schilsky, M. B. T.-W. D. (eds). Academic Press, pp. 183–185. doi: 10.1016/B978-0-12-811077-5.00016-5.

Fernández-Bachiller, M. I. *et al.* (2010) ‘Novel tacrine− 8-hydroxyquinoline hybrids as multifunctional agents for the treatment of Alzheimer’s disease, with neuroprotective, cholinergic, antioxidant, and copper-complexing properties’, *Journal of medicinal chemistry*, 53(13), pp. 4927–4937.

Ferrada, E. *et al.* (2007) ‘Stoichiometry and conditional stability constants of Cu(II) or Zn(II) clioquinol complexes; implications for Alzheimer’s and Huntington’s disease therapy’, *NeuroToxicology*, 28(3), pp. 445–449. doi: 10.1016/j.neuro.2007.02.004.

Di Ferrante, N. *et al.* (1975) ‘Lysyl Oxidase Deficiency in Ehlers–Danlos Syndrome Type V’, *Connective Tissue Research*, 3(1), pp. 49–53. doi: 10.3109/03008207509152341.

Ferrero-Miliani, L. *et al.* (2007) ‘Chronic inflammation: importance of NOD2 and NALP3 in interleukin-1β generation’, *Clinical & Experimental Immunology*, 147(2), pp. 227–235.

Figueiredo, R. T. *et al.* (2007) ‘Characterization of heme as activator of Toll-like receptor 4’, *Journal of Biological Chemistry*, 282(28), pp. 20221–20229.

Filiptsova, O. V *et al.* (2018) ‘The effect of the essential oils of lavender and rosemary on the human short-term memory’, *Alexandria Journal of Medicine*, 54(1), pp. 41–44. doi: 10.1016/j.ajme.2017.05.004.

Finney, L. *et al.* (2009) ‘Copper and angiogenesis: Unravelling a relationship key to cancer progression’, *Clinical and Experimental Pharmacology and Physiology*, 36(1), pp. 88–94. doi: 10.1111/j.1440-1681.2008.04969.x.

Fitch, C. D. *et al.* (1982) ‘Lysis of *Plasmodium falciparum* by ferriprotoporphyrin IX and a chloroquine-ferriprotoporphyrin IX complex.’, *Antimicrobial Agents and Chemotherapy*, 21(5), pp. 819–822.

Fitch, C. D. (2004) ‘Ferriprotoporphyrin IX, phospholipids, and the antimalarial actions of quinoline drugs’, *Life Sciences*, 74(16), pp. 1957–1972.

Fitch, C. D., Kanjananggulpan, P. and Mruk, J. S. (1986) ‘Mode of action of chloroquine and related drugs’, *International Symposium on Malaria*, pp. 235–240.

Flegg, J. A. *et al.* (2011) ‘Standardizing the measurement of parasite clearance in *falciparum* malaria: the parasite clearance estimator’, *Malaria journal*, 10(1), p. 339.

Fong, K. Y. and Wright, D. W. (2013) ‘Hemozoin and antimalarial drug discovery’, *Future Medicinal Chemistry*, 5(12), pp. 1437–1450. doi: 10.4155/fmc.13.113.

La Fontaine, S. and Mercer, J. F. B. (2007) ‘Trafficking of the copper-ATPases, ATP7A and ATP7B: Role in copper homeostasis’, *Archives of Biochemistry and Biophysics*, 463(2), pp. 149–167.

Fraser, R. S. and Creanor, J. (1975) ‘The mechanism of inhibition of ribonucleic acid synthesis by 8-hydroxyquinoline and the antibiotic lomofungin’, *The Biochemical Journal*, 147(3), pp. 401–410. Available at: http://www.ncbi.nlm.nih.gov/pubmed/810137.

Fu, S. *et al.* (2012) ‘Overcoming platinum resistance through the use of a copper-lowering agent’, *Molecular cancer therapeutics*, 11(6), pp. 1221–1225.

Fu, Y., Chang, F.-M. J. and Giedroc, D. P. (2014) ‘Copper transport and trafficking at the host–bacterial pathogen interface’, *Accounts of chemical research*, 47(12), pp. 3605–3613.

Gaetke, L. M., Chow-Johnson, H. S. and Chow, C. K. (2014) 'Copper: toxicological relevance and mechanisms', *Archives of Toxicology*, 88(11), pp. 1929–1938.

Gandhi, R. G. and Elshaboury, R. H. (2020) 'Artemisinin', in Ryan, E. T. et al. (eds) *Hunter's Tropical Medicine and Emerging Infectious Diseases*. 10th edn. London: Elsevier, pp. 1144–1146. doi: 10.1016/B978-0-323-55512-8.00163-0.

Garba, I. H., Ubom, G. a and Ejiogu, N. B. (2006) 'Serum copper concentration in adults with acute, uncomplicated *falciparum* malaria infection.', *Biological trace element research*, 113(2), pp. 125–130. doi: 10.1385/BTER:113:2:125.

Gershon, H., Gershon, M. and Clarke, D. D. (2003) 'Antifungal activity of substituted 8-quinolinol-5-and 7-sulfonic acids: a mechanism of action is suggested based on intramolecular synergism', *Mycopathologia*, 155(4), pp. 213–217.

Ghosh, R. *et al.* (2005) 'Eugenol causes melanoma growth suppression through inhibition of E2F1 transcriptional activity', *Journal of Biological Chemistry*, 280(7), pp. 5812–5819.

Gitau, E. N. *et al.* (2013) 'Plasma and cerebrospinal proteomes from children with cerebral malaria differ from those of children with other encephalopathies', *Journal of Infectious Diseases*, 208(9), pp. 1494–1503. doi: 10.1093/infdis/jit334.

Gordeuk, V. R., Thuma, P. E. and Brittenham, G. M. (1994) 'Iron chelation therapy for malaria.', *Advances in Experimental Medicine and Biology*, 356(1), pp. 371–383.

Goulart, H. R. *et al.* (2004) 'Terpenes arrest parasite development and inhibit biosynthesis of isoprenoids in *Plasmodium falciparum*', *Antimicrobial agents and chemotherapy*, 48(7), pp. 2502–2509.

Govender, P. (2019) *Malaria*, *Department: Health Province of KwaZulu-Natal*. Available at: http://www.kznhealth.gov.za/malariainfo.htm (Accessed: 14 May 2020).

Govindarajan, M. *et al.* (2012) 'Chemical composition and larvicidal activity of essential oil from Mentha spicata (Linn.) against three mosquito species', *Parasitology Research*, 110(5), pp. 2023–2032. doi: 10.1007/s00436-011-2731-7.

Govindarajan, M. *et al.* (2016) 'Larvicidal and repellent potential of Zingiber nimmonii (J. Graham) Dalzell (Zingiberaceae) essential oil: an eco-friendly tool against malaria, dengue, and lymphatic filariasis mosquito vectors?', *Parasitology Research*, 115(5), pp. 1807–1816. doi: 10.1007/s00436-016-4920-x.

Griess, P. (1879) 'Bemerkungen zu der Abhandlung der HH. Weselsky und Benedikt „Ueber einige Azoverbindungen"', *Berichte der deutschen chemischen Gesellschaft*, 12(1), pp. 426–428. doi: 10.1002/cber.187901201117.

Gülçin, İ. (2011) 'Antioxidant activity of eugenol: a structure-activity relationship study.', *Journal of Medicinal Food*, 14(9), pp. 975–85. doi: 10.1089/jmf.2010.0197.

Gülçin, I., Elmastat, M. and Aboul-Enein, H. Y. (2007) 'Determination of Antioxidant and Radical Scavenging Activity of Basil (Ocimum basilicum L. Family Lamiaceae)', *PHYTOTHERAPY RESEARCH*, 21, pp. 354–361. doi: 10.1002/ptr.2069.

Haigh, C. L. *et al.* (2016) 'A 2-Substituted 8-Hydroxyquinoline Stimulates Neural Stem Cell Proliferation by Modulating ROS Signalling', *Cell Biochemistry and Biophysics*, 74(3), pp. 297–306. doi: 10.1007/s12013-016-0747-4.

Ben Haj Yahia, I. *et al.* (2019) 'Comparative evaluation of Tunisian Mentha L. species essential oils: selection of potential antioxidant and antimicrobial agents', *Journal of Essential Oil Research*, 31(3), pp. 184–195. doi: 10.1080/10412905.2018.1550021.

Hajlaoui, H. *et al.* (2008) 'Comparison of chemical composition and antimicrobial activities of *Mentha longifolia* L. ssp.longifolia essential oil from two Tunisian localities (Gabes and Sidi Bouzid)', *Annals of Microbiology*, 58(3), p. 513. doi: 10.1007/BF03175551.

Halliwell, B. (2013) 'The antioxidant paradox: Less paradoxical now?', *British Journal of Clinical Pharmacology*, 75(3), pp. 637–644. doi: 10.1111/j.1365-2125.2012.04272.x.

Halliwell, B. and Gutterridge, J. (1990) 'Role of free radicals and catalytic metal ions in human diseases: An Overview', *Methods in Enzymology*, 186, pp. 1–85.

Hammond, C. R. (2005) 'The Elements', in *CRC Handbook of Chemistry and Physics*, pp. 1–36. doi: 10.1021/ja041017a.

Hamulakova, S. *et al.* (2016) 'Targeting copper(II)-induced oxidative stress and the acetylcholinesterase system in Alzheimer's disease using multifunctional tacrine-coumarin hybrid molecules', *Journal of Inorganic Biochemistry*, 161, pp. 52–62. doi: https://doi.org/10.1016/j.jinorgbio.2016.05.001.

Hamza, I. and Gitlin, J. D. (2002) 'Copper chaperones for cytochrome c oxidase and human disease', *Journal of Bioenergetics and Biomembranes*, 34(5), pp. 381–388. doi: 10.1023/A:1021254104012.

Harris, Z. L., Klomp, L. W. J. and Gitlin, J. D. (1998) 'Aceruloplasminemia: An inherited neurodegenerative disease with impairment of iron homeostasis', *Americal Journal of Clinical Nutrition*, 67, pp. 972S-977S. doi: 10.1196/annals.1306.024.

Hasanein, P., Sharifi, M. and Emamjomeh, A. (2017) 'Recent Studies on the Neuropharmacological Effects of Salvia officinalis L.: A Promising Candidate for Alzheimer's Disease', *Medicinal Chemistry*, 7. doi: 10.4172/2161-0444.1000479.

Havrylyuk, D. *et al.* (2018) 'Structure-activity relationships of anticancer ruthenium(II) complexes with substituted hydroxyquinolines', *European Journal of Medicinal Chemistry*, 156, pp. 790–799.

Hayat, F. *et al.* (2011) 'Antiprotozoal activity of chloroquinoline based chalcones', *European Journal of Medicinal Chemistry*, 46(5), pp. 1897–1905.

Hecht, S. M. (1987) 'DNA strand scission by activated bleomycin group antibiotics', in *Anticarcinogenesis and Radiation Protection*, pp. 437–440.

Hedera, P. (2019) 'Clinical management of Wilson disease', *Annals of translational medicine*, 7(2), pp. S66–S66. doi: 10.21037/atm.2019.03.18.

Hernández-Monjaraz, W. S. *et al.* (2018) 'Influence of iron and copper on the activity of laccases in *Fusarium oxysporum f. sp. lycopersici*', *Brazilian Journal of Microbiology*, pp. 269–275.

Holstein, S. A. and Hohl, R. J. (2003) 'Monoterpene regulation of Ras and Ras-related protein expression', *Journal of Lipid Research*, 44(6), pp. 1209–1215.

Hopkinson, R. J. *et al.* (2013) '5-Carboxy-8-hydroxyquinoline is a broad spectrum 2-oxoglutarate oxygenase inhibitor which causes iron translocation', *Chemical Science*, 4(8), p. 3110. doi: 10.1039/c3sc51122g.

Hou, J. *et al.* (2019) 'α-Pinene Induces Apoptotic Cell Death via Caspase Activation in Human Ovarian Cancer Cells', *Medical science monitor: International Medical Journal of Experimental and Clinical Research*, 25, pp. 6631–6638. doi: 10.12659/MSM.916419.

Houghton, P. *et al.* (2007) 'The sulphorhodamine (SRB) assay and other approaches to testing plant extracts and derived compounds for activities related to reputed anticancer activity', *Methods*, 42(4), pp. 377–387. doi: 10.1016/j.ymeth.2007.01.003.

Houwen, R. H. J. (2019) 'Chapter 19 - Zinc Therapy of Wilson Disease', in Weiss, K. H. and Schilsky, M. B. T.-W. D. (eds). Academic Press, pp. 203–207. doi: https://doi.org/10.1016/B978-0-12-811077-5.00019-0.

Husain, N. and Mahmood, R. (2019) 'Copper(II) generates ROS and RNS, impairs antioxidant system and damages membrane and DNA in human blood cells', *Environmental Science and*

Pollution Research, 26(20), pp. 20654–20668. doi: 10.1007/s11356-019-05345-1.

Indira, S. *et al.* (2019) 'Synthesis, spectral, electrochemical, *in-vitro* antimicrobial and antioxidant activities of bisphenolic mannich base and 8-hydroxyquinoline based mixed ligands and their transition metal complexes', *Journal of Molecular Structure*, 1198, p. 126886. doi: https://doi.org/10.1016/j.molstruc.2019.126886.

Ishida, S. *et al.* (2010) 'Enhancing tumor-specific uptake of the anticancer drug cisplatin with a copper chelator', *Cancer Cell*, 17(6), pp. 574–583.

Jagdale, A. D. *et al.* (2015) 'Citronellol: A potential antioxidant and aldose reductase inhibitor from *Cymbopogon citratus*', *International Journal of Pharmacy and Pharmaceutical Sciences*, 7(3), pp. 203–209.

Jeon, J.-H., Lee, C.-H. and Lee, H.-S. (2009) 'Antimicrobial Activities of 2-Methyl-8-Hydroxyquinoline and Its Derivatives against Human Intestinal Bacteria', *Journal of the Korean Society for Applied Biological Chemistry*, 52(2), pp. 202–205. doi: 10.3839/jksabc.2009.037.

Jiang, H. *et al.* (2011) 'Nitroxoline (8-hydroxy-5-nitroquinoline) is more a potent anti-cancer agent than clioquinol (5-chloro-7-iodo-8-quinoline)', *Cancer Letters*, 312(1), pp. 11–17. doi: 10.1016/j.canlet.2011.06.032.

Joshi, A. *et al.* (2019) 'Uptake of Intact Copper Oxide Nanoparticles Causes Acute Toxicity in Cultured Glial Cells', *Neurochemical Research*, 44(9), pp. 2156–2169. doi: 10.1007/s11064-019-02855-9.

Kakolwa, M. A. *et al.* (2018) 'Efficacy and safety of artemisinin-based combination therapy, and molecular markers for artemisinin and piperaquine resistance in Mainland Tanzania', *Malaria Journal*, 17(1), p. 369. doi: 10.1186/s12936-018-2524-x.

Kalaiyarasi, A. *et al.* (2019) 'Chemosensing, molecular docking and antioxidant studies of 8-aminoquinoline appended acylthiourea derivatives', *Journal of Molecular Structure*, 1185, pp. 450–460. doi: https://doi.org/10.1016/j.molstruc.2019.02.098.

Kalanon, M. and McFadden, G. I. (2010) 'Malaria, *Plasmodium falciparum* and its apicoplast', *Biochemical Society Transactions*, 38(3), pp. 775–782. doi: 10.1042/BST0380775.

Kalemba, D. and Kunicka, A. (2003) 'Antibacterial and antifungal properties of essential oils', *Current Medicinal Chemistry*, 10, pp. 813–829. doi: 10.2174/0929867033457719.

Kardos, J. *et al.* (2018) 'Copper signalling: causes and consequences', *Cell Communication and Signaling*, 16(1), p. 71. doi: 10.1186/s12964-018-0277-3.

Karpińska, G., Mazurek, A. P. and Dobrowolski, J. C. (2011) 'Hydroxyquinolines: Constitutional isomers and tautomers', *Computational and Theoretical Chemistry*, 972(1–3), pp. 48–56.

Katerji, M. *et al.* (2017) 'Chemosensitivity of U251 Cells to the Co-treatment of D-Penicillamine and Copper: Possible Implications on Wilson Disease Patients', *Frontiers in Molecular Neuroscience*, 10, p. 10. doi: 10.3389/fnmol.2017.00010.

Katsuno, K. *et al.* (2015) 'Hit and lead criteria in drug discovery for infectious diseases of the developing world', *Nature Reviews Drug Discovery*, 14, pp. 751–758.

Kaur, K. *et al.* (2009) 'Antimalarials from nature', *Bioorganic & Medicinal Chemistry*, 17(9), pp. 3229–3256. doi: 10.1016/j.bmc.2009.02.050.

Kavishe, R. A., Koenderink, J. B. and Alifrangis, M. (2017) 'Oxidative stress in malaria and artemisinin combination therapy: Pros and Cons', *FEBS Journal*, 284(16), pp. 2579–2591. doi: 10.1111/febs.14097.

Kawata, J. K., Kameda, M. and Miyazawa, M. (2008) 'Cyclooxygenase-2 inhibitory effects of monoterpenoids with a p-methane skeleton', *International Journal of Essential Oil Therapeutics*, 2, pp. 145–148.

Kedzia, B. *et al.* (1998) 'Investigation of essential oils and components with immunostimulating activity', *HERBA POLONICA*, 44(2), pp. 126–135.

Keepers, Y. P. *et al.* (1991) 'Comparisons of the sulphorodamine b protein and tetrazolium (MTT) assays for in vitro chemosensitivity testing.', *European Journal of Cancer*, 27(897), pp. 897–900.

Kenthirapalan, S. *et al.* (2014) 'Copper-transporting ATPase is important for malaria parasite fertility', *Molecular Microbiology*, 91(2), pp. 315–325. doi: 10.1111/mmi.12461.

Kepp, K. P. and Squitti, R. (2019) 'Copper imbalance in Alzheimer's disease: Convergence of the chemistry and the clinic', *Coordination Chemistry Reviews*, 397, pp. 168–187. doi: 10.1016/j.ccr.2019.06.018.

Khan, J., Kaushik, M. and Singh, S. (2019) 'Molecular Mechanisms of Action and Resistance of Antimalarial Drugs BT - Bacterial Adaptation to Co-resistance', in Mandal, S. M. and Paul, D. (eds). Singapore: Springer Singapore, pp. 267–296. doi: 10.1007/978-981-13-8503-2_14.

Khan, R. *et al.* (2020) 'Feasibility of Repurposing Clioquinol for Cancer Therapy', *Recent Patents on Anti-Cancer Drug Discovery*, 15(1), pp. 14–31. doi: 10.2174/1574892815666200227090259.

Khanikor, B. *et al.* (2013) 'Comparative mode of action of some terpene compounds against octopamine receptor and acetyl cholinesterase of mosquito and human system by the help of homology modeling and docking studies', *Journal of Applied Pharmaceutical Science*, 3(2), p. 6.

Kiernan, J. A. (2015) *Histological and histochemical methods : theory and practice*. 5th edn. Bloxham: Scion. Available at: http://search.ebscohost.com/login.aspx?direct=true&scope=site&db=nlebk&db=nlabk&AN=1020727.

Kim, H. *et al.* (1998) 'Crystal structure of fructose-1,6-bisphosphate aldolase from the human malaria parasite Plasmodium falciparum', *Biochemistry*, 37(13), pp. 4388–4396. doi: 10.1021/bi972233h\rbi972233h [pii].

Kiss, R. *et al.* (2016) 'Identification of 8-Hydroxyquinoline Derivatives Active Against Somatic V658F Mutant JAK1-Dependent Cells', *Archiv der Pharmazie - Chemistry in Life Sciences*, 349(12), pp. 925–933. doi: 10.1002/ardp.201600246.

Kodama, H. *et al.* (1988) 'Does CSF copper level in Wilson disease reflect copper accumulation in the brain?', *Pediatric Neurology*, 4(1), pp. 35–37. doi: 10.1016/0887-8994(88)90022-7.

Kodama, H., Fujisawa, C. and Bhadhprasit, W. (2012) 'Inherited copper transport disorders: biochemical mechanisms, diagnosis, and treatment.', *Current Drug Metabolism*, 13(3), pp. 237–50. doi: 10.2174/138920012799320455.

Konagaya, M. *et al.* (2004) 'Clinical analysis of longstanding subacute myelo-optico-neuropathy: sequelae of clioquinol at 32 years after its ban', *Journal of the Neurological Sciences*, 218(1), pp. 85–90. doi: 10.1016/j.jns.2003.11.007.

Kosnett, M. J. (2012) 'Heavy Metal Intoxication & Chelators', in Katzung, B. G., Masters, S. B., and Trevor, A. J. (eds) *Basic & Clinical Pharmacology*. 12th edn. New York, NY: The McGraw-Hill Companies. Available at: http://accesspharmacy.mhmedical.com/content.aspx?aid=55831845.

Kovalevich, J. and Langford, D. (2013) 'Considerations for the Use of SH-SY5Y Neuroblastoma Cells in Neurobiology', in *Methods in Molecular Biology*, pp. 9–21. doi: 10.1007/978-1-62703-640-5_2.

Krężel, A. and Maret, W. (2017) 'The Functions of Metamorphic Metallothioneins in Zinc and Copper Metabolism', *International Journal of Molecular Sciences*, 18(6), p. 1237. doi:

10.3390/ijms18061237.

Krishnaraju, A. V *et al.* (2005) 'Assessment of Bioactivity of Indian Medicinal Plants Using Brine Shrimp (Artemia salina) Lethality Assay', *International Journal of Applied Science and Engineering*, 3(2), pp. 125–134.

Kumar, G. L. and Kiernan, J. (eds) (2010) *Special Stains and H & E Second Edition Education Guide | Special Stains and H & E*. 2nd edn, *Dako*. 2nd edn. Carpinteria: Dako. Available at: http://www.dako.com/08066_special_stains_eduguide.pdf.

Lado, C. *et al.* (2004) 'Antioxidant property of volatile oils determined by the ferric reducing ability', *Zeitschrift fur Naturforschung*, 59(5–6), pp. 354–358.

Ladomersky, E. and Petris, M. J. (2015) 'Copper tolerance and virulence in bacteria', *Metallomics*, 7(6), pp. 957–964.

Lambros, C. and Vanderberg, J. P. (1979) 'Synchronization of *Plasmodium falciparum* erythrocyte stages in culture', *The Journal of Parasitology*, 65(3), pp. 418–420.

Lang, M., Kanost, M. R. and Gorman, M. J. (2012) 'Multicopper Oxidase-3 Is a Laccase Associated with the Peritrophic Matrix of *Anopheles gambiae*', *PLOS ONE*, 7(3), p. e33985. doi: 10.1371/journal.pone.0033985.

Lang, P. A. *et al.* (2007) 'Liver cell death and anemia in Wilson disease involve acid sphingomyelinase and ceramide', *Nature Medicine*, 13(2), p. 164—170. doi: 10.1038/nm1539.

Latorre, M., Troncoso, R. and Uauy, R. (2019) 'Biological Aspects of Copper', in Kerkar, N. and Roberts, E. A. B. T.-C. and T. P. on W. D. (eds) *Clinical and Translational Perspectives on Wilson Disease*. Academic Press, pp. 25–31. doi: 10.1016/B978-0-12-810532-0.00004-5.

Lawson, M. K. *et al.* (2016) 'Chelators in Iron and Copper Toxicity', *Current Pharmacology Reports*, 2(6), pp. 271–280. doi: 10.1007/s40495-016-0068-8.

Leanderson, P. and Tagesson, C. (1996) 'Iron bound to the lipophilic iron chelator, 8-hydroxyquinoline, causes DNA strand breakage in cultured lung cells', *Carcinogenesis*, 17(3), pp. 545–550.

Lee, D. C. and Ahn, Y.-J. (2013) 'Laboratory and simulated field bioassays to evaluate larvicidal activity of *Pinus densiflora* hydrodistillate, its constituents and structurally related compounds against *Aedes albopictus, Aedes aegypti* and Culex pipiens pallens in relation to their inhibi', *Insects*, 4(2), pp. 217–229.

Lee, K.-G. and Shibamoto, T. (2000) 'Antioxidant properties of aroma compounds isolated from soybeans and mung beans', *Journal of Agricultural and Food Chemistry*, 48(9), pp. 4290–4293.

Leung, F. Y. (1998) 'Trace elements that act as antioxidants in parenteral micronutrition', *Journal of Nutritional Biochemistry*, 9(6), pp. 304–307. doi: 10.1016/S0955-2863(98)00018-7.

Lewis, D. F. V *et al.* (1994) 'Safety evaluations of food chemicals by "compact" 1. A study of some acyclic terpenes', *Food and Chemical Toxicology*, 32(11), pp. 1053–1059.

Li, M. *et al.* (2017) 'Targeting reactive nitrogen species suppresses hereditary pancreatic cancer', *Proceedings of the National Academy of Sciences*, 114(30), pp. E6270–E6270. doi: 10.1073/pnas.1711704114.

Li, X. *et al.* (2010) 'Effect of noncompetitive proteasome inhibition on bortezomib resistance', *Journal of the National Cancer Institute*, 102(14), pp. 1069–1082. doi: 10.1093/jnci/djq198.

Liang, Z. D. *et al.* (2009) 'Mechanistic comparison of human high-affinity copper transporter 1-mediated transport between copper ion and cisplatin', *Molecular Pharmacology*, 76(4), pp. 843–853.

Liang, Z. D. *et al.* (2012) 'Mechanistic basis for overcoming platinum resistance using copper

chelating agents', *Molecular Cancer Therapeutics*, 11(11), pp. 2483–2494.

Lin, Z. X., Hoult, J. R. S. and Raman, A. (1999) 'Sulphorhodamine B assay for measuring proliferation of a pigmented melanocyte cell line and its application to the evaluation of crude drugs used in the treatment of vitiligo', *Journal of Ethnopharmacology*, 66(2), pp. 141–150. doi: 10.1016/S0378-8741(98)00199-8.

Lind, S. E., Park, J. S. and Drexler, J. W. (2009) 'Pyrithione and 8-hydroxyquinolines transport lead across erythrocyte membranes', *Translational Research*, 154(3), pp. 153–159. doi: 10.1016/j.trsl.2009.06.002.

Ling, L. *et al.* (2020) 'Genetic ablation of the mitoribosome in the malaria parasite *Plasmodium falciparum* sensitizes it to antimalarials that target mitochondrial functions', *Journal of Biological Chemistry*, (215), pp. 1–26. doi: 10.1074/jbc.ra120.012646.

Lis-Balcnin, M. *et al.* (1999) 'Differences in Bioactivity between the Enantiomers of α-Pinene', *Journal of Essential Oil Research*, 11(3), pp. 393–397. doi: 10.1080/10412905.1999.9701162.

Litwin, T., Dusek, P. and Członkowska, A. (2019) 'Neurological Wilson Disease', in Weiss, K. H. and Schilsky, M. B. T.-W. D. (eds) *Wilson Disease: Pathogenesis, Molecular Mechanisms, Diagnosis, Treatment and Monitoring*. 1st edn. New Haven: Academic Press, pp. 145–157. doi: 10.1016/B978-0-12-811077-5.00013-X.

Liu, L. *et al.* (2016) 'Copper deficiency in the lungs of TNF-α transgenic mice', *Frontiers in Physiology*, 7, p. 234.

Liu, N. (2015) 'Insecticide Resistance in Mosquitoes: Impact, Mechanisms, and Research Directions', *Annual Review of Entomology*, 60(1), pp. 537–559. doi: 10.1146/annurev-ento-010814-020828.

Lopez-Romero, J. C. *et al.* (2015) 'Antibacterial Effects and Mode of Action of Selected Essential Oils Components against *Escherichia coli* and *Staphylococcus aureus*', *Evidence-Based Complementary and Alternative Medicine*. Edited by V. De Feo, 2015, p. 795435. doi: 10.1155/2015/795435.

De Luca, A. *et al.* (2019) 'Copper homeostasis as target of both consolidated and innovative strategies of anti-tumor therapy', *Journal of Trace Elements in Medicine and Biology*, 55, pp. 204–213. doi: 10.1016/j.jtemb.2019.06.008.

Maarman, G. J. (2020) 'Making a case for metallothioneins conferring cardioprotection in pulmonary hypertension', *Medical Hypotheses*, 137, p. 109572. doi: 10.1016/j.mehy.2020.109572.

Mabeza, G. F. *et al.* (1999) 'Iron chelation therapy for malaria: a review', *Pharmacology & Therapeutics*, 81(1), pp. 53–75.

de Macedo, C. S. *et al.* (2002) 'Characterization of the isoprenoid chain of coenzyme Q in *Plasmodium falciparum*', *FEMS Microbiology Letters*, 207(1), pp. 13–20.

MacPherson, I. S. and Murphy, M. E. P. (2007) 'Type-2 copper-containing enzymes', *Cellular and Molecular Life Sciences*, 64(22), pp. 2887–2899. doi: 10.1007/s00018-007-7310-9.

Makler, M. T. *et al.* (1993) 'Parasite lactate dehydrogenase as an assay for *Plasmodium falciparum* drug sensitivity', *American Journal of Tropical Medicine and Hygiene*, 48(6), pp. 739–741.

Di Mambro, V. M. *et al.* (2003) 'Comparison of antioxidant activities of tocopherols alone and in pharmaceutical formulations', *International Journal of Pharmaceutics*, 262(1–2), pp. 93–99.

Manh, H. D. and Tuyet, O. T. (2020) 'Larvicidal and Repellent Activity of *Mentha arvensis L*. Essential Oil against Aedes aegypti', *Insects*, 11(3), p. 198. doi: 10.3390/insects11030198.

Manto, M. (2014) 'Abnormal Copper Homeostasis: Mechanisms and Roles in Neurodegeneration', *Toxics*, 2(2), pp. 327–345. doi: 10.3390/toxics2020327.

Manzl, C. *et al.* (2004) 'Copper-induced formation of reactive oxygen species causes cell death and disruption of calcium homeostasis in trout hepatocytes', *Toxicology*, 196(1), pp. 57–64. doi: 10.1016/j.tox.2003.11.001.

Marotti, M., Piccaglia, R. and Giovanelli, E. (1996) 'Differences in essential oil composition of basil (*Ocimum basilicum L*.) Italian cultivars related to morphological characteristics', *Journal of Agricultural and Food Chemistry*, 44(12), pp. 3926–3929.

Martín Santos, C. *et al.* (2013) 'Novel clioquinol and its analogous platinum complexes: importance, role of the halogen substitution and the hydroxyl group of the ligand.', *Dalton Transactions*, 42(37), pp. 13343–8. doi: 10.1039/c3dt51720a.

Mavondo, G. A. *et al.* (2019) 'Oxidative Stress in Malarial Diseases: *Plasmodium*-Human Host Interactions and Therapeutic Interventions', in Chakraborti, S. et al. (eds) *Oxidative Stress in Microbial Diseases*. Singapore: Springer Singapore, pp. 411–452. doi: 10.1007/978-981-13-8763-0_23.

Mazor, D. *et al.* (2006) 'Antioxidant properties of bucillamine: Possible mode of action', *Biochemical and Biophysical Research Communications*, 349(3), pp. 1171–1175.

McCord, J. M. (2004) 'Iron, Free Radicals, and Oxidative Injury', *The Journal of Nutrition*, 134(11), pp. 3171S-3172S. doi: 10.1093/jn/134.11.3171S.

Medici, V., Rossaro, L. and Sturniolo, G. C. (2007) 'Wilson disease-A practical approach to diagnosis, treatment and follow-up', *Digestive and Liver Disease*, 39(7), pp. 601–609. doi: 10.1016/j.dld.2006.12.095.

Merriam-Webster (2020) *8-Hydroxyquinolines*, *The Merriam-Webster.com Medical Dictionary*. Available at: https://www.merriam-webster.com/medical/8-hydroxyquinoline. (Accessed: 14 January 2020).

Mertens, M. *et al.* (2018) 'Glyphosate, a chelating agent—relevant for ecological risk assessment?', *Environmental Science and Pollution Research*, 25(6), pp. 5298–5317. doi: 10.1007/s11356-017-1080-1.

Meyer, B. *et al.* (1982) 'Brine Shrimp: A Convenient General Bioassay for Active Plant Constituents', *Planta Medica*, 45(05), pp. 31–34. doi: 10.1055/s-2007-971236.

Mezzaroba, L. *et al.* (2019) 'The role of zinc, copper, manganese and iron in neurodegenerative diseases', *NeuroToxicology*, 74, pp. 230–241. doi: 10.1016/j.neuro.2019.07.007.

Millenium Specialty Chemicals (1995) *Product Data Sheet: Citronellol Select*.

Miyake, Z. *et al.* (2020) 'Deferasirox Might be Effective for Microcytic Anemia and Neurological Symptoms Associated with Aceruloplasminemia: A Case Report and Review of the Literature', *Internal Medicine*, pp. 4178–19. doi: 10.2169/internalmedicine.4178-19.

Miyazawa, M. and Yamafuji, C. (2005) 'Inhibition of acetylcholinesterase activity by bicyclic monoterpenoids', *Journal of Agricultural and Food Chemistry*, 53(5), pp. 1765–1768.

Moret, V. *et al.* (2009) 'Discovery of a new family of bis-8-hydroxyquinoline substituted benzylamines with pro-apoptotic activity in cancer cells: Synthesis, structure?activity relationship, and action mechanism studies', *European Journal of Medicinal Chemistry*, 44(2), pp. 558–567. doi: 10.1016/j.ejmech.2008.03.042.

Mosmann, T. (1983) 'Rapid Colorimetric assay for cellular growth and survival: application to proliferation and cytotoxicity assay', *Journal of Immunological Methods*, 65(1–2), pp. 55–63. doi: 10.1016/0022-1759(83)90303-4.

Mot, A. I. and Crouch, P. J. (2017) 'Biometals and Alzheimer's Disease', in White, A. R. et al. (eds) *Biometals in Neurodegenerative Diseases: Mechanisms and Therapeutics*. London: Academic Press, pp. 1–17. doi: 10.1016/B978-0-12-804562-6.00001-4.

Moura, I. C. *et al.* (2001) 'Limonene arrests parasite development and inhibits isoprenylation of proteins in *Plasmodium falciparum*', *Antimicrobial Agents and Chemotherapy*, 45(9), pp. 2553–2558.

MPMP (2020) *Mitochondrial copper transport pathways to cytochrome C oxidase subunits*, *Malaria Parasite Metabolic Pathways*. Available at: http://mpmp.huji.ac.il/maps/Cu_CCO.html (Accessed: 21 May 2020).

Murray, C. K. and J. W. B. (2009) 'Rapid Diagnosis of Malaria', *Interdisciplinary Perspectives on Infectious Diseases*, 2009. doi: 10.1155/2009/415953.

Mustapha, O. (2017) *The effect of terpenes on the life cycle of the malaria parasite*. University of the Witwatersrand. Available at: http://wiredspace.wits.ac.za/bitstream/handle/10539/25775/Obaidiyah Mustapha.pdf?sequence=1&isAllowed=y.

Nagababu, E. *et al.* (2010) 'Assessment of antioxidant activity of eugenol *in vitro* and *in vivo*', *Methods in Molecular Biology*, 610, pp. 165–180. doi: 10.1007/978-1-60327-029-8_10.

Narsaria, N. *et al.* (2012) 'Oxidative stress in children with severe malaria', *Journal of Tropical Pediatrics*, 58(2), pp. 147–150. doi: 10.1093/tropej/fmr043.

Nazer, M. R., Darvishi, M. and Qolampour, A. (2018) 'The Protective Role of Menthone Against Indomethacin-Induced Gastric Ulcers in Rat Model TT -', *GMJ Medicine*, 2(1), pp. 33–37. doi: 10.29088/GMJM.2018.33.

NCSS (2020) 'Linear regression and correlation', in *NCSS Statisitical software*, pp. 1–56. Available at: https://ncss-wpengine.netdna-ssl.com/wp-content/themes/ncss/pdf/Procedures/NCSS/Linear_Regression_and_Correlation.pdf.

NDoH South Africa (2018) 'National guidelines for the prevention of malaria, South Africa, 2018', pp. 1–42.

Neldner, K. H. (1977) 'The halogenated 8-hydroxyquinolines.', *International Journal of Dermatology*, 16(4), pp. 267–73. Available at: http://www.ncbi.nlm.nih.gov/pubmed/140848.

Neumann, W., Gulati, A. and Nolan, E. M. (2017) 'Metal homeostasis in infectious disease: recent advances in bacterial metallophores and the human metal-withholding response', *Current Opinion in Chemical Biology*, 37, pp. 10–18.

Neves Carvalho, A. *et al.* (2017) 'Oxidative stress and antioxidants in neurological diseases: is there still hope?', *Current Drug Targets*, 18(6), pp. 705–718.

Niederau, C. (2018) 'Wilson's Disease', in Mauss, S. et al. (eds) *Hepatology - A Clinical Textbook*. 9th edn. Simon Collins.

Nittis, T. and Gitlin, J. D. (2002) 'The copper-iron connection: Hereditary accruloplasminemia', *Seminars in Hematology*, 39(4), pp. 282–289.

Nizamutdinova, I. T. *et al.* (2016) 'Mast cells and histamine are triggering the NF-κB-mediated reactions of adult and aged perilymphatic mesenteric tissues to acute inflammation', *Aging*, 8(11), pp. 3065–3090. doi: 10.18632/aging.101113.

Nunes, R. R. *et al.* (2019) 'Brazilian malaria molecular targets (BraMMT): Selected receptors for virtual high-throughput screening experiments', *Memorias do Instituto Oswaldo Cruz*, 114(2), pp. 1–10. doi: 10.1590/0074-02760180465.

Oliver, S. V and Brooke, B. D. (2016) 'The Role of Oxidative Stress in the Longevity and Insecticide Resistance Phenotype of the Major Malaria Vectors *Anopheles arabiensis* and *Anopheles funestus*', *PloS one*, 11(3), pp. e0151049–e0151049. doi: 10.1371/journal.pone.0151049.

Oliver, S. V and Brooke, B. D. (2018) 'The effect of commercial herbicide exposure on the life history and insecticide resistance phenotypes of the major malaria vector *Anopheles*

arabiensis (*Diptera: culicidae*)', *Acta Tropica*, 188, pp. 152–160. doi: 10.1016/j.actatropica.2018.08.030.

Oliveri, V. *et al.* (2014) 'Multifunctional 8-Hydroxyquinoline-Appended Cyclodextrins as New Inhibitors of Metal-Induced Protein Aggregation', *Chemistry – A European Journal*, 20(29), pp. 8954–8964. doi: 10.1002/chem.201402690.

Oliveri, V. *et al.* (2017) 'Amino- and chloro-8-hydroxyquinolines and their copper complexes as proteasome inhibitors and antiproliferative agents', *Metallomics*, 9(10), pp. 1439–1446. doi: 10.1039/C7MT00156H.

Olliaro, P. L. *et al.* (2001) 'Possible modes of action of the artemisinin-type compounds', *Trends in Parasitology*, 17(3), pp. 122–126. doi: 10.1016/S1471-4922(00)01838-9.

Omoto, A. *et al.* (2005) 'Copper chelation with tetrathiomolybdate suppresses adjuvant-induced arthritis and inflammation-associated cachexia in rats.', *Arthritis Research & Therapy*, 7(6), pp. R1174-82. doi: 10.1186/ar1801.

Ondrejkovičová, M. *et al.* (2020) 'New mutation of the ceruloplasmin gene in the case of a neurologically asymptomatic patient with microcytic anaemia, obesity and supposed Wilson's disease', *BMC Gastroenterology*, 20(1), pp. 1–6. doi: 10.1186/s12876-020-01237-8.

Osanloo, M. *et al.* (2018) 'Larvicidal activity of essential oil of *Syzygium aromaticum* (Clove) in comparison with its major constituent, eugenol, against *Anopheles stephensi*', *Journal of arthropod-borne diseases*, 12(4), p. 361.

Ozek, T. *et al.* (2010) 'Enantiomeric distribution of some linalool containing essential oils and their biological activities', *Records of Natural Products*, 4(4), pp. 180–192.

Pan, Q. *et al.* (2009) 'Antiangiogenic tetrathiomolybdate protects against Her2/neu-induced breast carcinoma by hypoplastic remodeling of the mammary gland', *Clinical Cancer Research*. 2009/11/24, 15(23), pp. 7441–7446. doi: 10.1158/1078-0432.CCR-09-1361.

Pape, V. F. S. *et al.* (2018) 'Impact of copper and iron binding properties on the anticancer activity of 8-hydroxyquinoline derived Mannich bases', *Dalton Transactions*, 47(47), pp. 17032–17045. doi: 10.1039/c8dt03088j.

Parkinson, C. J. *et al.* (2019) 'Development of pyridyl thiosemicarbazones as highly potent agents for the treatment of malaria after oral administration', *Journal of Antimicrobial Chemotherapy*, 74(10), pp. 2965–2973. doi: 10.1093/jac/dkz290.

Pauli, A. (2001) 'Antimicrobial properties of essential oil constituents', *The International Journal of Aromatherapy*, 11(3), pp. 1–8.

Pavela, R., Kaffkova, K. and KUMŠTA, M. (2014) 'Chemical composition and larvicidal activity of essential oils from different *Mentha L*. and *Pulegium* species against *Culex quinquefasciatus* say (Diptera: Culicidae).', *Plant Protection Science*, 50(1).

Pavela, R., Vrchotová, N. and Tříska, J. (2009) 'Mosquitocidal activities of thyme oils (*Thymus vulgaris L.*) against *Culex quinquefasciatus* (Diptera: Culicidae)', *Parasitology Research*, 105(5), p. 1365.

Peña, M. M., Lee, J. and Thiele, D. J. (1999) 'A delicate balance: homeostatic control of copper uptake and distribution.', *The Journal of Nutrition*, 129(7), pp. 1251–1260.

Peng, Z. *et al.* (2014) 'A multicopper oxidase-related protein is essential for insect viability, longevity and ovary development', *PloS one*, 9(10), pp. e111344–e111344. doi: 10.1371/journal.pone.0111344.

Percário, S. *et al.* (2012) 'Oxidative stress in Malaria', *International Journal of Molecular Sciences*, 13(12), pp. 16346–16372. doi: 10.3390/ijms131216346.

Pérez G, S. *et al.* (2011) 'Anti-inflammatory Activity of Some Essential Oils', *Journal of Essential Oil Research*, 23(5), pp. 38–44. doi: 10.1080/10412905.2011.9700480.

Phan Trong Giao *et al.* (2001) 'Artemisinin for treatment of uncomplicated falciparum malaria: Is there a place for monotherapy?', *American Journal of Tropical Medicine and Hygiene*, 65(6), pp. 690–695.

Phillips, M. A. and Stanley, S. L. (2011) 'Chemotherapy of Protozoal Infections: *Amebiasis, Giardiasis, Trichomoniasis, Trypanosomiasis, Leishmaniasis*, and Other Protozoal Infections', in Brunton, L. L., Chabner, B. A., and Knollmann, B. C. (eds) *Goodman & Gilman's: The Pharmacological Basis of Therapeutics*. 12th edn. New York, NY: McGraw-Hill Education. Available at: http://accesspharmacy.mhmedical.com/content.aspx?aid=1127870390.

Pimentel, D. (1995) 'Amounts of pesticides reaching target pests: environmental impacts and ethics', *Journal of Agricultural and environmental Ethics*, 8(1), pp. 17–29.

Popović-Djordjević, J. *et al.* (2019) '*Calamintha incana*: Essential oil composition and biological activity', *Industrial Crops and Products*, 128, pp. 162–166. doi: 10.1016/j.indcrop.2018.11.003.

Postma, N. *et al.* (1996) 'Oxidative stress in malaria ; implications for prevention and therapy .', *Pharmacy World and Science*, 18(4), pp. 121–129.

Pradeepa, V. *et al.* (2016) 'Potential mode of action of a novel plumbagin as a mosquito repellent against the malarial vector *Anopheles stephensi*, (Culicidae: Diptera)', *Pesticide Biochemistry and Physiology*, 134, pp. 84–93. doi: 10.1016/j.pestbp.2016.04.001.

Pramod, K. and Ansari, S. (2010) 'Eugenol: A Natural Compound with Versatile Pharmacological Actions', *Natural Product Communications*, 5, pp. 1999–2006.

Preechapornkul, P. *et al.* (2010) 'Optimizing the Culture of *Plasmodium*', *The Southeast Asian Journal of Tropical Medicine and Public Health*, 41(4), pp. 761–769.

Prohaska, J. R. *et al.* (1990) 'Effect of dietary copper deficiency on the distribution of dopamine and norepinephrine in mice and rats.', *The Journal of Nutritional Biochemistry*, 1(3), pp. 149–154.

Prohaska, J. R. (2008) 'Role of copper transporters in copper homeostasis 1 – 4', *The American Journal of Clinical Nutrition*, 88, pp. 826–829.

Pubchem (2020a) *PubChem*, *National Library of Medicine*. Available at: https://pubchem.ncbi.nlm.nih.gov/ (Accessed: 12 May 2020).

Pubchem (2020b) *PubChem Database*, *National Center for Biotechnology Information. PubChem Database. Copper 8-hydroxyquinoline, CID=54598431*. Available at: https://pubchem.ncbi.nlm.nih.gov/compound/Copper-8-hydroxyquinoline (Accessed: 10 May 2020).

Radfar, A. *et al.* (2009) 'Synchronous culture of *Plasmodium falciparum* at high parasitemia levels', *Nature Protocols*, 4(11), pp. 1828–1844. doi: 10.1038/nprot.2009.198.

Rahnama, R., Tulaby Dezfuly, Z. and Alishahi, M. (2018) 'Acute Toxicity of Herbicides on the Survival of Adult Shrimp, *Artemia Franciscana*', *Iranian Journal of Toxicology*, 12(6), pp. 45–51. Available at: http://ijt.arakmu.ac.ir/article-1-710-en.html.

Rajkumar, S. and Jebanesan, A. (2007) 'Repellent activity of selected plant essential oils against the malarial fever mosquito *Anopheles stephensi*', *Tropical Biomedicine*, 24(2), pp. 71–75.

Raphael, T. J. and Kuttan*, G. (2003) 'Immunomodulatory Activity of Naturally Occurring Monoterpenes Carvone, Limonene, and Perillic Acid', *Immunopharmacology and Immunotoxicology*, 25(2), pp. 285–294. doi: 10.1081/IPH-120020476.

Rasoloson, D. *et al.* (2004) 'Copper pathways in *Plasmodium falciparum* infected erythrocytes indicate an efflux role for the copper P-ATPase.', *The Biochemical Journal*, 381(Pt 3), pp. 803–11. doi: 10.1042/BJ20040335.

Rehman, K. *et al.* (2014) 'Haemolysis associated with the treatment of malaria with artemisinin derivatives: a systematic review of current evidence', *International Journal of Infectious Diseases*, 29, pp. 268–273. doi: 10.1016/j.ijid.2014.09.007.

Riddiford, L. M. (2009) 'Molting', in Resh, V. H. and Cardé, R. T. B. T.-E. of I. (Second E. (eds) *Encyclopedia of Insects*. 2nd edn. San Diego: Academic Press, pp. 649–654. doi: 10.1016/B978-0-12-374144-8.00179-X.

Říha, M. *et al.* (2013) 'Novel method for rapid copper chelation assessment confirmed low affinity of D-penicillamine for copper in comparison with trientine and 8-hydroxyquinolines', *Journal of Inorganic Biochemistry*, 123, pp. 80–87.

Ringwald, P. *et al.* (1999) '*In Vitro* Culture and Drug Sensitivity Assay of *Plasmodium falciparu*m with Nonserum Substitute and Acute-Phase Sera', *Journal of Clinical Micobiology*, 37(3), pp. 700–705.

Ringwald, P. (2014) 'Status report on artemisinin resistance', *Global Malaria Programme*, (January), pp. 1–7. doi: 10.1017/CBO9781107415324.004.

Ringwald, P. (2016) 'Artemisinin and artemisinin-based combination therapy resistance', *Global Malaria Programme*, (October), pp. 1–8. Available at: http://apps.who.int/iris/bitstream/10665/208820/1/WHO_HTM_GMP_2016.5_eng.pdf?ua=1.

Rivera-Mancía, S. *et al.* (2010) 'The transition metals copper and iron in neurodegenerative diseases', *Chemico-Biological Interactions*, 186(2), pp. 184–199.

Roberts, E. A. (2019) 'Trientine for Wilson Disease: Contemporary Issues', in Weiss, K. H. and Schilsky, M. B. T.-W. D. (eds) *Wilson Disease: Pathogenesis, Molecular Mechanisms, Diagnosis, Treatment and Monitoring*. 1st edn. Academic Press, pp. 187–195. doi: 10.1016/B978-0-12-811077-5.00017-7.

Roberts, E. A. and Schilsky, M. L. (2008) 'Diagnosis and treatment of Wilson disease: An update', *Hepatology*, 47(6), pp. 2089–2111. doi: 10.1002/hep.22261.

Robinett, N. G. *et al.* (2019) 'Exploiting the vulnerable active site of a copper-only superoxide dismutase to disrupt fungal pathogenesis', *Journal of Biological Chemistry* , 294(8), pp. 2700–2713. doi: 10.1074/jbc.RA118.007095.

De Romaña, D. L. *et al.* (2011) 'Risks and benefits of copper in light of new insights of copper homeostasis', *Journal of Trace Elements in Medicine and Biology*, 25(1), pp. 3–13.

Rosenthal, P. J. (2015) 'Antiprotozoal Drugs', in Katzung, B. G. and Trevor, A. J. (eds) *Basic & Clinical Pharmacology*. 13th edn. New York, NY: McGraw-Hill Medical. Available at: http://accesspharmacy.mhmedical.com/content.aspx?aid=1104849660.

Rossiter, D. and Blockman, M. (eds) (2020) *South African Medicines Formulary*. 13th edn. Cape Town: South African Medical Association.

Rupp, C. and Weiss, K. H. (2019) 'Tetrathiomolybdate', in Weiss, K. H. and Schilsky, M. B. T.-W. D. (eds) *Wilson Disease: Pathogenesis, Molecular Mechanisms, Diagnosis, Treatment and Monitoring*. 1st edn. Academic Press, pp. 197–201. doi: 10.1016/B978-0-12-811077-5.00018-9.

Ryan, T. M. *et al.* (2015) 'Stabilization of nontoxic Ajβ-oligomers: Insights into the mechanism of action of hydroxyquinolines in alzheimer's disease', *Journal of Neuroscience*, 35(7), pp. 2871–2884. doi: 10.1523/JNEUROSCI.2912-14.2015.

Ryvolova, M. *et al.* (2011) 'Analytical Methods for Metallothionein Detection', *Current Analytical Chemistry*, 7, pp. 243–261. doi: 10.2174/1573411011107030243.

Saad, A. A. *et al.* (2013) 'Zinc, copper and C-reactive protein in children with severe *Plasmodium falciparum* malaria in an area of unstable malaria transmission in eastern Sudan', *Journal of Tropical Pediatrics*, 59(2), pp. 150–153. doi: 10.1093/tropej/fms056.

Sacchetti, G. *et al.* (2005) 'Comparative evaluation of 11 essential oils of different origin as functional antioxidants, antiradicals and antimicrobials in foods', *Food Chemistry*, 91(4), pp. 621–632.

Sadiq, S. *et al.* (2012) 'Metal toxicity at the synapse: presynaptic, postsynaptic, and long-term effects', *Journal of Toxicology*, 2012, pp. 1–42.

Safadi, M. El *et al.* (2017) 'Cyclen-based chelators for the inhibition of Aβ aggregation: Synthesis, anti-oxidant and aggregation evaluation', *Inorganica Chimica Acta*, 467, pp. 343–350. doi: 10.1016/j.ica.2017.07.060.

Saito, K. *et al.* (2019) 'Potential role of serotonin as a biological reductant associated with copper transportation', *Journal of Inorganic Biochemistry*, 199, p. 110770. doi: 10.1016/j.jinorgbio.2019.110770.

Scheibel, L. W. and Adler, A. (1980) 'Antimalarial Activity of Selected Aromatic Chelators', *Molecular Pharmacology*, 18(2), pp. 320 LP – 325. Available at: http://molpharm.aspetjournals.org/content/18/2/320.abstract.

Scheibel, L. W. and Adler, A. (1981) 'Antimalarial activity of selected aromatic chelators. II. Substituted quinolines and quinoline-N-oxides.', *Molecular Pharmacology*, 20(1), pp. 218–23. Available at: http://www.ncbi.nlm.nih.gov/pubmed/6793844.

Scheibel, L. W. and Adler, A. (1982) 'Antimalarial activity of selected aromatic chelators. III. 8-Hydroxyquinolines (oxines) substituted in positions 5 and 7, and oxines annelated in position 5,6 by an aromatic ring.', *Molecular Pharmacology*, 22(1), pp. 140 LP – 144. Available at: http://molpharm.aspetjournals.org/content/22/1/140.abstract.

Scheibel, L. W. and Stanton, G. G. (1986) 'Antimalarial activity of selected aromatic chelators. IV. Cation uptake by *Plasmodium falciparum* in the presence of oxines and siderochromes.', *Molecular Pharmacology*, 30(4), pp. 364–9. Available at: http://www.ncbi.nlm.nih.gov/pubmed/2945090.

Scheiber, I. F., Mercer, J. F. B. and Dringen, R. (2010) 'Copper accumulation by cultured astrocytes', *Neurochemistry International*, 56(3), pp. 451–460.

Schraufstatter, I. U. *et al.* (1986) 'Oxidant injury of cells. DNA strand-breaks activate polyadenosine diphosphate-ribose polymerase and lead to depletion of nicotinamide adenine dinucleotide.', *The Journal of Clinical Investigation*, 77(4), pp. 1312–1320.

Schuhmacher, A., Reichling, J. and Schnitzler, P. (2003) 'Virucidal effect of peppermint oil on the enveloped viruses herpes simplex virus type 1 and type 2 in vitro', *Phytomedicine*, 10(6), pp. 504–510. doi: 10.1078/094471103322331467.

Schwartz, E. (2012) 'Prophylaxis of malaria', *Mediterranean Journal of Hematology and Infectious Diseases*, 4(1). doi: 10.4084/MJHID.2012.045.

Seatlholo, S. T. (2007) *The Biological Activity of Specific Essential Oil Constituents*. University of the Witwatersrand. Available at: http://wiredspace.wits.ac.za/bitstream/handle/10539/4668/Seatlholo TS 9605308D MSc.pdf?sequence=1&isAllowed=y.

Sebei, K. *et al.* (2015) 'Chemical composition and antibacterial activities of seven Eucalyptus species essential oils leaves', *Biological Research*, 48(1), p. 7. doi: 10.1186/0717-6287-48-7.

Sedaghat, M. M. *et al.* (2011) 'Chemical composition and larvicidal activity of essential oil of *Cupressus arizonica E.L*. Greene against malaria vector *Anopheles stephensi* Liston (Diptera: Culicidae)', *Pharmacognosy Research*, 3(2), pp. 135–139. doi: 10.4103/0974-8490.81962.

Shah, S. *et al.* (2016) '8-Hydroxyquinolines Are Boosting Agents of Copper-Related Toxicity in *Mycobacterium tuberculosis*', *Antimicrobial Agents and Chemotherapy*, 60(10), pp. 5765 LP – 5776. doi: 10.1128/AAC.00325-16.

Shanbhag, V. *et al.* (2019) 'ATP7A delivers copper to the lysyl oxidase family of enzymes and promotes tumorigenesis and metastasis', *Proceedings of the National Academy of Sciences*, 116(14), pp. 6836 LP – 6841. doi: 10.1073/pnas.1817473116.

Sharma, O. P. and Bhat, T. K. (2009) 'DPPH antioxidant assay revisited', *Food Chemistry*, 113(4), pp. 1202–1205.

Sharma, V. and Singh, S. (2019) 'Mechanistic and Structural Insights into Oxidative Stress in Malaria and Anti-malarial Drug Metabolism', in Chakraborti, S. et al. (eds) *Oxidative Stress in Microbial Diseases*. Singapore: Springer Singapore, pp. 531–538. doi: 10.1007/978-981-13-8763-0_28.

Shi, H., Hudson, L. G. and Liu, K. J. (2004) 'Oxidative stress and apoptosis in metal ion-induced carcinogenesis', *Free Radical Biology and Medicine*, 37(5), pp. 582–593.

Shousha, S. and Mitchell, T. R. (1983) 'Orcein staining of leukocytes', *The Histochemical Journal*, 15(6), pp. 563–569. doi: 10.1007/BF01954147.

Sibon, I. *et al.* (2005) 'Lysyl oxidase deficiency: a new cause of human arterial dissection', *Heart*, 91(5), pp. e33–e33. doi: 10.1136/hrt.2004.053074.

Sidhu, A. B. S., Verdier-Pinard, D. and Fidock, D. A. (2002) 'Chloroquine resistance in *Plasmodium falciparum* malaria parasites conferred by pfcrt mutations', *Science*, 298(5591), pp. 210–213. doi: 10.1126/science.1074045.

Sikka, S. C. and Bartolome, A. R. (2018) 'Chapter 36 - Perfumery, Essential Oils, and Household Chemicals Affecting Reproductive and Sexual Health', in Sikka, S. C. and Hellstrom, W. J. G. B. T.-B. I. A. M. R. and S. H. (eds) *Bioenvironmental Issues Affecting Men's Reproductive and Sexual Health*. 1st edn. Boston: Academic Press, pp. 557–569. doi: 10.1016/B978-0-12-801299-4.00036-0.

Da Silva, A. C. R. *et al.* (2012) 'Biological activities of a-pinene and β-pinene enantiomers', *Molecules*, 17(6), pp. 6305–6316.

Singh, R. P., Sharad, S. and Kapur, S. (2004) 'Free radicals and oxidative stress in neurodegenerative diseases: relevance of dietary antioxidants', *Journal Indian Academy of Clinical Medicine*, 5(3), pp. 218–25. doi: 10.1016/j.canlet.2012.05.012.

Singh, S. V. *et al.* (2017) 'A phenolic glycoside from *Flacourtia indica* induces heme mediated oxidative stress in *Plasmodium falciparum* and attenuates malaria pathogenesis in mice', *Phytomedicine*, 30, pp. 1–9. doi: 10.1016/j.phymed.2017.04.010.

Singh, Y. P. *et al.* (2019) 'A review on iron chelators as potential therapeutic agents for the treatment of Alzheimer's and Parkinson's diseases', *Molecular Diversity*, 23(2), pp. 509–526. doi: 10.1007/s11030-018-9878-4.

South African Department of Health (2020) *EML Clinical Guideline*. South Africa.

Srinivasan, R. *et al.* (2008) 'Tolerance of house fly, *Musca domestica L*.(Diptera: Muscidae) to dichlorvos (76% EC) an insecticide used for fly control in the tsunami-hit coastal villages of southern India', *Acta Tropica*, 105(2), pp. 187–190.

Srisung, S. *et al.* (2013) 'Antimicrobial activity of 8-hydroxyquinoline and transition metal complexes', *International Journal of Pharmacology*, 9(2), pp. 170–175. doi: 10.3923/ijp.2013.170.175.

Sritabutra, D. *et al.* (2011) 'Evaluation of herbal essential oil as repellents against *Aedes aegypti (L.) and Anopheles dirus* Peyton & Harrion', *Asian Pacific Journal of Tropical Biomedicine*, 1(1), pp. S124–S128.

Standen, M., Connellan, P. and Leach, D. (2006) 'Natural killer cell activity and lymphocyte activation: Investigating the effects of a selection of essential oils and components in vitro', *Centre for Phytochemistry and Pharmacology Papers*, 16. doi: 10.1016/j.ijat.2006.09.006.

Stefanakis, M. K. *et al.* (2013) 'Antibacterial activity of essential oils from plants of the genus Origanum', *Food Control*, 34(2), pp. 539–546. doi: 10.1016/j.foodcont.2013.05.024.

Stover, K. R., Travis King, S. and Robinson, J. (2012) 'Artemether-lumefantrina: Una Opción para la Malaria', *Annals of Pharmacotherapy*, 46(4), pp. 567–577. doi: 10.1345/aph.1Q539.

Strausak, D. *et al.* (2001) 'Copper in disorders with neurological symptoms: Alzheimer's, Menkes, and Wilson diseases', *Brain Research Bulletin*, 55(2), pp. 175–185.

Strober, W. (1997) 'Trypan blue exclusion test of cell viability', *Current Protocols in Immunology*, Appendix 3, p. A.3B.1-A.3B.2. doi: 10.1002/0471142735.ima03bs21.

Su, V. *et al.* (2008) '*Plasmodium falciparum* growth is arrested by monoterpenes from eucalyptus oil', *Flavour and Fragrance Journal*, 23(5), pp. 315–318.

Su, Y.-W. *et al.* (2010) 'Inhibitory Effects of Citronellol and Geraniol on Nitric Oxide and Prostaglandin E-2 Production in Macrophages', *Planta medica*, 76, pp. 1666–1671. doi: 10.1055/s-0030-1249947.

Sullivan, V. K., Burnett, F. R. and Cousins, R. J. (1998) 'Metallothionein expression is increased in monocytes and erythrocytes of young men during zinc supplementation.', *The Journal of Nutrition*, 128, pp. 707–713. Available at: http://jn.nutrition.org/content/128/4/707.short.

Sun, T.-S. *et al.* (2014) 'Reciprocal functions of Cryptococcus neoformans copper homeostasis machinery during pulmonary infection and meningoencephalitis', *Nature Communications*, 5(1), pp. 1–13.

Sureshkumar, B. *et al.* (2020) 'Quinoline derivatives as possible lead compounds for anti-malarial drugs: Spectroscopic, DFT and MD study', *Arabian Journal of Chemistry*, 13(1), pp. 632–648. doi: 10.1016/j.arabjc.2017.07.006.

Syed, A. A. and Syeda, A. (2007) 'Neocuproine and bathocuproine as new reagents for the spectrophotometric determination of certain proton pump inhibitors', *Bulletin of the Chemical Society of Ethiopia*, 21(3), pp. 315–321.

Takeda, A. *et al.* (2010) 'Impairment of recognition memory and hippocampal long-term potentiation after acute exposure to clioquinol', *Neuroscience*, 171(2), pp. 443–450. doi: 10.1016/j.neuroscience.2010.09.017.

Tamargo, J., Le Heuzey, J.-Y. and Mabo, P. (2015) 'Narrow therapeutic index drugs: a clinical pharmacological consideration to flecainide', *European Journal of Clinical Pharmacology*, 71(5), pp. 549–567. doi: 10.1007/s00228-015-1832-0.

Tapiero, H. and Tew, K. D. (2003) 'Trace elements in human physiology and pathology: Zinc and metallothioneins', *Biomedicine and Pharmacotherapy*, 57(9), pp. 399–411.

Tapiero, H., Townsend, D. M. and Tew, K. D. (2003) 'Trace elements in human physiology and pathology. Copper', *Biomedicine and Pharmacotherapy*, 57(9), pp. 386–398.

Tardito, S. *et al.* (2011) 'Copper Binding Agents Acting as Copper Ionophores Lead to Caspase Inhibition and Paraptotic Cell Death in Human Cancer Cells', *Journal of the American Chemical Society*, 133(16), pp. 6235–6242. doi: 10.1021/ja109413c.

Tardito, S. *et al.* (2012) 'Copper-dependent cytotoxicity of 8-hydroxyquinoline derivatives correlates with their hydrophobicity and does not require caspase activation', *Journal of Medicinal Chemistry*, 55(23), pp. 10448–10459. doi: 10.1021/jm301053a.

Terada, K. and Sugiyama, T. (2002) 'Intracellular Copper Transport and ATP7B, the Wilson's Disease Protein', in Massaro, E. J. (ed.) *Handbook of Copper Pharmacology and Toxicology*. Totowa, NJ: Humana Press, pp. 227–234. doi: 10.1007/978-1-59259-288-3_13.

Tikar, S. N. *et al.* (2011) 'Resistance Status of the Malaria Vector Mosquitoes, *Anopheles stephensi and Anopheles subpictus* Towards Adulticides and Larvicides in Arid and Semi-Arid

Areas of India.', *Journal of Insect Science*, 11(85), p. 85. doi: 10.1673/031.011.8501.

Tilley, L., Loria, P. and Foley, M. (2001) 'Chloroquine and other quinoline antimalarials', in *Antimalarial Chemotherapy*, pp. 87–121.

Tisato, F. *et al.* (2010) 'Copper in diseases and treatments, and copper-based anticancer strategies', *Medicinal Research Reviews*, 30(4), pp. 708–749. doi: 10.1002/med.20174.

Tiwari, M. K. *et al.* (2019) 'Copper ion / H2O2 oxidation of Cu/Zn-Superoxide dismutase: Implications for enzymatic activity and antioxidant action', *Redox Biology*, 26, p. 101262. doi: 10.1016/j.redox.2019.101262.

Toghiani, S. *et al.* (2016) 'Effect of ascorbic acid and menthone on the caspase 3 in the sperm cells of acyclovir treated rats', *Acta Medica Mediterranea*, 32(4), pp. 1213–1219.

Toyoshima, I. (2017) 'Toxic effect of clioquinol on vesicular transport in axons of dorsal root ganglion cells', *Journal of the Neurological Sciences*, 381, p. 502. doi: 10.1016/j.jns.2017.08.3623.

Trager, W. and Jensen, J. B. (1976) 'Human malaria parasites in continuous culture', *Science*, 193(4254), pp. 673–675. Available at: http://www.sciencemag.org/content/193/4254/673.short.

Tsui, M. T. K., Wang, W.-X. and Chu, L. M. (2005) 'Influence of glyphosate and its formulation (Roundup®) on the toxicity and bioavailability of metals to Ceriodaphnia dubia', *Environmental Pollution*, 138(1), pp. 59–68.

Tu, Y.-J., Njus, D. and Schlegel, H. B. (2017) 'A theoretical study of ascorbic acid oxidation and HOO˙/O2˙− radical scavenging', *Organic & Biomolecular Chemistry*, 15(20), pp. 4417–4431. doi: 10.1039/C7OB00791D.

Turnaturi, R., Oliveri, V. and Vecchio, G. (2016) 'Biotin-8-hydroxyquinoline conjugates and their metal complexes: Exploring the chemical properties and the antioxidant activity', *Polyhedron*, 110, pp. 254–260.

UniProtKB (2020a) *UniProtKB - A0A2R3SKL9 (A0A2R3SKL9_PLAFA)*, *UniProt*. Available at: https://www.uniprot.org/uniprot/A0A2R3SKL9 (Accessed: 21 May 2020).

UniProtKB (2020b) *UniProtKB - Q7QBA0 (Q7QBA0_ANOGA)*, *UniProt*. Available at: https://www.uniprot.org/uniprot/Q7QBA0 (Accessed: 21 May 2020).

UniProtKB (2020c) *UniProtKB - Q95034 (Q95034_PLAFA)*, *UnitProt*. Available at: https://www.uniprot.org/uniprot/Q95034 (Accessed: 21 May 2020).

Upadhyay, S., Torres, G. and Lin, X. (2013) 'Laccases involved in 1,8-dihydroxynaphthalene melanin biosynthesis in Aspergillus fumigatus are regulated by developmental factors and copper homeostasis', *Eukaryotic Cell*. 2013/10/11, 12(12), pp. 1641–1652. doi: 10.1128/EC.00217-13.

Di Vaira, M. *et al.* (2004) 'Clioquinol, a drug for Alzheimer's disease specifically interfering with brain metal metabolism: Structural characterization of its zinc(II) and copper(II) complexes', *Inorganic Chemistry*, 43(13), pp. 3795–3797. doi: 10.1021/ic0494051.

Vairo, F. P. e *et al.* (2019) 'A systematic review and evidence-based guideline for diagnosis and treatment of Menkes disease', *Molecular Genetics and Metabolism*, 126(1), pp. 6–13. doi: 10.1016/j.ymgme.2018.12.005.

Valentine, J. S., Doucette, P. A. and Potter, S. (2005) 'Copper-Zinc Superoxide Dismutase and Amyotrophic Lateral Sclerosis', *Annual Review of Biochemistry*, 74, pp. 563–593. doi: 10.1146/annurev.biochem.72.121801.161647.

Valko, M. *et al.* (2006) 'Free radicals, metals and antioxidants in oxidative stress-induced cancer', *Chemico-Biological Interactions*, 160(1), pp. 1–40.

Vanka, R. *et al.* (2020) 'Molecular targets in cerebral malaria for developing novel therapeutic strategies', *Brain Research Bulletin*, 157, pp. 100–107. doi: 10.1016/j.brainresbull.2020.01.020.

Venkateswara, R. *et al.* (2007) 'Toxicity of organophosphates on morphology and locomotor behavior in brine shrimp, Artemia salina', *Archives of Environmental Contamination and Toxicology*, 53(2), pp. 227–232. doi: 10.1007/s00244-006-0226-9.

Venter, N. *et al.* (2017) 'Benchmarking insecticide resistance intensity bioassays for Anopheles malaria vector species against resistance phenotypes of known epidemiological significance', *Parasites & Vectors*, 10(1), p. 198.

Viola-Rhenals, M., Rieber, M. S. M. and Rieber, M. S. M. (2006) 'Suppression of survival in human SKBR3 breast carcinoma in response to metal-chelator complexes is preferential for copper-dithiocarbamate', *Biochemical Pharmacology*, 71(6), pp. 722–734.

Vittorio, O. *et al.* (2016) 'Dextran-Catechin: An anticancer chemically-modified natural compound targeting copper that attenuates neuroblastoma growth', *Oncotarget*, 7(30), pp. 47479–47493. doi: 10.18632/oncotarget.10201.

Waitumbi, J. and Warburg, A. (1998) 'Phlebotomus papatasi saliva inhibits protein phosphatase activity and nitric oxide production by murine macrophages', *Infection and Immunity*, 66(4), pp. 1534–1537. Available at: http://www.ncbi.nlm.nih.gov/pubmed/9529078.

Wang, L. *et al.* (2020) 'Current understanding of metal ions in the pathogenesis of Alzheimer's disease', *Translational Neurodegeneration*, 9(1), pp. 1–13. doi: 10.1186/s40035-020-00189-z.

Wang, T.-H., Hsia, S.-M. and Shieh, T.-M. (2016) 'Lysyl Oxidase and the Tumor Microenvironment', *International Journal of Molecular Sciences*, 18(1), p. 62. doi: 10.3390/ijms18010062.

Wang, T. T. *et al.* (2010) 'In vitro studies on the antioxidant and protective effect of 2-substituted -8-hydroxyquinoline derivatives against H2O2-induced oxidative stress in BMSCs', *Chemical Biology and Drug Design*, 75(2), pp. 214–222. doi: 10.1111/j.1747-0285.2009.00925.x.

Wang, X., Garrick, M. D. and Collins, J. F. (2019) 'Animal Models of Normal and Disturbed Iron and Copper Metabolism', *The Journal of Nutrition*, 149(12), pp. 2085–2100. doi: 10.1093/jn/nxz172.

Wang, Y. *et al.* (2017) 'Clinical efficacy and safety of Chinese herbal medicine for Wilson's disease: A systematic review of 9 randomized controlled trials', *Complementary Therapies in Medicine*, 20(3), pp. 143–154.

Warrell, D. *et al.* (2010) 'Malaria', in *Oxford Textbook of Medicine*. 5th edn. Oxford University Press. doi: 10.1093/med/9780199204854.001.1.

Weiss, K. H. *et al.* (2017) 'Bis-choline tetrathiomolybdate in patients with Wilson's disease: an open-label, multicentre, phase 2 study', *The Lancet Gastroenterology & Hepatology*, 1253(17), pp. 1–8. doi: 10.1016/S2468-1253(17)30293-5.

White, N. J. (2008) 'Qinghaosu (artemisinin): the price of success', *Science*, 320(5874), pp. 330–334.

WHO (2005) 'Guidelines for laboratory and field testing of mosquito larvicides', *World Health Organization*, pp. 1–41. doi: Ref: WHO/CDS/WHOPES/GCDPP/2005.11.

WHO (2016) *World Malaria Report*, *World Health Organization*. doi: 10.4135/9781452276151.n221.

WHO (2019) *World Malaria Report 2019. Geneva.* Available at: https://www.who.int/publications-detail/world-malaria-report-2019.

Wiebe, A. *et al.* (2017) 'Geographical distributions of African malaria vector sibling species and evidence for insecticide resistance', *Malaria Journal*, 16(1), p. 85.

Wiemann, P. *et al.* (2017) 'Aspergillus fumigatus copper export machinery and reactive oxygen intermediate defense counter host copper-mediated oxidative antimicrobial offense', *Cell Reports*, 19(5), pp. 1008–1021.

Wongsrichanalai, C. *et al.* (2002) 'Epidemiology of drug-resistant malaria', *Lancet Infectious Diseases*, 2(4), pp. 209–218. doi: 10.1016/S1473-3099(02)00239-6.

Yamada, K. A. and Sherman, I. W. (1981) 'Purine metabolism by the avian malarial parasite Plasmodium lophurae', *Molecular and Biochemical Parasitology*, 3(4), pp. 253–264. doi: 10.1016/0166-6851(81)90056-6.

Yang, X. *et al.* (2018) 'Novel 8-hydroxyquinoline derivatives targeting β-amyloid aggregation, metal chelation and oxidative stress against Alzheimer's disease', *Bioorganic & Medicinal Chemistry*, 26(12), pp. 3191–3201.

Yassin, M. S. *et al.* (2000) 'Changes in uptake of vitamin B12 and trace metals in brains of mice treated with clioquinol', *Journal of the Neurological Sciences*, 173(1), pp. 40–44. doi: 10.1016/S0022-510X(99)00297-X.

Yeh, I. and Altman, R. B. (2006) 'Drug Targets for Plasmodium falciparum: a post-genomic review/survey.', *Mini Reviews in Medicinal Chemistry*, 6(2), pp. 177–202. doi: 10.2174/138955706775475957.

Yoo, C.-B. *et al.* (2005) 'Eugenol isolated from the essential oil of Eugenia caryophyllata induces a reactive oxygen species-mediated apoptosis in HL-60 human promyelocytic leukemia cells', *Cancer Letters*, 225(1), pp. 41–52. doi: 10.1016/j.canlet.2004.11.018.

Yu, H. *et al.* (2009) 'Clioquinol targets zinc to lysosomes in human cancer cells.', *The Biochemical Journal*, 417(1), pp. 133–139. doi: 10.1042/BJ20081421.

Yu, Z. *et al.* (2010) 'Preparation of polyamine-functionalized copper specific adsorbents for selective adsorption of copper', *Colloids and Surfaces B: Biointerfaces*, 78(2), pp. 222–228. doi: 10.1016/j.colsurfb.2010.03.004.

Yu, Z. *et al.* (2019) 'Blockage of SLC31A1-dependent copper absorption increases pancreatic cancer cell autophagy to resist cell death', *Cell Proliferation*. 2019/01/31, 52(2), pp. e12568–e12568. doi: 10.1111/cpr.12568.

Yunta, C. *et al.* (2019) 'Cross-resistance profiles of malaria mosquito P450s associated with pyrethroid resistance against WHO insecticides', *Pesticide Biochemistry and Physiology*, 161, pp. 61–67.

Zahran, H. E.-D. M. and Abdelgaleil, S. A. M. (2011) 'Insecticidal and developmental inhibitory properties of monoterpenes on Culex pipiens L.(Diptera: Culicidae)', *Journal of Asia-Pacific Entomology*, 14(1), pp. 46–51.

Zatta, P. and Frank, A. (2007) 'Copper deficiency and neurological disorders in man and animals', *Brain Research Reviews*, 54(1), pp. 19–33.

Zhang, J., Krugliak, M. and Ginsburg, H. (1999) 'The fate of ferriprotorphyrin IX in malaria infected erythrocytes in conjunction with the mode of action of antimalarial drugs', *Molecular and Biochemical Parasitology*, 99(1), pp. 129–141. doi: 10.1016/S0166-6851(99)00008-0.

Zhang, P. *et al.* (2013) 'Study of anti-inflammatory activities of α-d-glucosylated eugenol', *Archives of Pharmacal Research*, 36(1), pp. 109–115.

Zheng, H. *et al.* (2005) 'Design, synthesis, and evaluation of novel bifunctional iron-chelators as potential agents for neuroprotection in Alzheimer's, Parkinson's, and other neurodegenerative diseases', *Bioorganic and Medicinal Chemistry*, 13(3), pp. 773–783.

Zhou, C.-F. *et al.* (2013) 'Subacute toxicity of copper and glyphosate and their interaction to

earthworm (Eisenia fetida)', *Environmental Pollution*, 180, pp. 71–77.

Zhou, J. *et al.* (2004) 'Effect of α -pinene on nuclear translocation of NF-κB in THP-1 cells', *Acta Pharmacologica Sinica*, 25(4), pp. 480–484.

Zivanovic, S., Chi, S. and Draughon, A. F. (2005) 'Antimicrobial Activity of Chitosan Films Enriched with Essential Oils', *Journal of Food Science*, 70(1), pp. M45–M51. doi: 10.1111/j.1365-2621.2005.tb09045.x.

Van Zyl, R. L. *et al.* (1993) 'Malaria pigment and extracellular iron: possible target for iron chelating agents', *Biochemical Pharmacology*, 45(7), pp. 1431–1436.

Van Zyl, R. L. *et al.* (2006) 'The biological activities of 20 nature identical essential oil constituents', *Journal of Essential Oil Research*, 18(sup1), pp. 129–133.

Van Zyl, R. L. *et al.* (2008) 'Antiplasmodial activities of some abietane diterpenes from the leaves of five Plectranthus species', *South African Journal of Science*, 104(1–2), pp. 62–64.

Van Zyl, R. L. (2016) 'The malaria season is upon us', *South African Family Practice*, 58(5), pp. 68–72. doi: 10.4102/safp.v58i5.4551.

Appendix A. Ethics

A.1: Clearance certificate

UNIVERSITY OF THE WITWATERSRAND, JOHANNESBURG	HUMAN RESEARCH ETHICS COMMITTEE (MEDICAL)

Office of the Deputy Vice-Chancellor (Research & Post Graduate Affairs)

TO: Professor R van Zyl
School of Therapeutic Sciences
Department of Pharmacy and Pharmacology
Medical School
University

E-mail: Robyn.vanzyl@wits.ac.za

CC: Supervisor: Not applicable <>
and <HREC-Medical ResearchOffice@wits.ac.za>

FROM: Iain Burns
Human Research Ethics Committee (Medical)
Tel: 011 717 1252

E-mail: Iain.Burns@wits.ac.za

DATE: 2019/06/10

REF: *R14/49*

PROTOCOL NO: **M190579** *(This is your ethics application study reference number. Please quote this reference number in all correspondence relating to this study)*

PROJECT TITLE: *The chemotherapeutic properties of novel synthetic and natural compounds*

Please find attached the Clearance Certificate for the above project. I hope it goes well and that an article in a recognized publication comes out of it. This will reflect well on your professional standing and contribute to the Government funding of the University.

MSWorks2000/Iain0007/Clearscan.wps

UNIVERSITY OF THE WITWATERSRAND JOHANNESBURG

R14/49 Professor R van Zyl

HUMAN RESEARCH ETHICS COMMITTEE (MEDICAL)
CLEARANCE CERTIFICATE NO. M190579

NAME: (Principal Investigator)	Professor R van Zyl
DEPARTMENT:	School of Therapeutic Sciences Department of Pharmacy and Pharmacology Medical School University
PROJECT TITLE:	The chemotherapeutic properties of novel synthetic and natural compounds
DATE CONSIDERED:	Ad hoc
DECISION:	Approved unconditionally
CONDITIONS:	Renewal of M140669
SUPERVISOR:	Not applicable
APPROVED BY:	Dr CB Penny, Chairperson, HREC (Medical)
DATE OF APPROVAL:	2019/06/10

This clearance certificate is valid for 5 years from date of approval. Extension may be applied for.

DECLARATION OF INVESTIGATORS

To be completed in duplicate and **ONE COPY** returned to the Research Office Secretary on the 3rd Floor, Phillip Tobias Building, Parktown, University of the Witwatersrand, Johannesburg.

I/we fully understand the conditions under which I am/we are authorized to carry out the above-mentioned research and I/we undertake to ensure compliance with these conditions. Should any departure be contemplated, from the research protocol as approved, I/we undertake to submit details to the Committee. I agree to submit a yearly progress report. When a funder requires annual re-certification, the application date will be one year after the date when the study was initially reviewed. In this case, the study was initially reviewed in **May** and will therefore reports and re-certification will be due early in the month of **May** each year. Unreported changes to the application may invalidate the clearance given by the HREC (Medical).

Principal Investigator Signature

01/07/2019
Date

PLEASE QUOTE THE CLEARANCE CERTIFICATE NUMBER IN ALL ENQUIRIES

R14/49 Dr Robyn L van Zyl

HUMAN RESEARCH ETHICS COMMITTEE (MEDICAL)

CLEARANCE CERTIFICATE NO. M140669

NAME: (Principal Investigator) Dr Robyn L van Zyl

DEPARTMENT: Pharmacy & Pharmacology
Medical School

PROJECT TITLE: The Chemotherapeutic Properties of Novel Synthetic and Natural Compounds (Renewal previously M090532)

DATE CONSIDERED: 29/05/2009 (Initial Approval) 26/06/2014 (Renewal)

DECISION: Approved unconditionally

CONDITIONS:

SUPERVISOR:

APPROVED BY: Professor PE Cleaton-Jones, Chairperson, HREC (Medical)

DATE OF APPROVAL: 26/06/2014

This clearance certificate is valid for 5 years from date of approval. Extension may be applied for.

DECLARATION OF INVESTIGATORS

To be completed in duplicate and **ONE COPY** returned to the Secretary in Room 10004, 10th floor, Senate House, University.

I/we fully understand the conditions under which I am/we are authorized to carry out the above-mentioned research and I/we undertake to ensure compliance with these conditions. Should any departure be contemplated, from the research protocol as approved, I/we undertake to resubmit the application to the Committee. **I agree to submit a yearly progress report**.

Principal Investigator Signature

Date 21-07-2014

PLEASE QUOTE THE PROTOCOL NUMBER IN ALL ENQUIRIES

UNIVERSITY OF THE WITWATERSRAND, JOHANNESBURG

Human Research Ethics Committee (Medical)
50 years 1966-2016

Research Office Secretariat: Faculty of Health Sciences, Phillip Tobias Building, 3rd Floor, Office 301, 29 Princess of Wales Terrace, Parktown, 2193 Tel +27 (0)11-717-1252 /1234/2656/2700
Private Bag 3, Wits 2050, email: zanele.ndlovu@wits.ac.za
Office email: hrec-medical.researchoffice@wits.ac.za
Website: www.wits.ac.za/research/about-our-research/ethics-and-research-integrity/

November 23, 2017

It has come to my attention that there is some misunderstanding concerning waivers for a few postgraduate students in the Pharmacology Division, Department of Pharmacy and Pharmacology. The waivers below are all that is needed for ethics approval for the listed postgraduate students' research.

Each postgraduate received fresh blood weekly needed to grow malaria parasites from healthy volunteers in an approved project (renewal number M140669; original number M 090532) of Prof R L van Zyl.

Waiver details:
W-CJ-130301-3 Prof R L van Zyl, Mr T I Mahlangu – student no 667999.
W-CJ-150330-2 Prof R L van Zyl, Mrs N Jansen van Vuuren – student no 0748672W.
W-CJ-160129-2 Prof R L van Zyl, Ms P Thabana – student no 609529.
W-CJ-161129-1 Ms F Kathrada – student no 0602240N, Prof R L van Zyl.

UNIVERSITY OF THE WITWATERSRAND
PROF PE CLEATON-JONES
HREC (MEDICAL)
2017 -11- 23
JOHANNESBURG

Professor Peter Cleaton-Jones
Chair

Copies: HREC (Medical) Secretariat: Zanele Ndlovu, Rhulani Mkanzi, Lebo Moeng.

A.2: Human cell lines, blood, and plasma

Human Research Ethics Committee (Medical)

Research Office Secretariat: Senate House Room SH 10005, 10th floor. Tel +27 (0)11-717-1252
Medical School Secretariat: Medical School Room 10M07, 10th Floor. Tel +27 (0)11-717-2700
Private Bag 3, Wits 2050, www.wits.ac.za. Fax +27 (0)11-717-1265

Ref: W-CJ-131030-1 30/10/2013

TO WHOM IT MAY CONCERN:

Waiver: This certifies that the following research does not require clearance from the Human Research Ethics Committee (Medical).

Investigator: Prof R van Zyl.

Project title: The chemotherapeutic properties of novel synthetics and natural compounds.

Reason: This is a laboratory study in which human blood and plasma for the in vitro maintenance of *Plasmodium falciparum* for experimental purposes such as drug sensitivity and toxicity studies. There are no human participants.

UNIVERSITY OF THE WITWATERSRAND
PROF PE CLEATON - JONES
HREC (MEDICAL)
2013 -10- 30
JOHANNESBURG

Professor Peter Cleaton-Jones

Chair: Human Research Ethics Committee (Medical)

Copy - HREC(Medical) Secretariat : Anisa Keshav, Zanele Ndlovu.

Human Research Ethics Committee (Medical)

Research Office Secretariat: Senate House Room SH10005, 10th floor. Tel +27 (0)11-717-1252
Medical School Secretariat: Tobias Health Sciences Building, 2nd floor Tel +27 (0)11-717-2700
Private Bag 3, Wits 2050, www.wits.ac.za. Fax +27 (0)11-717-1265

Ref: W-CJ-150330-2 30/03/2015

TO WHOM IT MAY CONCERN:

Waiver: This certifies that the following research does not require clearance from the Human Research Ethics Committee (Medical).

Investigator: **Prof R L van Zyl, Mrs N Jansen van Vuuren (student no. 0748672W).**

Project title: **The chemotherapeutic properties of novel metal chelating agents and essential oils.**

Reason: This is a laboratory study using commercial cell lines – Graham, SH-SY5Y, K562, MCF-7, Caco2 and T-29. There are no human participants

UNIVERSITY OF THE WITWATERSRAND
PROF PE CLEATON-JONES
2015 -03- 30
JOHANNESBURG

Professor Peter Cleaton-Jones

Chair: Human Research Ethics Committee (Medical)

Copy – HREC (Medical) Secretariat: Zanele Ndlovu, Langutani Masingi.

A.3: Artemia

UNIVERSITY OF THE WITWATERSRAND JOHANNESBURG

ANIMAL RESEARCH ETHICS COMMITTEE (AREC)

Registration number: AREC0101210-002

Solomon Mahlangu House
10th Floor, Room 10004
Jorissen Street
Braamfontein, Johannesburg

7 November 2017

To whom it may concern,

Re: Waiver from Animal Ethics Screening Committee of the University of the Witwatersrand

This letter serves to confirm that Associate Professor Robyn van Zyl (Department of Pharmacy and Pharmacology, School of Therapeutic Sciences, University of the Witwatersrand) does not require full animal ethics clearance for her studies which use *Artemia* (Brine shrimp) as a toxicological model to evaluate known or novel synthetic and natural compounds.

Reasons: *Artemia* eggs and *naupili* are used in the study. No animals or animal products are used in the study.

Conditions: All approved biosafety and biosecurity SOPs should be adhered to.

Should you require any further information, do not hesitate to contact me.

Yours sincerely,

Kennedy Erlwanger

(Chairman: Animal Research Ethics Committee, University of the Witwatersrand)

Reference: R van Zyl Waiver (Artemia) 07-11-2017-O

Assoc Prof Kennedy H. Erlwanger
School of Physiology
Faculty of Health Sciences, University of the Witwatersrand
7 York Road, Parktown, 2193
SOUTH AFRICA
Tel: +27 (0)11 717 3454
Email: Kennedy.Erlwanger@wits.ac.za

A.4: Larvae

UNIVERSITY OF THE WITWATERSRAND JOHANNESBURG

ANIMAL RESEARCH ETHICS COMMITTEE (AREC)

Registration number: AREC0101210-002

Solomon Mahlangu House
10th Floor, Room 10004
Jorissen Street
Braamfontein, Johannesburg

7 November 2017

To whom it may concern,

Re: Waiver from Animal Ethics Screening Committee of the University of the Witwatersrand

This letter serves to confirm that Associate Professor Robyn van Zyl (Department of Pharmacy and Pharmacology, School of Therapeutic Sciences, University of the Witwatersrand) does not require full animal ethics clearance for her studies which use *Anopheles* mosquito species to evaluate known or novel synthetic and natural compounds as potential insecticides against *Anopheles* species.

Reasons: Mosquito eggs and larva are used in the study. No animals or animal products are used in the study.

Conditions: All approved biosafety and biosecurity SOPs should be adhered to.

Should you require any further information, do not hesitate to contact me.

Yours sincerely,

Kennedy Erlwanger

(Chairman: Animal Research Ethics Committee, University of the Witwatersrand)

Reference: R van Zyl –Anopheles Waiver 07-11-2017-O

Assoc Prof Kennedy H. Erlwanger
School of Physiology
Faculty of Health Sciences, University of the Witwatersrand
7 York Road, Parktown, 2193
SOUTH AFRICA
Tel: +27 (0)11 717 2454
Email: Kennedy.Erlwanger@wits.ac.za

UNIVERSITY OF THE WITWATERSRAND JOHANNESBURG

ANIMAL RESEARCH ETHICS COMMITTEE (AREC)

Registration number: AREC0101210-002

Solomon Mahlangu House
10th Floor, Room 10004
Jorissen Street
Braamfontein, Johannesburg

24 November 2017

To whom it may concern,

Re: Professor R van Zyl Waiver (for MSc students) from Animal Research Ethics Committee of the University of the Witwatersrand

This letter serves to confirm that Associate Professor Robyn van Zyl (Department of Pharmacy and Pharmacology, School of Therapeutic Sciences, University of the Witwatersrand) does not require full animal ethics clearance for her studies undertaken by the students detailed below. She has previously been granted a waiver for the studies as detailed in the documents referenced *R van Zyl (Artemia) 07-11-2017-O and R van Zyl-Anopheles waiver 07-11-2017-O*. The students and studies covered by the waiver letters:

1. Ms Fatima Kathrada [0602240N]: The effect of 7-chloroquinoline derivatives on the life cycle of the malaria parasite.

2. Mr Sahil Lala [358351]: The effect of quinolone heterocyclic derivatives on the malaria parasite and Anopheles vector.

3. Ms Teboho Malimabe [152675]: The effect of novel quinoxaline derivatives on the life cycle of malaria parasite and vector.

4. Ms Natasha Jansen van Vuuren [071867W]: The effect of novel compounds on copper homeostasis in *Plasmodium falciparum* and neuroblastoma cells.

5. Mr Thulani Mahlangu [667999]: The chemotherapeutic properties of novel quinazolines and bis-hydrazones compounds.

6. Ms Puleng Thabana [609529: The effect of novel oxo-1, 6 dihydropyrimidine and 2-(quinolone-8-yloyxy) acetohydrazone derivatives on the life cycle of the malaria parasite.

7. Ms W Ramashia [572354]: Transcription analysis of an immune factor in a main Africa malaria vector *Anopheles funestus*.

Conditions: All previously requisite biosafety and biosecurity SOPs should be adhered to.

Should you require any further information, do not hesitate to contact me.

Yours sincerely,

Kennedy Erlwanger

(Chairman: Animal Research Ethics Committee, University of the Witwatersrand)

Reference: R van Zyl –Anopheles & Artemia PGrad students Waiver 07-11-2017-O

Assoc Prof Kennedy H. Erlwanger
School of Physiology
Faculty of Health Sciences, University of the Witwatersrand
7 York Road, Parktown, 2193
SOUTH AFRICA
Tel: +27 (0)11 717 2454
Email: Kennedy.Erlwanger@wits.ac.za

A.5: Biosafety

UNIVERSITY OF THE WITWATERSRAND, JOHANNESBURG

Research Office

INSTITUTIONAL BIOSAFETY COMMITTEE (IBC)
(R 14/16)

CLEARANCE CERTIFICATE **PROTOCOL NUMBER: 20190404**

BRIEF DESCRIPTION OF APPLICATION:

Chemotherapeutic properties of novel synthetic and natural compounds

APPLICANT: Prof RL van Zyl et al

SUPERVISOR: Pharmacy and Pharmacology

SCHOOL/DEPARTMENT : School of Therapeutic Sciences

DATE CONSIDERED: 24 February 2020

EXPIRY DATE: 24 February 2025

DECISION OF COMMITTEE: Approved unconditionally
Renewal 20090503 Dr R van Zyl

1. This clearance certificate expires on 24 February 2025 and may be renewed on application
2. An annual report must be provided on the anniversary date of this certificate, for as long as the project continues
3. Notification of any proposed modifications must be submitted on the attached form
4. Unreported changes to the application may invalidate the clearance given by the IBC

DATE: 13 March 2020

CHAIRPERSON: _____
(Professor J Larkin)

DECLARATION OF APPLICANT:

To be completed in duplicate and **one copy** returned to the Research Office, Phillip Tobias Building, Room 301, 3rd Floor, 29 Princess of Wales Terrace, Parktown, Faculty of Health Sciences, University.

1. I have read, understood and accepted the approval conditions above
2. I agree to submit a yearly progress report to the Committee and to submit an interim report on the form provided, in the event of any significant unforeseen event, *e.g.* suspension of a drug trial, temporary closure or relocation of my laboratory, etc
3. I note that the University Safety Officer, or his/her representative, may at any reasonable time inspect my laboratory or trial site to ensure compliance with current Health and Safety legislation. I undertake to offer my full co-operation in any such inspection.
4. I have read, understood and will comply with the *recommended standard operating procedures for the handling of biohazardous materials* posted at http://web.wits.ac.za/Academic/Research/Biosafety.htm
5. I declare (delete as appropriate) that:
    a. I have all the approvals required by statute or regulation and by the funding agencies supporting this work, or
    b. that I will not begin work until such approvals are obtained

Signed: _____ **Date:** _____

PLEASE QUOTE THE PROTOCOL NUMBER IN ALL ENQUIRIES

Appendix B. Methods

The following method was attempted in the course of this project however the results not included due to the assay not working or producing repeatable results.

B.1: The tritiated hypoxanthine-incorporation assay

The malaria parasite requires purines and pyrimidines for the synthesis of nucleic acids. The parasite is able to synthesize its own pyrimidines; however it cannot synthesize purines (Yamada and Sherman, 1981). It has been proven that the parasite utilizes the purines of the host red blood cells, mainly salvaging the purine, hypoxanthine. Hypoxanthine utilization is a measure of parasitic metabolism and decreased utilization would indicate the inhibition of parasite viability (Yamada and Sherman, 1981). Therefore, the tritiated hypoxanthine incorporation assay measures the inhibition of hypoxanthine incorporation into the parasitic DNA by a test/control compound using radio-labelled ^{3}H-hypoxanthine (Desjardins *et al.*, 1979; Van Zyl *et al.*, 2008).

The parasite suspension was adjusted to 0.5% parasitaemia and 1% haematocrit in fresh red blood cells and hypoxanthine negative culture media, screened at 200 µM for test compounds (25 µL) and incubated for 24 hours. Test compounds showing activity greater than 60% were plated with serial dilutions at a starting concentration of 200 µM (Figure B.1). The candle jar method was used to ensure an ideal environment for parasitic homeostasis (Trager and Jensen, 1976). Quinine and chloroquine were the positive controls and a 1% haematocrit parasite free solution was the negative control. Labelled ^{3}H-hypoxanthine (25 µL) was added to the plate and further incubated for 24 hours. The ^{3}H-DNA was harvested on glass fibre filter paper using a semi-automated cell harvester.

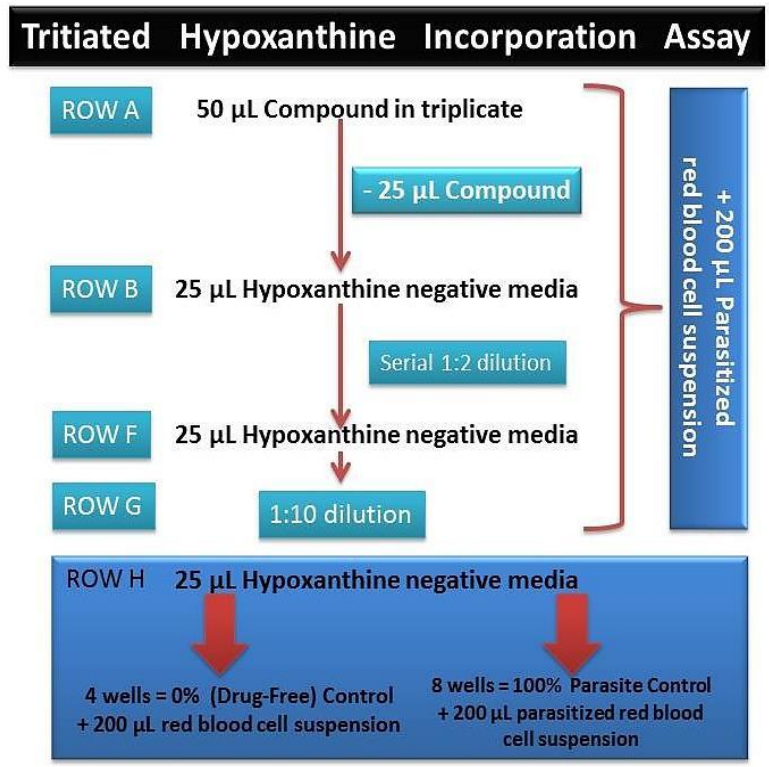

Figure B.1: A flow diagram of the organisation of the experimental plate for the tritiated hypoxanthine incorporation assay.

The effect on percentage parasitaemia by compounds as determined by the ^{3}H-hypoxanthine incorporation of *P. falciparum*.

The plate containing test/control drugs and parasitized suspension was placed in a candle-jar and incubated at 37°C for 24 hours in a micro-aerobic environment, containing sterile ddH_2O (Trager and Jensen, 1976). Subsequently, 10 µL ^{3}H-hypoxanthine (5mCi; Amersham Life Science, UK) diluted in 2.7 mL hypoxanthine-negative experimental culture media per plate, was plated into all wells and incubated in the candle jar for a further 24 hours at 37°C. The parasite DNA was isolated using a Titertek® cell harvester onto GFB-filter mats. The filter mats were dried overnight and beta scintillation fluid (6 mL; Perkin-Elmer) added to each sample bag. The incorporated ^{3}H-hypoxanthine was counted on a Wallac™ beta scintillation counter and the results were expressed as counts per minute (CPM). The percentage parasite growth was calculated using Equation 19.

$$\% \text{ Parasite growth} = \frac{CPM_{TC} - CPM_{\text{Mean RBC control}}}{CPM_{\text{mean parasite control}} - CPM_{\text{Mean RBC control}}}$$

Equation 19: The percentage parasite growth in response to incubation to test compounds

Where CPM = counts per minute, TC = Test compound, RBC = red blood cell

Appendix C. Results

C.1: Metal complexation

Table C.1: The metal complexation effects of EOCs

EOCS	% Copper (I) complexation	% Copper (II) complexation	EOCS	Copper (I) complexation	% Copper (II) complexation
***Cis*-nerolidol**	4.92 ± 0.85	1.64 ± 0.50	**(-)-β-Pinene**	18.86 ± 2.52	13.56 ± 2.45
***Trans*-nerolidol**	11.84 ± 2.90	8.28 ± 1.42	**(+)-β-Pinene**	17.08 ± 2.56	10.83 ± 2.43
***Trans*-geraniol**	10.64 ± 2.68	9.30 ± 1.11	**(-)-Fenchone**	12.38 ± 2.36	20.22 ± 3.60
***Cis*-geraniol**	11.21 ± 2.36	9.96 ± 1.22	**(+)-Fenchone**	9.50 ± 2.82	29.77 ± 1.20
Geranyl acetate	13.84 ± 3.18	24.76 ± 7.69	**(+)-Borneol**	9.09 ± 5.36	10.22 ± 1.92
Farnesol	12.20 ± 1.94	31.62 ± 0.25	**(-)-Borneol**	9.86 ± 2.66	6.60 ± 1.71
(±)-Linalool	11.30 ± 3.04	24.79 ± 5.15	**(-)-Bornyl acetate**	15.40 ± 2.10	6.60 ± 7.06
(-)-Linalool	12.71 ± 3.19	15.33 ± 0.61	**(±)-Camphor**	12.17 ± 2.24	6.76 ± 4.81
Linalyl acetate	9.31 ± 2.92	18.52 ± 2.86	**(1R)-(+)-Camphor**	14.76 ± 2.21	6.06 ± 4.84
(-)-Citronellal	12.89 ± 4.50	27.79 ± 1.87	**(-)-Camphor**	11.14 ± 2.38	6.96 ± 5.05
(-)-Menthone	11.17 ± 2.64	39.41 ± 7.48	**(1R)-(-)-Camphorquinone**	8.86 ± 1.13	6.06 ± 2.70
(±)-Menthol	8.65 ± 2.32	8.67 ± 1.20	**(±)-Camphorquinone**	7.67 ± 2.27	8.73 ± 1.54
Carvacrol	10.12 ± 2.70	7.37 ± 1.82	**(1S)-(+)-Camphorquinone**	15.72 ± 5.92	6.50 ± 1.34
(+)-Carvone	11.86 ± 0.85	30.79 ± 3.02	**(-)-Caryophyllene oxide**	4.21 ± 2.20	7.61 ± 1.95
(-)-Carvone	10.14 ± 1.18	27.17 ± 3.90	**(+)-*Trans*-caryophyllene**	14.32 ± 6.54	6.26 ± 1.21
(-)-Pulegone	9.72 ± 0.84	41.71 ± 8.62	**(-)-α-Thujone**	12.03 ± 3.64	9.43 ± 1.70
(+)-Pulegone	8.83 ± 1.26	21.00 ± 3.63	**(±)-α-b-Thujone**	5.43 ± 2.17	9.83 ± 2.09
(R)-(+)-Limonene	11.90 ± 2.87	12.96 ± 2.72	**Artemisia ketone**	18.58 ± 3.33	13.23 ± 2.67
(S)-(-)-Limonene	11.90 ± 2.56	3.83 ± 1.02	**α-Humulene**	16.38 ± 3.83	1.15 ± 0.03
(+)-Terpinen-4-ol	12.24 ± 2.42	8.45 ± 2.10	**Ocimene**	12.21 ± 3.32	6.72 ± 0.80
(-)-Terpinen-4-ol	17.78 ± 2.41	26.20 ± 3.92	**(±)-Lavandulol acetate**	16.76 ± 3.67	4.73 ± 1.72
1,8-Cineole	13.45 ± 3.04	24.68 ± 4.83	**Myrcene**	0.39 ± 0.14	5.08 ± 1.50
1,4-Cineole	11.61 ± 1.95	4.72 ± 0.72	**ρ-Cymene**	9.39 ± 2.07	21.80 ± 3.60
α-Bisabolol	8.49 ± 2.60	3.59 ± 0.28			

C.2: Copper chelation

IC_{50} values for Copper (I) Chelation and Copper (II) Chelation:

Copper (I) Chelation: (-)-menthone 42.71 ± 1.81; (-)-β-pinene 9.04 ± 2.28; (+)-β-pinene 11.28 ± 2.23; α-humulene 13.41 ± 4.59.

Copper (II) Chelation: (+)-carvone 12.03 ± 1.13; (-)-pulegone 10.87 ± 0.09; (+)-pulegone 48.97 ± 7.30; (-)-terpinen-4-ol 40.46 ± 3.27; eucalyptol (1,8-cineole) 49.75 ± 2.95; ρ-cymene 46.05 ± 7.71; (-)-fenchone 29.24 ± 3.04; (+)-fenchone 42.22 ± 3.07.

C.3: Copper reduction

Table C.2: The Trolox™ equivalent antioxidant capacity (TEAC), as determined by the copper reduction assay.

Compounds	TEAC at 200 µM	Compounds	TEAC at 200 µM
5-Nitro-8-OH	14.94 ± 2.50	**O-phenanthroline monohydrate**	4.77 ± 1.03
5-HSO_3-8-OH	12.63 ± 0.40	**Bathophenanthroline disulfonic acid**	4.25 ± 0.85
N-butyl-2,2-imino-di-(8-OH)	10.68 ± 0.37	**Cupral**	3.99 ± 0.88
5-Carboxy-8-OH	10.54 ± 1.68	**BHT**	3.94 ± 1.00
8-Chloro-2-OH	10.39 ± 2.34	**5,7-Dibromo-8-OH**	3.87 ± 0.78
8-Fluoro-4-OH	8.54 ± 1.61	**Tetrathiomolybdate**	3.83 ± 0.76
5,7-Dichloro-2-CH_3-8-OH	6.79 ± 1.11	**TET**	3.80 ± 0.82
4-OH	6.52 ± 0.90	**Methotrexate**	3.79 ± 0.83
5-Chloro-8-OH	6.14 ± 1.60	**Antimycin A**	3.65 ± 0.71
5,7-Diiodo-8-OH	5.82 ± 0.49	**5-Chloro-7-bromo-8-OH**	3.41 ± 1.03
Cupferron	5.36 ±0.95	**Dihydroartemisinin**	3.40 ± 0.72
5,7-Dichloro-8-OH	5.08 ± 0.67	**5-Chloro-7-iodo-8-OH**	2.88 ± 0.48
5-HSO_3-7-iodo-8-OH	4.91 ± 0.76	**D-Penicillamine**	2.75 ± 0.56

Table C.3: The Trolox™ equivalent antioxidant capacity (TEAC), as determined by the copper reduction assay**.**

Essential Oils	TEAC at 200 µM	Essential Oils	TEAC at 200 µM	Essential Oils	TEAC at 200 µM
Linalyl acetate	8.88 ± 1.68	***Cis*-nerolidol**	5.36 ±0.95	**Artemisia ketone**	2.84 ± 0.31
(-)-Fenchone	8.51 ± 0.72	**(-)-Carvone**	2.75 ± 0.56	**(+)-β-Pinene**	2.84 ± 0.10
(-)-β-Pinene	8.25 ± 0.53	**(+)-Borneol**	4.77 ± 1.03	**(±)-Lavandulol acetate**	2.81 ± 0.21
(-)-Menthone	7.97 ± 1.75	***Trans*-geraniol**	4.25 ± 0.85	**(1S)-(+)-Camphorquinone**	2.77 ± 0.28
ρ-Cymene	7.84 ± 1.92	**(-)-Pulegone**	3.99 ± 0.88	**(+)-Fenchone**	2.73 ± 0.52
Geranyl acetate	7.39 ± 1.13	**(-)-Borneol**	3.94 ± 1.00	**Myrcene**	2.64 ± 0.17
(±)-Linalool	7.16 ± 1.52	**(-)-Terpinen-4-ol**	3.83 ± 0.76	**(+)-Pulegone**	2.54 ± 0.36
(-)-Citronellal	7.16 ± 1.54	**(S)-(-)-β-Citronellol**	3.80 ± 0.82	**(1R)-(+)-Camphor**	2.52 ± 0.25
(1R)-(-)-Camphorquinone	6.75 ± 0.35	***Trans*-nerolidol**	3.79 ± 0.83	**(±)-Camphorquinone**	2.39 ± 0.55
1,4-Cineole	6.78 ± 1.11	**(-)-α-Pinene**	3.65 ± 0.71	**(-)-α-Thujone**	2.34 ± 0.43
(±)-Menthol	6.74 ± 1.37	**(-)-Bornyl acetate**	3.40 ± 0.72	**(+)-Terpinen-4-ol**	2.30 ± 0.20
(+)-α-Pinene	6.63 ± 0.90	**(+)-*Trans*-caryophyllene**	3.22 ± 0.23	**(-)-Camphor**	2.30 ± 0.57
(±)-α-β-Thujone	6.45 ± 1.31	**Ocimene**	3.04 ± 0.16	**(S)-(-)-Limonene**	2.29 ± 0.20
1,8-Cineole	5.97 ± 0.88	**(-)-Linalool**	2.97 ± 0.36	**(±)-Camphor**	2.28 ± 0.32
α-Bisabolol	5.62 ± 0.40	**α-Humulene**	2.92 ± 0.47	**(-)-Caryophyllene oxide**	2.07 ± 0.49

C.4: Antimalarial investigations

Table C.4: The percentage inhibition of ferriprotoporphyrin biomineralization inhibited by EOCs.

EOCs	% inhibition of ferriprotoporphyrin biomineralization at 200 µM	EOCs	% inhibition of ferriprotoporphyrin biomineralization at 200 µM
***Trans*-nerolidol**	30.44 ± 4.23	**(±)-Camphor**	14.45 ± 2.02
ρ-Cymene	26.78 ± 2.14	**(-)-α-Pinene**	13.70 ± 1.52
(-)-Caryophyllene oxide	26.15 ± 1.29	**(-)-Carvone**	13.53 ± 0.37
(+)-β-Pinene	24.43 ± 2.65	**1,8-Cineole**	12.57 ± 1.22
Linalyl acetate	21.74 ± 2.70	**(+)-Fenchone**	11.50 ± 1.28
(-)-Menthone	19.81 ± 2.38	**Farnesol**	8.33 ± 0.92
Geranyl acetate	17.59 ± 0.80	**(R)-(+)-Limonene**	8.07 ± 0.78
Eugenol	22.91 ± 1.15	**(+)-Carvone**	7.19 ± 0.94
1,4-Cineole	23.91 ± 1.98	**Thymol**	7.18 ± 0.41
α-Bisabolol	22.35 ± 2.12	**(±)-Linalool**	6.79 ± 0.42
(+)-Borneol	21.94 ± 1.48	**(1R)-(-)-Camphorquinone**	4.60 ± 0.65
(-)-Bornyl acetate	21.47 ± 1.17	**(-)-Fenchone**	1.25 ± 0.21
ρ-Cymene	26.78 ± 2.14	**(±)-Camphorquinone**	≤ 0.01
(-)-Caryophyllene oxide	26.15 ± 1.29	**(1S)-(+)-Camphorquinone**	≤ 0.01
(+)-β-Pinene	24.43 ± 2.65	**α-Humulene**	≤ 0.01
(-)-β-Pinene	17.89 ± 1.17		

C.5: Effect on RBCs and neuroblastoma cells

Table C.5: The percentage cellular viability of the neuroblastoma cell line, as determined by the MTT and SRB assays

EOCs	MTT viability assay	SRB viability assay
	% Cellular viability	
***Cis*-nerolidol**	84.18 ± 9.04	81.80 ± 1.47
***Trans*-nerolidol**	85.77 ± 9.04	84.94 ± 1.05
***Trans*-geraniol**	102.05 ± 21.67	102.22 ± 0.31
***Cis*-geraniol**	85.42 ± 12.64	104.88 ± 0.68
Citral	64.47 ± 2.14	88.52 ± 5.66
Farnesol	4.77 ± 0.91	96.05 ± 7.24
(-)-Linalool	62.13 ± 0.73	122.83 ± 3.33
(+)-Pulegone	59.67 ± 1.73	127.86 ± 7.40
(R)-(+)-Limonene	74.78 ± 19.61	122.83 ± 2.90
(S)-(-)-Limonene	83.56 ± 22.19	127.86 ± 5.38
(-)-Terpinen-4-ol	48.03 ± 13.12	91.59 ± 8.56
1,4 Cineole	61.78 ± 1.86	102.63 ± 4.34
α-Bisabolol	74.01 ± 14.50	67.90 ± 3.56
ρ-Cymene	80.39 ± 24.77	61.06 ± 6.91
(-)-Caryophyllene oxide	80.11 ± 1.50	Not determined
(+)-*Trans*-caryophyllene	51.45 ± 5.74	Not determined
(-)-α-Thujone	75.86 ± 3.69	Not determined
(±)-α-b-Thujone	70.34 ± 6.80	Not determined
α-Humulene	75.75 ± 0.60	121.92 ± 6.13
Ocimene	93.86 ± 6.06	Not determined
(±)-Lavandulol acetate	85.32 ± 4.56	128.14 ± 0.91
Myrcene	82.26 ± 14.63	127.21 ± 6.77
AA	82.6 ± 8.3 Significant difference [No (P = 0.06)] IC_{50} value: 10.0 ± 2.0	95.8 ± 5.4 Significant difference [No (P = 0.10)]

Table C.6: The percentage cellular viability of the neuroblastoma cell line, as determined by the MTT and SRB assays

EOCs	MTT viability assay	SRB viability assay	EOCs	MTT viability assay	SRB viability assay
Copper (I)	2.1 ± 0.8	73.9 ± 9.6	**Carvacrol**	70.84 ± 4.97)	68.67 ± 3.45
Copper (II)	2.5 ± 0.7	65.1 ± 1.8	**2-Mercapto-thiazoline**	71.39 ± 9.61	78.90 ± 6.62
Camptothecin	8.80 ± 1.70	40.70 ± 3.80	**Artemisia ketone**	71.86 ± 10.46	73.33 ± 8.22
(-)-α-Pinene	12.16 ± 1.48	100	**(+)-Fenchone**	73.93 ± 23.20	68.05 ± 6.55
(1S)-(+)-Camphorquinone	12.46 ± 4.47	66.32 ± 0.74	**(-)-Bornyl acetate**	73.97 ± 1.99	66.71 ± 2.47
Geranyl acetate	13.42 ± 1.14	100	**(-)-Fenchone**	74.82 ± 17.21	≥ 100
Eugenol	20.63 ± 1.20	89.65 ± 7.20	**(-)-β-Pinene**	75.39 ± 4.69	86.66 ± 3.13
(+)-α-Pinene	21.31 ± 2.52	73.72 ± 4.77	**(±)-Camphor**	75.76 ± 17.05	87.92 ± 7.53
(±)-Linalool	34.36 ± 0.98	89.93 ± 0.26	**(-)-Camphor**	76.74 ± 7.43	≥ 100
Linalyl acetate	35.29 ± 6.00	92.07 ± 8.06	**(+)-β-Pinene**	78.52 ± 5.61	88.31 ± 8.75
(+)-Terpinen-4-ol	37.96 ± 2.47	102.99 ± 5.68	**Thymol**	80.38 ± 17.06	89.93 ± 4.55
(-)-Citronellal	39.69 ± 3.42	66.02 ± 6.53	**(+)-Borneol**	81.74 ± 4.24	93.90 ± 4.33
(-)-Pulegone	49.45 ± 5.85	68.21± 9.09	**(±)-Menthone**	82.93 ± 0.17	69.36 ± 0.56
(-)-Menthone	5.51 ± 0.87	93.18 ± 9.05	**(-)-Borneol**	83.65 ± 2.36	56.30 ± 2.27
(S)-(-)-(β)-Citronellol	52.24 ± 2.48	106.81 ± 8.03	**(-)-Carvone**	85.97 ± 9.11	93.75 ± 2.95
(±)-Menthol	55.03 ± 6.11	100	**Methotrexate**	86.31 ± 3.52	100
1,8-Cineole	55.65 ± 4.88	82.34 ± 3.73	**(+)-Carvone**	95.04 ± 5.83)	95.03 ± 5.09
(1R)-(+)-Camphor	58.16 ± 4.58	68.54 ± 4.47	**(±)-Camphor-quinone**	97.39 ± 6.95	78.28 ± 2.66
(1R)-(-)-Camphorquinone	58.3 ± 5.8	41.9 ± 2.1			

Table C.7: The effect of incubation with copper and EOCs on percentage cellular viability.

EOCs	% Protective effect against Copper (I)	Effect on Cellular Viability	% Protective effect against Copper (II)	Effect on Cellular Viability
***Cis*-nerolidol**	-72.57 ± 0.58	↓	-76.94 ± 1.51	↓
***Trans*-nerolidol**	-60.95 ± 1.69	↓	-82.47 ± 2.79	↓
***Trans*-geraniol**	-91.39 ± 2.58	↓	-86.07 ± 1.91	↓
***Cis*-geraniol**	-74.32 ± 1.31	↓	-81.71 ± 1.91	↓
(±)-Linalool	-		-33.95 ± 0.16	↓
(-)-Linalool	-		-57.39 ± 2.00	↓
(-)-Menthone	-49.45 ± 1.51	↓	-	
(±)-Menthol	-89.54 ± 1.26	↓	-	
Carvacrol	-78.02 ± 1.46	↓	-84.44 ± 0.58	↓
(+)-Carvone	-52.16 ± 2.65	↓	-55.24 ± 0.95	↓
(-)-Carvone	-62.28 ± 1.50	↓	-62.85 ± 2.03	↓
(+)-Pulegone	-48.69 ± 2.86	↓	-57.76 ± 1.39	↓
(R)-(+)-Limonene	-59.03 ± 2.74	↓	-73.64 ± 0.29	↓
(S)-(-)-Limonene	-76.52 ± 0.63	↓	-81.71 ± 0.05	↓
(-)-Terpinen-4-ol	-41.35 ± 1.23	↓	-	
1,4 Cineole	-59.57 ± 0.17	↓	-58.53 ± 1.84	↓
α-Bisabolol	-70.17 ± 0.13	↓	-72.70 ± 0.59	↓
ρ-Cymene	-75.80 ± 0.07	↓	-79.15 ± 0.26	↓
(-)-β-Pinene	-70.67 ± 0.17	↓	-73.63 ± 0.28	↓
(+)-β-Pinene	-67.27 ± 0.21	↓	-66.39 ± 1.84	↓
(-)-Fenchone	-64.87 ± 0.05	↓	-69.29 ± 1.77	↓
(+)-Fenchone	-66.00 ± 0.04	↓	-74.22 ± 1.38	↓
(+)-Borneol	-69.41 ± 0.18	↓	-70.42 ± 0.63	↓
(-)-Borneol	-62.20 ± 0.07	↓	-67.56 ± 2.99	↓
(-)-Bornyl acetate	-70.10 ± 0.07	↓	-59.15 ± 28.50	↓
(±)-Camphor	-63.91 ± 0.07	↓	-40.23 ± 50.45	↓
(1R)-(+)-Camphor	-81.38 ± 0.14	↓	-	
(-)-Camphor	-57.99 ± 0.23	↓	-	
(1R)-(-)-Camphorquinone	-67.19 ± 0.25	↓	-78.79 ± 4.18	↓
(±)-Camphorquinone	-		-34.98 ± 1.06	↓
(1S)-(+)-Camphorquinone	-42.42 ± 1.00	↓	-	
(-)-Caryophyllene oxide	-68.81 ± 0.31	↓	-78.91 ± 0.52	↓
(-)-α-Thujone	-65.64 ± 2.83	↓	-74.16 ± 0.97	↓
(±)-α-b-Thujone	-59.85 ± 2.83	↓	-67.93 ± 1.38	↓
Artemisia ketone	-74.19 ± 1.51	↓	-69.90 ± 1.66	↓
α-Humulene	-67.64 ± 3.24	↓	-66.73 ± 2.10	↓
Ocimene	-88.23 ± 4.08	↓	-88.05 ± 0.35	↓
(±)-Lavandulol acetate	-76.43 ± 5.22	↓	-82.11 ±0.46	↓
Myrcene	-51.79 ± 9.39	↓	-68.35 ± 0.42	↓

Table C.8: Adherent cell counting

EOC/8-OH derivative/compounds	% Cellular viability		% Change in cellular viability	Effect on viability
	24 hours	48 hours		
(-)-α-Pinene	92.51	61.15	32.56	decreased
(-)-β-Pinene	91.57	80.42	11.77	decreased
(±)-Menthone	87.83	83.90	4.33	decreased
2-Mercaptothiazoline	59.42	75.93	-16.77	increased
Citral	51.85	60.36	-8.57	increased
Thymol	96.39	78.79	18.42	decreased
5,7-Dimethyl-8-OH	90.06	63.64	27.47	decreased
5-Nitro-8-OH	61.69	45.95	16.39	decreased
5-Amino-8-OH	73.40	78.67	-5.16	increased
5-Chloro-7-bromo-8-OH	67.03	69.23	-2.03	increased
5,7-Dichloro-8-OH	51.82	55.26	-3.37	increased
2-Amino-8-OH	81.24	62.50	19.54	decreased
5-H_3SO_4-7-iodo-8-OH	72.14	56.76	16.05	decreased
5,7-Cl_2-2-CH_3-8-OH	79.46	75.00	4.85	decreased
5,7-Dibromo-8-OH	57.84	72.22	-14.59	increased
5-Cl-7-iodo-8-OH	37.40	54.55	-17.50	increased
5,7-Diiodo-8-OH	39.93	62.96	-23.55	increased
N-butyl-2,2-imino-di-8-OH	60.25	47.01	13.82	decreased
5-HSO_3 -8-OH	84.42	77.14	7.77	decreased
8-Chloro-2-OH	81.27	67.65	14.28	decreased
5-Carboxy-8OH	86.29	79.45	7.32	decreased
Camptothecin	54.83	44.44	10.86	decreased
Chloroquine	66.36	51.16	15.84	decreased
Quinine	95.91	91.30	5.05	decreased
D-penicillamine	96.12	98.39	-2.01	increased
Neocuproine	84.40	40.00	45.94	decreased
Tetrathiomolybdate	95.39	83.91	12.13	decreased

Table C.9: The protective effect of the EOCs on red blood cells treated with copper.

EOC	% Haemolytic protective effect	Effect of compound with copper (I)	% Haemolytic protective effect	Effect of compound with copper (II)
***Cis*-nerolidol**	-11.08 ± 1.63	↑ lysis	-13.96 ± 3.17	↑ lysis
***Trans*-nerolidol**	-14.95 ± 4.50	↑ lysis	-13.95 ± 2.45	↑ lysis
***Trans*-geraniol**	-15.49 ± 5.63	↑ lysis	-16.17 ± 3.79	↑ lysis
***Cis*-geraniol**	-15.60 ± 2.13	↑ lysis	-16.92 ± 2.21	↑ lysis
(-)-Linalool	-80.98 ± 5.41	↑ lysis	-33.37 ± 14.20	↑ lysis
Linalyl acetate	-70.59 ± 3.03	↑ lysis	-4.94 ± 3.31	↑ lysis
(S)-(-)-β-Citronellol	-72.98 ± 3.89	↑ lysis	-2.25 ± 0.89	↑ lysis
(-)-Menthone	-94.48 ± 4.84	↑ lysis	-33.43 ± 3.61	↑ lysis
(+)-Pulegone	-81.06 ± 7.91	↑ lysis	-63.26 ± 3.69	↑ lysis
(R)-(+)-Limonene	-14.95 ± 3.62	↑ lysis	-13.39 ± 1.47	↑ lysis
(S)-(-)-Limonene	-17.09 ± 4.69	↑ lysis	-15.78 ± 3.78	↑ lysis
(+)-Terpinen-4-ol	-80.48 ± 4.01	↑ lysis	-126.13 ± 16.91	↑ lysis
1,4 Cineole	-63.62 ± 10.43	↑ lysis	-237.34 ± 1.78	↑ lysis
α-Bisabolol	-18.94 ± 1.97	↑ lysis	-16.78 ± 0.63	↑ lysis
ρ-Cymene	-6.87 ± 1.32	↑ lysis	-4.97 ± 0.76	↑ lysis
(-)-β-Pinene	-48.86 ± 4.48	↑ lysis	-3.83 ± 1.33	↑ lysis
(+)-β-Pinene	-57.07 ± 3.49	↑ lysis	-11.95 ± 3.12	↑ lysis
(-)-Fenchone	-4.31 ± 1.25	↑ lysis	-10.14 ± 1.73	↑ lysis
(+)-Fenchone	-5.13 ± 2.82	↑ lysis	-8.21 ± 1.19	↑ lysis
(+)-Borneol	-18.34 ± 1.90	↑ lysis	-18.88 ± 5.59	↑ lysis
(-)-Borneol	-17.08 ± 0.69	↑ lysis	-20.05 ± 3.25	↑ lysis
(-)-Bornyl acetate	-16.77 ± 0.50	↑ lysis	-18.18 ± 2.55	↑ lysis
(±)-Camphor	-19.32 ± 4.85	↑ lysis	-17.82 ± 2.89	↑ lysis
(1R)-(+)-Camphor	-18.59 ± 4.65	↑ lysis	-18.20 ± 1.12	↑ lysis
(-)-Camphor	-19.81 ± 3.34	↑ lysis	-18.67 ± 0.48	↑ lysis
(1R)-(-)-Camphorquinone	-85.97 ± 6.35	↑ lysis	See Figure 5.16	
(±)-Camphorquinone	-78.20 ± 1.86	↑ lysis	-37.19 ± 3.30	↑ lysis
(1S)-(+)-Camphorquinone	-119.66 ± 5.20	↑ lysis	-38.83 ± 2.36	↑ lysis
(-)-Caryophyllene oxide	-98.13 ± 3.93	↑ lysis	-588.65 ± 14.56	↑ lysis
(+)-*Trans*-caryophyllene	-59.38 ± 9.98	↑ lysis	-24.52 ± 5.82	↑ lysis
(-)-α-Thujone	-25.16 ± 0.58	↑ lysis	-21.26 ± 5.82	↑ lysis
(±)-α-b-Thujone	-19.73 ± 0.17	↑ lysis	-19.28 ± 4.72	↑ lysis
Thymol	-8.99 ± 0.84	↑ lysis	See Figure 5.16	
Artemisia ketone	-51.78 ± 8.31	↑ lysis	-9.14 ± 0.26	↑ lysis
α-Humulene	-54.36 ± 0.88	↑ lysis	-69.02 ± 0.24	↑ lysis
Ocimene	-79.40 ± 3.15	↑ lysis	-12.00 ± 0.85	↑ lysis
(±)-Lavandulol acetate	-18.89 ± 3.88	↑ lysis	-7.22 ± 0.97	↑ lysis

C.6: Antioxidant activity

Table C.10: The percentage free radical scavenged (≥ 60%) by the EOC's and control compounds.

EOCs	% FRS at 200 µM
***Trans*-geraniol**	1.71 ± 0.33
***Cis*-geraniol**	1.77 ± 0.38
(±)-Linalool	3.23 ± 0.19
(-)-Linalool	0.64 ± 0.27
Linalyl acetate	1.52 ± 0.26
(-)-Citronellal	2.01 ± 0.23
(±)-Menthol	2.27 ± 0.48
Carvacrol	3.13 ± 0.62
(+)-Pulegone	1.25 ± 0.43
(R)-(+)-Limonene	1.48 ± 0.26
(S)-(-)-Limonene	1.61 ± 0.44
(+)-Terpinen-4-ol	2.15 ± 0.45
(-)-Terpinen-4-ol	0.64 ± 0.07
1,8-Cineole	2.25 ± 0.41
1,4-Cineole	2.06 ± 0.32
ρ-Cymene	1.60 ± 0.32
(+)-β-Pinene	1.95 ± 0.41
(+)-Fenchone	1.89 ± 0.44
(+)-Borneol	≤ 0.01
(-)-Borneol	≤ 0.01
(±)-Camphor	≤ 0.01
(1R)-(+)-Camphor	≤ 0.01
(-)-Camphor	≤ 0.01
(1R)-(-)-Camphorquinone	≤ 0.01
(±)-Camphorquinone	≤ 0.01
(1S)-(+)-Camphorquinone	≤ 0.01
(-)-Caryophyllene oxide	≤ 0.01
(+)-*Trans*-caryophyllene	1.44 ± 0.63
(-)-α-Thujone	1.71 ± 0.66
α-Humulene	1.56 ± 0.35
Myrcene	1.47 ± 0.36

Table C.11: Percentage lipid peroxidation inhibited.

Compounds	% Lipid peroxidation inhibited	IC_{50} Value
Neocuproine	3.56 ± 1.63	
Tetrathiomolybdate	45.53 ± 5.79	4.30 ± 0.25
TET	18.00 ± 2.94	
BHT	38.03 ± 0.93	7.73 ± 1.28
BHA	30.23 ± 1.87	
Quinine	2.44 ± 4.05	
Chloroquine	2.74 ± 3.29	
Ascorbic Acid	88.12 ± 1.94	34.37 ± 3.32
Trolox	68.79 ± 1.75	15.19 ± 3.58
EDTA	44.91 ± 6.53	
Camptothecin	15.21 ± 2.60	
Cupral	52.68 ± 1.94	
Dihydroartemisinin	8.84 ± 3.12	
Methotrexate	10.23 ± 2.86	

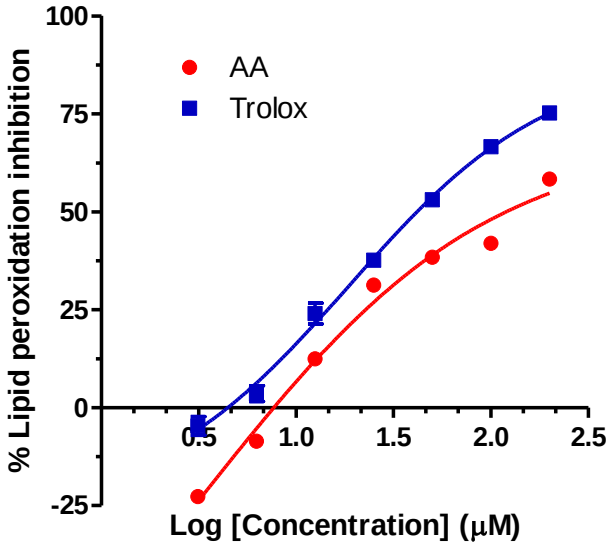

Figure C.1: The log-sigmoid dose response curve of the lipid peroxidation inhibition activity of the most active AA and BHA.

Table C.12: Percentage lipid peroxidation induced

Essential oil constituents	% Lipid peroxidation inhibited
Citral	57.30 ± 1.84
Geranyl acetate	53.62 ± 2.18
Farnesol	51.91 ± 2.43
(±)-Linalool	57.02 ± 2.66
(-)-Linalool	54.46 ± 1.64
Linalyl acetate	57.12 ± 0.79
(-)-Citronellal	56.52 ± 3.18
(S)-(-)-β-Citronellol	52.09 ± 1.76
(-)-Menthone	54.61 ± 0.96
(+)-Carvone	48.31 ± 4.36
(-)-Carvone	51.63 ± 1.26
(-)-Pulegone	53.38 ± 2.51
(+)-Pulegone	52.58 ± 3.47
(+)-Terpinen-4-ol	53.41 ± 1.23
(-)-Terpinen-4-ol	51.39 ± 4.06
(-)-α-Pinene	49.35 ± 1.56
(-)-Fenchone	49.84 ± 3.20
(+)-Fenchone	52.68 ± 2.34
(1R)-(-)-Camphorquinone	55.27 ± 4.20
Artemisia ketone	50.26 ± 2.60
α-Humulene	53.16 ± 0.86
(±)-Lavandulol acetate	45.14 ± 1.04
Myrcene	49.17 ± 3.31

Table C.13: The percentage nitrite in the Griess reagent assay.

Compounds/EOCs	% Nitrite
D-Penicillamine	17.36 ± 1.87
Chloroquine	12.52 ± 2.26
Quinine	16.77 ± 2.91
TET	21.32 ± 0.85
Neocuproine	16.80 ± 3.31
Camptothecin	11.53 ± 1.89
EDTA	22.34 ± 4.87
Dihydroartemisinin	19.36 ± 3.46
Trolox	17.01 ± 3.08
BHA	16.51 ± 2.40
BHT	16.52 ± 1.65
L-Penicillamine	22.71 ± 0.92
Cupferron	≤ 0.01
Bathocupriene	12.05 ± 2.01
Cupral	24.68 ± 1.99
Methotrexate	8.28 ± 0.18
Carvacrol	23.70 ± 4.98
***Trans*-nerolidol**	23.68 ± 4.41
(+)-Terpinen-4-ol	23.58 ± 4.47
Artemisia ketone	22.91 ± 3.71
(-)-Pulegone	22.87 ± 2.30
α-Bisabolol	22.86 ± 4.30
1,4-Cineole	22.84 ± 4.84
(+)-Borneol	19.72 ± 2.14
Myrcene	19.22 ± 0.94
ρ-Cymene	18.84 ± 1.58
(±)-Camphorquinone	18.01 ± 0.46
α-Humulene	16.90 ± 3.14

C.7: Larvicidal activity

Table C.14: The larvicidal activity of EOCs after 24 hours.

EOCs	% Mortality
Artemisia ketone	14.00 ± 5.50 [Yes (P = 0.01)]
α-Humulene	13.00 ± 5.70 [Yes (P = 0.01)]
(±)-Menthol	13.00 ± 2.70 [Yes (P = 0.01)]
(-)-Bornyl acetate	12.00 ± 5.70 [Yes (P = 0.01)]
(±)-Camphor	12.00 ± 5.70 [Yes (P = 0.01)]
2-Mercaptothiazoline	18.00 ± 8.40 [Yes (P = 0.01)]

Appendix D. Discussion

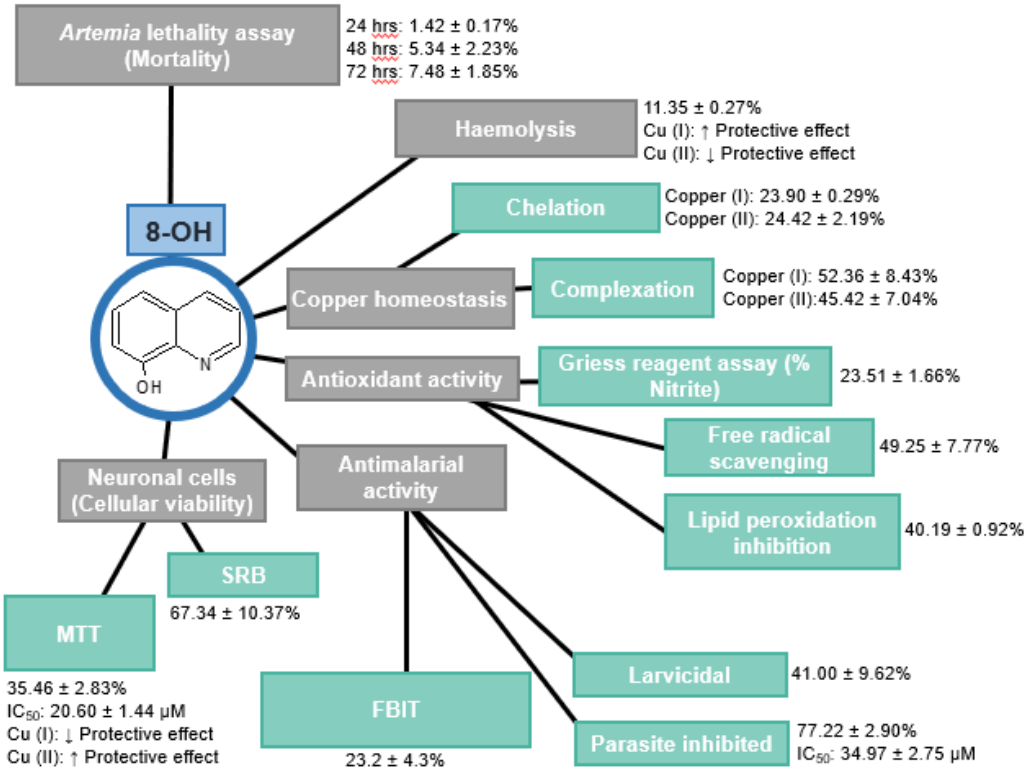

Figure D.1: The summary of activity for 8-OH

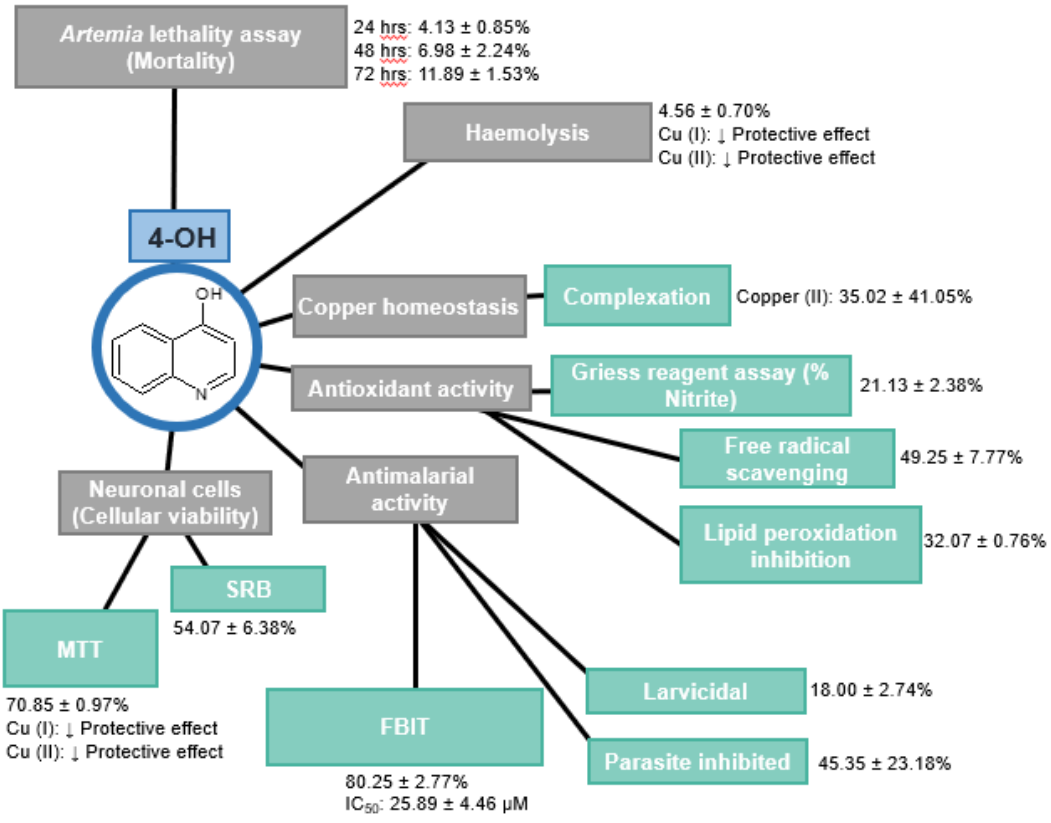

Figure D.2: The summary of activity for 4-OH

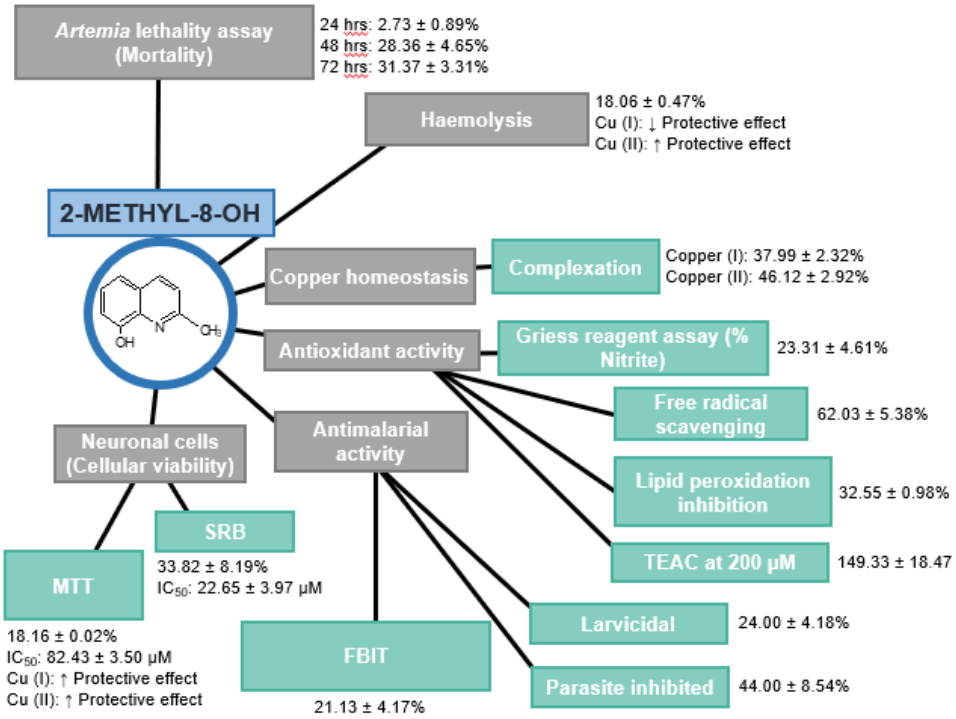

Figure D.3: The summary of activity for 2-methyl-8-OH

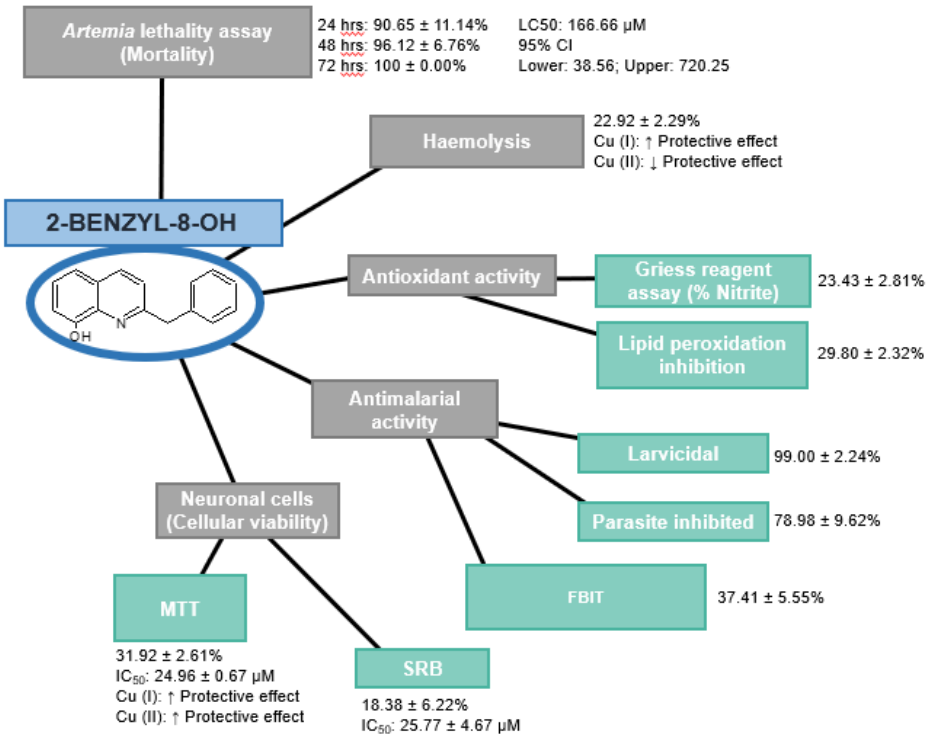

Figure D.4: The summary of activity for 2-benzyl-8-OH

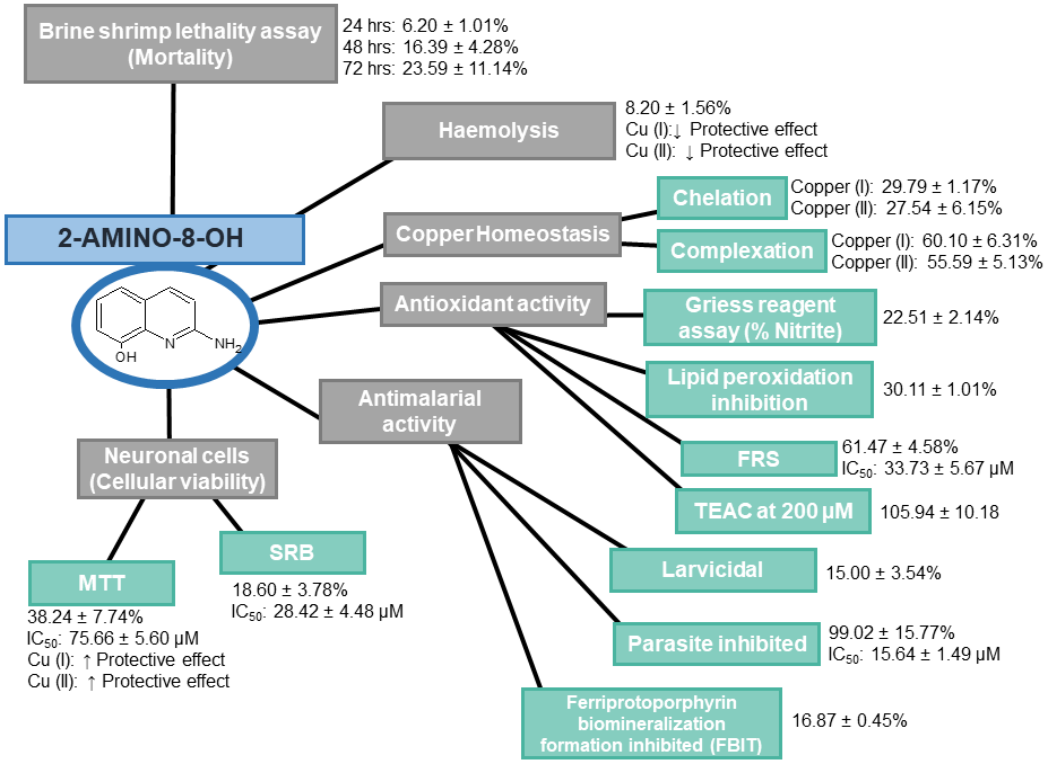

Figure D.5: The summary of activity for 2-amino-8-OH

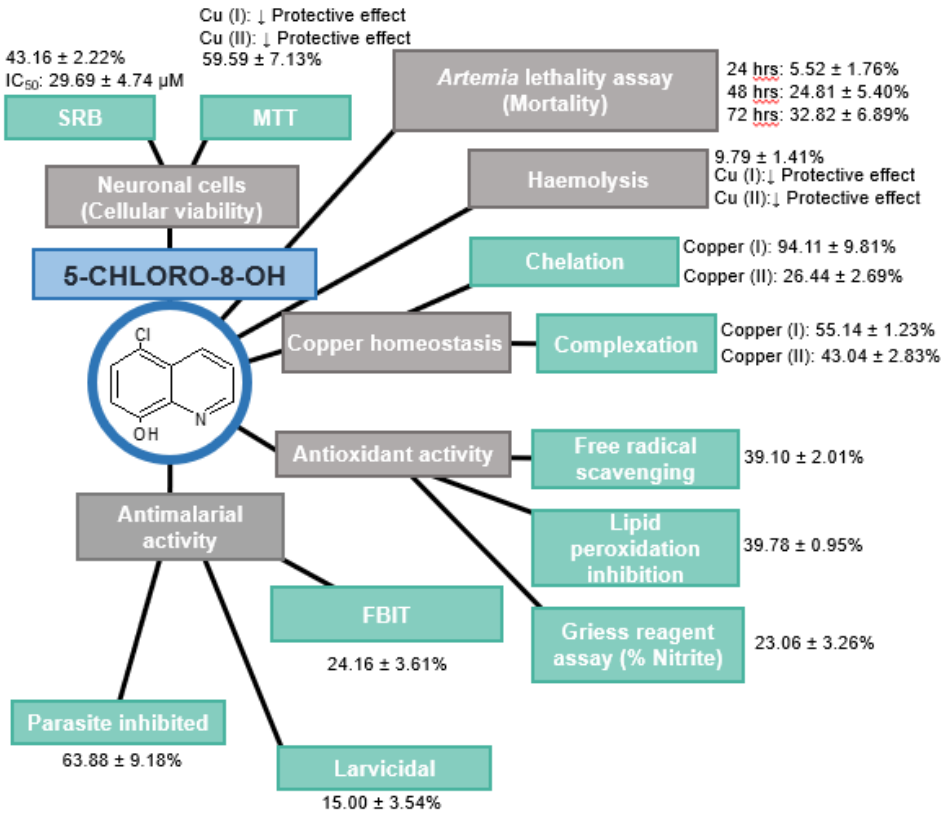

Figure D.6: The summary of activity for 5-chloro-8-OH

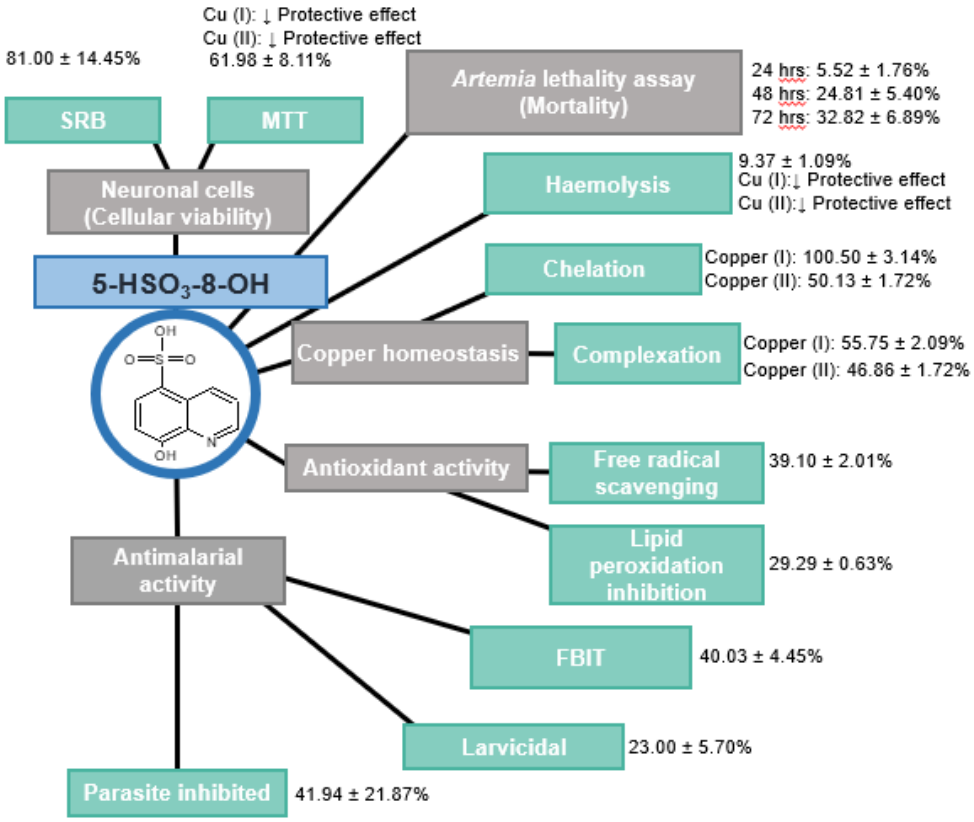

Figure D.7: The summary of activity for 5-HSO_3-8-OH

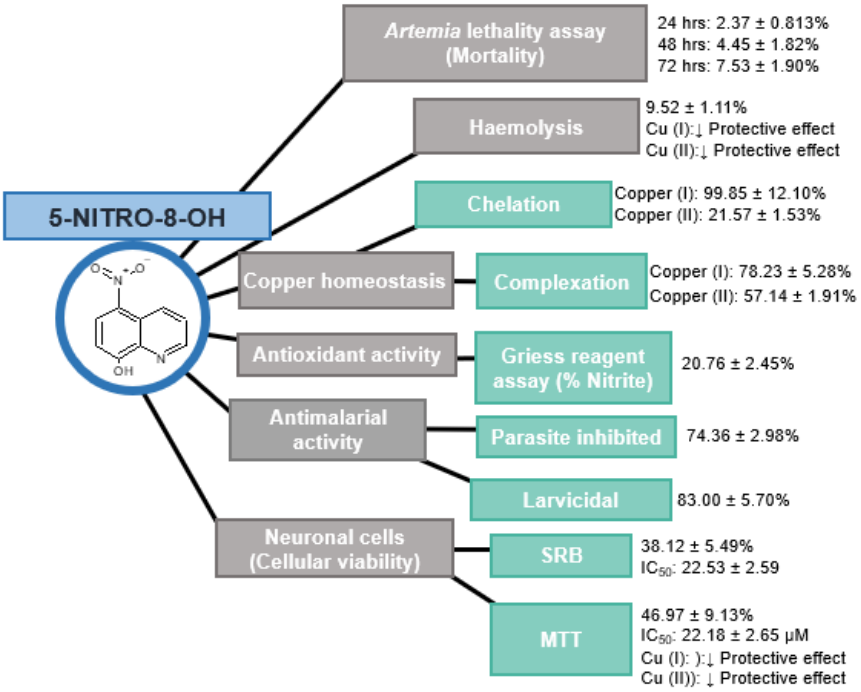

Figure D.8: The summary of activity for 5-nitro-8-OH

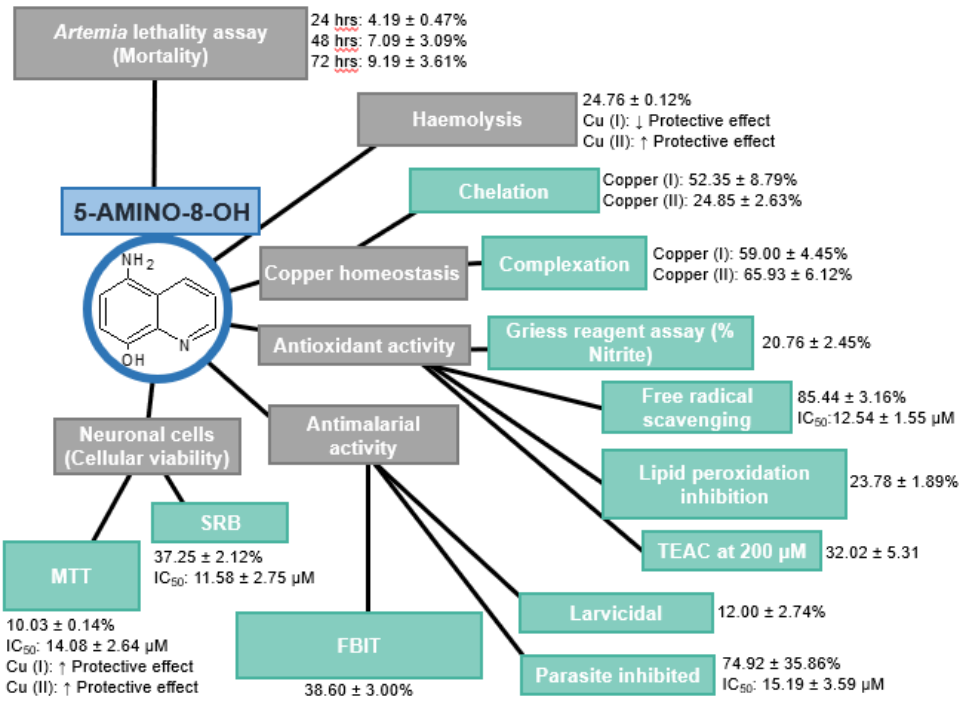

Figure D.9: The summary of activity for 5-amino-8-OH

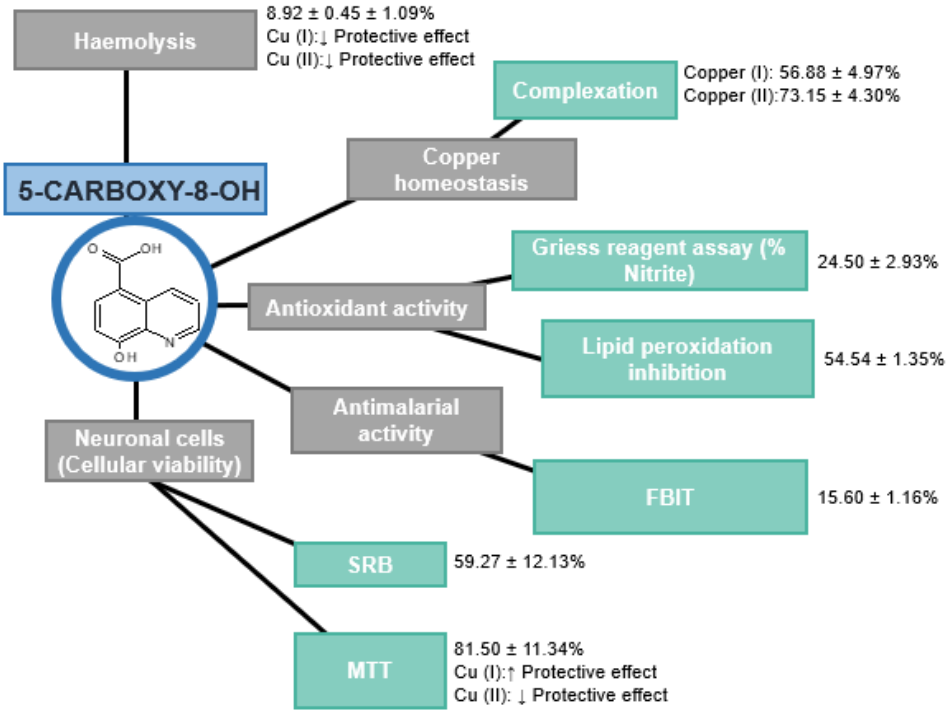

Figure D.10: The summary of activity for 5-carboxy-8-OH

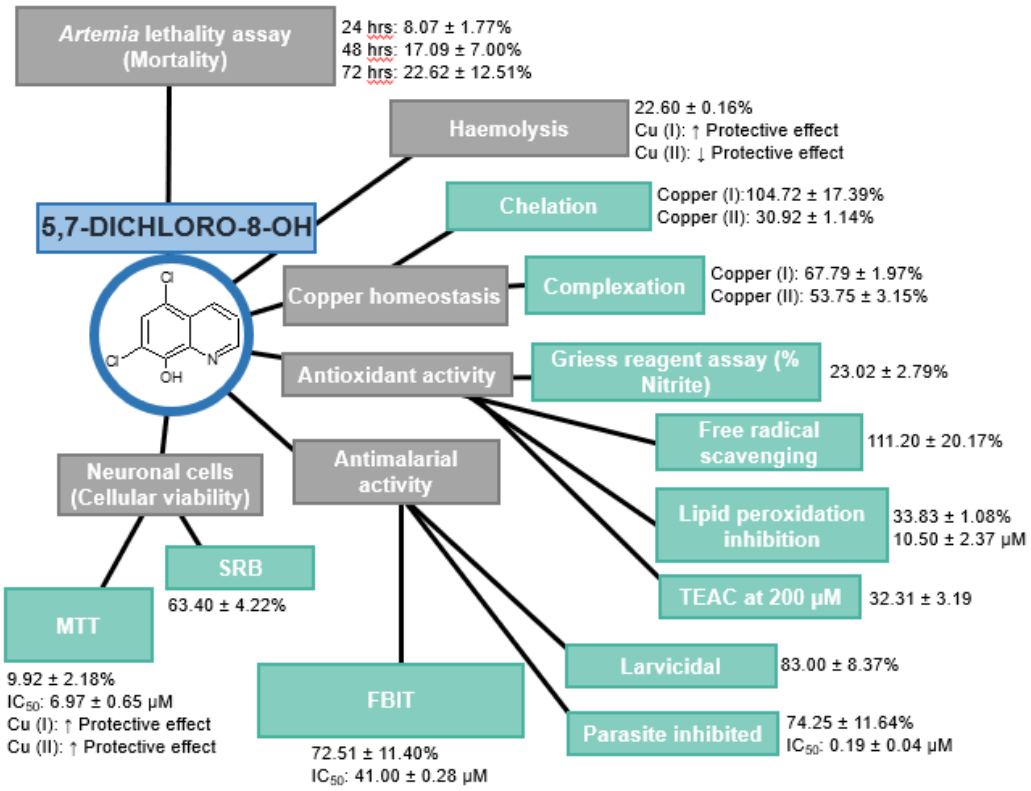

Figure D.11: The summary of activity for 5,7-dichloro-8-OH

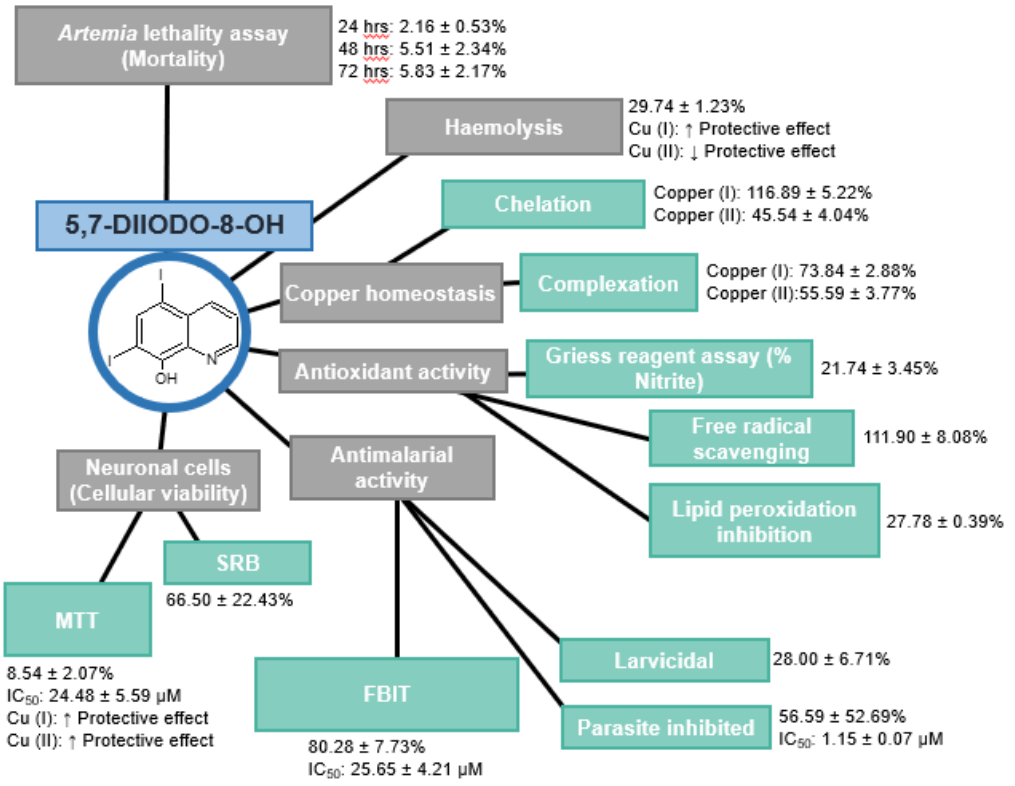

Figure D.12: The summary of activity for 5,7-diiodo-8-OH

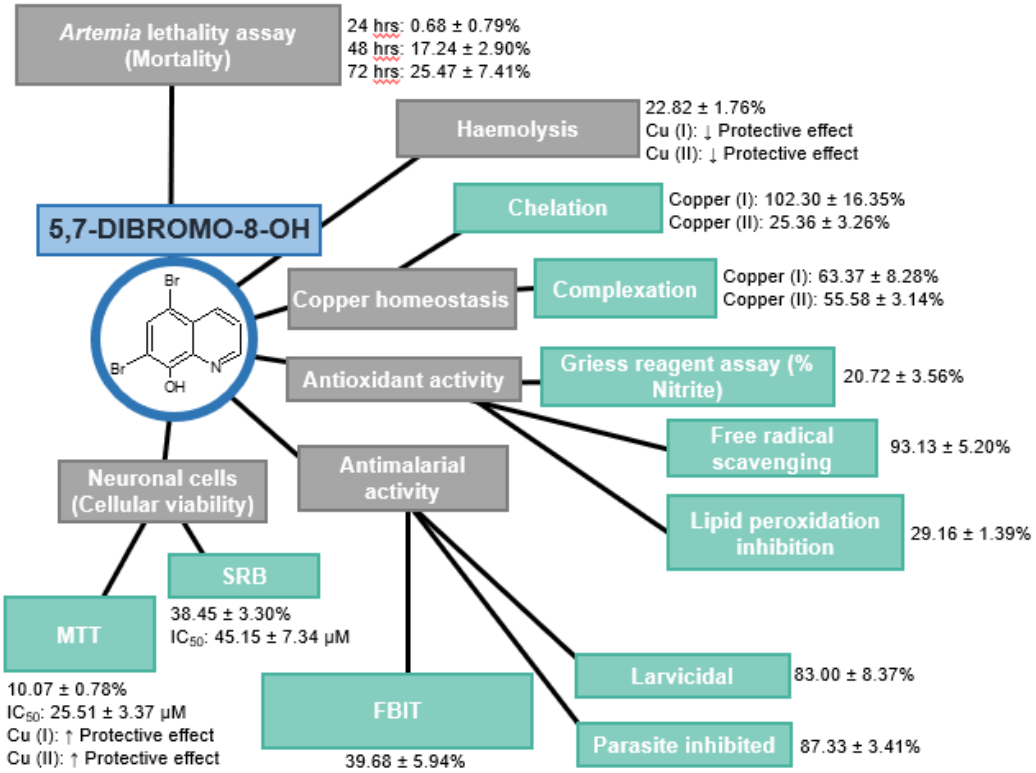

Figure D.13: The summary of activity for 5,7-dibromo-8-OH

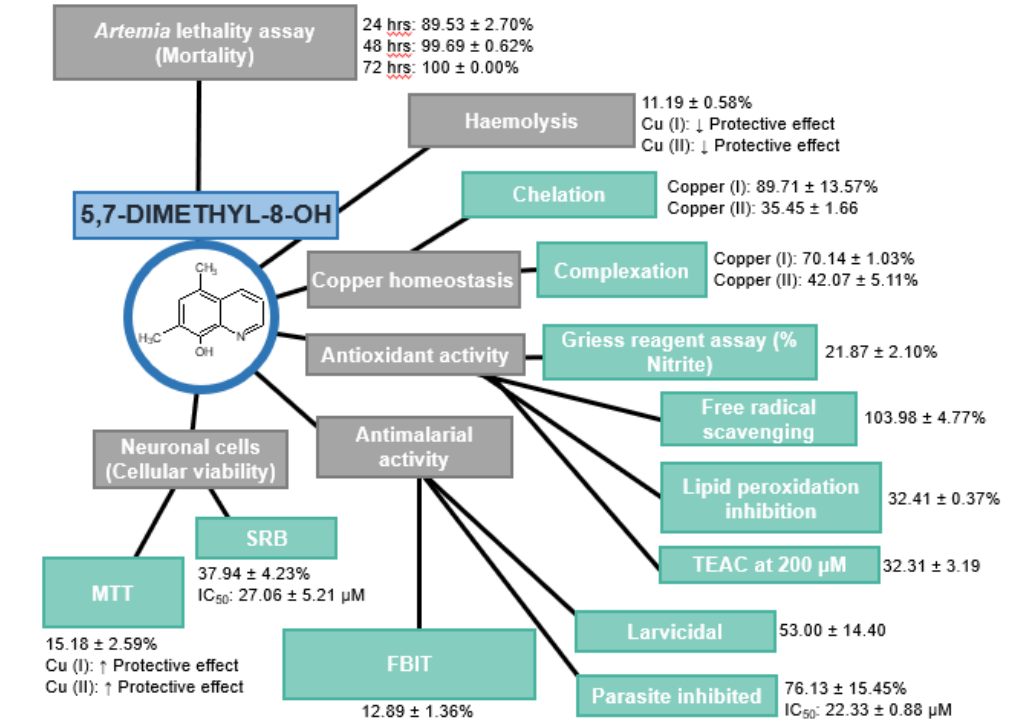

Figure D.14: The summary of activity for 5,7-dimethyl-8-OH

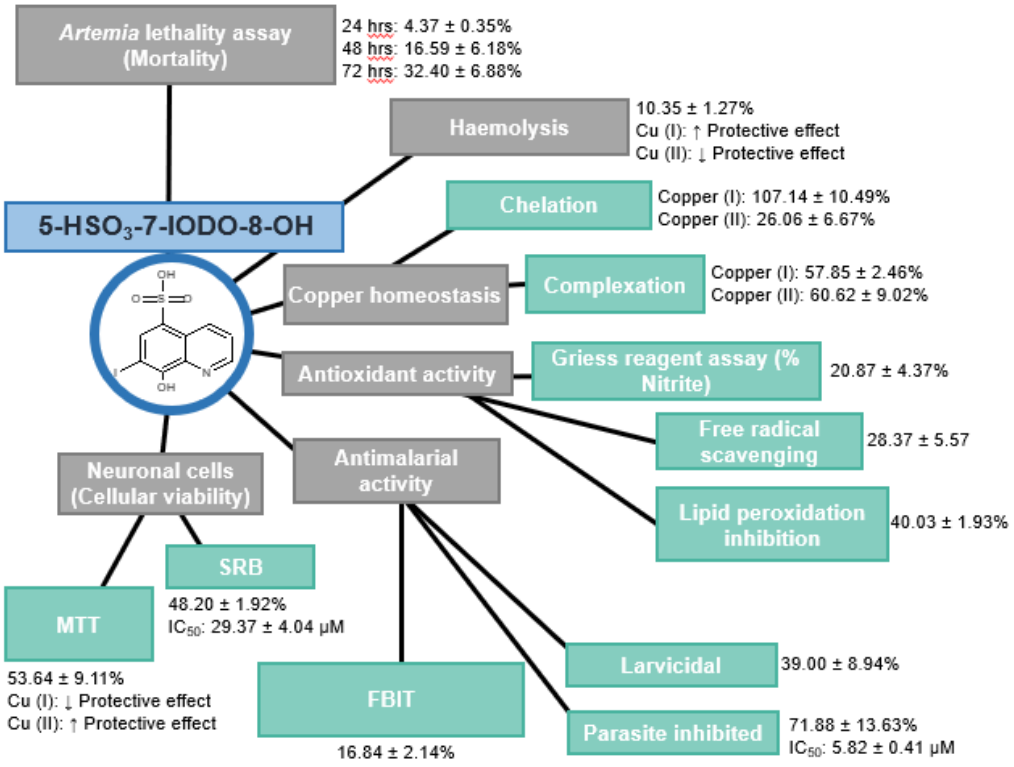

Figure D.15: The summary of activity for 5-HSO_3-7-iodo-8-OH

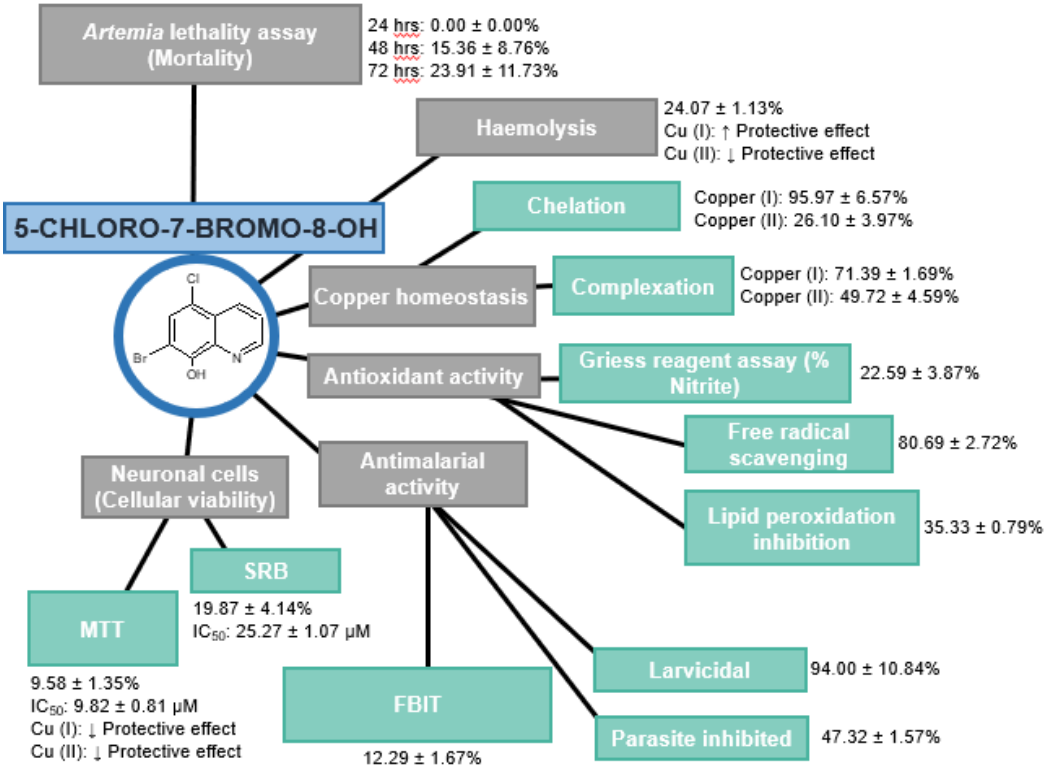

Figure D.16: The summary of activity for 5-chloro-7-bromo-8-OH

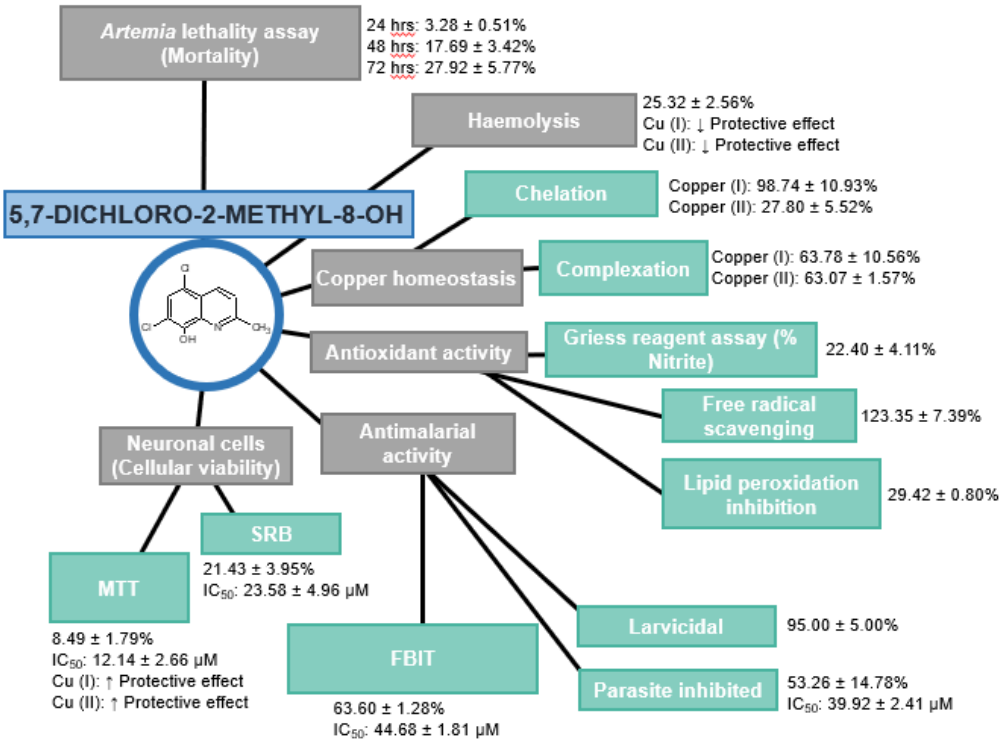

Figure D.17: The summary of activity for 5,7-dichloro-2-methyl-8-OH

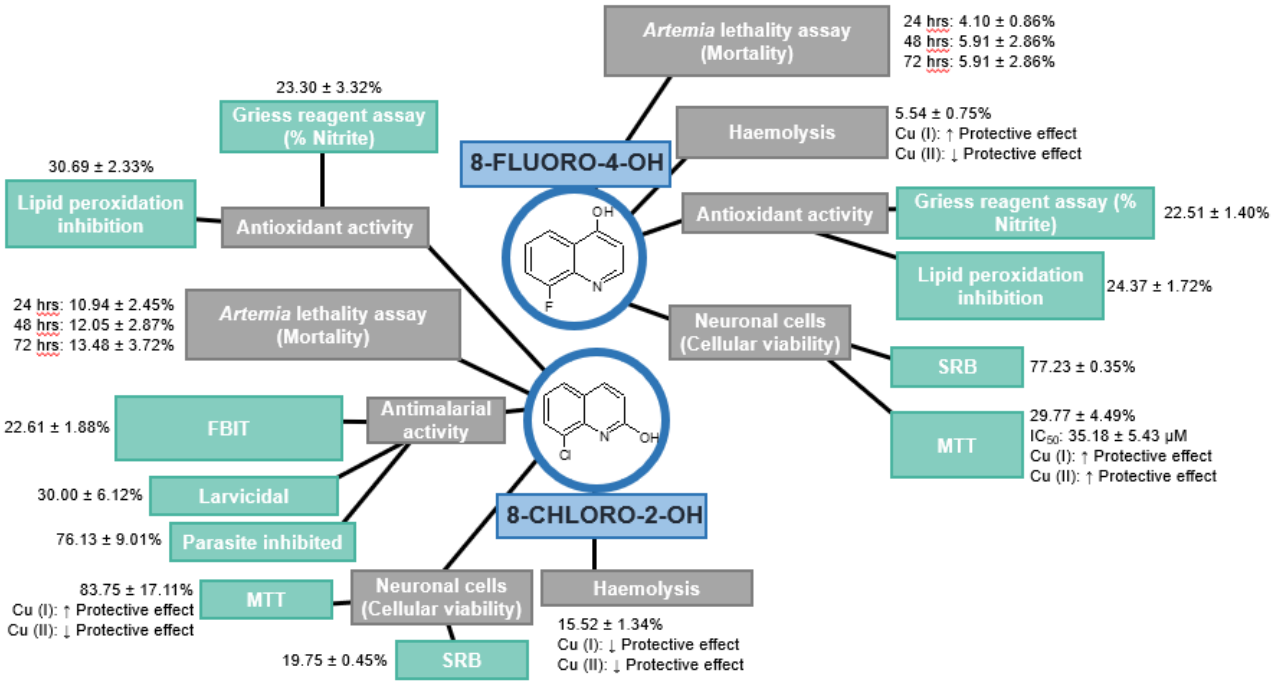

Figure D.18: The summary of activity for 8-fluoro-4-OH and 8-chloro-2-OH